

**AD-A168 975**

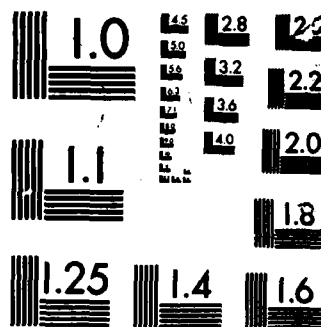
KRASH DYNAMICS ANALYSIS MODELING - TRANSPORT AIRPLANE  
 CONTROLLED IMPACT D. (U) LOCKHEED AIRCRAFT CORP DUBURANK  
 CALIF 6 WITTLIN ET AL. MAR 86 LR-38776 DOT/FAR/CT-85/9  
 DTFA83-84-C-00004 F/G 1/2

1/2

**UNCLASSIFIED**

F/G 1/2

NL



2

DOT/FAA/CT-85/9

# KRASH Dynamics Analysis Modeling — Transport Airplane Controlled Impact Demonstration Test

AD-A168 975

Gil Wittlin  
Bill LaBarge

Prepared by  
Lockheed-California Company  
Burbank, California

May 1985  
(Revised March 1986)  
Final Report

This document is available to the U.S. public  
through the National Technical Information  
Service, Springfield, Virginia 22161.



U.S. Department of Transportation  
**Federal Aviation Administration**  
Technical Center  
Atlantic City Airport, N.J. 08405

DTIC  
ELECTE  
JUN 20 1986  
S D E

DTIC FILE COPY

86

026

#### **NOTICE**

**This document is disseminated under the sponsorship of the Department of Transportation in the interest of information exchange. The United States Government assumes no liability for the contents or use thereof.**

**The United States Government does not endorse products or manufacturers. Trade or manufacturer's names appear herein solely because they are considered essential to the object of this report.**

1. Report No. DOT/FAA/CT-85/9		2. Government Accession No.		3. Recipient's Catalog No.	
4. Title and Subtitle KRASH DYNAMICS ANALYSIS MODELING - TRANSPORT AIRPLANE CONTROLLED IMPACT DEMONSTRATION TEST		5. Report Date May 1985 (Revised March 1986)			
		6. Performing Organization Code			
7. Author(s) G. Wittlin, W.L. LaBarge		8. Performing Organization Report No. LR 30776			
9. Performing Organization Name and Address Lockheed-California Company Burbank, CA 91520		10. Work Unit No.			
		11. Contract or Grant No. DTFA03-84-C-00004			
12. Sponsoring Agency Name and Address U.S. Department of Transportation Federal Aviation Administration Technical Center Atlantic City Airport, NJ 08405		13. Type of Report and Period Covered			
		14. Sponsoring Agency Code Final Jan. 1984 - Sept. 1984			
15. Supplementary Notes					
16. Abstract <p>A transport airplane Controlled Impact Demonstration (CID) test is analyzed with program KRASH. Prior to modeling the test condition, supporting analysis of both narrow-body and wide-body transport airplane frame segments were modeled with KRASH and compared to existing test results. The results of the analysis are utilized as input data for the KRASH CID model. Prior to the CID test a narrow-body transport airplane was impacted with the ground, via a free fall drop, to obtain structure crush and damage data. KRASH modeling of this test was used to refine the CID KRASH model. The CID KRASH model is exercised to obtain anticipated floor accelerations, underside crush, fuselage forces, and deflections. All KRASH modeling is performed utilizing current enhancement features. The latest KRASH85 input-output format is described in a separate report. Contained in this report are descriptions of the following:</p> <ul style="list-style-type: none"> <li>• Recent KRASH85 coding changes to enhance its usage</li> <li>• KRASH models and results for both narrow-body and wide-body transport airplane frame section drop tests</li> <li>• KRASH model and results for a narrow-body transport airplane drop test</li> <li>• KRASH model and results for a CID test to be performed.</li> <li>• Conclusions based on the CID pre-test analysis results</li> </ul>					
17. Key Words (Suggested by Author(s)) KRASH, crashworthiness, crash dynamics computer simulation, controlled impact demonstration, CID, analytical predictions transport airplane			18. Distribution Statement This document is available to the U.S. public through the National Technical Information Services, Springfield, VA 22161		
19. Security Classif. (of this report) UNCL.		20. Security Classif. (of this page) UNCL.		21. No. of Pages 173	
22. Price*					

# FOREWORD

This report was prepared by the Lockheed-California Company, under contract DTFA03-84-C-00004, sponsored by the Federal Aviation Administration Technical Center. This report describes the analytical modeling effort performed from January 1984 through September 1984. The latest KRASH input-output format incorporated during the same time period are described in report DOT/FAA/CT-85-10. The work was administered under the direction of L. Neri and C. Caiafa of the FAA.

The Lockheed-California Company effort was performed by Gil Wittlin with support from M. A. Gamon and W. L. LaBarge. The Lockheed effort was performed within the Flutter and Dynamics Department.

Accession For	
NTIS GRA&I	<input checked="" type="checkbox"/>
DTIC TAB	<input type="checkbox"/>
Unannounced	<input type="checkbox"/>
Justification	
By	
Distribution/	
Availability Codes	
Dist	Avail and/or Special
A-1	

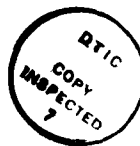


## TABLE OF CONTENTS

Section	Page
FOREWORD	iii
EXECUTIVE SUMMARY	v
LIST OF FIGURES	ix
LIST OF TABLES	xv
1 INTRODUCTION	1-1
1.1 BACKGROUND	1-1
1.2 PROGRAM OBJECTIVE	1-1
2 KRASH ENHANCEMENTS	2-1
2.1 BACKGROUND	2-1
2.2 KRASH85 MODIFICATIONS	2-1
2.2.1 Revised Plastic Hinge Moment	2-1
2.2.2 Gear-Oleo Element Metering Pin	2-5
2.2.3 Load-Interaction Curves	2-5
2.2.4 Expanded Initial Condition (IC) Subroutine	2-9
2.2.5 Comprehensive Energy Balance Code	2-9
2.2.6 c.g. Time Histories	2-9
2.2.7 Arbitrary Mass Numbering	2-11
3 FUSELAGE SECTION TESTS AND ANALYSES	3-1
3.1 NARROW BODY AIRPLANE FUSELAGE SECTIONS	3-1
3.2 WIDEBODY AIRPLANE FUSELAGE SECTION TEST	3-7
4 PRELIMINARY KRASH ANALYSIS	4-1
4.1 GEARS-RETRACTED ANALYSIS	4-1
4.2 COMPARISONS WITH GEARS-EXTENDED AND SLOPE IMPACTS	4-11
4.3 SEAT/OCCUPANT RESPONSE TO A LONGITUDINAL PULSE	4-17
4.4 TEST IMPACT CONDITION SELECTION	4-23
5 NARROW-BODY AIRPLANE IMPACT DATA	5-1
5.1 AIRPLANE IMPACT TEST	5-1

# TABLE OF CONTENTS (Continued)

Section		Page
5.2	KRASH MODELING OF IMPACT TEST	5-14
5.3	REVISED CID STICK MODEL RESULTS	5-18
6	CID PRE-TEST ANALYSIS	6-1
6.1	KRASH MODEL	6-1
6.2	KRASH ANALYSIS RESULTS	6-8
6.3	SUMMARY OF CID PRE-TEST ANALYSIS RESULTS	6-16
7	CONCLUSIONS	7-1
	REFERENCES	R-1
	APPENDICES	
A.	KRASH DATA SET ECHOES	
A.1	NARROW-BODY AIRPLANE KRASH FRAME MODEL	A-1
A.2	WIDE-BODY AIRPLANE KRASH FRAME MODEL	A-4
A.3	KRASH CID AIRPLANE STICK MODEL	A-7
A.4	KRASH CID AIRPLANE EXPANDED MODEL	A-13
B.	KRASH TIME HISTORY RESPONSES - EXPANDED MODEL	B-1
C.	DISTRIBUTION LIST	C-1



## TABLE OF CONTENTS

Section	Page
FOREWORD	iii
SUMMARY	v
LIST OF FIGURES	ix
LIST OF TABLES	ix
1 INTRODUCTION	1-1
2 USER'S GUIDE	2-1
2.1 OVERALL KRASH85 ANALYSIS SYSTEM	2-1
2.2 KRASH85 INPUT	2-8
2.3 OUTPUT AND SAMPLE CASE	2-93
2.3.1 KRASHIC Output	2-93
2.3.1.1 Echo of Input Data	2-93
2.3.1.2 Formatted Print-Out of Input Data	2-94
2.3.1.3 Miscellaneous Calculated Data	2-122
2.3.1.3.1 Model Parameters	2-123
2.3.1.3.2 Beam Loads and Deflections Corresponding to Yielding	2-123
2.3.1.3.3 Overall Vehicle Forces/Accelerations at Time Zero	2-123
2.3.1.3.4 Individual Mass Forces/Accelerations At Time Zero	2-124
2.3.2 MSCTRAN Output	2-125
2.3.2.1 Executive Control Deck Echo	2-125
2.3.2.2 Case Control Deck Echo	2-125
2.3.2.3 Input Bulk Data Deck Echo	2-125
2.3.2.4 Sorted Bulk Data Deck Echo	2-144
2.3.2.5 Displacement Vector	2-144
2.3.2.6 Load Vector	2-145

# LIST OF FIGURES (Continued)

Figure		Page
3-16	Passenger Cabin Floor Acceleration Time History	3-14
3-17	DC-10 Frame Model (Revised)	3-16
3-18	Passenger Cabin Floor Acceleration Time History(Revised Model)	3-16
3-19	Comparison of Widebody Frame Section Analysis and Test Results	3-18
3-20	Results of Narrow-Body Airplane Fuselage Center Section Test	3-18
3-21	Acceleration Time Histories Measured in Anthropomorphic Dummies Located in Fuselage Center Section	3-19
4-1	Outline of Analytical Approach	4-2
4-2	CID KRASH Stick Model	4-3
4-3	CID Model Frame Crush Springs	4-5
4-4	CID Model Hard Point Springs	4-6
4-5	Combined Load Ratios, for Fuselage Underside Load-Deflection Variations	4-8
4-6	Combined Load Ratios, Comparisons for 'No Lift' and Reduced Fuselage Stiffness	4-8
4-7	Combined Shear-Moment Loads as a Function of MLG Bulkhead Load Deflection Representation	4-9
4-8	Model Hard Point Load-Deflection Variations	4-9
4-9	Fuselage Damage as Function of Sink Speed, KRASH Analysis, 1° Nose-Up Impact	4-10
4-10	Duplication of Known Test Load-Deflection Curve Using Metering Pin Coding in KRASH85	4-12
4-11	Oleo Metering Pin Damping Constant Versus Gear Compression	4-12
4-12	Single Gear Model Analysis Results	4-14
4-13	Initial Impact Conditions; Ramp Versus Air-to-Ground Impact	4-15
4-14	KRASH Results, Air-To-Ground Versus Ground-To-Ground Impacts	4-16
4-15	KRASH CID Model Accelerations at FS960 (Mass 6)	4-18
4-16	Effect of Different Floor Longitudinal Pulse Representations on Occupant Response	4-19

# LIST OF FIGURES (Continued)

Figure		Page
4-17	KRASH CID Model Accelerations at FS620 (Mass 4)	4-20
4-18	KRASH CID Model Accelerations at FS820 (Mass 5)	4-21
4-19	KRASH Seat - Occupant Longitudinal Pulse Analysis Results	4-22
5-1	Pre-Test Setup - B707 Impact Test	5-2
5-2	Post-Test View - B707 Impact Test	5-2
5-3	Forward Lower Fuselage Damage - Left Side Looking Aft	5-3
5-4	Wing Root Fairing - Right Hand Trailing Edge	5-3
5-5	Left Wing Inboard Pylon Failure	5-4
5-6	Left Hand Inboard Pylon - Upper Longeron Fracture	5-4
5-7	Left Hand Landing Gear Well - View Looking Aft - Vertical Keel to FS960 Bulkhead	5-5
5-8	Close Up View of Vertical Keel and FS960 Bulkhead Intersection	5-5
5-9	Left Hand Landing Gear Wheel Well - FS820 Bulkhead, Looking Forward	5-6
5-10	Left Hand Landing Gear Wheel Well - FS820 Bulkhead - Tracing Web Crack	5-6
5-11	Left Hand Landing Gear Wheel Well - FS820 Bulkhead - Tracing Web Crack to Floor	5-7
5-12	Left Hand Landing Gear Wheel Well - FS820 Bulkhead - Floor Intersection	5-7
5-13	Centerline Frame Fracture Forward of FS620 Bulkhead - Forward Cargo Bay	5-8
5-14	Sidewall Frame Damage Aft Region of Forward Cargo Bay (Just Forward of FS620)	5-8
5-15	Aft Cargo Bay Looking Forward to FS960 Bulkhead	5-9
5-16	Close Up View of Stringer/Doubler Failure at FS960 Bulkhead	5-9
5-17	FS1010 - 104C Frame Damage	5-10
5-18	FS1100 - 1120 Frame Damage	5-10
5-19	Lower Wing Box and Keel Left Hand Side View Shows Crushed Ducting	5-11
5-20	Cabin Floor Looking Aft - Center Decking Removed FS820 to FS940	5-12

# LIST OF FIGURES (Continued)

Figure		Page
5-21	Cabin Floor Transverse Beams - Looking Aft from FS820	5-12
5-22	Looking at Left Hand Side of FS820 Bulkhead	5-13
5-23	Fractures at FS820 Bulkhead and Cabin Floor Interface - Right Hand Side View	5-13
5-24	Fracture at FS820 Bulkhead and Cabin Floor Interface - Close-Up View	5-14
5-25	Revisions to CID Model Frame Crush Springs	5-16
5-26	Revisions to CID Model Hard Point Springs	5-17
5-27	Maximum Allowable Moment and Shear Envelope - Negative Bending	5-20
5-28	Maximum Allowable Moment and Shear Envelope - Negative Bending	5-21
5-29	Maximum Allowable Moment and Shear Envelope - Negative Bending	5-22
5-30	Comparison of Pre-CID KRASH Stick Model Accelerations for Planned Symmetrical Impact Condition - Original Versus Revised Load Deflection Curves	5-24
5-31	Comparison Pre-CID DRASH Stick Model LIC and Fuselage Crush for the Planned Impact Condition - Original Versus Revised Load-Deflection Curves	5-25
5-32	Acceleration Response at FS300, Condition No. 3	5-27
5-33	Acceleration Response at FS460, Condition No. 3	5-28
5-34	Acceleration Response at FS620, Condition No. 3	5-29
5-35	Acceleration Response at FS820, Condition No. 3	5-30
5-36	Acceleration Response at FS960, Condition No. 3	5-31
5-37	Acceleration Response at FS1040, Condition No. 3	5-32
5-38	Acceleration Response at FS1200, Condition No.3	5-33
5-39	Acceleration Response at FS1400, Condition No. 3	5-34

# LIST OF FIGURES (Continued)

Figure		Page
6-1	Expanded CID KRASH Model	6-2
6-2	KRASH Models Parameters	6-4
6-3	CID Pre-Test Analysis - Vertical Acceleration Pulses, 17 Ft/Sec, +1 <sup>0</sup> Nose-Up	6-18
6-4	CID Pre-Test Peak Acceleration Versus Fuselage Station Obtained from KRASH Analysis	6-20
6-5	Comparison of PRE-CID KRASH Stick Model Analyses Versus Expanded Model Results for Planned Symmetrical Impact Condition	6-21
6-6	Comparison of Pre-CID KRASH Stick and Expanded Models Analyses Results for Planned Symmetrical Impact Condition	6-22
6-7	Pre-CID Tests KRASH Analysis Results for Planned Symmetrical Impact Condition	6-23

# LIST OF TABLES

Table		Page
2-1	Previous Modifications to Program KRASH (Reference 8)	2-2
2-2	The Features Unique to KRASH83	2-3
2-3	KRASH85 Enhancement Features	2-4
4-1	KRASH Model Fuselage Mass Point Locations	4-4
4-2	Gear-Up Versus Gear Extended Analysis Results	4-13
5-1	Qualitative Comparison of KRASH Stick Model and B707 Airplane Impact Test	5-15
5-2	Comparison of Analysis Results	5-19
6-1	Static Deflections	6-3
6-2	Comparison of Beam Initial LIC Ratios	6-6
6-3	CID Model Mass Description	6-6
6-4	CID Model Beam Description	6-7
6-5	Analysis Results, Fuselage Crush	6-9
6-6	Impact Sequence	6-10
6-7	Analysis Results, Yield/Rupture Sequence	6-11
6-8	Analysis Results, Beam Deflection	6-12
6-9	Analysis Results, Peak Vertical Acceleration	6-13
6-10	Summary of Fuselage Peak Shear and Moment Loads and LIC Ratios	6-13
6-11	Comparison of Peak Acceleration With and Without Fuselage Shell Shear Representation	6-14
6-12	Comparison of Peak Crushing With and Without Fuselage Shell Shear Representation	6-14
6-13	Comparison of Beam Deflections for Modeling With and Without Fuselage Shell Shear Representation	6-15
6-14	Summary of Beam Peak Deflection Range	6-17

## EXECUTIVE SUMMARY

The analysis of a Controlled Impact Demonstration (CID) test using program KRASH is described. In support of the CID test, several frame segments as well as a complete narrow-body airplane were impacted and responses such as underside fuselage crush, mass accelerations and/or reaction loads were obtained. KRASH model results were compared to the results obtained from supporting tests. The test data were used to refine the KRASH CID models. The revised KRASH models were used to predict the responses from the planned CID conditions impact. The predicted responses indicate that at the planned impact condition the floor peak vertical accelerations will vary from 8 to 12 g's throughout the length of the passenger floor, and that the fuselage underside crushing magnitude and distribution will be approximately the same as was noted in the supporting narrow-body full airplane impact test. Similarly, the predicted response indicates that the peak longitudinal acceleration range between 3 to 6 g's throughout the cabin floor under the same impact condition. The airframe structural integrity as depicted by the fuselage moment/shear distribution was shown to be marginal at the wing center section and satisfactory at the other locations.

Improvements were made to the KRASH coding. A KRASH85 release has been documented in report DOT/FAA/CT-85/10.

## SECTION 1

### INTRODUCTION

#### 1.1 BACKGROUND

The major domestic transport airplane manufacturers, under FAA and NASA sponsorship, reviewed jet transport accidents for the period 1959 to 1978. The results of these studies are presented in references 1, 2, and 3 and are summarized in reference 4. The data contained in these reports form the basis for developing candidate crash scenarios for FAR 25 narrow- and wide-body jet powered transport (reference 5) category airplanes. Analytical modeling of transport airplanes crash scenarios has been performed previously (reference 6). However, insufficient test data were available to validate the results of that study. To fully evaluate the appropriateness of crash scenarios for design considerations, it is necessary to predict airframe structure dynamic responses with a reasonable degree of accuracy. To achieve confidence in analytical procedures, it is necessary for predictions to compare favorably with test data. Where predictions differ from test data it is important to identify changes in modeling techniques and/or applied methodology. Program KRASH, developed under U.S. Army (reference 7) and FAA (reference 8) sponsorship, is used in this study to determine airframe response for an impact test involving a narrow-body jet transport.

#### 1.2 PROGRAM OBJECTIVE

The major objective of this effort is the development of modeling techniques for future application to a wide range of impact conditions. The overall task effort flow diagram is shown in figure 1-1. The thrust of the effort described in this report is the application of program KRASH to a Controlled Impact Demonstration (CID) test involving a narrow-body jet transport airplane. Frame segment tests, as well as a preliminary narrow-body airplane impact test, provided quantitative and qualitative data which were useful in assessing the KRASH



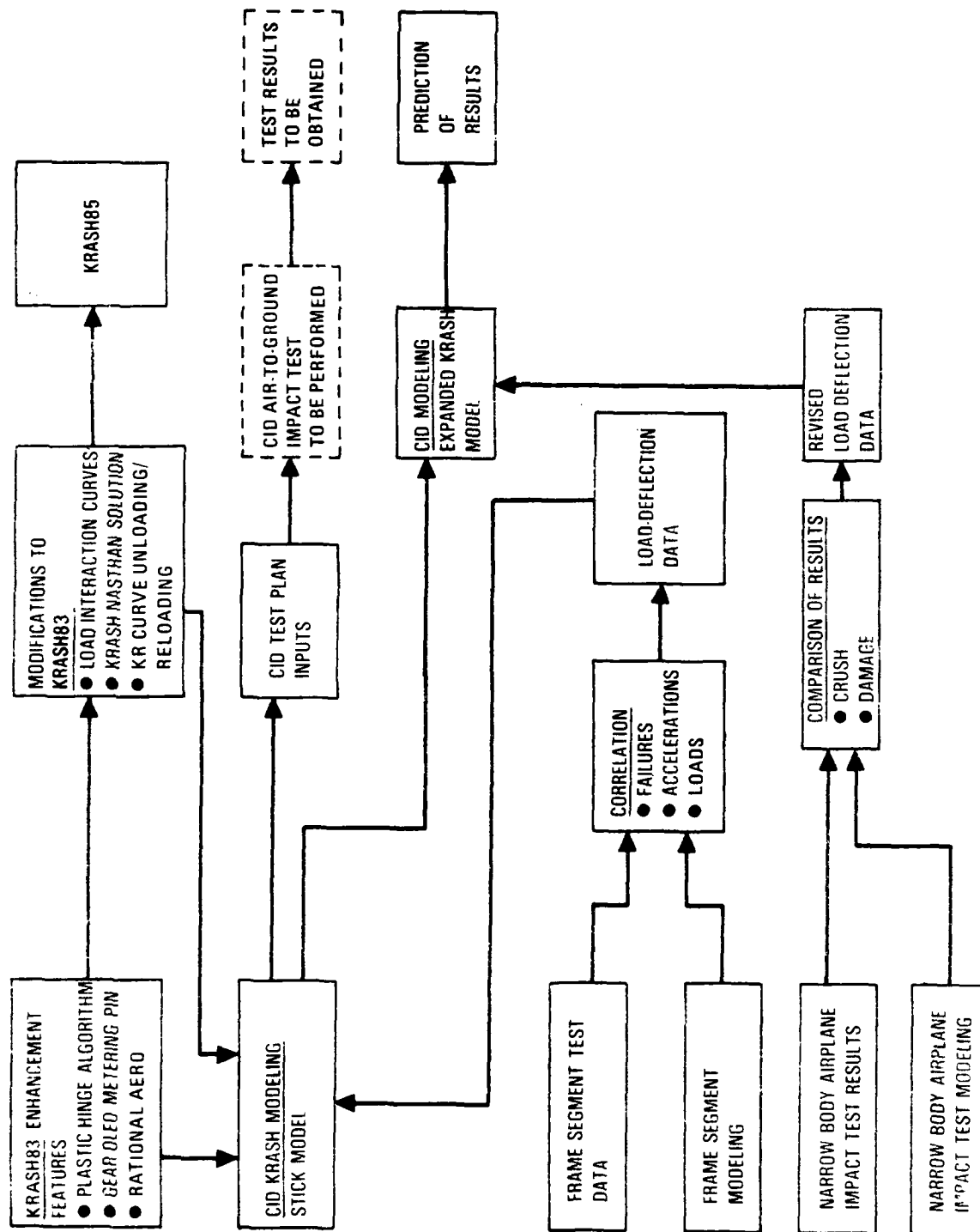


FIGURE 1-1. TASK EFFORT FLOW DIAGRAM

models and methodology. The Task effort involved the use of updated features of KRASH85 as they became available. The comparison of results and potential modifications to KRASH or the modeling techniques are to be included in a subsequent Task effort.

## SECTION 2

### KRASH ENHANCEMENTS

#### 2.1 BACKGROUND

KRASH79 was released to the public after having been validated under FAA sponsorship (reference 8) for general aviation airplane modeling application. A summary of modifications, incorporated into KRASH79, is provided in table 2-1. Subsequent to KRASH79 release, additional enhancement features were incorporated into the program. This updated version designated KRASH83 was provided to the FAA at the onset of the study described in this report. A summary of these features is provided in table 2-2. In addition, several improvements were identified to be incorporated into KRASH during the course of the current effort. These features are shown in table 2-3. The more significant improvements to create the current KRASH85 version are briefly described in the following section and in detail in reference 9.

#### 2.2 KRASH85 MODIFICATIONS

##### 2.2.1 Revised Plastic Hinge Moment

This feature corrects a deficiency in the previous KRASH79 coding involving unloading of an element when the plastic hinge option was used. The plastic hinge coding now properly models unloading and reloading, allowing the formation of hysteresis loops representing the growth of element strain energy during cyclic loading. Figure 2-1 illustrates typical hysteresis loops obtained in KRASH85 for a test case that forces cyclic bending of a plastic hinge beam. This change provides an alternative to the use of the stiffness reduction factor (KR) tables when modeling nonlinear bending. The KR table formulation was not sufficiently rigorous to guarantee that negative values for strain energy (which is not physically possible) will not occur. This capability is

TABLE 2-1. PREVIOUS MODIFICATIONS TO PROGRAM KRASH (REFERENCE 8)

- Sloped impact surface (rigid or flexible)
- Cabin volume change
- Member directional stress
- Element linear stiffness computations
- Nonlinear curve computations
- Member frequency, yield forces and loads computations
- External spring force and compression data
- Separation of crushing and friction energy
- Symmetrical airplane modeling
- Massless node representations
- More stable stiffness and damping formulation
- Flexible ground
- Unsymmetrical axial load-deflection curves, including deadband allowance
- Expanded beam end-fixity combinations
- Plastic hinge element
- Shock strut element
- Expanded force and deflection for rupture of beams
- Energy tolerance cutoffs
- Mass impulse calculations
- Low-pass filtering of acceleration data
- Beam structural damping forces
- External spring damping
- Increased program size to 150 beam elements and 180 beam nonlinear degrees of freedom
- Mass location plots
- Acceleration pulse input
- Restart
- Summaries
  - (a) beam element rupture and yield
  - (b) external spring loads and deflections
  - (c) plastic hinge occurrence
  - (d) time history plots of mass responses and impulses, beam forces, deflections, stresses, strain energy and damping energy, external spring force and deflections, occupant DRI's, and cg translational velocities.

TABLE 2-2. THE FEATURES UNIQUE TO KRASH83

- Revised plastic hinge unloading/reloading algorithm (eliminates instabilities caused by coupled bending motions with KR coding)
- Inclusion of metering pin in oleo model
- Saving of mass displacement data for post-processing
- Addition of rational aerodynamic force/moment calculations for each mass
- Provision for input of force or moment time histories for each mass
- Addition of label cards in input format
- Provision for overriding run termination due to energy growth
- Revised input and output formats to accommodate additional features
- Corrections of minor coding errors
  - Elimination of DRI mass from cg velocity calculation
  - Corrections of plot array dimension errors in PREPLOT
  - Corrections in GENMOD for acceleration input tables
  - Correction of internal beam lateral deflection print/plot output
  - Provision for user input specification for vertical beams
  - Capability to run case with NSP = 0, no external springs
  - External spring load truncation altered to avoid premature cutoff

TABLE 2-3. KRASH85 ENHANCEMENT FEATURES

Modification	
o	Expand IC subroutine to compute balanced beam loads (interfaces with NASTRAN)
o	Provide for failure criteria based on approximate combined loading
o	Recode energy balance to include effects of input forces or accelerations for specified masses
o	Correct KR unloading/reloading so that loads are limited in both directions (uncoupled X, $\phi$ directions)
o	Calculation of CG forces, accelerations, velocities and displacements time histories
o	Develop user-independent beam orientation algorithm
o	Saving of acceleration and forces for data transmittal
o	Printout and/or plot of beam forces in mass axis
o	Addition of tire vertical spring coding
o	Compute total moment and shear distribution at any station
o	Input masses in arbitrary numbering scheme

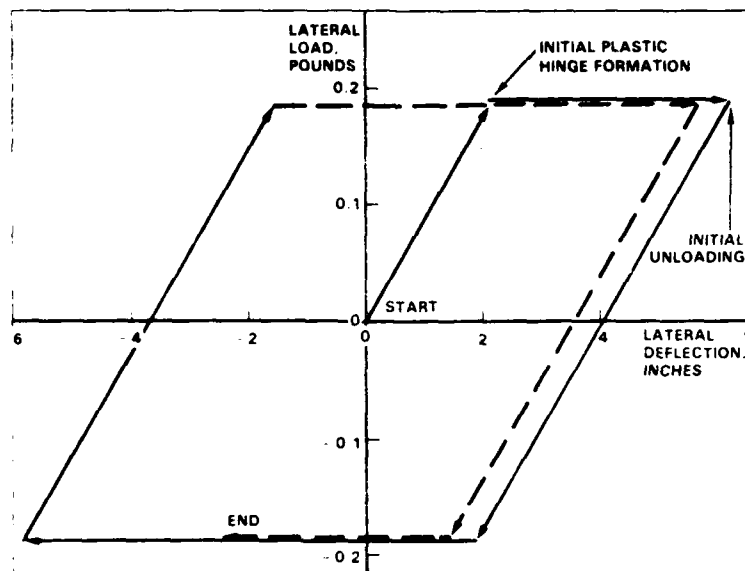


FIGURE 2-1. THE FORMATION OF HYSTERESIS LOOPS FOR LATERAL BENDING OF PLASTIC HINGE ELEMENTS FROM KRASH85

important for modeling frame segments. The program prints out a summary which provides the following information on plastic hinge moment formation:

- Beam number and end ( $i^{\text{th}}$  and/or  $j^{\text{th}}$ )
- Time of occurrence
- Direction

As in the previous coding the user still identifies beams that can form plastic hinge moments by an end fixity (pinned) designation and beam shape factor.

#### 2.2.2 Gear-Oleo Element Metering Pin

Since a metering pin is such a common feature in a transport airplane landing gear, the ability to model the varying damping characteristics is necessary to properly analyze transport airplane landing gears. This is particularly true because of the high sink rates involved in crash landings, which yield high strut closure velocities wherein the damping force is predominant. The KRASH coding has been organized so as to determine the metering pin damping versus stroke characteristics needed to match a given load-deflection curve. In effect, the program can be run in an "inverted mode," in which the user inputs a known load-deflection curve (from drop test data), and the program calculates the metering pin characteristics (damping constant versus stroke) required to achieve the input load-deflection curve. The output metering pin curve can then be used in subsequent analyses of the gear for other conditions. The feature is useful when the actual profile of the metering pin is not available, but drop test data are available. Figure 2-2 illustrates a comparison of results of test and analysis for a transport airplane main gear drop test at 12 ft/sec, using KRASH with a metering pin derived as described above. The degree of correlation evident in figure 2-2 represents an order of magnitude improvement over what was obtainable using a trial and error procedure to try to deduce the proper metering pin characteristics, without the "inverted mode" provision.

#### 2.2.3 Load-Interaction Curves

KRASH85 includes load interaction curve (LIC) data for failure prediction. Figure 2-3 shows a typical set of interaction curves for fuselage bending and

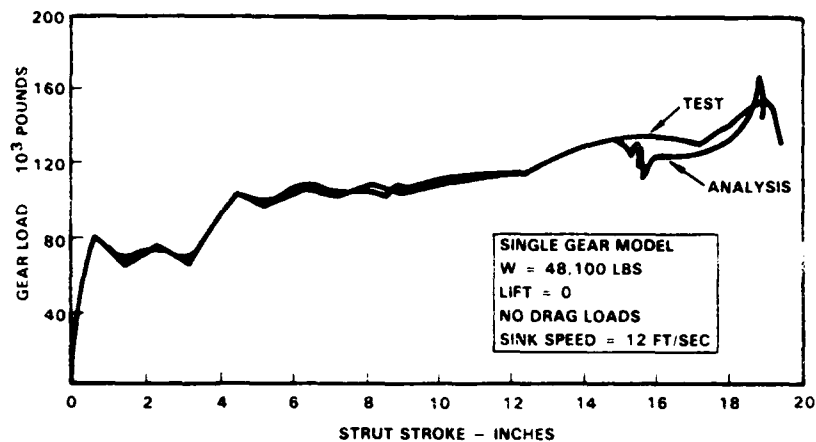


FIGURE 2-2. DUPLICATION OF KNOWN TEST-LOAD-DEFLECTION CURVE USING METERING PIN CODING IN KRASH85

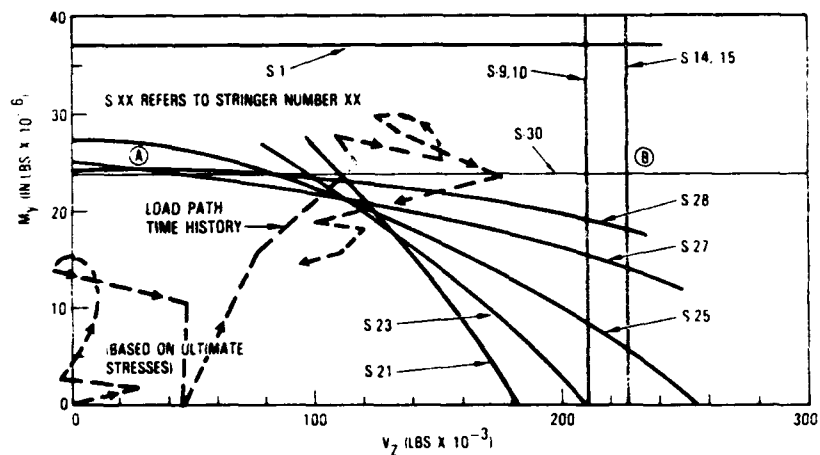


FIGURE 2-3. MAXIMUM ALLOWABLE MOMENT AND SHEAR ENVELOPE - NEGATIVE BENDING



shear at a particular airplane fuselage station. Figure 2-4 identifies the stringers at a representative frame location. The user can specify interaction curves at a maximum of 40 locations which can be anywhere. The user is not restricted to using the end points of the beam. Up to 20 straight line segments can be used to define each load-interaction curve.

At each location the program calculates the following:

- The internal beam loads, in KRASH sign convention, at the load interaction point.
- These loads are transformed to correspond to the standard structural load sign convention employed by the Lockheed-California Company (Calac).
- The Calac-convention loads are then transformed to a user-specified sign convention. One of six such sign conventions may be selected by the user. If no convention is specified, the loads are left in the Calac sign convention.
- The two interaction loads are selected from the six loads calculated.

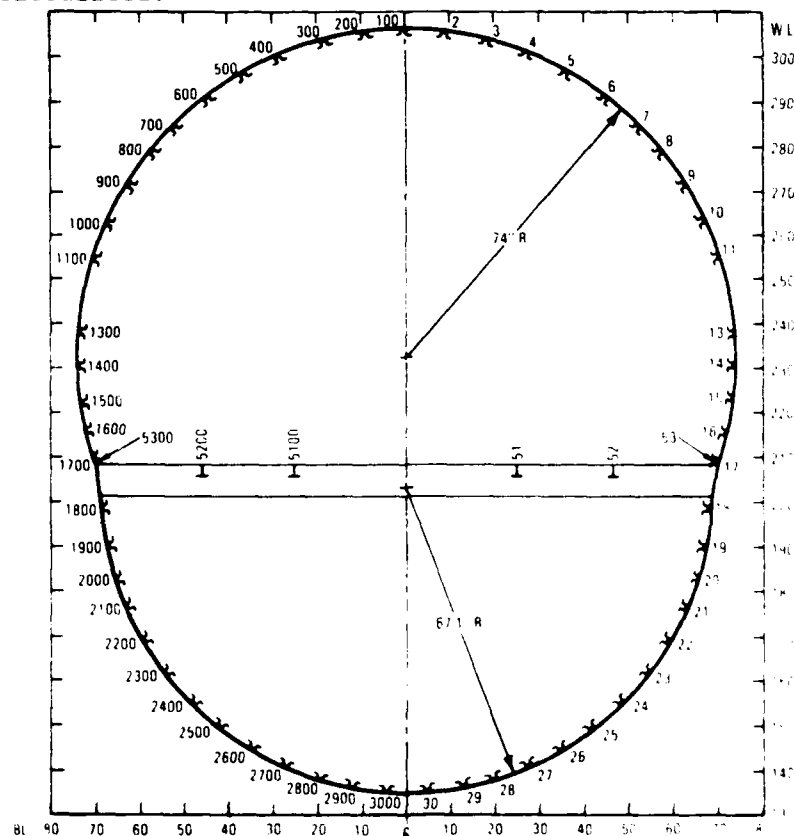


FIGURE 2-4. TYPICAL CROSS SECTION WITH STIFFENER LOCATIONS - REAR VIEW

- A load ratio for each load interaction line. A ratio greater than one indicates that a load interaction curve has been exceeded, signifying that at least one element has failed in some manner. KRASH85 is coded to allow complete rupture of a beam element if an input maximum load ratio is exceeded.

At the conclusion of the computer run the following is printed:

- Time histories of the following quantities for each load interaction curve.
  - o X Load (fuselage vertical shear in figure 2-3)
  - o Y Load (fuselage vertical bending in figure 2-3)
  - o Maximum load ratio at each time
  - o Input load interaction line number corresponding to the maximum load ratio at that time.
- A summary which shows the peak maximum load ratio for each interaction curve and the overall maximum load ratio.

The user has the option of saving the load-interaction curve time history data in an output file, which can be used for subsequent post-processing. A post-processing program has been developed (independent of KRASH85) to generate load interaction curve x-y plots. These data can be plotted to show the time-varying path of the calculated x-y loads, superimposed on the load-interaction curve (as illustrated by the dashed line in figure 2-3).

While the load interaction data output provides a great deal of useful information not previously available, considerable caution must be exercised by the user in its interpretation. A maximum load ratio greater than one does not, by itself, indicate complete failure of the corresponding fuselage section. The output data have been used in conjunction with the actual manufacturer-supplied interaction diagrams to assess the extent of damage at each location. For example, suppose that the computed combined loads were as shown by points A and B in figure 2-3. For point A stringers S27 through S30 could fail. For point B several additional stringer elements could fail (S-9 through S-15 and S-21 through S-30). Usually the input data for running KRASH is the minimum necessary to define the inner boundary in figure 2-3. The current KRASH85 coding does not define which stringers fail.

#### 2.2.4 Expanded Initial Condition (IC) Subroutine

The expanded IC subroutine allows for interfacing with NASTRAN (MSC version) to obtain a statically balanced set of loads and displacements. The overall flow diagram is shown in figure 2-5. For a complete analysis, including the determination of balanced initial conditions, steps 1, 2, and 3 are all executed. Each step involves a separate computer program, and the runs are performed sequentially. A single submittal is adequate to accomplish all 3 steps. The vehicle is properly balanced at time zero. The masses are deflected from their original positions to be compatible with the forces acting. The forces considered in the balance equations include: gravity, externally applied forces, aerodynamic lift, inertia relief loads, and mass accelerations.

#### 2.2.5 Comprehensive Energy Balance Code

The energy balance equations in KRASH79 did not account for externally applied loads; i.e., force, aerodynamic lift, mass accelerations. As a result, while the total energy could deviate substantially from 100 percent, the solution was stable. However, the growth in energy caused confusion in interpreting analysis results. The effect of all externally applied forces are now accurately accounted for. Thus, growth of total energy in excess of 1 percent would be considered suspect with regard to model validity.

#### 2.2.6 c.g. Time Histories

KRASH79 contains a summary of c.g. velocity versus time, which is plotted at the end of each run. This feature is still retained. However, KRASH85 in addition contains a summary print of the following quantities:

- Time
- External forces in x, y, z directions
- Accelerations in x, y, z directions
- Velocities in x, y, z directions
- Displacements in x, y, z directions

A cross plot of force versus deflection yields a load-deflection curve. When using KRASH85 to model a substructure; i.e., frame section, this output could be used to develop an equivalent load-deflection curve as input into a larger model.

#### 2.2.7 Arbitrary Mass Numbering

KRASH85 accepts user supplied mass point identification numbers. The modification can be thought of conceptually as a mass point number pre-processor and a mass point number post-processor. The pre-processor converts external mass point numbers to internal mass point numbers. The external mass point numbers are supplied by the user as part of the input while the internal mass point numbers are defined by the program. The internal mass numbers are consistent with the numbering system previously used in earlier versions of program KRASH. After conversion program KRASH85 is executed using the internal mass point numbers. After execution is completed the post-processor converts the internal mass point numbers to external mass point numbers for output. In the modification, two new subroutines (INPT and INPTPL) were added. In these subroutines, two arrays (MASS and IMASS) are defined which cross reference the external mass point numbers to internal mass point numbers and vice versa.

The external mass point identification numbers are input in columns 71 and 72 on Card 200 (MASS POINT DATA). The identification numbers cannot be less than zero or greater than 99. If they are, program execution will be halted. If any of the numbers are left blank or set equal to zero, the program will automatically assign sequential identification numbers to all mass points in the order of input. This option accommodates previously developed input data sets.

When the RUNMOD=2 option is used, the program automatically assigns an external mass point identification number to the image mass point generated under this option. The identification number assigned is 100 greater than the identification number of the mass point used in defining the image mass point. For example, if the input mass point identification number is 96 then the image mass point identification number will be 196.

## SECTION 3

### FUSELAGE SECTION TESTS AND ANALYSES

#### 3.1 NARROW BODY AIRPLANE FUSELAGE SECTIONS

Two narrow-body fuselage forward sections were subjected to a vertical impact. The first test was conducted at that NASA-Langley test facility. The results of the test are reported in reference 10. The Pre and post impact conditions are shown in figures 3-1 and 3-2. The 120-inch long (six-bay) specimen was subjected to a 20 ft/sec vertical velocity impact. The weight, including seats and occupant representations, is approximately 5100 pounds. A two-dimensional KRASH model was established to represent a typical frame. The post impact configuration predicted by the analytical model is shown in figure 3-3.

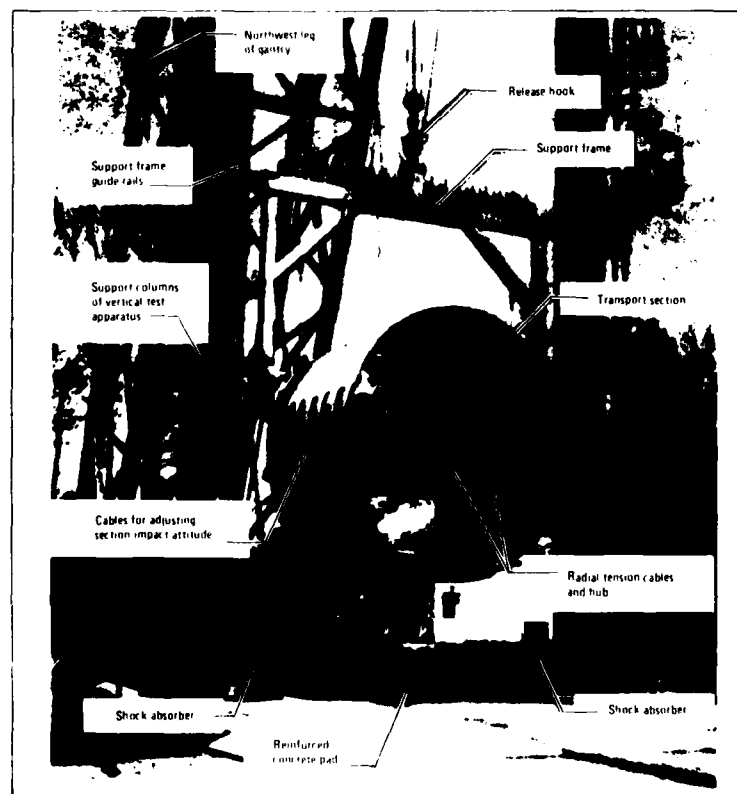


FIGURE 3-1. TRANSPORT SECTION SUSPENDED IN VERTICAL TEST APPARATUS

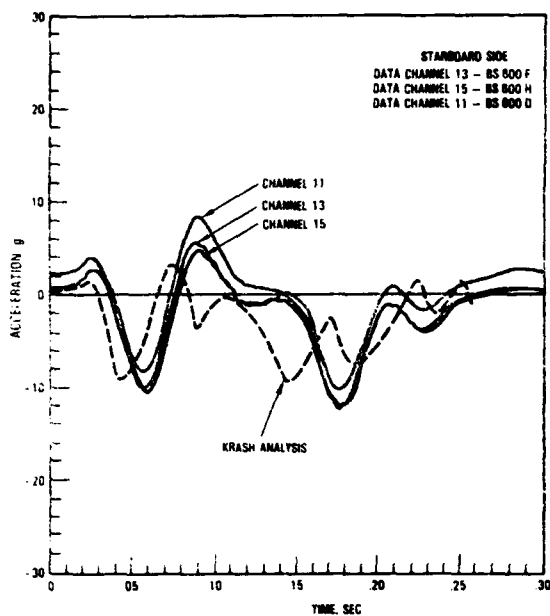


The KRASH symmetrical model, representing a typical frame, consists of 11 masses and 12 beams. An echo of the KRASH model is provided in Appendix A, Section A-1. The comparison of the analysis and test results is shown in figure 3-4 for three airframe and one occupant location. The KRASH model assumes that the mass associated with each frame is the same and that the weight on the port (left) side is also equal to weight on the starboard (right) side. The actual weight distribution between port and starboard sides for the test article was closer to 60/40. The frame designations for the test specimen are 600, 600D, 600E, 600F, 600G, 600H and 600J, each of which are 20 inches apart.

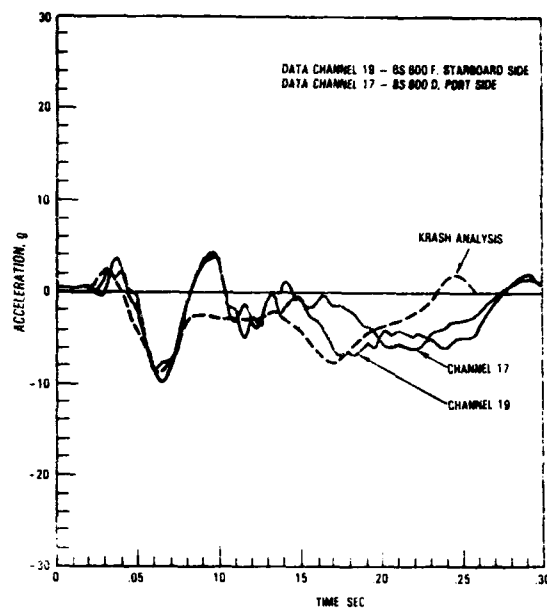
Figure 3-4 shows that for measurement locations several frames apart (40 to 80 inches), the responses do not differ substantially. The same is true when comparing starboard and portside responses (floor beam/inboard seat rail). Even the lighter mass roof peak responses, located 40 inches apart, are within 20 percent and 10 milliseconds of their acceleration and time of occurrence, respectively.

The analysis results, at all comparative locations, approximate the measured response peaks generally within 20 percent in amplitude and within 20 milliseconds with respect to the occurrence of the peak response. Thus, the representation of a single frame, while not exact at every location, approximates the segment response. This indicates that, while failure modes can vary along the length and width of the structure, a simplified representation can satisfactorily predict the responses "on the average". More detailed modeling would not necessarily predict the response more accurately or reliably and most likely would require significantly more time and computer cost. The analogy of predicting failures "on the average" for this model, is similar to the conclusions obtained in a previous study (reference 11) in which crush behavior of fuselage under-floor segments were determined, using simplified approximate procedures.

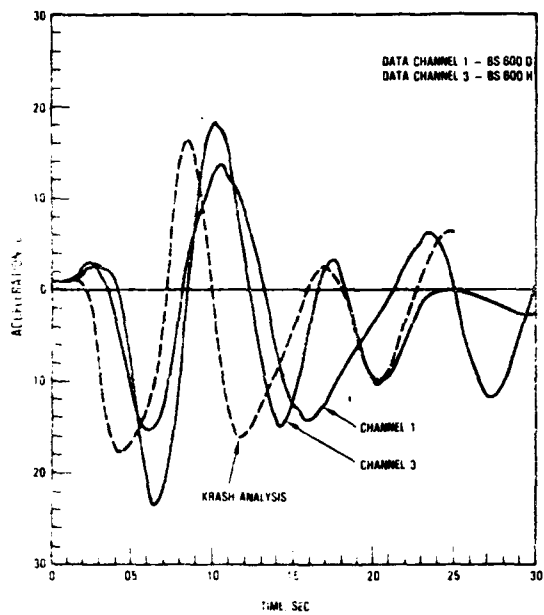
As noted earlier, program KRASH was modified to compute c.g. forces, accelerations, velocities, and displacements versus time. With this algorithm a load-versus-time deflection curve characteristic of the overall structure behavior was obtained directly from the analysis results. Since the test setup did not include load cells from which reaction loads could be measured directly, no comparison can be made for this parameter. A three-dimensional plot of the analysis generated load, deflection and time parameters is shown in figure 3-5.



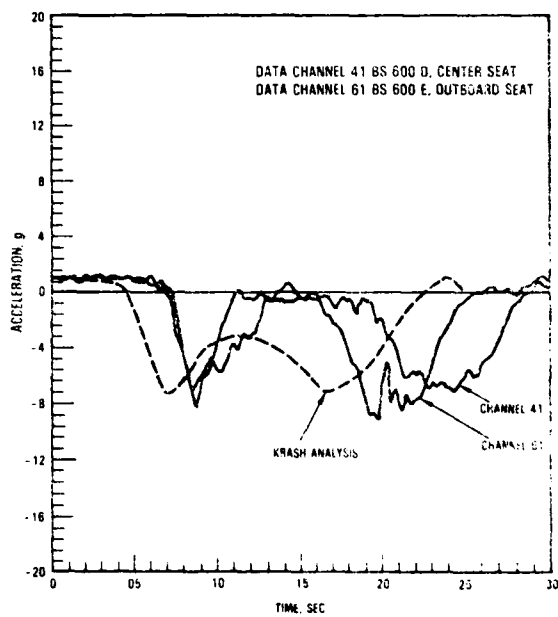
(a) Frame Floor Beam,  
Starboard Side



(b) Floor Beam/Inboard  
Seat Rail



(c) Roof



(d) Pelvis

FIGURE 3-4. KRASH FRAME ANALYSIS VERSUS TEST RESULTS



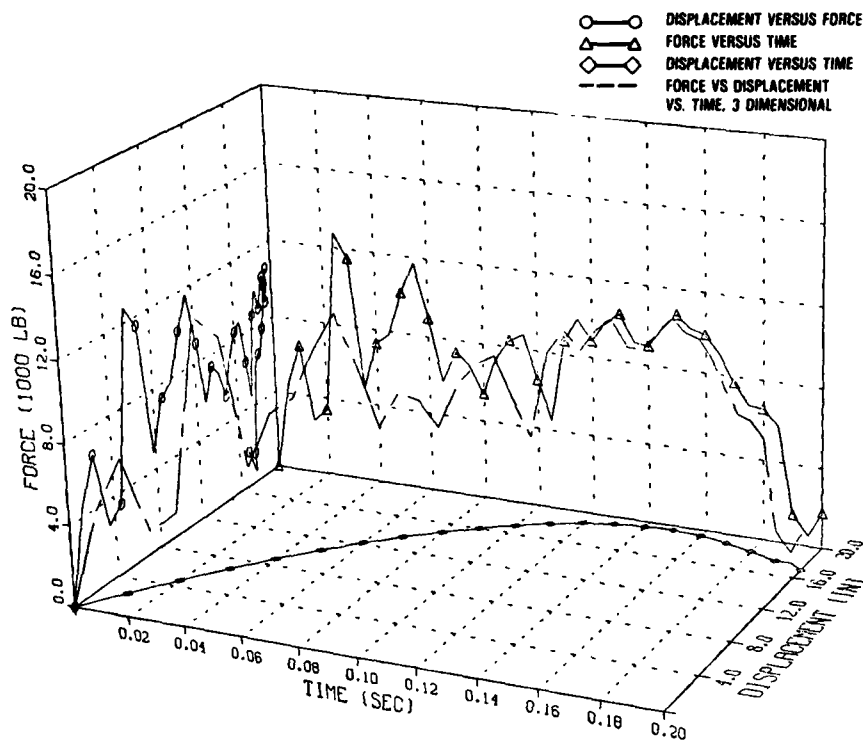


FIGURE 3-5. B707 FRAME (NO CARGO) LOAD-DEFLECTION TIME HISTORY

For inputs into a larger KRASH airframe model the load deflection curve is approximated by the dashed line in figure 3-6. The energy, as computed by the area under the load-deflection curve, agrees with the amount of energy to be dissipated based on the mass, velocity and crush distance involved. The approximately 20 inches of crush obtained in the analysis is consistent with the measured results.

The second test of a B707 fuselage section (reference 12) was performed at the FAA Technical Center test facility in Pomona, N.J. The 120 inch long instrumented, forward fuselage section was impacted at a velocity of 20 ft/sec. The section was representative of stations 460 through 580. The NASA section was representative of stations 600 through 600J. The total weight for the FAA 6 bay segment was 6440 pounds, of which 1860 pounds was cargo luggage. The post test configuration for the FAA test is shown in figure 3-7. Of interest in the FAA test, was the presence of luggage on the cargo floor which minimized the extent to which a cusp was formed at the extreme lower centerline. The KRASH representation for

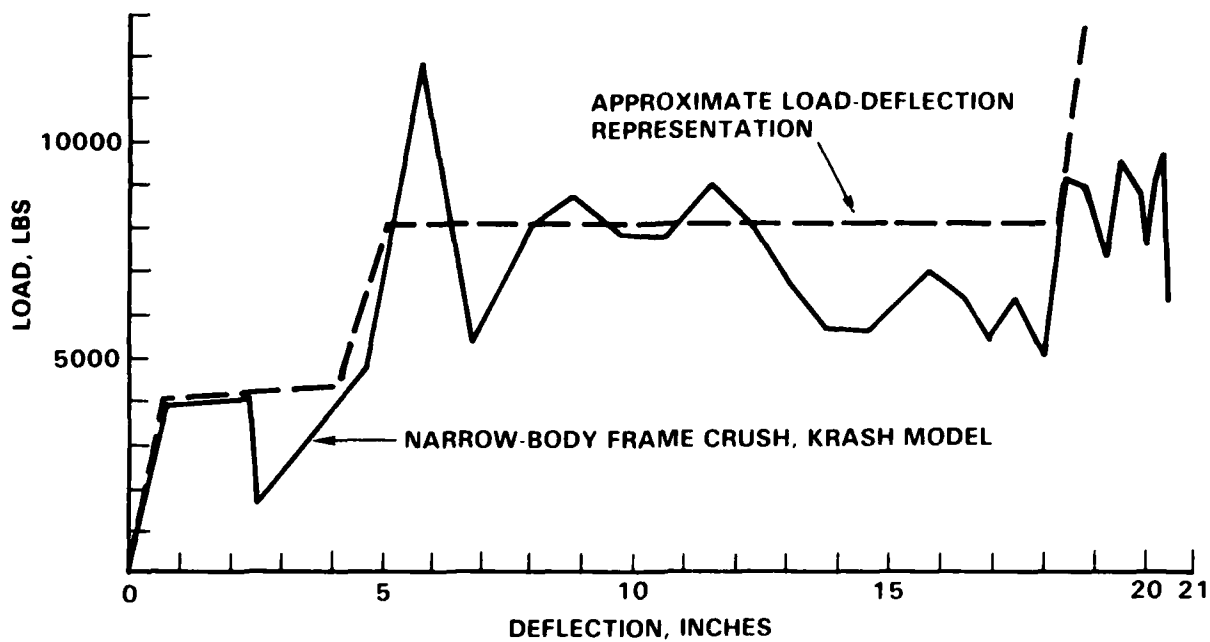


FIGURE 3-6. FRAME LOAD-DEFLECTION OBTAINED BY KRASH ANALYSIS

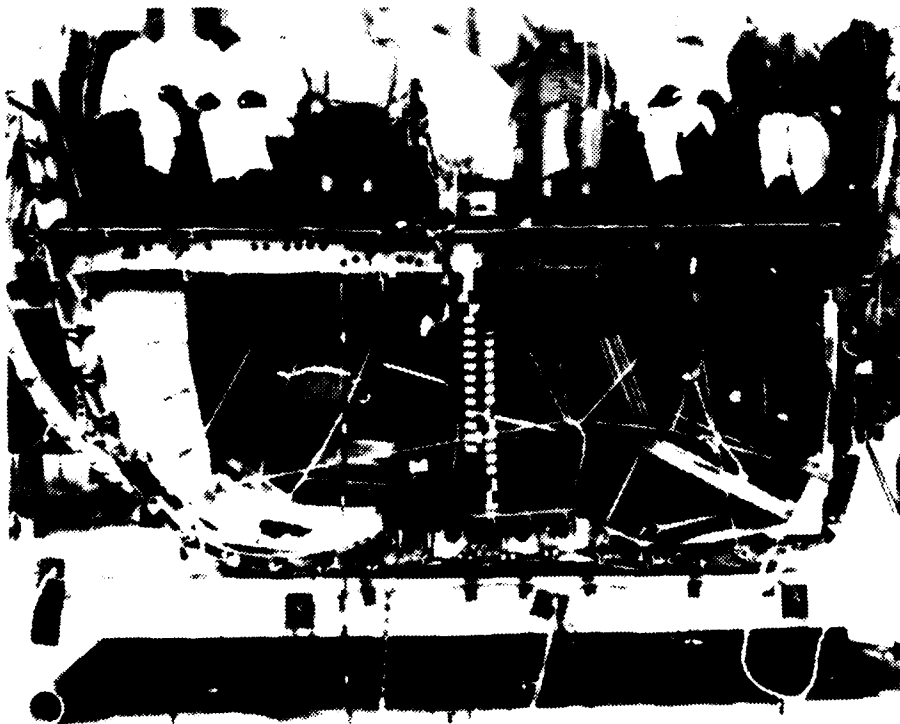


FIGURE 3-7. POST-TEST VIEW OF TRANSPORT AIRPLANE SECTION WITH CARGO

this test is the same model as shown in figure 3-3, except for added mass representing the luggage at locations 1 and 7.

The results of the KRASH analysis are compared to FAA test data in figures 3-8 through 3-11. Figure 3-8 shows the c.g. displacement versus time for analysis and test. The test data are obtained via double integration of midcenter vertical acceleration data. The peak displacements occur very close in time and differ by approximately 1.5 inches or less than 10 percent.

Figure 3-9 compares load cell force versus vertical displacement for analysis and test. The force from the analysis is based on scaling up the weight of the frame model to that of the total weight of the test article. Figure 3-10 shows the force versus time comparisons. The comparisons in figures 3-9 and 3-10 show good agreement with peak values, as well as with the time of occurrence. Figure 3-11 compares passenger floor vertical accelerations for test and analysis. The test data are from the midspan of the floor and were filtered at 60 Hz. The location for the analysis acceleration is at the inboard seat-floor attachment BL24.8 and was filtered at 50 Hz. The primary peak acceleration is within 10 percent in magnitude but occurs later in the analysis than shown in the test. The second deceleration peaks are in phase and approximately 20 percent apart in peak value. Both the test and analysis show a third peak deceleration value at 0.150 msec. The analysis peak deceleration for the third peak is -9g as compared to -4g for the test. Thereafter both analysis and test show a substantial decrease in response.

### 3.2 WIDEBODY AIRPLANE FUSELAGE SECTION TEST

A wide-body aft fuselage section was subjected to an impact having a 20 ft/sec vertical velocity in the same manner as were the narrow-body fuselage sections noted earlier. The weight, including one partial row of occupants, was approximately 5000 pounds. The pre- and post-impact configurations are shown in figure 3-12. The major damage was failure of the vertical supports for the cargo floor structure.

The frame model developed for use in program KRASH is illustrated in figure 3-13. It is a symmetric, half frame representation of a single bay of the DC-10 fuselage section used in the drop test. The model consists of fourteen

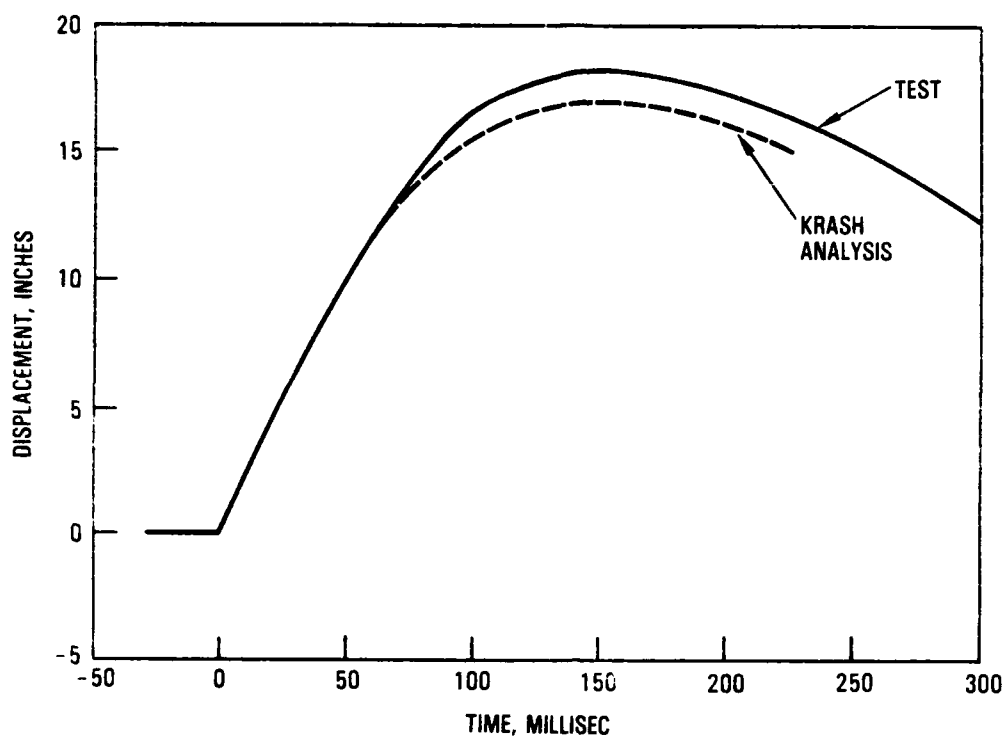


FIGURE 3-8. COMPARISON OF FAA TEST AND KRASH ANALYSIS, VERTICAL DISPLACEMENT VERSUS TIME

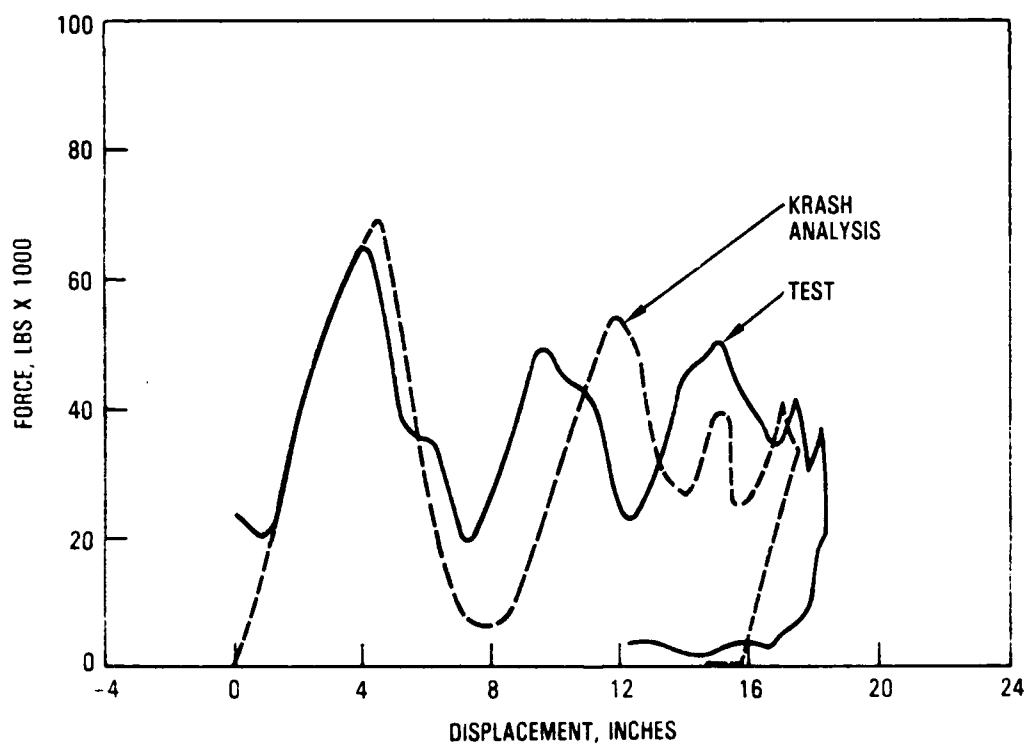


FIGURE 3-9. COMPARISON OF FAA TEST AND KRASH ANALYSIS, FORCE VERSUS DISPLACEMENT

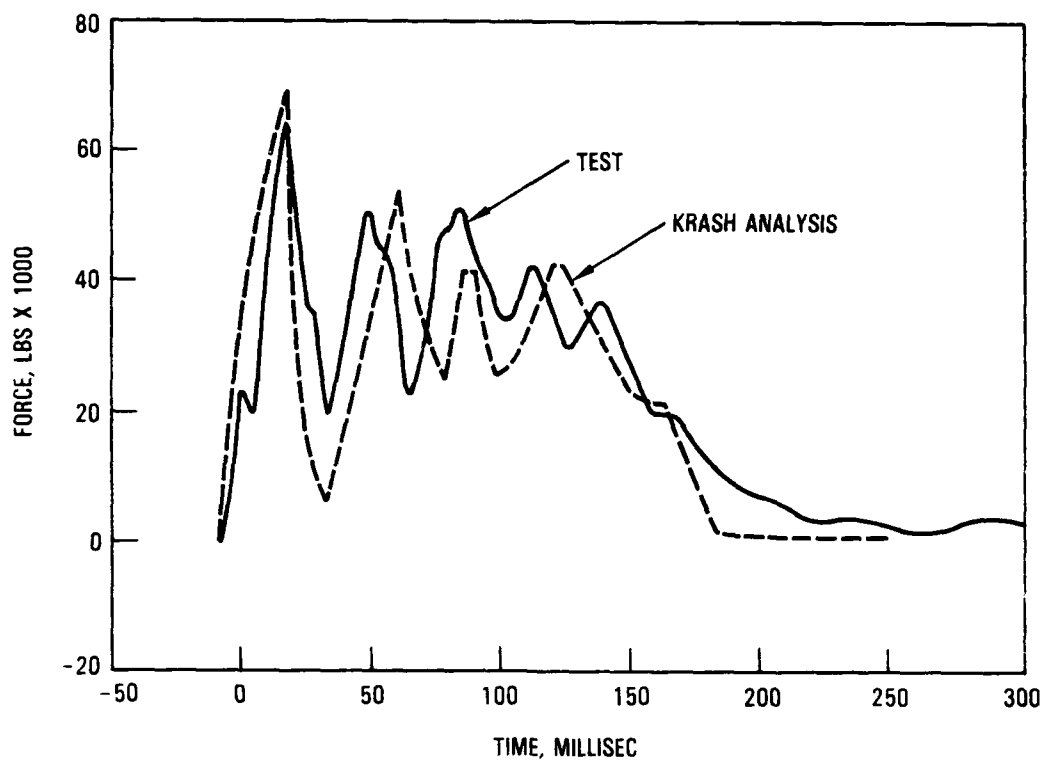


FIGURE 3-10. COMPARISON OF FAA TEST AND KRASH ANALYSIS, FORCE VERSUS TIME

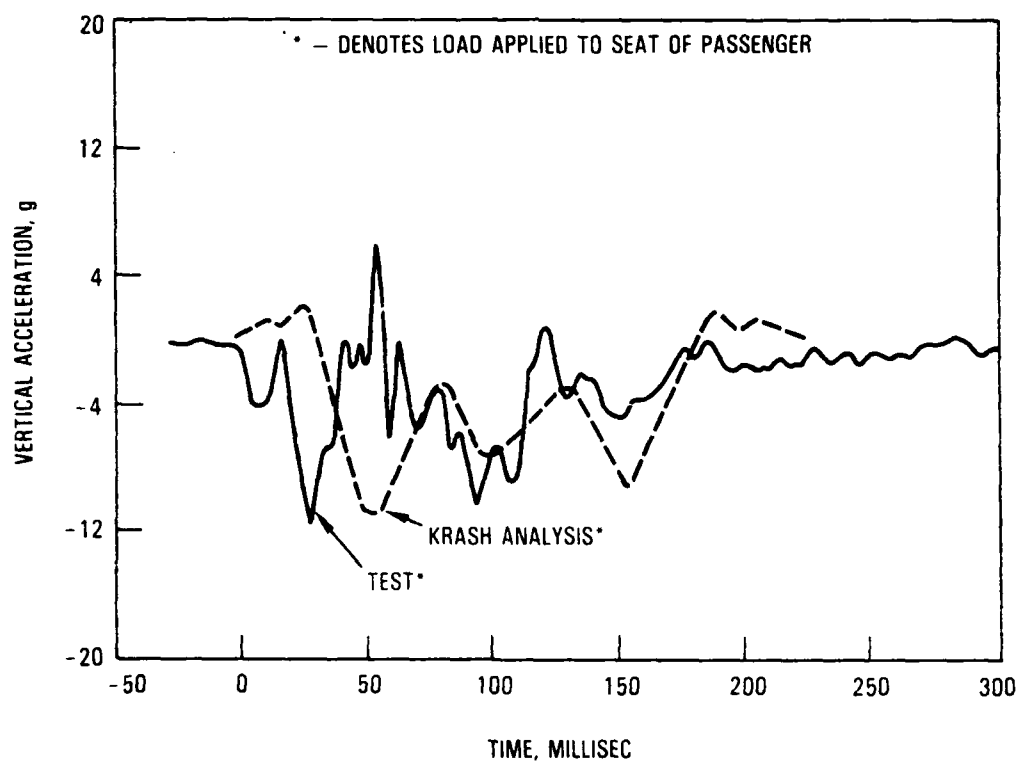
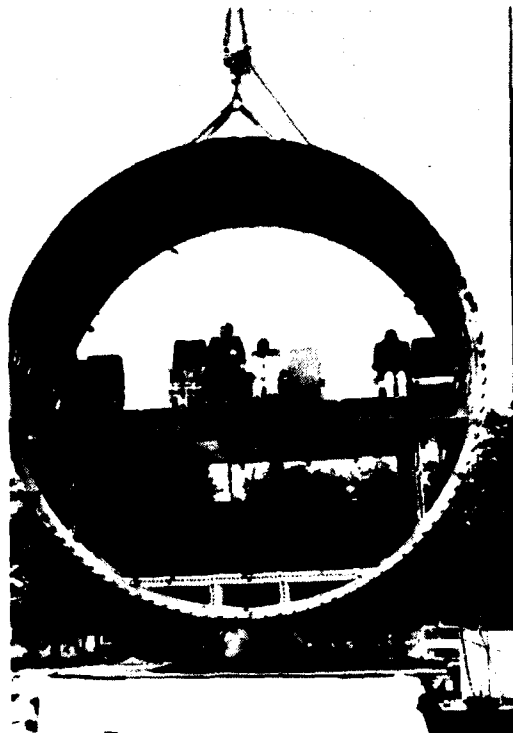
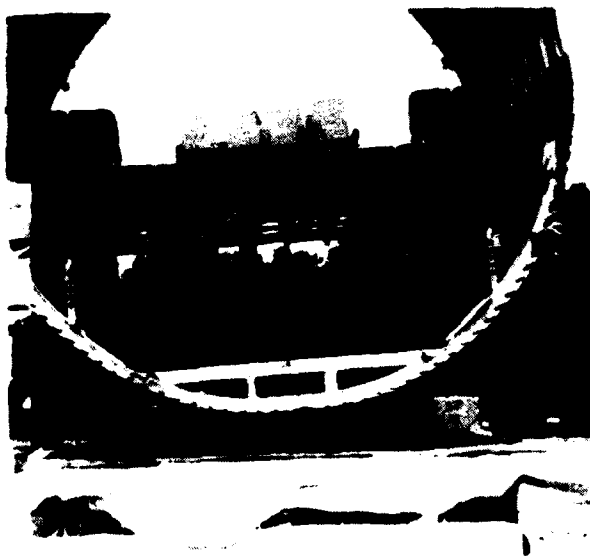


FIGURE 3-11. COMPARISON OF FAA TEST AND KRASH ANALYSIS, PASSENGER FLOOR VERTICAL ACCELERATION



(a) Pre-test



Overview



Close-Up of Cargo  
Floor Vertical Supports

(b) Post-test

FIGURE 3-12. DC-10 FUSELAGE SECTION TEST

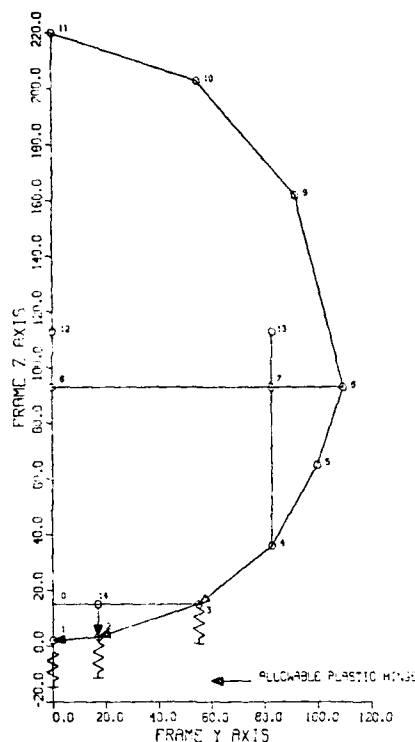


FIGURE 3-13. DC-10 FRAME MODEL

mass elements interconnected by sixteen beams elements. Three crushing springs are provided to transfer the impact load to the frame model. The frame model represents a portion of the test section with a weight of 1235.0 pounds. An echo of the KRASH frame model is shown in the Appendix, Section A-2.

Plastic hinges are allowed in the cargo floor region as noted by the arrows in figure 3-13. Plastic hinge moments are allowed about both beam y and beam x axes except for the cargo floor post (beam 2-14) for which a plastic hinge moment is allowed about the beam z axis only. Rupture produced by a moment about the beam y axis, equivalent to the allowable plastic hinge moment, is also allowed at the mass 2 end of the cargo floor post.

The frame model was used to simulate a flat (zero pitch) impact having a 20 ft/sec drop velocity. The resulting load deflection time history of the frame c.g. is shown in figure 3-14. The analysis results indicate that during the drop a maximum displacement of 6.3 inches is reached approximately 0.045 seconds after impact. A maximum load of approximately 37,000 pounds

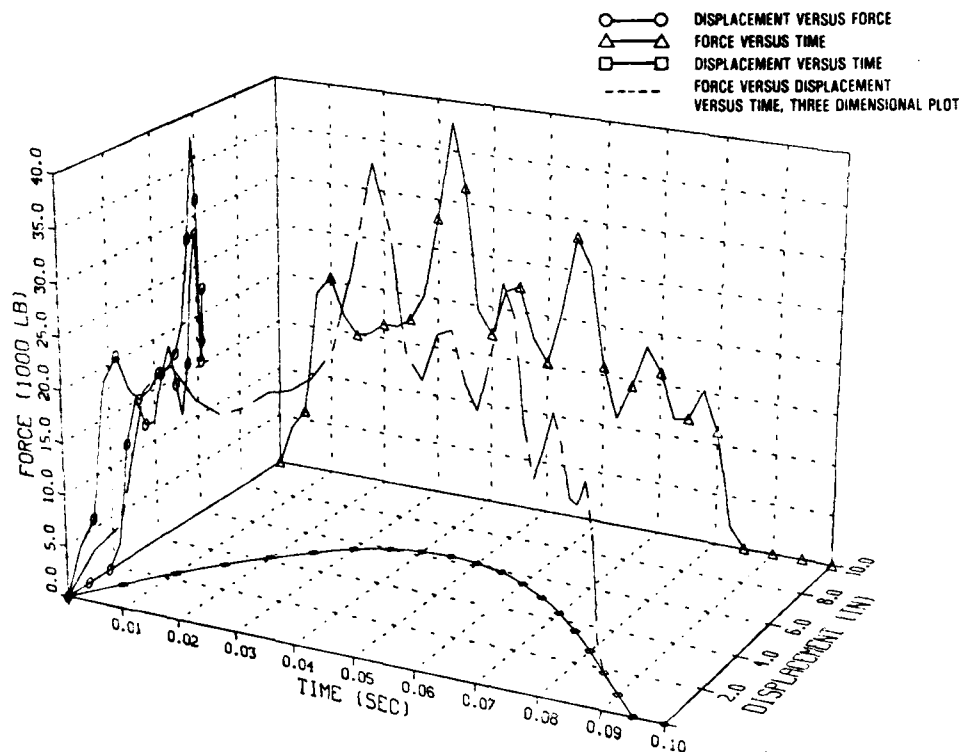


FIGURE 3-14. DC-10 FRAME LOAD-DEFLECTION TIME HISTORY

occurs approximately 0.0125 second prior to the occurrence of the peak displacement. After reaching maximum displacement, the frame rebounds and leaves the ground at approximately 0.085 second after impact.

During impact an exchange of energy takes place as shown in figure 3-15. At impact the total energy is divided between gravitational potential energy\* and kinetic energy. At the time of maximum c.g. displacement all of the kinetic energy and a small percentage of the potential energy has been converted into strain energy and crushing energy. The strain energy is associated with the deflection of the beam elements and the crushing energy is associated with the deflection of the crushing springs. Note that at the time the frame leaves the ground (time = 0.085 sec) the potential energy has been restored to its original value while part of the kinetic energy has been permanently transformed into strain and crushing energy. This permanent transfer results in

\*The potential energy is based on a selected reference plane.



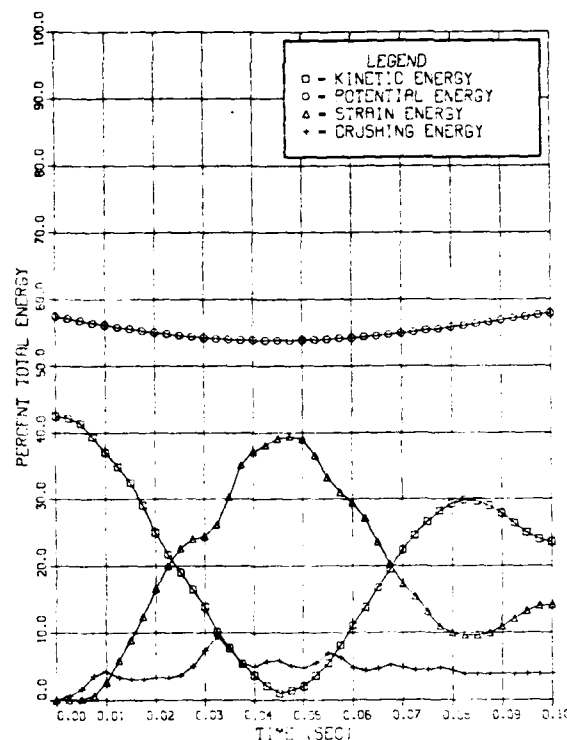


FIGURE 3-15. ENERGY DISTRIBUTION - PERCENT OF TOTAL

the plastic deformation of some of the beam elements and permanent set of the crushing springs. The resultant "permanent set" of the c.g. is approximately 1.8 to 2.0 inches.

In the time period following ground contact the structure below the cargo floor deforms. A plastic hinge is formed about the frame x axis at the attachment of the cargo floor post (beam 2-14) and the frame beam element. In addition, plastic hinges are formed at masses 1 and 3. The frame's y and z axes are defined in figure 3-13. The frame x axis is normal to the plane containing the y and z axes.

Passenger vertical acceleration time histories (masses 12 and 13) are shown in figure 3-16. Maximum vertical accelerations of approximately 33 g's and 51 g's, respectively, are experienced by the two masses. The base duration associated with the peak accelerations at the floor are < 50 milliseconds.

Data available from the test consisted of personal observations, photos, and a video tape record of the test. The analysis was performed prior to the

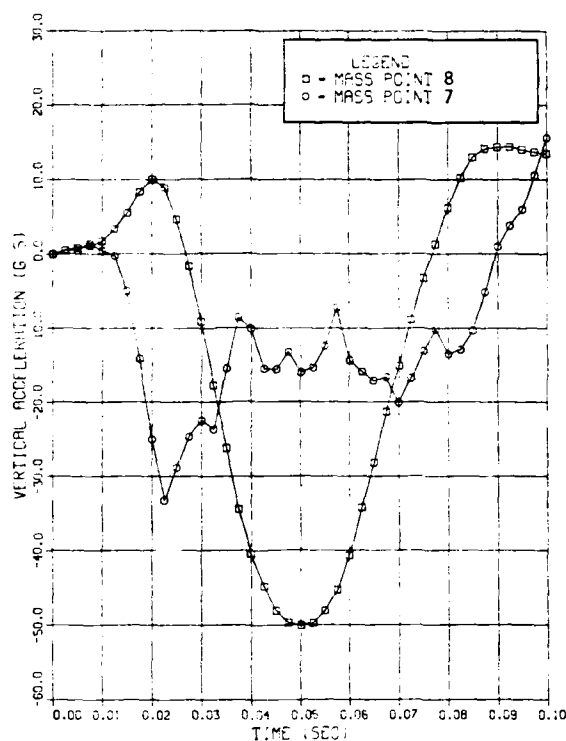


FIGURE 3-16. PASSENGER CABIN FLOOR ACCELERATION TIME HISTORY

availability of acceleration response data. A post-test inspection indicated that there was apparent damage to the regular aircraft seats. An onboard experimental seat suffered a slightly bent frame. The weight of the section is considered to be relatively light, which most likely accounts for the slight damage (all of which occurs below the cargo floor) and the high floor accelerations. Comparison of the predicted response of local structure in the region of the cargo floor with the observed post-test results reveals the following:

Predicted Results

Cargo floor post plastic hinge formed about the frame x axis - probable rivet failure.

No plastic hinge formation of cargo floor post about the frame y axis.

Observed Results

No apparent frame x axis plastic hinge formed in cargo floor post - no rivet failure.

Cargo floor post plastic hinge formed about frame y axis - rupture of posts at attachment to frame.

### Predicted Results

Plastic hinge formed in lower frame at center line of frame model.

No plastic hinge allowed in the passenger cabin floor beam.

Maximum c.g. deflection occurs at 0.045 second after impact.

### Observed Results

Plastic hinge formed in lower frame at center line of frame model.

Plastic hinge appears to form in the passenger cabin floor beam near the frame center line (mass point 8 in figure 3-13).

Maximum crushing of structure in cargo floor region occurs approximately 0.05-0.06 second after impact.

After review of the photos and video tape, the frame model was modified as follows:

- Cargo floor post beam connecting mass 2 to mass 14. Massless nodes were introduced to simulate the offset of neutral axes at the attachment of the cargo floor post to the frame and to the cargo floor beam.

The frame x axis plastic hinge was removed. Rupture is allowed at a moment equivalent to the frame y axis plastic hinge moment.

- Passenger cabin floor beam connecting mass 7 to mass 8. A plastic hinge is allowed at the attachment of the beam to mass 8.

The revised model is shown in figure 3-17.

Using the revised model two cases were run. Each of the runs simulated a drop velocity of 20 ft/sec. One of the runs was at a zero pitch angle while the second is at a 2 degree nose down pitch angle. With the new model, failure of the cargo floor post due to bending about the frame y axis was duplicated during the 2 degree pitch case but not during the zero pitch case. Thus this failure mode appears to be sensitive to the pitch angle of the frame at the time of impact. The large moments about the frame x axis observed in the earlier run are still prevalent in both runs using the revised model.

Results of the two runs using the revised frame model show that the maximum vertical acceleration response levels of the passenger cabin floor (masses 7 and 8) are sensitive to the degree of plastic hinge formation in the cabin floor beam. The acceleration levels for masses 7 and 8 are shown in figure 3-18 for the 2 degree pitch case. The maximum acceleration levels are 34 g's and 33 g's for masses 7 and 8, respectively. For the zero degree impact case the maximum acceleration levels are 36 g's and 33 g's, respectively.

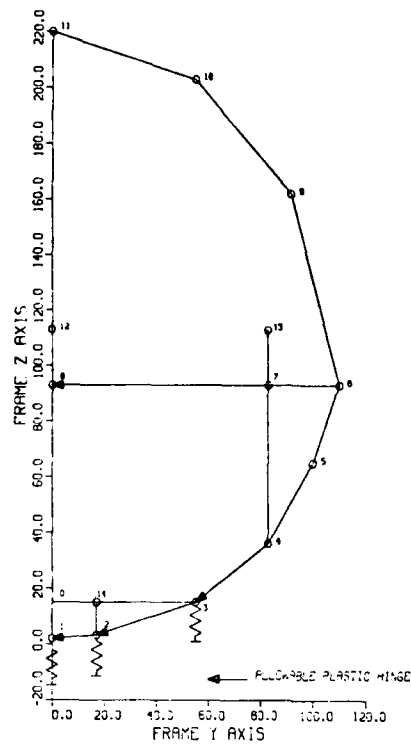


FIGURE 3-17. DC-10 FRAME MODEL (REVISED)

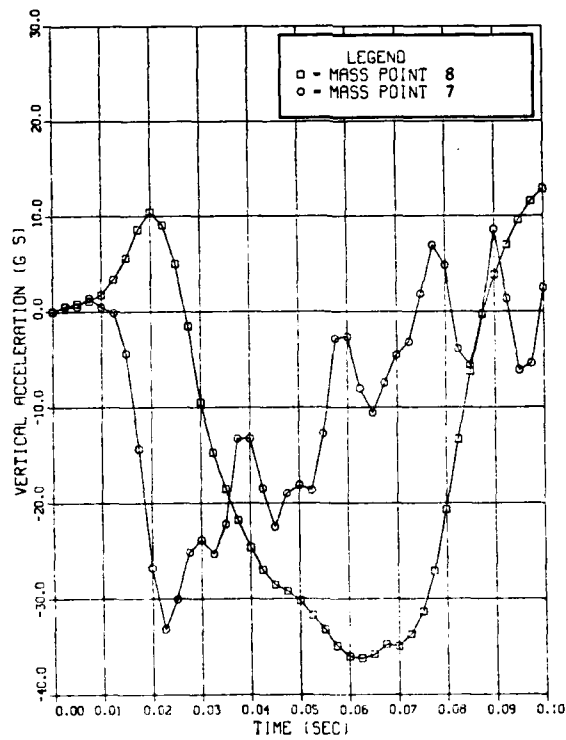


FIGURE 3-18. PASSENGER CABIN FLOOR ACCELERATION TIME HISTORY (REVISED MODEL)

The c.g. loads and displacements predicted during the zero pitch and 2 degree pitch cases using the revised model were not significantly different than those obtained using the original frame model. The maximum c.g. loads and deflections are 39,000 pounds, 6.2 inches and 38,000 pounds, 6.4 inches for the zero pitch and 2 degree pitch cases, respectively.

Subsequent to revising the frame model, test acceleration response data were reported in reference 13. Figure 3-19 shows a comparison between the analysis and test results at two passenger cabin floor locations. In both instances the peak levels are in good agreement. However, the time of occurrence of the peak response or the duration differs between the test and analysis results. The assumption of a plastic hinge at the floor centerline for the analytical model could tend to result in a more plastic (longer duration) response than is observed in the test data.

The discussion to this point has been confined to frame segment tests and analyses. Frame sections are considered soft compared to stiff bulkheads, and as such the passenger cabin floor responses tend to be muted. The DC-10 section responses are high in magnitude compared to the B707 frame sections due to 1) low test mass loading and 2) the type of construction (i.e., floor posts which provide an alternate load path). Hard points, such as those located at major bulkheads, are more likely to transmit high magnitude, short duration pulses to the passenger cabin floor. A test of a B707 fuselage center section is reported in reference 14. The post-test results including floor time history responses are shown in figure 3-20. The test specimen which weighed approximately 8000 lbs., including anthropomorphic dummies, exhibited little deformation and floor vertical peak responses between 60g to 90g, with a pulse base duration of around 20 milliseconds. A section more fully loaded and with wing mass might exhibit more crushing and lower broader response levels.

The occupant vertical responses for a location in proximity to the floor responses (figure 3-20) is shown in figure 3-21. From the curves in figure 3-21 it can be observed that the pelvic peak vertical response is around 36g to 44g for a nearly triangular pulse with a base duration of 40 milliseconds. Thus the dummy response is lower and broader than that exhibited at

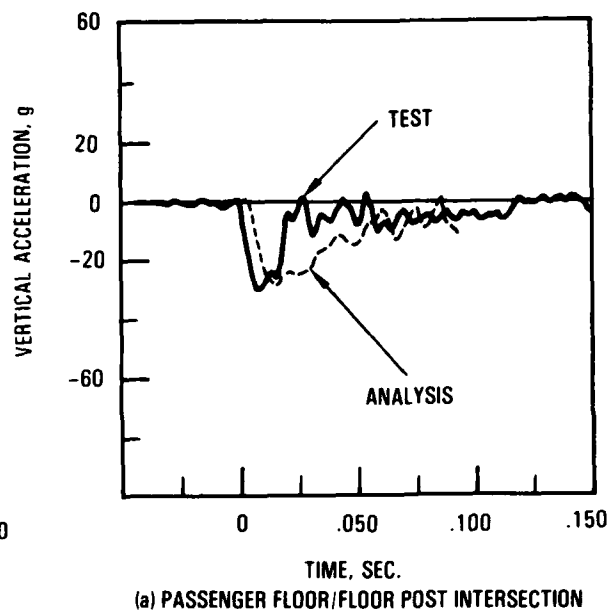
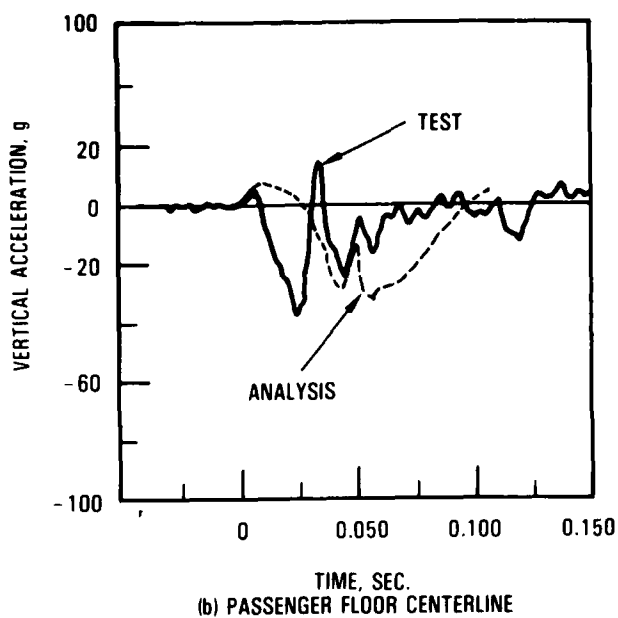


FIGURE 3-19. COMPARISON OF WIDEBODY FRAME SECTION ANALYSIS AND TESTS RESULTS

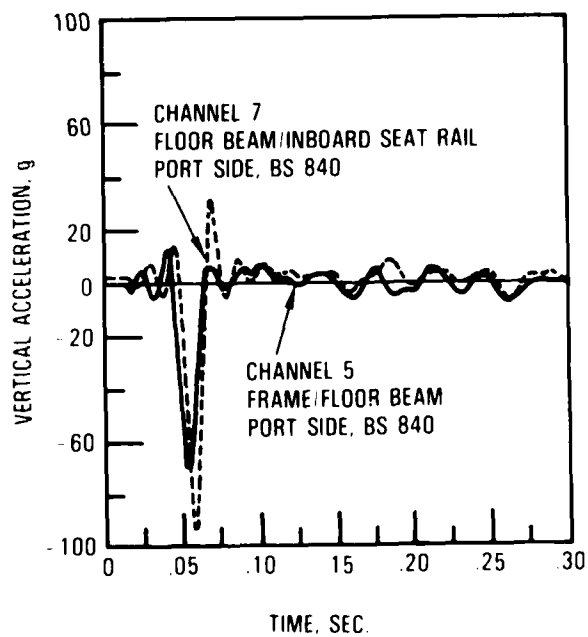
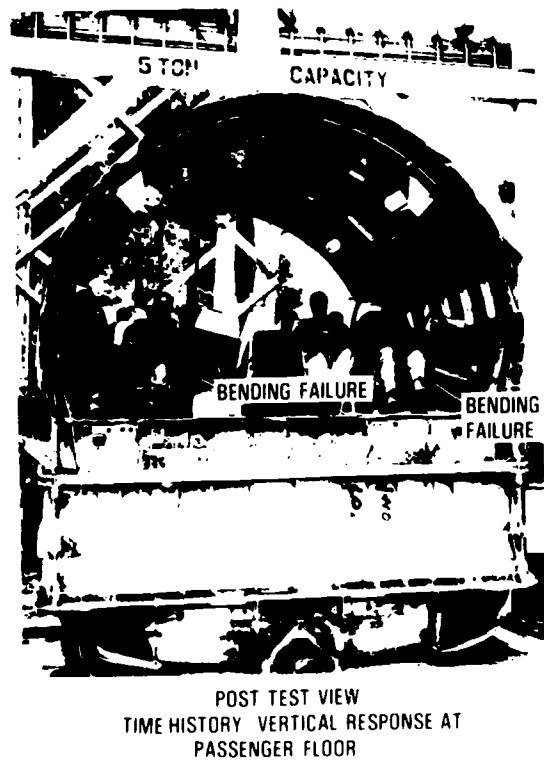


FIGURE 3-20. RESULTS OF NARROW-BODY AIRPLANE FUESLAGE CENTER SECTION TEST

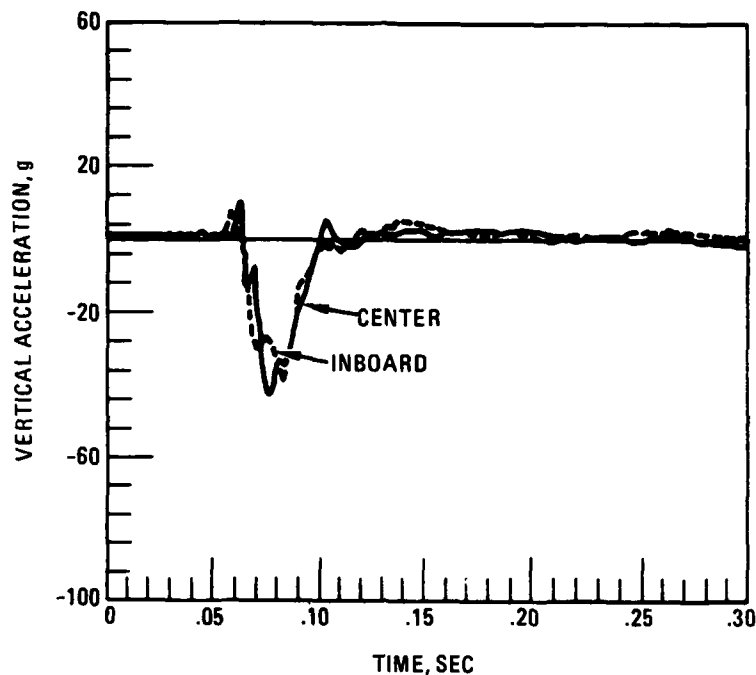


FIGURE 3-21. ACCELERATION TIME HISTORIES MEASURED IN ANTHROPOMORPHIC DUMMIES LOCATED IN FUSELAGE CENTER SECTION

the floor. By contrast a corresponding dummy response for the B707 drop test is closer to 8g peak, 100 millisecond base duration and between triangular and trapezoidal in shape (figure 3-4). To what degree the occupant could be exposed to a serious injury due to vertical loading depends on how injury criteria are specified and measured. For combined loading (vertical-longitudinal or longitudinal-lateral) the criteria can get more difficult to define.

## SECTION 4

### PRELIMINARY KRASH ANALYSIS

#### 4.1 GEARS-RETRACTED ANALYSIS

The flow diagram, shown in figure 4-1, outlines the procedure being followed to assess the effect of sink speed on airframe structural integrity using the available structural data and state-of-the-art analysis. A KRASH stick model was established to facilitate providing inputs into the Controlled Impact Demonstration (CID) test plan with regard to a desirable test impact condition. The stick model is shown in figure 4-2. The model consists of 27 masses and 26 beam elements. For the analysis a symmetrical half-airplane model consisting of 19 masses and 18 beam elements is used. The beam stiffness and mass properties are derived from manufacturer provided data. The model accounts for lower fuselage crushing and major bulkhead loads through the use of external (ground contact) springs along the fuselage. The frame crushing characteristics are developed from separate KRASH model analyses of narrow-body fuselage section tests, as described in Section 3. Bulkhead load-deflection characteristics are obtained from results of a narrow-body bulkhead segment test and previous wide-body airplane analyses (reference 7). The fuselage mass point locations and designations are identified in table 4-1. The difference between the KRASH model fuselage station and airplane body station designations is due to three extra frames in the forebody between station 600 and 620 and two less frames in the aftbody between station 960 and 1020. The fuselage frame and bulkhead load-deflection curves used with the stick model are shown in figures 4-3 and 4-4, respectively. The load range investigated is between the solid and dashed lines. The objective of this initial effort is to obtain overall fuselage shears, moments and accelerations. Preliminary estimates of fuselage shear and moment capability were obtained from manufacturer provided data. The data are in the form of moment versus shear at several locations. A typical moment-shear interaction curve was shown earlier in figure 2-3. For each interaction curve the stringers, whose locations are shown in figure 2-4, can be identified.



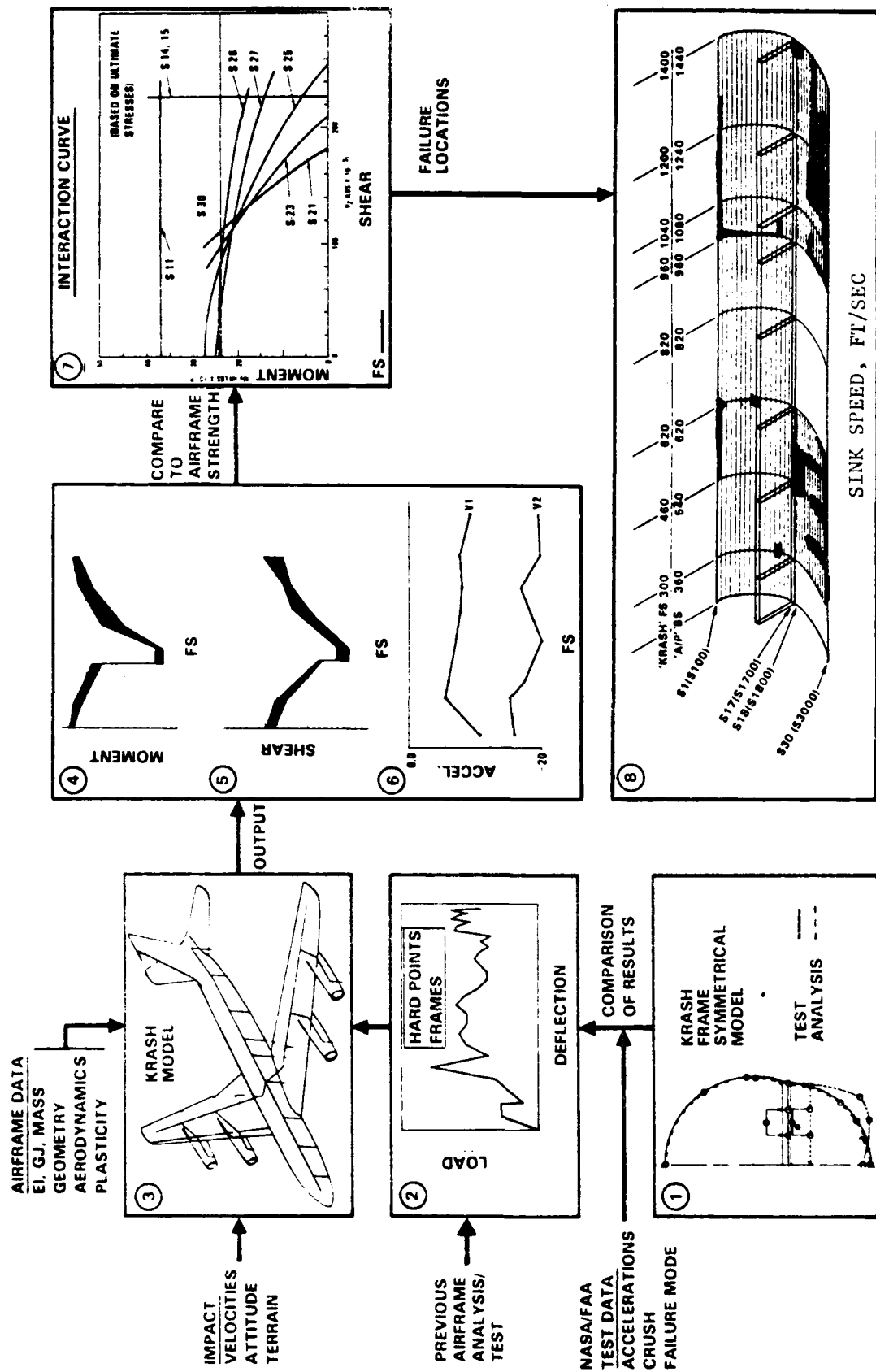


FIGURE 4-1. OUTLINE OF ANALYTICAL APPROACH:

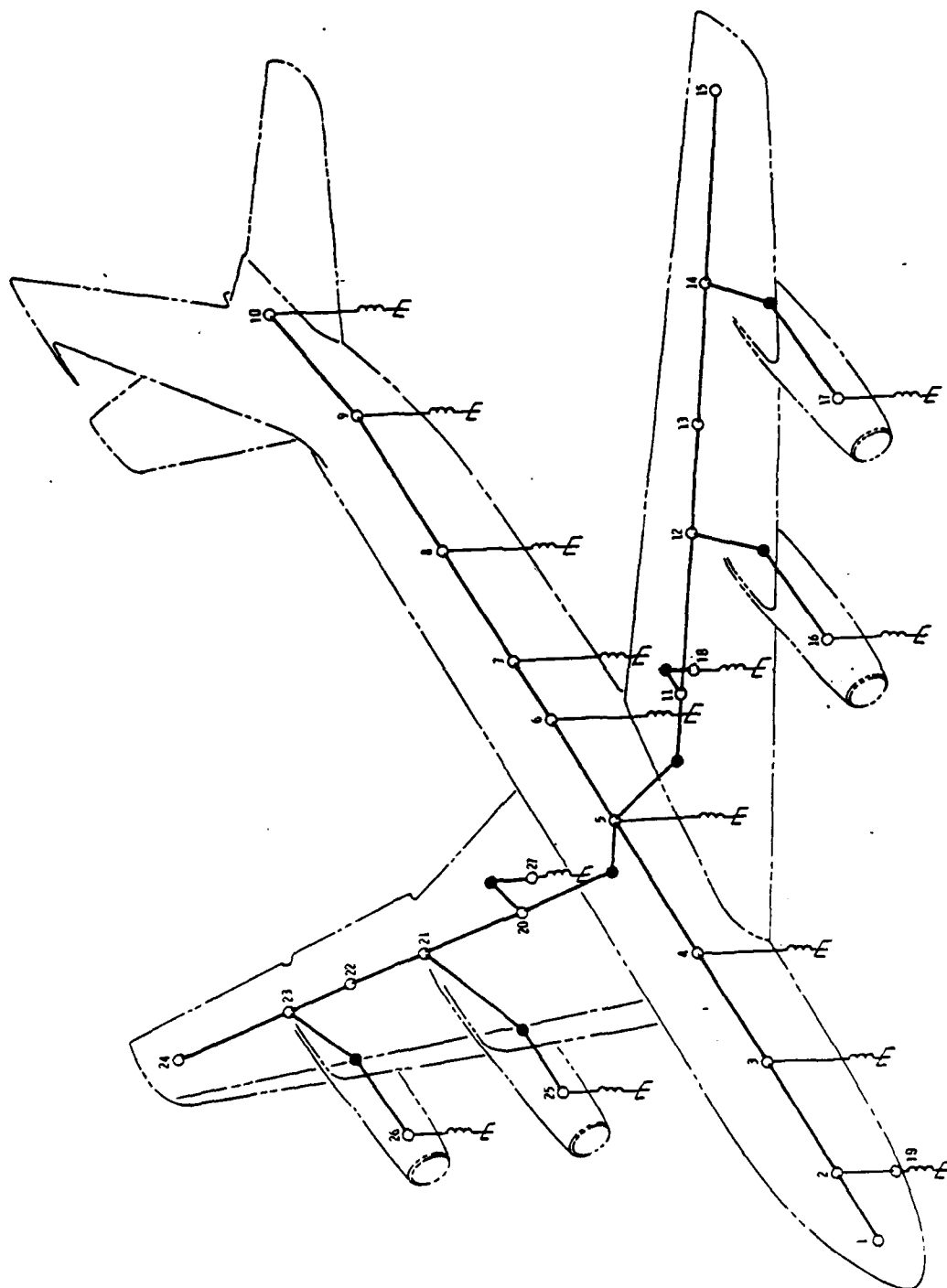
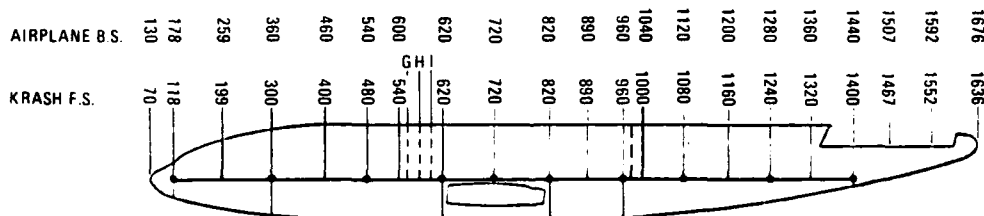


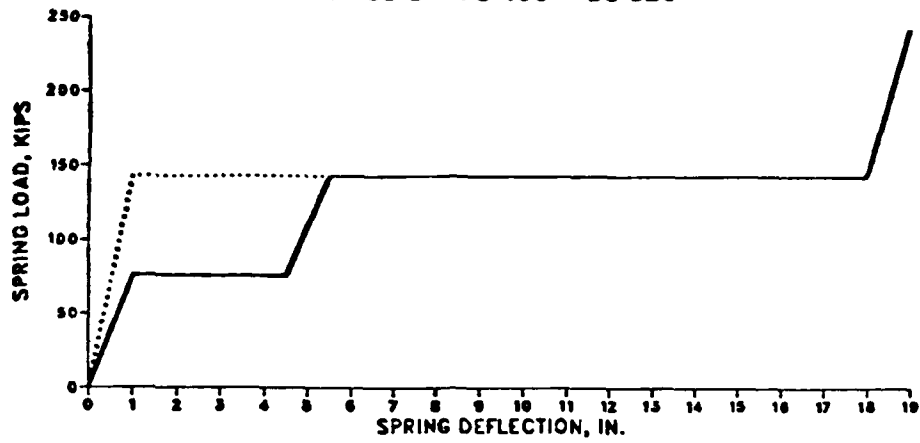
FIGURE 4-2. CID KRASH STICK MODEL

TABLE 4-1. KRASH MODEL FUSELAGE MASS POINT LOCATIONS

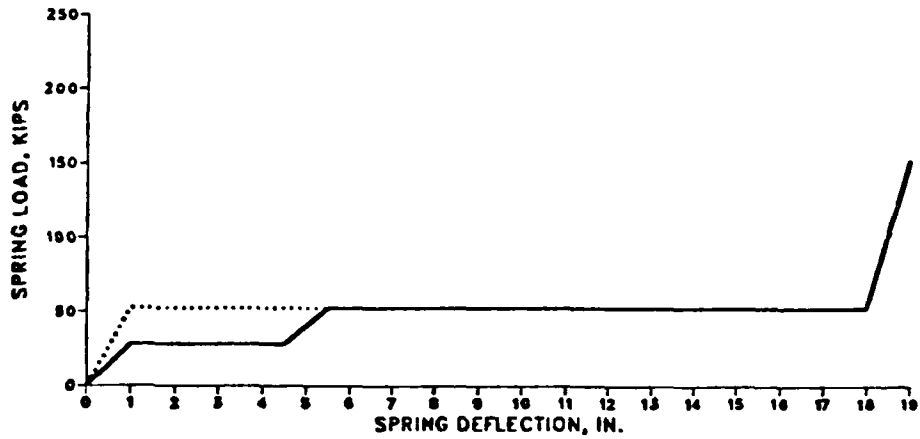
MASS NO.	KRASH FUSELAGE STATION	AIRPLANE BODY STATION	LOCATION REPRESENTATION
1	199	259	Nose Gear Wheel Well, forward bulkhead
2	300	360	Nose Gear Wheel Well, rear bulkhead
3	460	520	Forward fuselage frames
4	620	620	Wing center section, forward
5	820	820	Wing center section, rear
6	960	960	Main landing gear rear bulkhead
7	1040	1080	Mid fuselage frames
8	1200	1240	Mid-aft fuselage frames
9	1400	1440	Aft pressure bulkhead
10	1570	1610	Empennage



FORWARD FUSELAGE FRAMES  
MASS 3 - FS 460 - BS 520



MID FUSELAGE FRAMES  
MASS 7 - FS 1040 - BS 1080



AFT FUSELAGE FRAMES  
MASS 8 - FS 1200 - BS 1240

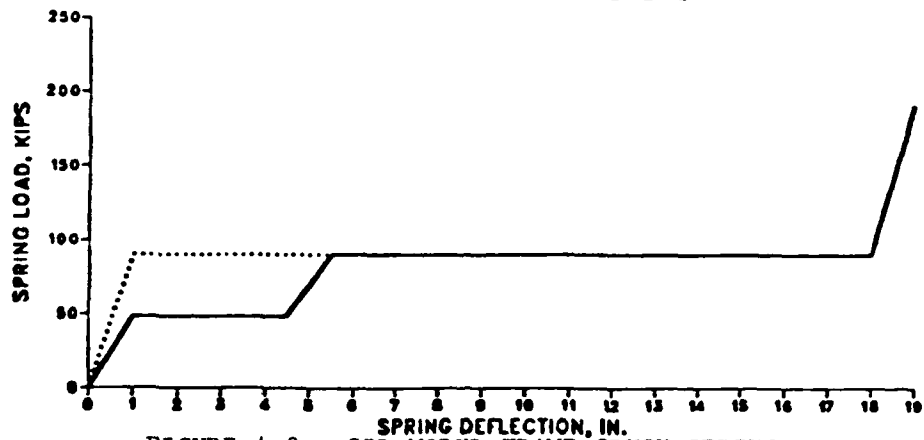
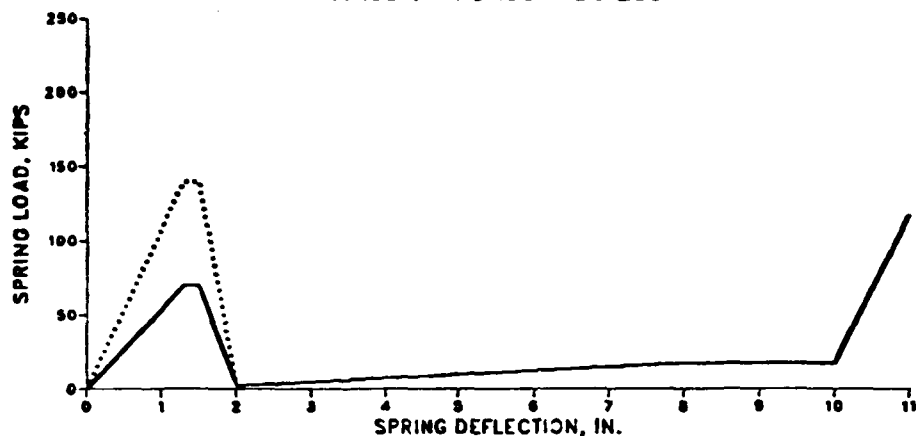
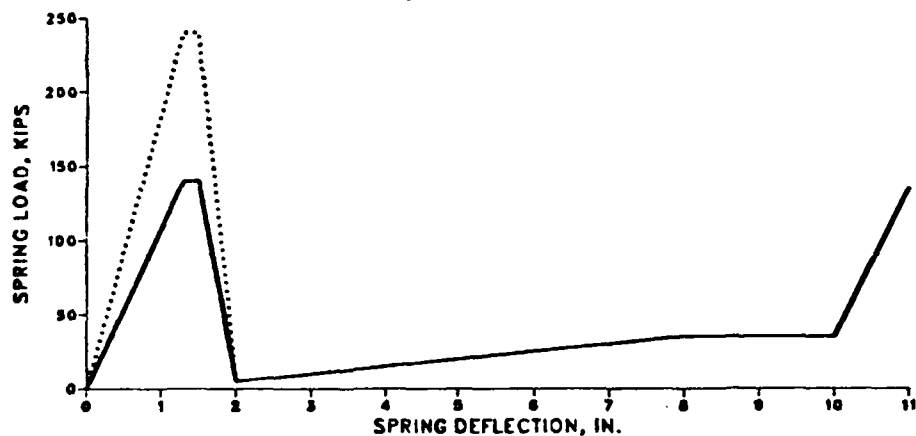


FIGURE 4-3. CID MODEL FRAME CRUSH SPRINGS

NG WHEEL WELL FWD BULKHEAD  
MASS 1 - FS 199 - BS 259



NG WHEEL WELL AFT BULKHEAD  
MASS 2 - FS 300 - BS 360



WING CENTER SECTION MASS 4 - FS 620 - BS 620      WING CENTER SECTION MASS 5 - FS 820 - BS 820      MLG WHEEL WELL AFT BULKHEAD MASS 6 - FS 960 - BS 960

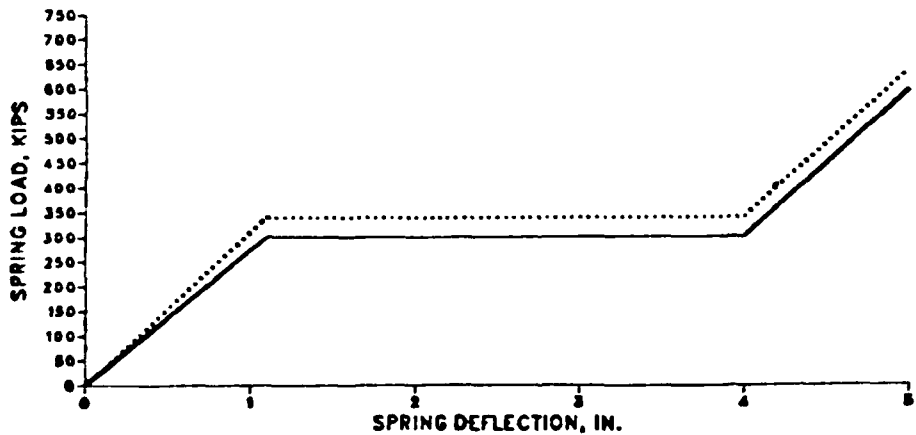


FIGURE 4-4. CID MODEL HARD POINT SPRINGS

The lower stringers are subject to failure due to compression and crushing loads. The middle stringers (S9 through S20) are vulnerable to high shear loads. The upper stringers would most likely fail under high bending tensile loads. The results of the load-interaction analysis are used in a qualitative sense to determine the relative sensitivity of regions of the airframe with gears-up to a range of impact velocities from 8 to 17 ft/sec, for a 155 knot forward velocity and one-degree nose-up attitude condition. The revised IC subroutine, in which KRASH-NASTRAN combined usage provides a static balance for an assumed 1g aerodynamic loading distribution, was used. As part of this initial study a sensitivity analysis was performed to ascertain how the results are affected by changes in the input data parameters. The solid and dotted lines in figures 4-3 and 4-4 indicate the range in load variation investigated. Figures 4-5 and 4-6 present results in the form of normalized LIC ratios for changes in fuselage underside load-deflection characteristics as noted in figures 4-3 and 4-4, as well as changes with regard to fuselage stiffness or plasticity and initial aerodynamic loading. Lower loads are experienced for a softer fuselage, increased plasticity and for a no lift condition, as can be observed in figures 4-5 and 4-6.

Figure 4-7 shows results in the form of normalized LIC ratio as a function of changes in hard point load-deflection characteristics as noted in figure 4-8. The variations noted in figure 4-8 differ from those previously described in figure 4-4 in that the spring bottoming characteristics are affected. The response of the airframe is very sensitive to the hard point inputs, more so than to the soft frames. For the case analyzed, the aft fuselage loads increase substantially as a result of "bottoming" on hard points.

A qualitative assessment of the gear-up condition is shown in figure 4-9. The structure damage obtained from the stick model analysis is shown for a range of impact velocity conditions from 10 ft/sec to 17 ft/sec. The darkened regions in figure 4-9 indicate areas where potentially severe damage could occur. It is difficult to determine the degree of damage (i.e., separation) using the model and data described. An interpretation given to these results indicates a potential for aft fuselage separation to occur at a 17 ft/sec impact velocity. The stick model approach provides an overview of trends and an

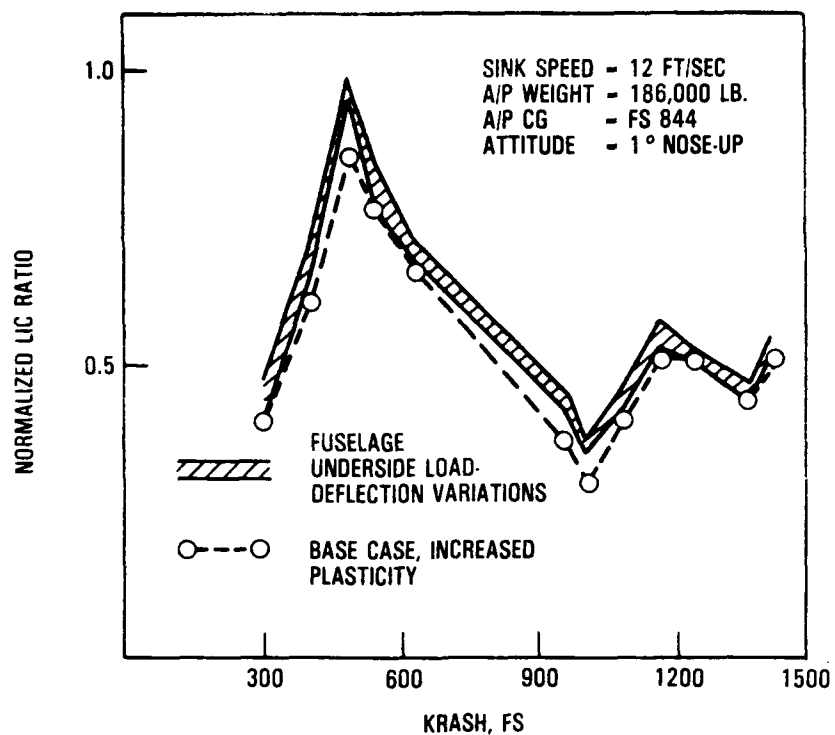


FIGURE 4-5. COMBINED LOAD RATIOS, FOR FUSELAGE UNDERSIDE LOAD-DEFLECTION VARIATIONS

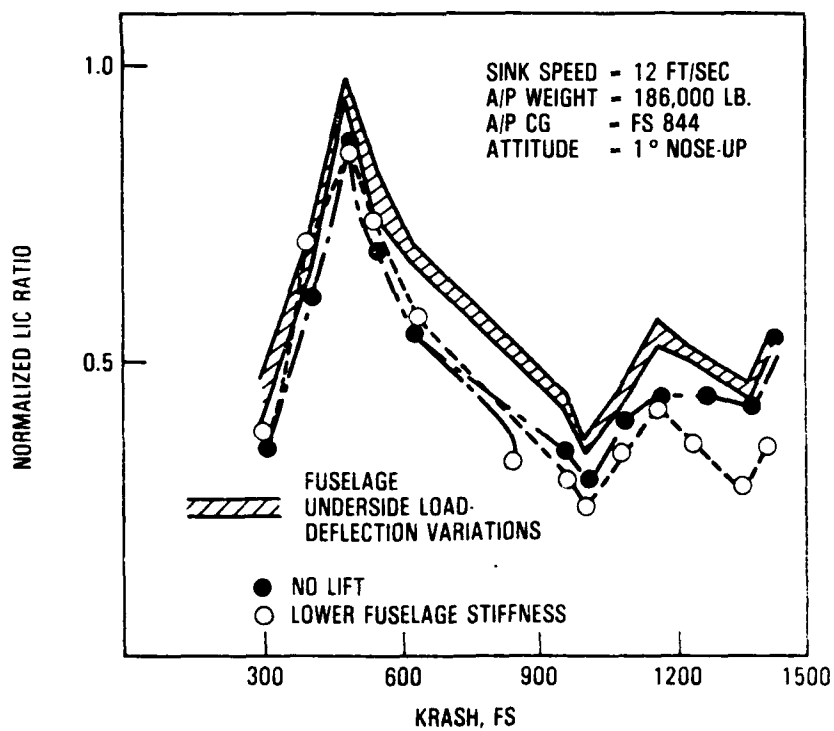


FIGURE 4-6. COMBINED LOAD RATIOS, COMPARISONS FOR 'NO LIFT' AND REDUCED FUSELAGE STIFFNESS

# RESPONSE SENSITIVITY STUDY SINK SPEED-12FT/SEC

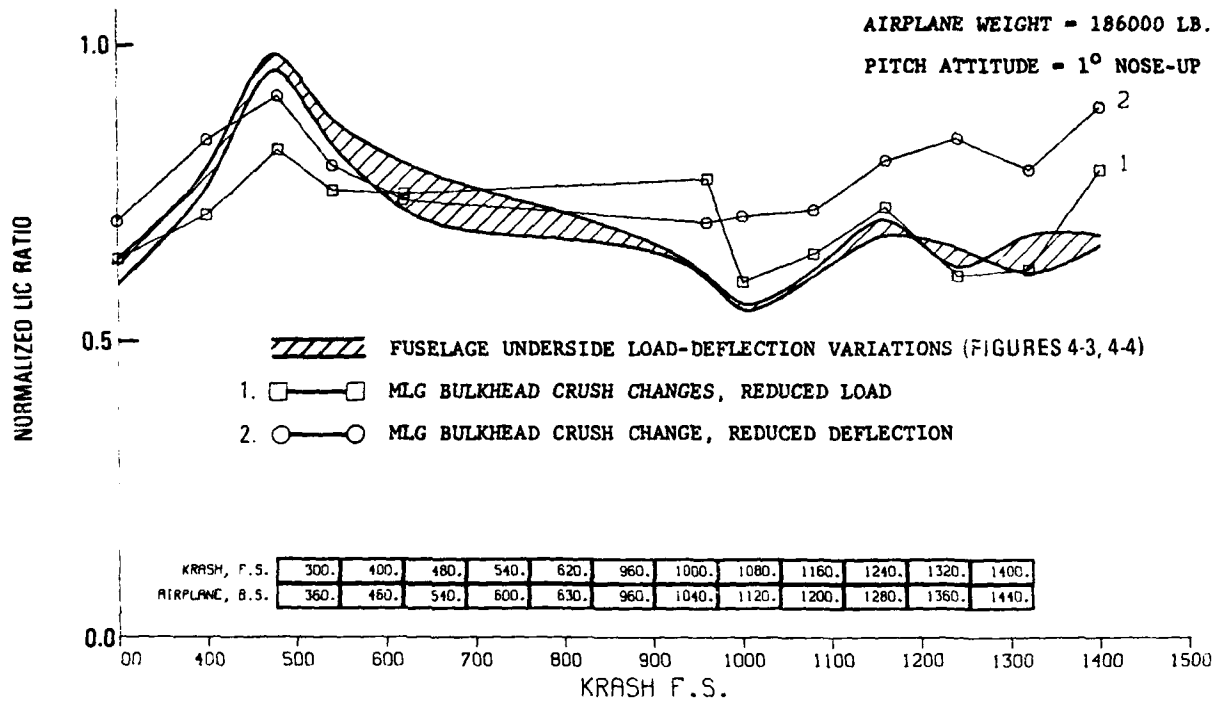


FIGURE 4-7. COMBINED SHEAR-MOMENT LOADS AS A FUNCTION OF MLG BULKHEAD LOAD-DEFLECTION REPRESENTATION

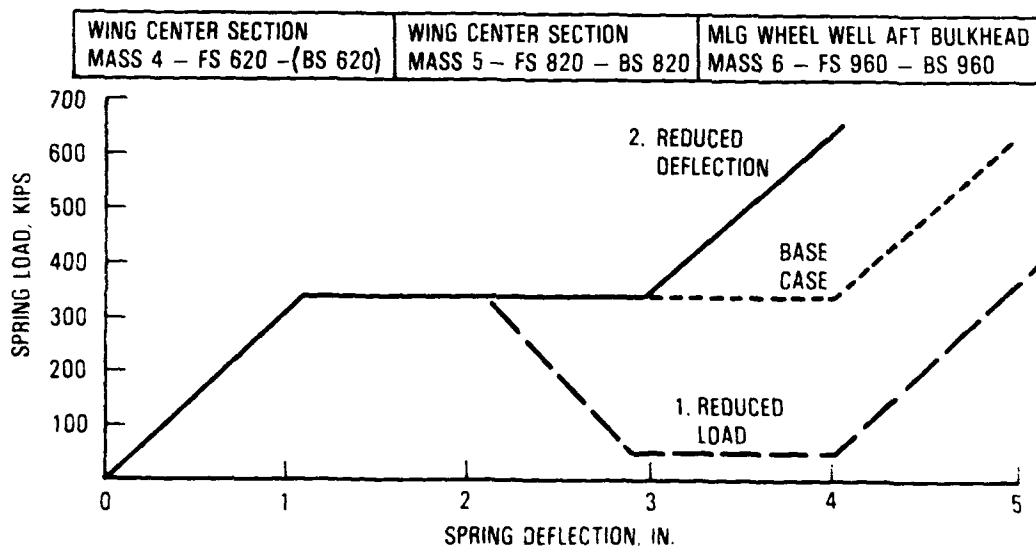
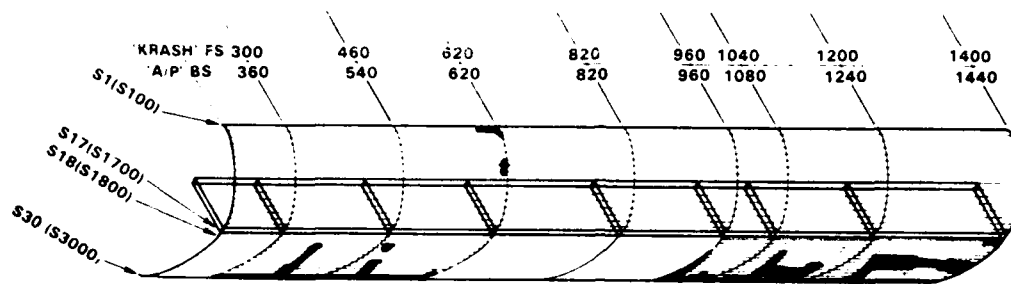
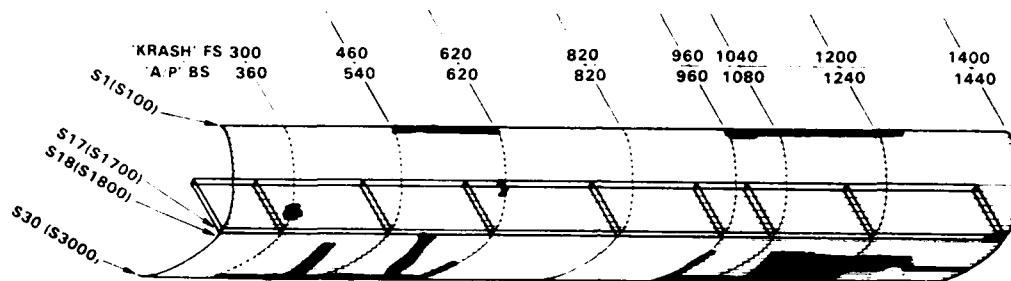


FIGURE 4-8. MODEL HARD POINT LOAD-DEFLECTION VARIATIONS

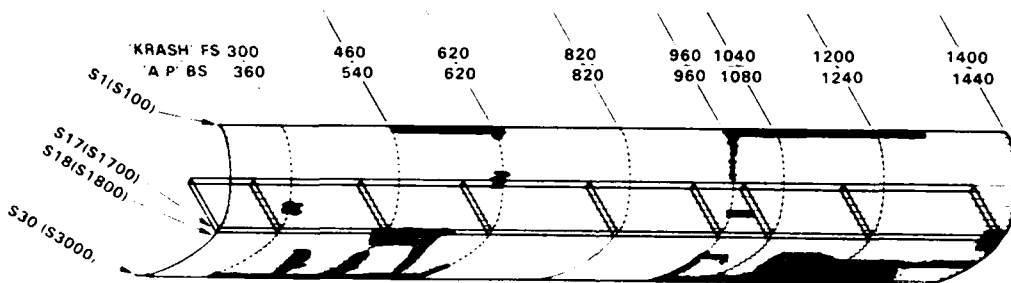




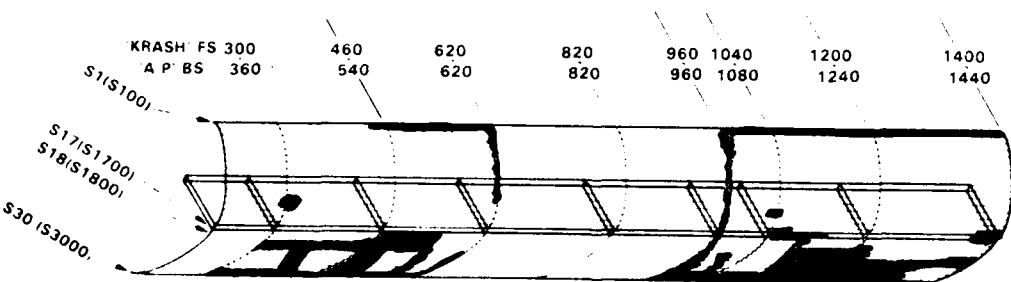
SINK SPEED - 10 FT/SEC



SINK SPEED - 12 FT/SEC



SINK SPEED - 14 FT/SEC



SINK SPEED - 17 FT/SEC

FIGURE 4-9. FUSELAGE DAMAGE AS FUNCTION OF SINK SPEED, KRASH ANALYSIS, 1° NOSE-UP IMPACT

insight into potentially critical regions. However, the approach has limitations with regard to 1) incorporating the effects of local plasticity, 2) the sensitivity to representation of fuselage underside structure, particularly hard points, and 3) the accuracy of available airframe structural capability data.

#### 4.2 COMPARISONS WITH GEARS-EXTENDED AND SLOPE IMPACTS

Comparisons were also made between the gear-up and gear-extended configurations. The procedure for performing gear-extended analysis was as follows:

1. The manufacturer-provided main gear load-stroke drop test data at 12 ft/sec was matched, using the KRASH oleo metering pin coding. The comparison is shown in figure 4-10. The tests were conducted at a landing weight, with an equivalent single gear weight of 48100 pounds.
2. Based on the matching of the test data with a simulated oleo metering pin, the damping ( $C_D$ ) versus stroke characteristic of the metering pin is derived (see figure 4-11).
3. Using the metering pin characteristics, shown in figure 4-11, high sink speed conditions are then run with the KRASH stick model including landing gears.

The results of the gear-extended analysis, following the approach outlined above, are compared to the gear-up analysis results in table 4-2. From table 4-2, it can be observed that a full gear stroke is anticipated up to a 20 ft/sec vertical sink speed impact. However, at 20 ft/sec impact sink speed, while the gear may not fail, the combined load ratio ( $>1.0$ ) could result in fuselage failure at the MLG bulkhead (BS 960). Based on the stick model analysis, the gear-extended condition in the impact velocity range of 18 to 20 ft/sec appears to be comparable to a gears-up impact velocity of 8 to 12 ft/sec. The analysis results indicate that the fuselage average overall accelerations are lower for the gears-extended than for the gears-up condition. To ascertain the validity of the above-noted comparison, a single gear model was run for impact sink speeds of 10, 20 and 30 ft/sec. The results of these analyses are shown in figure 4-12. A takeoff weight is used for these results, with an equivalent single gear weight of 92,335 pounds. These simple model results illustrate that up to an impact velocity of 20 ft/sec, one might expect to obtain a large percentage of the stroking capability of the gear. At a 30 ft/sec sink rate the stroke, based on a MLG load capability of 350 to

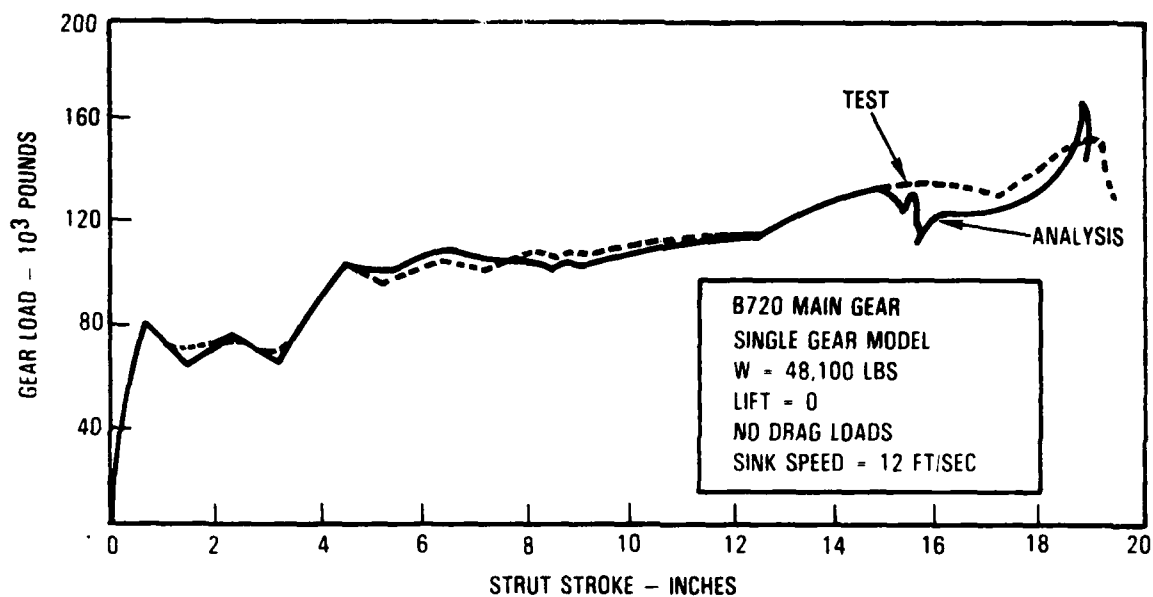


FIGURE 4-10. DUPLICATION OF KNOWN TEST LOAD-DEFLECTION CURVE USING METERING PIN CODING IN KRASH85

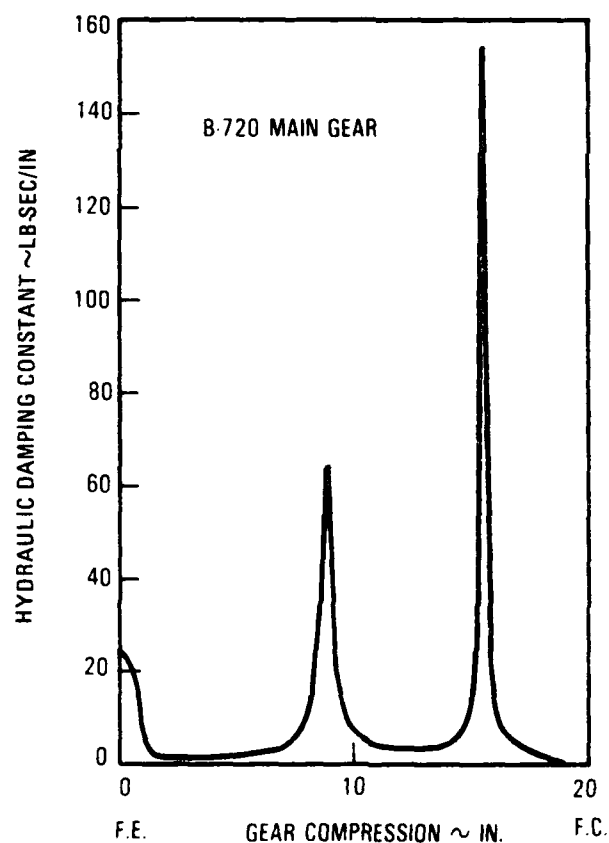


FIGURE 4-11. OLEO METERING PIN DAMPING CONSTANT VERSUS GEAR COMPRESSION

TABLE 4-2. GEAR-UP VERSUS GEAR EXTENDED ANALYSIS RESULTS

CONFIGURATION	IMPACT SINK SPEED FT/SEC	AVERAGE VERTICAL ACCELERATION "G's"	COMBINED MOMENT-SHEAR LOAD RATIO	
			BS 620	BS 960
Gears-Retracted	8	8.1	.89	.93
	10	9.9	1.3	1.05
	12	12.8	1.4	1.08
	14	14.3	1.4	1.21
	17	18.7	1.4	1.88
Gears-Down	18*	6.6	.48	.84
	20**	7.8	.72	1.13

+1<sup>0</sup> Nose-Up Attitude, 186,000 Lb. Airplane

\* 18.8 Inch Stroke, No Gear Failure

\*\* 19.0 Inch Stroke, No Gear Failure

\*\*\*These values are high. Subsequent airplane drop test data (see Section 5) indicates that hardpoint springs at FS 620, 820 960 do not 'bottom out' at the deflections used in this analysis.

430 KIPS, might reduce to  $\approx 35$  percent of its maximum stroke. Based on airplane taxi design considerations, one could anticipate a MLG for the CID airplane to be capable of 360 to 420 KIPS vertical load. Current widebody airplane Main Landing Gears are designed for a vertical load in excess of 600 KIPS/Gear.

Since previous transport airplane crash tests were of the ground-to-ground variety the question of "how the planned CID air-to-ground impact compares with a ground-to-ground (ramp) impact?" is of interest. Figure 4-13 illustrates the ramp initial impact conditions (representative of ground-to-ground) that are comparable to air-to-ground initial impact conditions with regard to initial velocities and contact points. Using KRASH, a comparison of results was made for a ramp impact such as the L1649 test (reference 15) versus the planned air-to-ground impact. For both impacts, it was assumed that the forward velocity and sink speed, respectively, were equal. The two impact conditions are depicted as conditions IIA and V, in figure 4-13. The results, shown in figure 4-14, indicate that the combined shear-moment load as depicted by the LIC ratio normalized to the peak value is lower for the ground-to-ground impact, except at the forward end. The LIC ratios for the air-to-ground

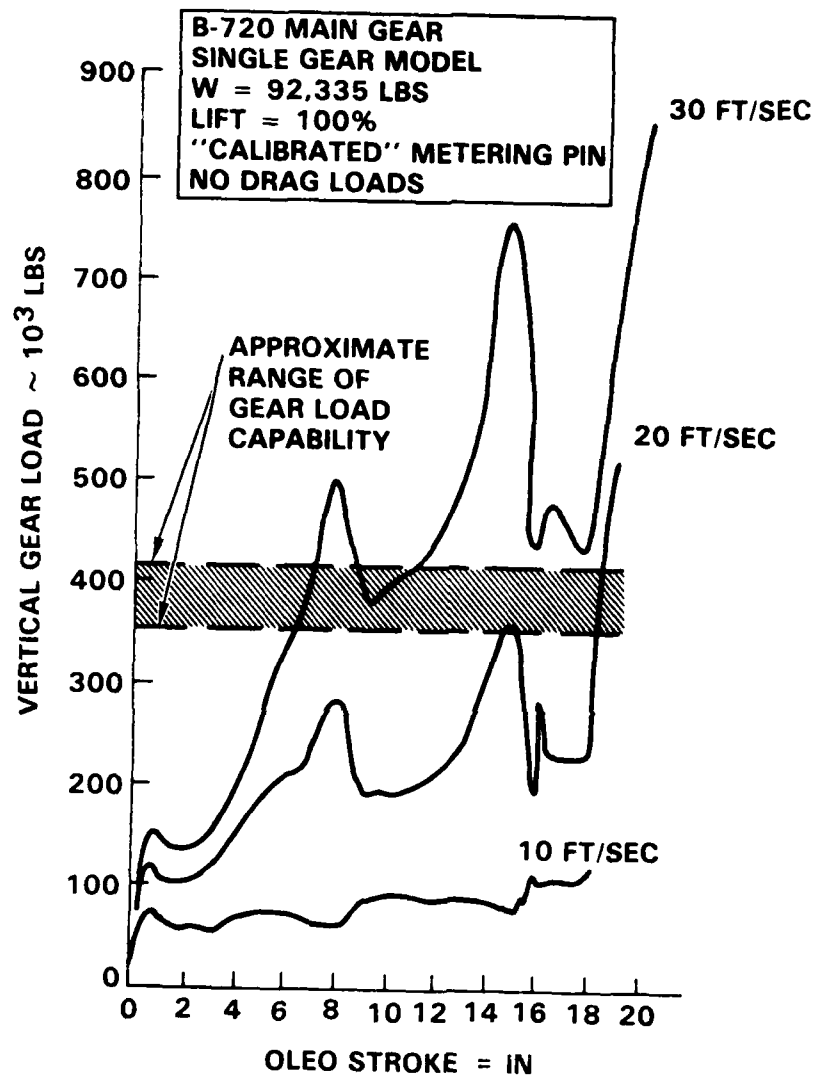


FIGURE 4-12. SINGLE GEAR MODEL ANALYSIS RESULTS

### RAMP IMPACT

(II)

$$V = 262 \text{ FT/SEC}, \theta_S = 6^\circ$$

$$V_N = V \sin \theta_S \approx 27.4 \text{ FT/SEC}$$

$$V_H = V \cos \theta_S \approx 260 \text{ FT/SEC}$$

### AIR-TO-GROUND IMPACT

(IV)

$$V = 262 \text{ FT/SEC}, \theta = 6^\circ$$

$$V_Z = V \sin \theta = V_N \approx 27.4 \text{ FT/SEC}$$

$$V_X = V \cos \theta = V_H \approx 260 \text{ FT/SEC}$$

(III)

A)  $V = 262 \text{ FT/SEC}, \theta_S = 3.7^\circ$

$$V_H = V \cos \theta_S \approx 261.5 \text{ FT/SEC}$$

$$V_N = V \sin \theta_S = 17 \text{ FT/SEC}$$

(V)

A)  $V = 262 \text{ FT/SEC}$

$$\theta = 1^\circ \text{ NOSE-UP}$$

$$\gamma = 3.7^\circ \text{ (NEGATIVE IN DIVE)}$$

$$V_X = V \cos \gamma = 261.5 \text{ FT/SEC}$$

$$V_Z = V \sin \gamma = 17 \text{ FT/SEC}$$

B)  $V = 162 \text{ FT/SEC}, \gamma = 3.7^\circ$

$$V_X = V \cos \gamma \approx 161.5 \text{ FT/SEC}$$

$$V_Z = V \sin \gamma = 10.5 \text{ FT/SEC}$$

(III)

AIRPLANE IMPACTS  
SLOPE AT RELATIVE  
ANGLE =  $(\theta + \theta_S)$   
TO FLAT GROUND

$$V = 262 \text{ FT/SEC}, \theta_S = 3.7^\circ, \theta = 1^\circ$$

$$V_H = V \cos \theta_S = 261.5 \text{ FT/SEC}$$

$$V_N = V \sin \theta_S = 17 \text{ FT/SEC}$$

(V)

$$V = 262 \text{ FT/SEC}$$

$$\theta = 1^\circ \text{ NOSE UP}$$

$$\gamma = 3.7^\circ \text{ (NEGATIVE IN DIVE)}$$

$$V_X = V \cos \gamma \approx 261.5 \text{ FT/SEC}$$

$$V_Z = V \sin \gamma = 17 \text{ FT/SEC}$$

FIGURE 4-13. INITIAL IMPACT CONDITIONS; RAMP VERSUS AIR-TO-GROUND IMPACT

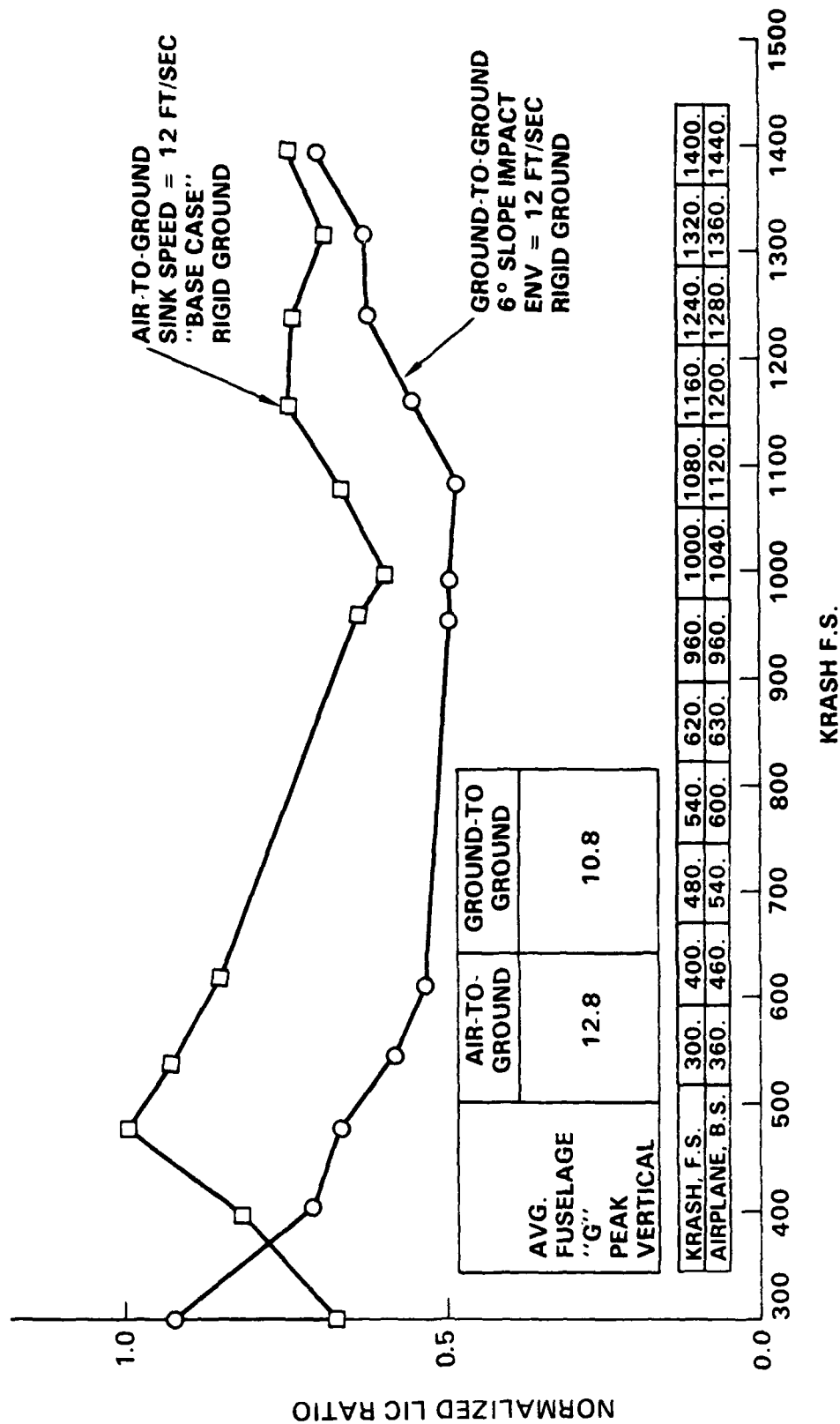


FIGURE 4-14. KRAH RESULTS, AIR-TO-GROUND VERSUS GROUND-TO-GROUND IMPACTS

condition are high in the aftbody due to 'slapdown' as the airplane rotates onto the aft section after initial impact. Since both analyses are for a rigid ground one would anticipate longitudinal accelerations to be low and comparable for both conditions. As can be observed from figure 4-13 a ramp impact similar to that shown in condition III would be a closer approximation of the planned air-to-ground impact (condition V).

#### 4.3 SEAT/OCCUPANT RESPONSE TO A LONGITUDINAL PULSE

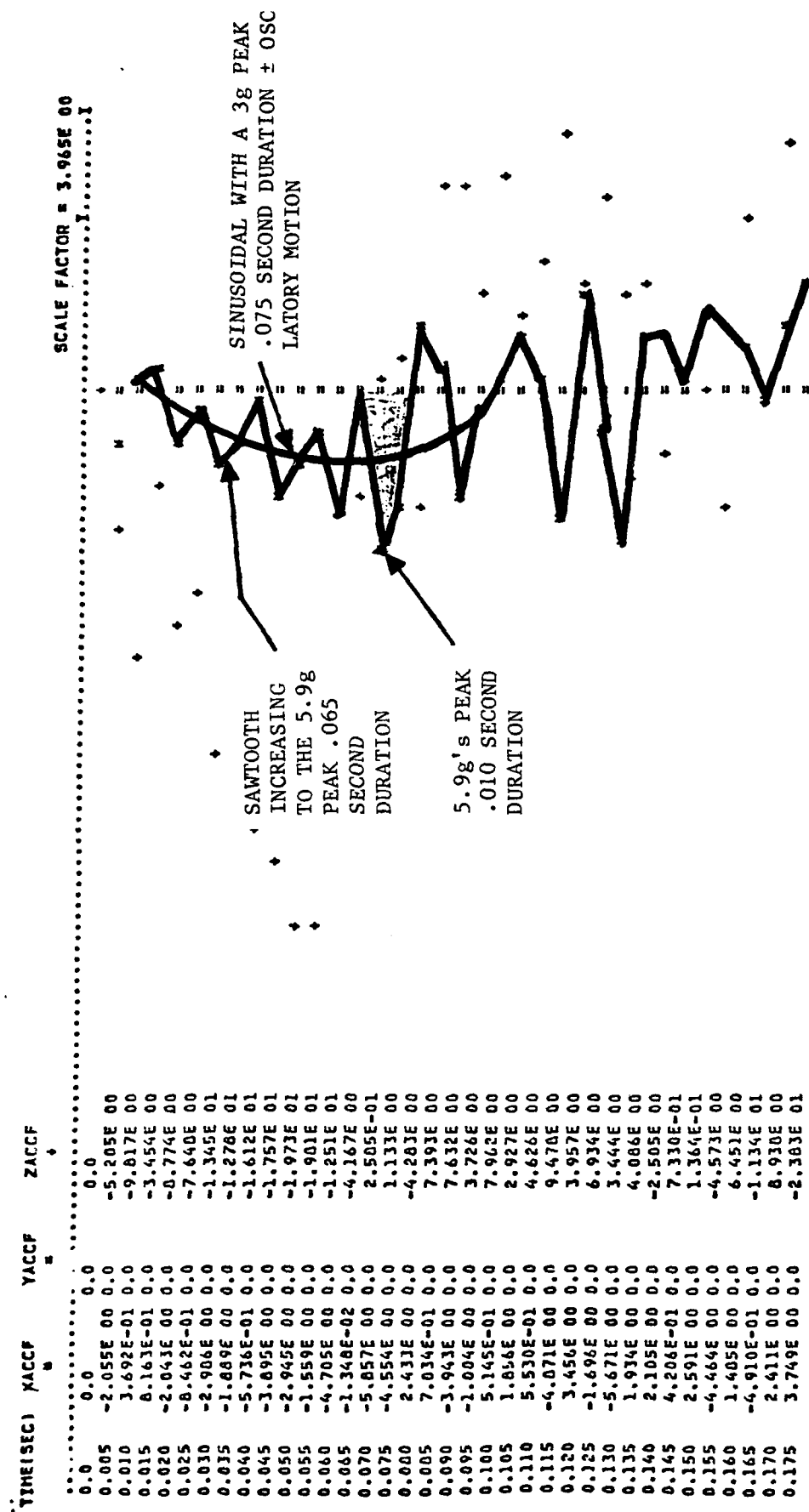
Seat-occupant analyses were performed with the KRASH model developed under a previous transport airplane crash dynamics study (reference 6). A review of the KRASH stick model results shows that the responses, at any particular location, can possibly be described in several ways. For example, for the gears-up impact condition ( $V_x = 155$  kts,  $V_v = 17$  ft/sec,  $1^\circ$  nose-up) figure 4-15 shows that the longitudinal pulse shape at FS 960, can be described as:

- A. Triangular, 5.9g peak acceleration, 0.010 second base
- B. Sawtooth, increasing to the 5.9g peak acceleration, 0.07 second duration
- C.  $\approx$ sinusoidal, with a 3g peak acceleration, 0.065 second duration.

For each of these pulses the occupant would respond differently. Figure 4-16 shows the results of an analysis using the KRASH occupant-seat model developed and correlated with CAMI-seat longitudinal pulse test data (reference 6). The data provided in figure 4-16 demonstrate that for the half sine and sawtooth pulses, the occupant could experience 4.9g to 5.3g accelerations at the pelvis. For the 0.01 second triangular pulse the same response would be barely over 1g. For lap belt only restraints, the occupant rotations are shown to be  $4.5^\circ$ ,  $27.2^\circ$  and  $25^\circ$ , for cases A, B, and C, respectively.

The analytically determined pulses at FS 620 (wing leading edge) and FS 820 (wing trailing edge) are shown in figures 4-17 and 4-18). They can be characterized as trapezoidal with a peak acceleration of 3.2g to 3.3g and a base duration of 0.050 to 0.055 seconds. The corresponding pelvic responses from the KRASH seat model, shown as case G in figure 4-19, indicate a 5.8g acceleration response and occupant rotation of 29.5 degrees. Cases D, E, F, in figure 4-18, illustrate response as a functions of other pulses. Case D





XACCF = Longitudinal Accel.  
YACCF = Lateral Accel.  
ZACCF = Vertical Accel.

FIGURE 4-15. KRASH CID MODEL ACCELERATIONS AT FS960 (MASS 6)

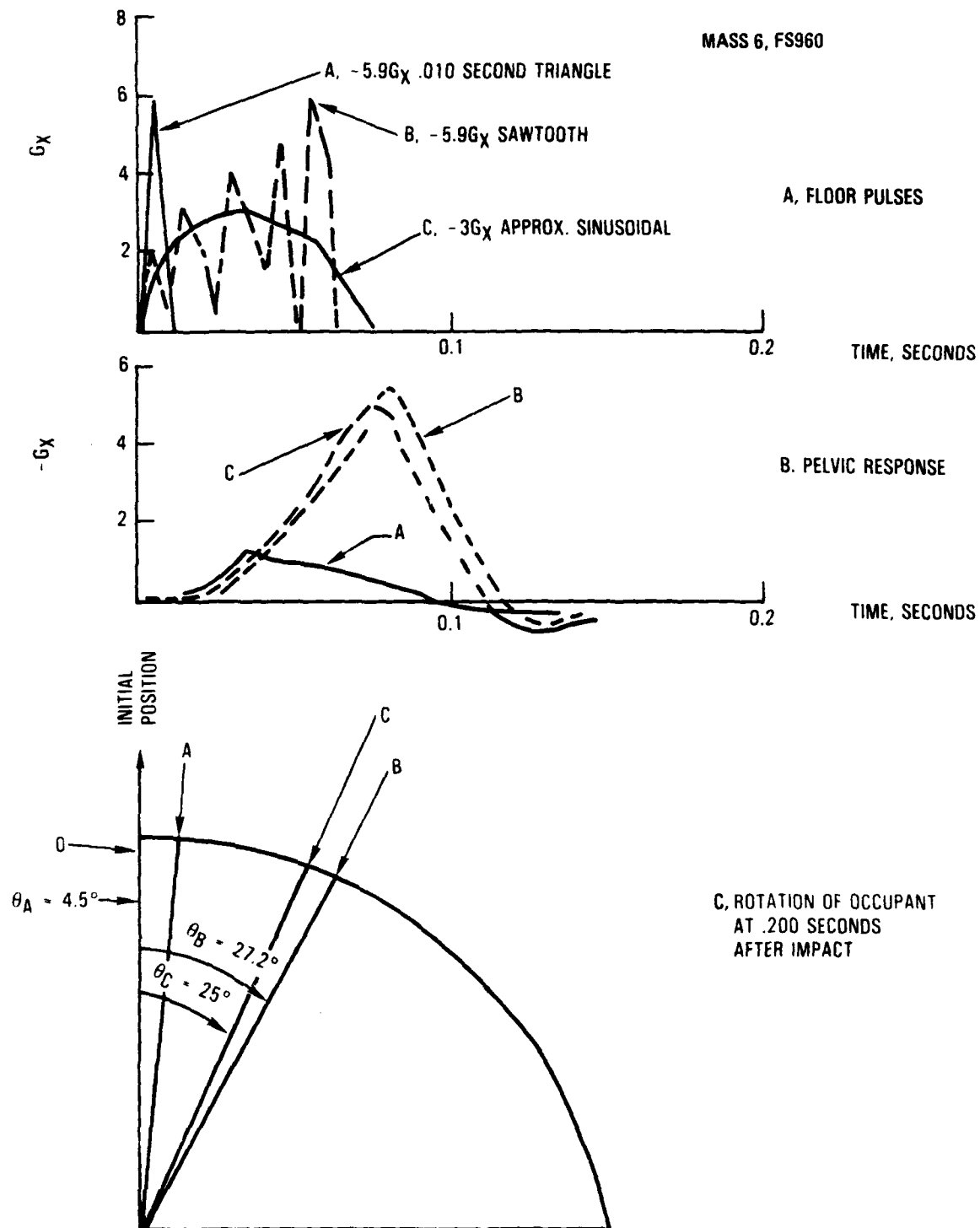
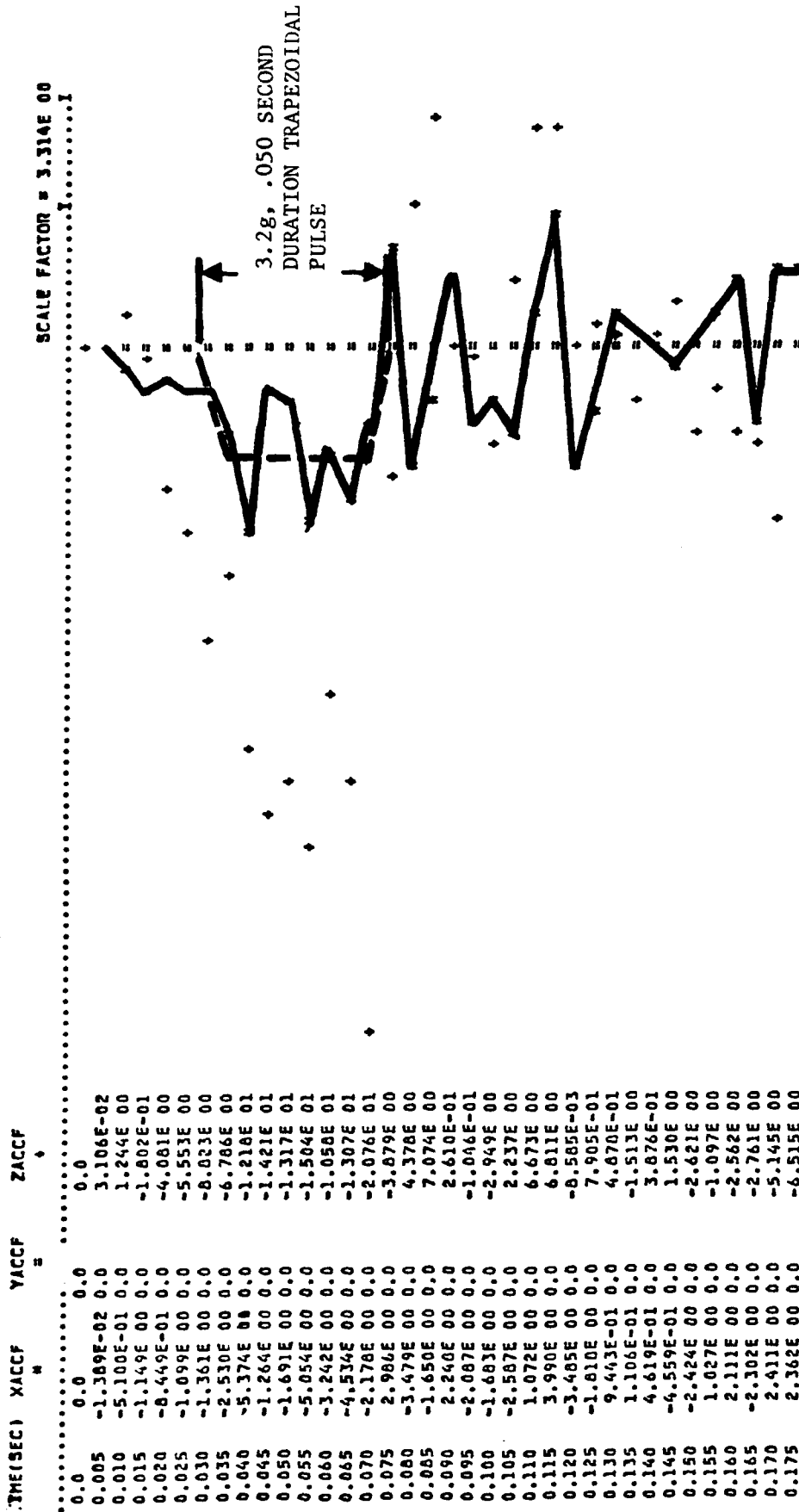


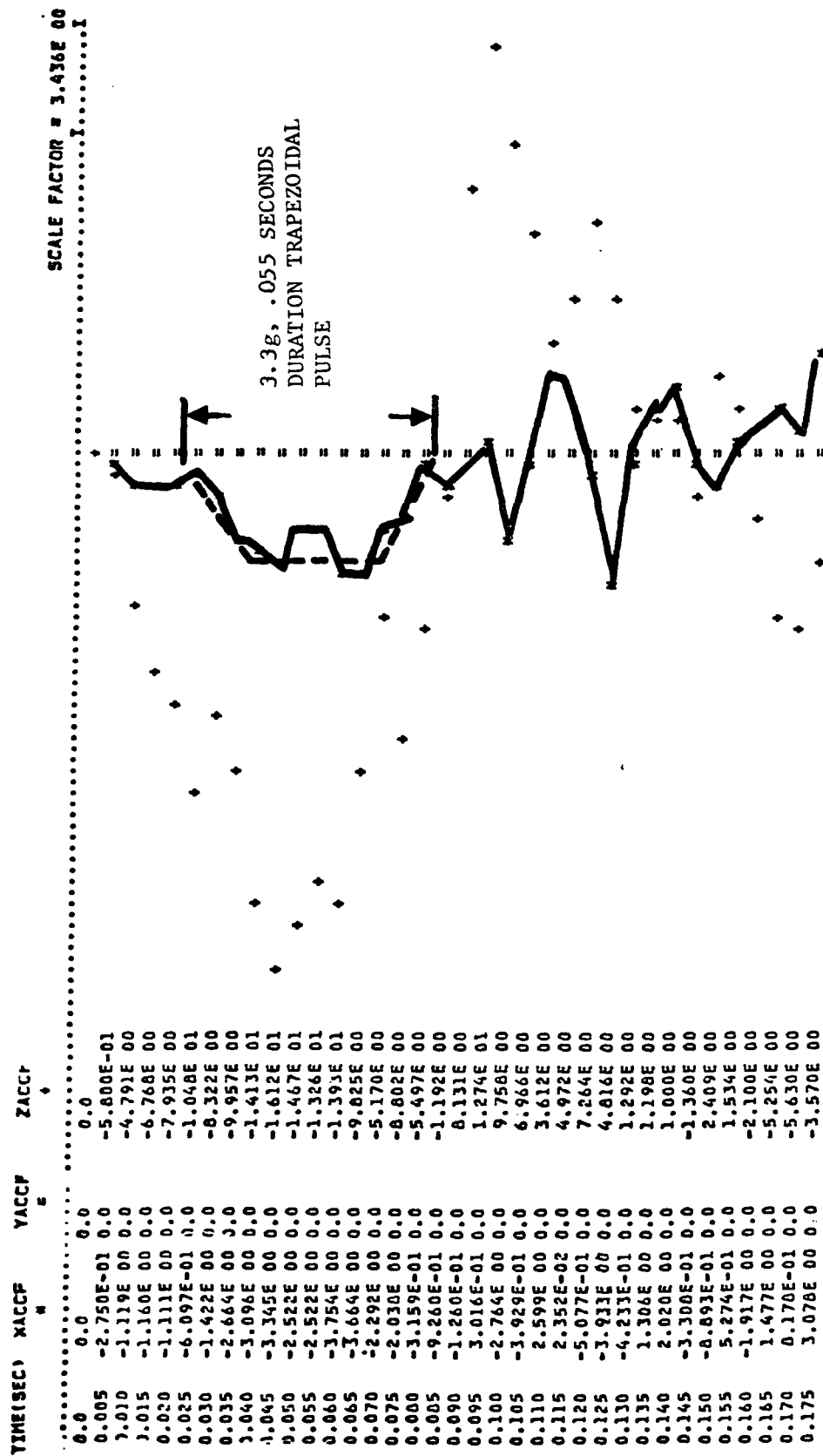
FIGURE 4-16. EFFECT OF DIFFERENCE FLOOR LONGITUDINAL PULSE REPRESENTATIONS ON OCCUPANT RESPONSE

# MASS 4 FILTERED ACCELERATION(G'S), FS620, 50 HZ. FILTER



XACCF = Longitudinal Accel.  
YACCF = Lateral Accel.  
ZACCF = Vertical Accel.

FIGURE 4-17. KRASH CID MODEL ACCELERATIONS AT FS620 (MASS 4)



XACCF = Longitudinal Accel.  
YACCF = Lateral Accel.  
ZACCF = Vertical Accel.

FIGURE 4-18. KRASH CID MODEL ACCELERATIONS AT FS820 (MASS 5)

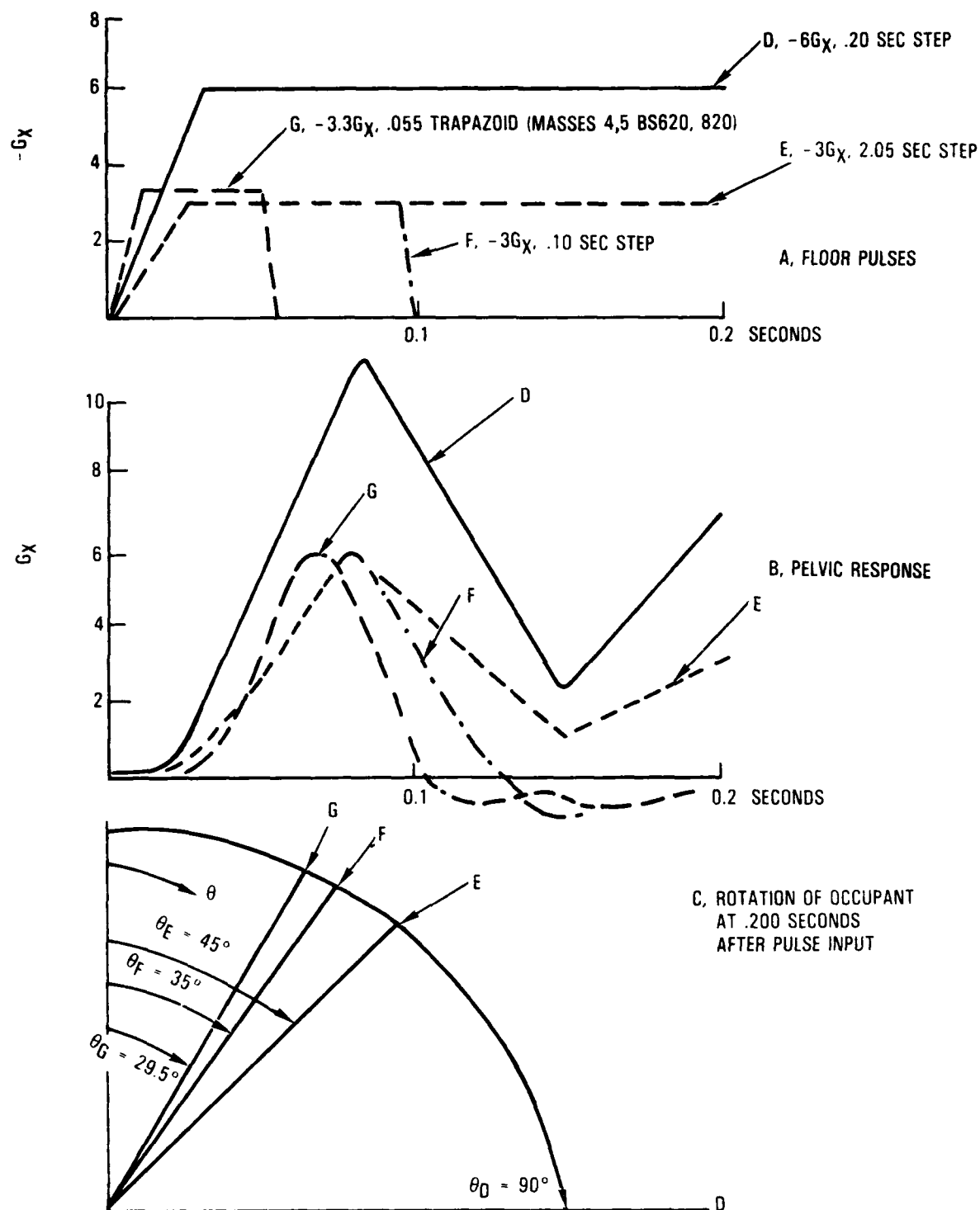


FIGURE 4-19. KRASH SEAT - OCCUPANT LONGITUDINAL PULSE ANALYSIS RESULTS

represents the condition which was tested at CAMI and with which KRASH results were compared in reference 6.

From the results shown in figures 4-16 and 4-18, it is clear that when defining pulses, it is important to consider the total pulse and not a segment of the pulse. Furthermore, the subjective interpretation of the pulse could lead to different conclusions with regard to occupant response. The KRASH obtained longitudinal pulses for the condition described could result in 5g to 6g pelvic responses for lap-belt only restrained occupant and rotations up to 30 degrees.

#### 4.4 TEST IMPACT CONDITION SELECTION

Since the CID test involves combined Crashworthiness and Antimisting Kerosene (AMK) objectives it was recognized that the test impact conditions could be compromised. The responsible agencies selected a 17 ft/sec sink speed at impact with the airplane in a 1 degree nose-up attitude and a flight path speed of 155 knots. From the results of the preliminary analysis presented, this condition indicated the evidence of loads severe enough to challenge the structural integrity of the airframe. The extent to which damage would occur appeared to be very dependent on the hard point load-deflection characteristics and the amount of initial aft fuselage down bending provided by the aerodynamics. The CID test as described is expected to provide relatively high vertical but low longitudinal floor pulses. The previously performed L1649 test (reference 15) provided both moderate/high vertical and longitudinal impact forces. The extreme of a high longitudinal combined with a low vertical impact force is not covered in either this or the previous L1649 test. However, it is reasonable to expect that an analysis whose results have been correlated for the other combinations of loading will be satisfactory for this latter condition. Improved methodology, via KRASH, for future applications, is a major goal of this test program. With the successful acquisition of data relating input and output responses, failure modes and airframe deformation, it will be possible to achieve such a goal.

## SECTION 5

### NARROW-BODY AIRPLANE IMPACT DATA

#### 5.1 AIRPLANE IMPACT TEST

A B707-131 airplane weighing 195,000 pounds and with a c.g. at FS855.14, was used in the performance of a drop test at Laurinburg, N.C. on 29 June 1984. The purpose of the test was to evaluate the airframe strength characteristics for an aircraft similar to the CID test article under comparable impact conditions (+1<sup>0</sup> nose up, 17 ft/sec impact sink speed). The B707-131 airplane is 100 inches longer (20 inches forward of FS620, 80 inches aft of FS960) than the CID test article, but, basically of the same construction and design. High speed film coverage was provided. Pre- and post-test views of the test configuration are shown in figures 5-1 and 5-2, respectively. Damage to the aircraft was reviewed immediately after the impact and several weeks later, after the test vehicle had been lifted off the ground. Figures 5-3 through 5-24 show the damage that was sustained by the airplane as a result of the impact. Figures 5-3 and 5-4 show damage to the fuselage underside. It was estimated that the crush was about 2 inches, aft of the nose gear bulkhead; 4 inches, forward of the wing leading edge (FS620); and 11 to 13 inches, aft of the MLG Rear Bulkhead (FS960). The inboard wing engine pylons failed noticeably at the upper strut attach points from the pylon to the wing. Figures 5-5 and 5-6 depict the engine pylon failure. Figures 5-7 through 5-12 show damage to the vertical centerline keel and FS960 bulkhead. The bulkhead web crack is traced from the lower section up through to the floor in figures 5-9 through 5-12. Damage to the forward cargo bay at or forward of FS620 is shown in figures 5-13 and 5-14. The lower fuselage has been crushed and frame failures are noted on the centerline and along the sidewall. Figures 5-15 through 5-18 shows damage that occurred in the aft cargo bay from FS60 to FS1120. The extent of damage is

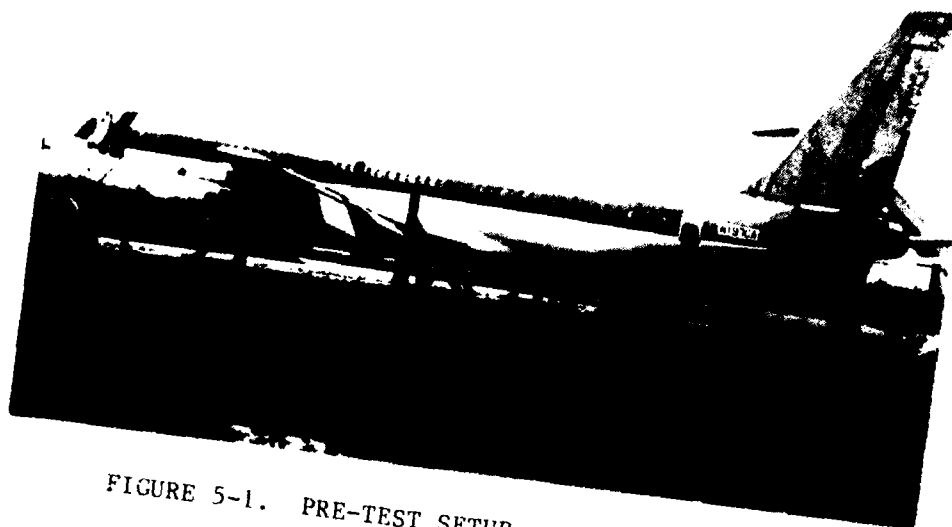


FIGURE 5-1. PRE-TEST SETUP - B707 IMPACT TEST



FIGURE 5-2. POST-TEST VIEW - B707 IMPACT TEST





FIGURE 5-3. FORWARD LOWER FUSELAGE DAMAGE - LEFT SIDE LOOKING AFT



FIGURE 5-4. WING ROOT FAIRING - RIGHT HAND TRAILING EDGE



FIGURE 5-5. LEFT WING INBOARD PYLON FAILURE

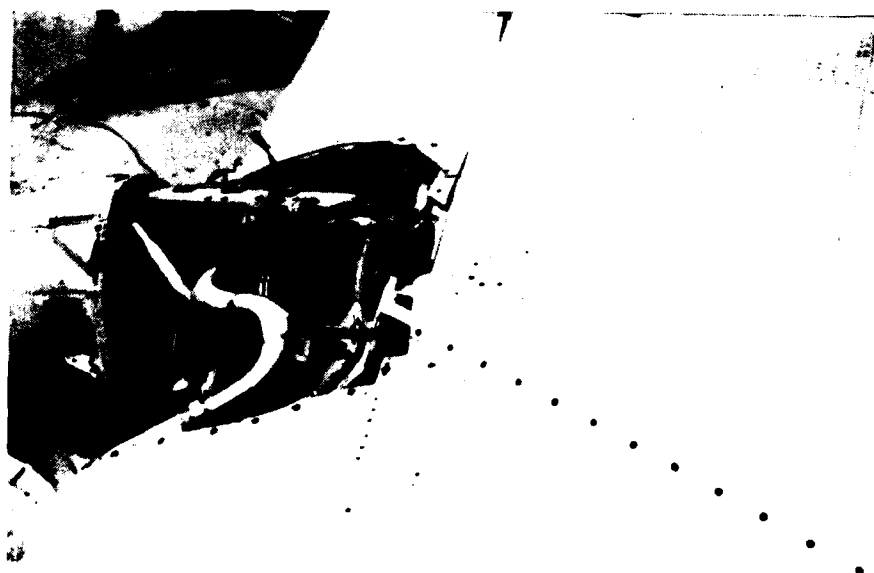


FIGURE 5-6. LEFT HAND INBOARD PYLON -  
UPPER LONGERON FRACTURE



FIGURE 5-7. LEFT HAND LANDING GEAR WELL- VIEW LOOKING AFT -  
VERTICAL KEEL TO FS960 BULKHEAD

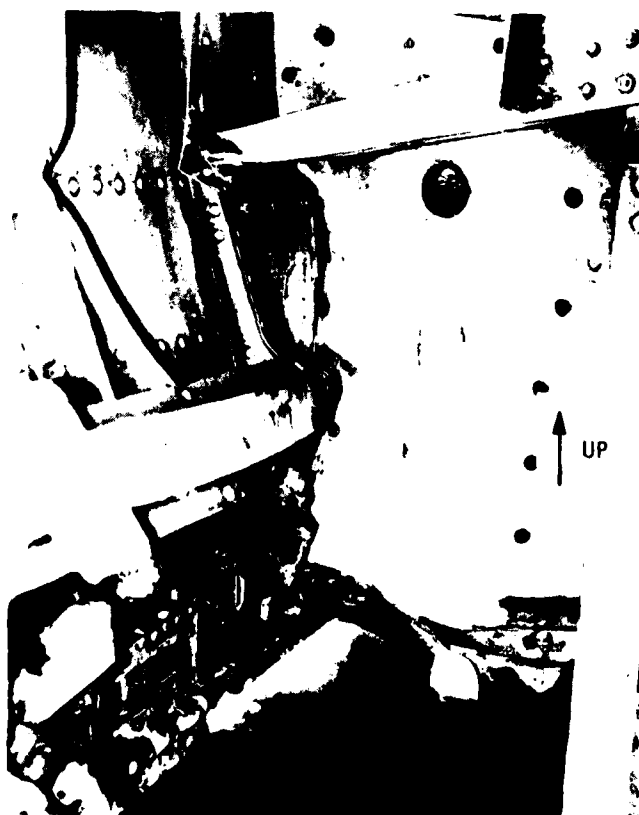


FIGURE 5-8. CLOSE UP VIEW OF VERTICAL KEEL  
AND FS960 BULKHEAD INTERSECTION

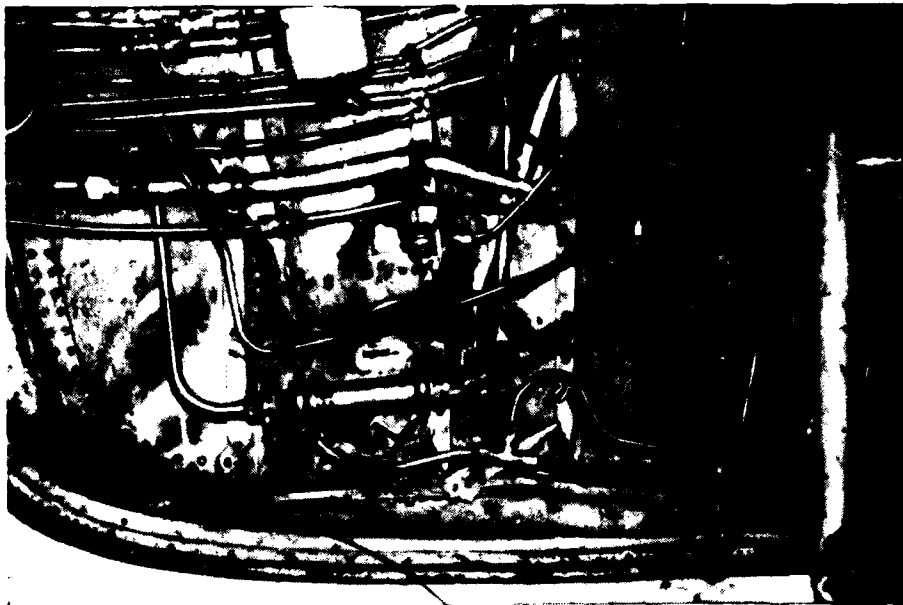


FIGURE 5-9. LEFT HAND LANDING GEAR WHEEL WELL -  
FS820 BULKHEAD, LOOKING FORWARD

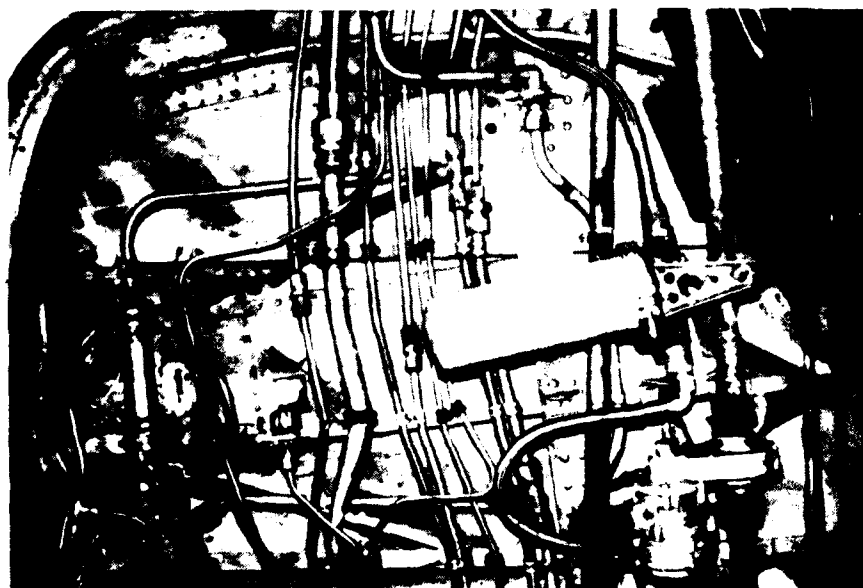


FIGURE 5-10. LEFT HAND LANDING GEAR WHEEL WELL -  
FS820 BULKHEAD - TRACING WEB CRACK



FIGURE 5-11. LEFT HAND LANDING GEAR WHEEL WELL -  
FS820 TRACING WEB CRACK TO FLOOR

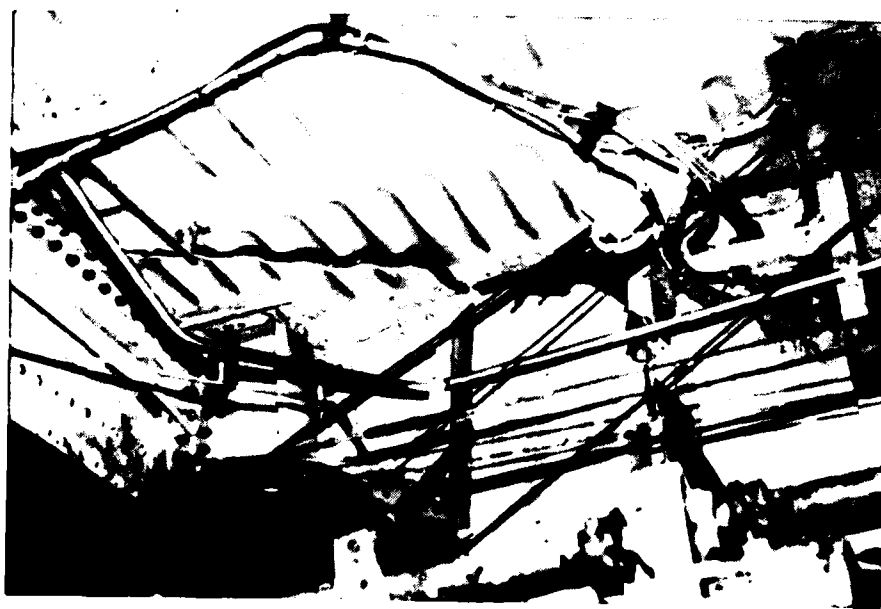


FIGURE 5-12. LEFT HAND LANDING GEAR WHEEL WELL -  
FS820 BULKHEAD - FLOOR INTERSECTION



FIGURE 5-13. CENTERLINE FRAME FRACTURE OF FS620 BULKHEAD - FORWARD CARGO BAY

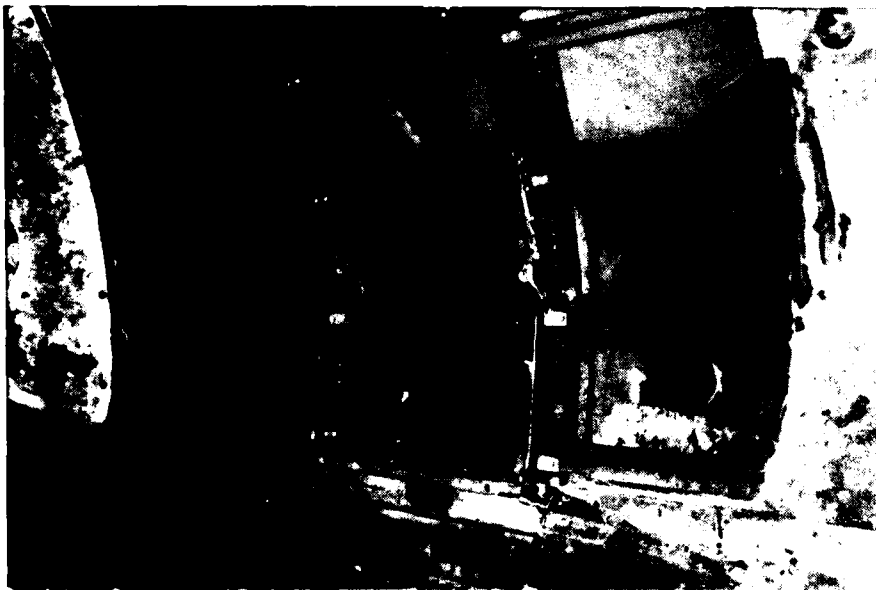


FIGURE 5-14. SIDEWALL FRAME DAMAGE AFT REGION OF FORWARD CARGO BAY (JUST FORWARD OF FS620)



FIGURE 5-15. AFT CARGO BAY LOOKING FORWARD  
TO FS960 BULKHEAD



FIGURE 5-16. CLOSE UP VIEW OF STRINGER/DOUBLER FAILURE  
AT FS960 BULKHEAD



FIGURE 5-17. FS1010 - 1040 FRAME DAMAGE



FIGURE 5-18. FS1100 - 1130 FRAME DAMAGE



more severe in the aft region as compared with the forward cargo bay. The relative severity of damage in the forward and aft region based on the analysis is consistent with the amount of crushing measured along the fuselage. From figure 5-19 it can be seen that the crushed ducting along the wing box keel (FS620-820) indicates that the structure had deflected at least 6 inches. Interior passenger floor damage is depicted in figures 5-20 through 5-24. The bulkhead at the wing trailing edge (FS820) ruptured and pushed the floor at that point up at least 4 inches at the center. The transverse beams and seat tracks have been severed. The frames between FS820 and 960 exhibit damage and an out-board bulge of the fuselage above the floor was noticeable after the impact. Since the onboard seats were not attached, but piled on the floor prior to the test, and no floor accelerations were recorded, it is difficult to ascertain the potential for seat failure throughout the airplane.

The test, conducted at Laurinburg, provided results with regard to structural damage and failure modes for a severe impact. Since the test lacked forward velocity and initial aerodynamic loading, there may be differences in responses when compared to the CID test. Bearing this fact in mind, the results were used to help refine the CID model prior to its planned test. The



FIGURE 5-19. LOWER WING BOX AND KEEL LEFT HAND SIDE VIEW SHOWS CRUSHED DUCTING

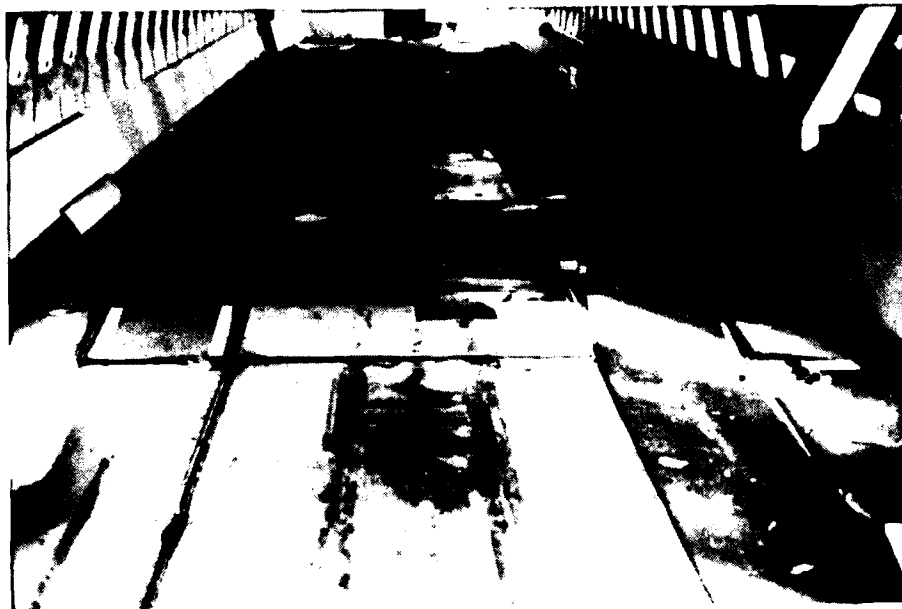


FIGURE 5-20. CABIN FLOOR LOOKING AFT - CENTER  
DECKING REMOVED FS820 TO FS940

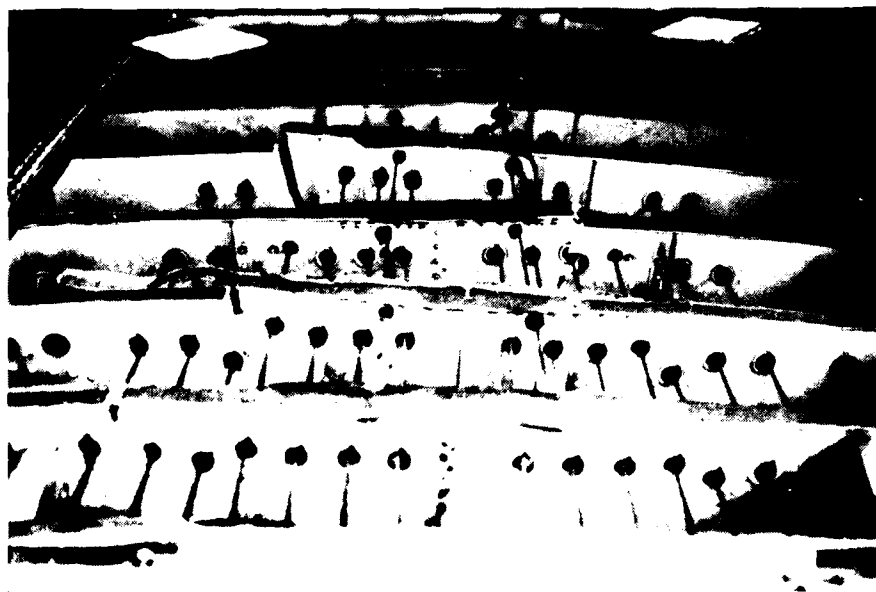


Figure 5-21. CABIN FLOOR TRANSVERSE BEAMS -  
LOOKING AFT FROM FS820



FIGURE 5-22. LOOKING AT LEFT HAND SIDE OF  
FS820 BULKHEAD

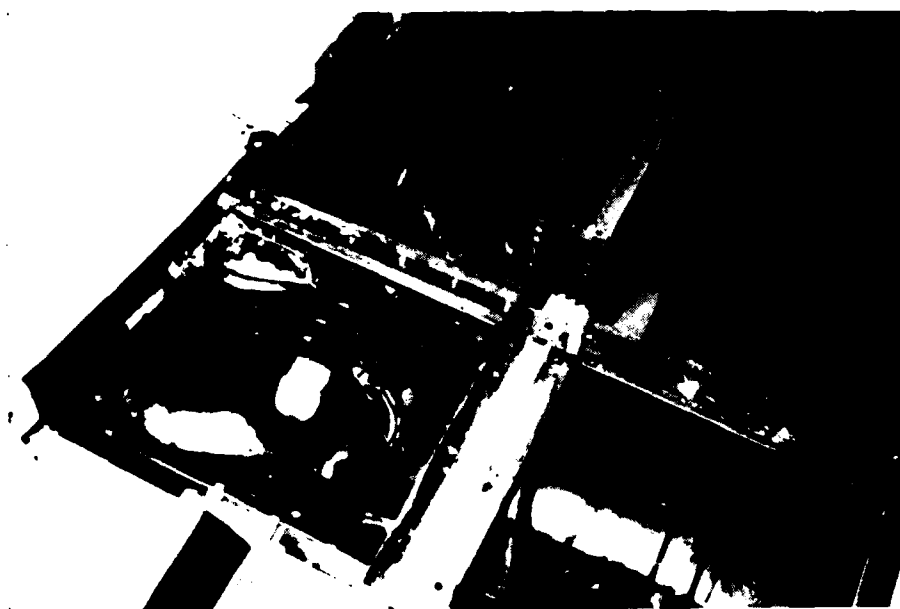


FIGURE 5-23. FRACTURES AT FS820 BULKHEAD AND CABIN FLOOR  
INTERFACE - RIGHT HAND SIDE VIEW



FIGURE 5-24. FRACTURE AT FS820 BULKHEAD AND CABIN FLOOR INTERFACE - CLOSE-UP VIEW

procedure, by which the results were incorporated into the modeling, is described in the following section.

## 5.2 KRASH MODELING OF IMPACT TEST

The CID KRASH stick model, shown in figure 4-2, was modified to reflect the longer B707 airplane. The appropriate weight and c.g. and the available shear and moment interaction curves were modified to reflect strength consistent with the increased size. The crush springs were modified to reflect both the appropriate crushing distribution, as well as the loads that might be experienced, as related to the damage shown in figures 5-3 through 5-24. The stick model results are compared to the test results in table 5-1.

One discrepancy noted in the analysis results versus that of the test is the extremely high moment-shear interaction curve values in the forward fuselage from FS460 to 620. The curves are based on compression failures and, thus, the high ratio exaggerates the damage. Nevertheless the analysis indicates more

TABLE 5-1. QUALITATIVE COMPARISON OF KRASH STICK  
MODEL AND B707 AIRPLANE IMPACT TEST

KRASH ANALYSIS RESULTS	TEST RESULTS
1. High Shear Loads in FS 820-960 Region	Keel damage FS 820-960 Bulkhead Damage at FS 820 and 960. See Figures 5-7 through 5-12 and 5-20 through 5-24.
2. No significant Bending Moment as evidence by low interaction curve levels, particularly in aft fuselage	Cargo Floor damage show evidence of crushing in lower region and frame failures. See Figures 5-13 through 5-18
3. Severe crushing of fuselage aft of MLG bulkhead FS 960 (5" to 6") crush forward of wing leading edge	Damage aft of FS 960 much more extensive than fwd of FS 620. See Figure 5-13 through 5-18, Figure 5-3 and 5-4
4. Approximately 6" to 9" inches of crush in wheel well region	6" Ducting in wheel well region shows evidence of complete crush. See Figure 5-19
5. Shows engine crushing accounts for approximately 10% of the total energy. Outboard engine also contacts ground and contributes to energy absorption	While the inboard engine fails at its upper attach points it remains lodged between wing and ground. See Figures 5-5 and 5-6

damage than is observed from a review of the post-test configuration. The stick model has limitations with regard to matching the level of detail damage experienced during the test. Since the fuselage is represented by only several mass points in the region of interest (FS 300-1200), the overall accelerations are lower than one might anticipate from the nature of abrupt failures noted. Local failures, such as shearing of webs, cannot be represented. Since one beam represents connectivity between major regions of structure, it is difficult for the input data to represent the overall nonlinearities. For example, major floor disruption locally, as occurred at FS820 during the test, would have to be represented by a beam rupture or highly nonlinear behavior. In the math model, this could result in separation of sections. In the test the upper fuselage shell maintains its integrity even though the floor has failed. The expanded CID model has more opportunity to represent discrete failures. However, even that model will have limitations for local failures. The contribution of the B707 impact test results is that it allows for a refinement to the crush representation of the fuselage frames and hard points. These refinements are shown in figures 5-25 and 5-26, respectively. The refinements evolved from several iterations using the KRASH stick model (figure 4-2). The purpose of the

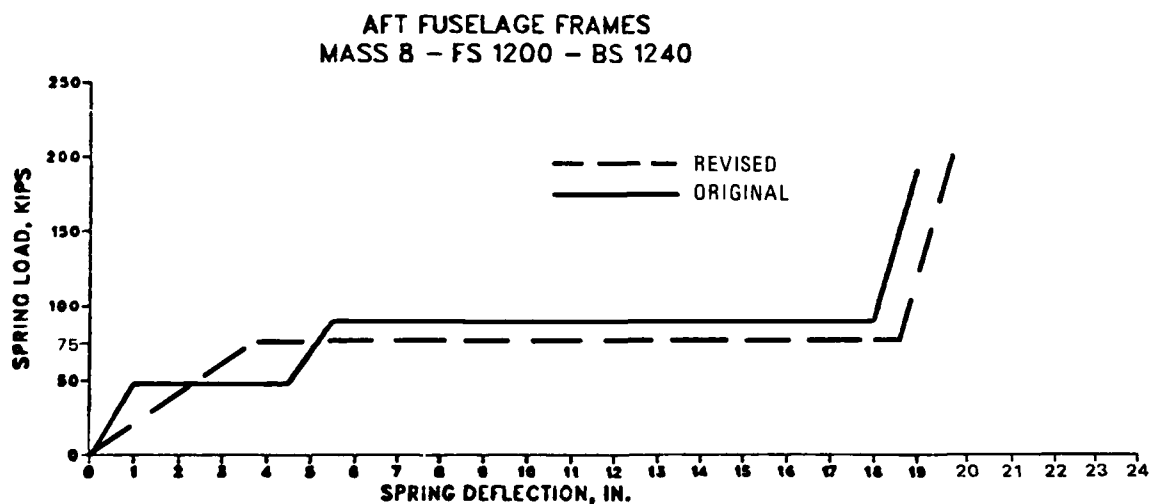
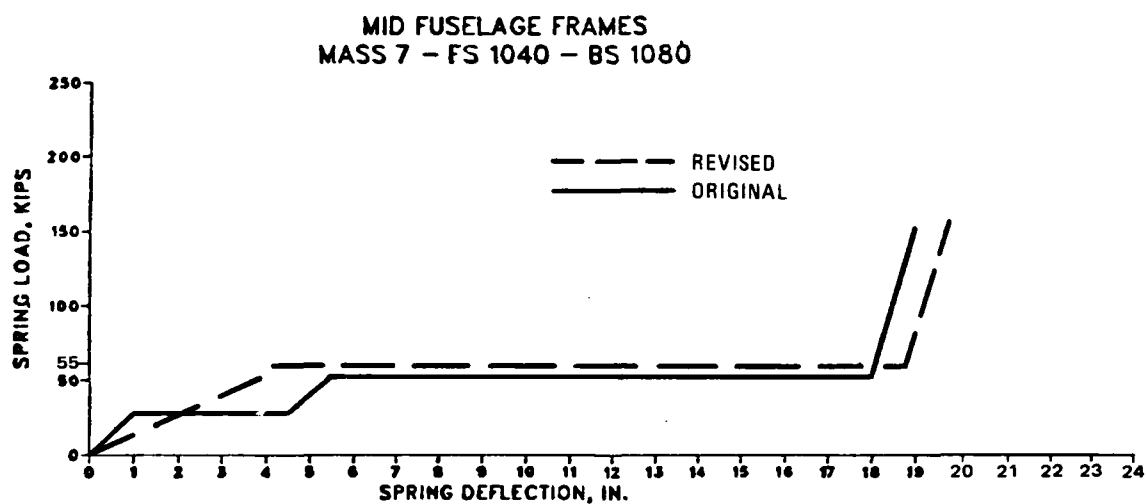
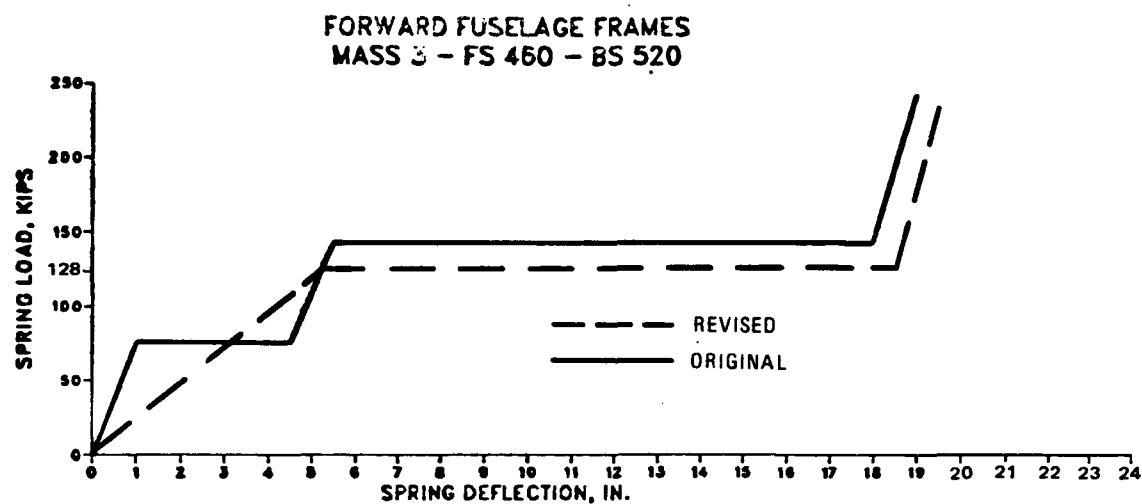


FIGURE 5-25. REVISIONS TO CID MODEL FRAME CRUSH SPRINGS

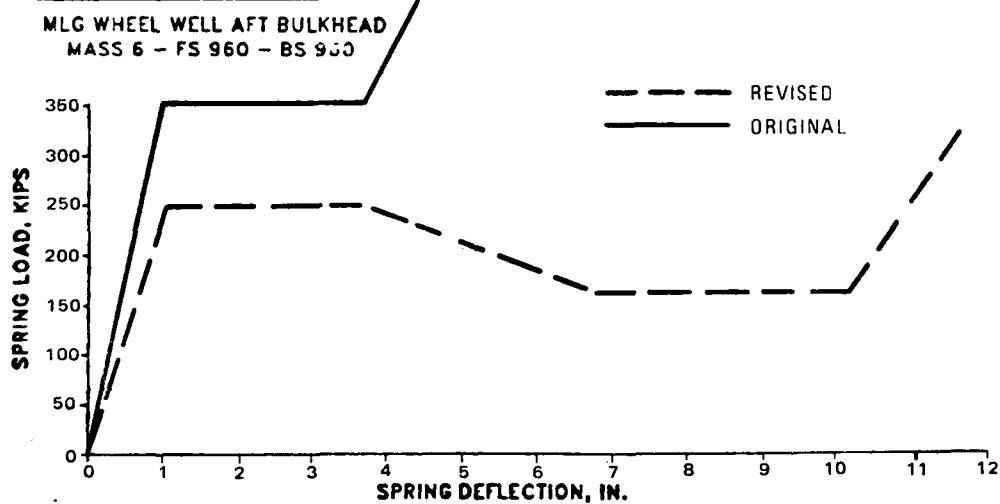
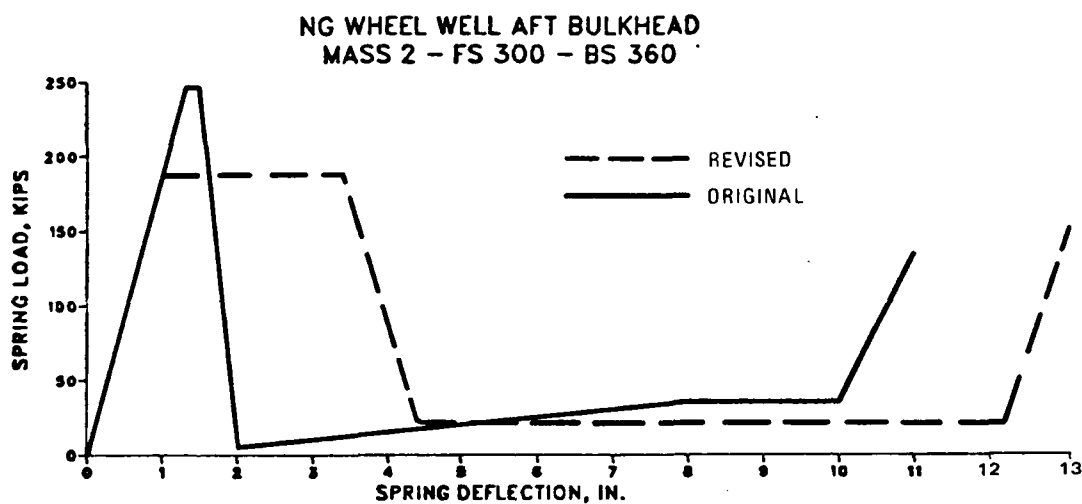
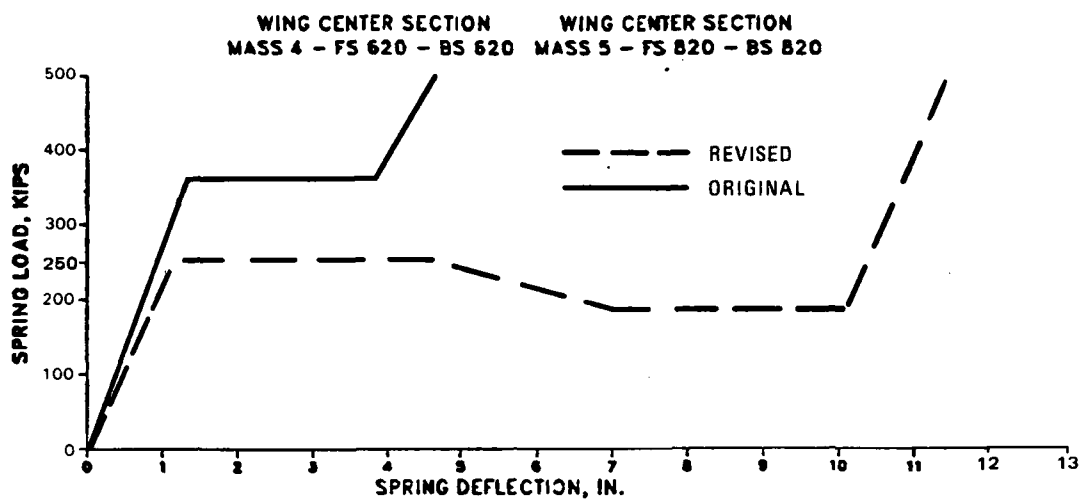


FIGURE 5-26. REVISIONS TO CID MODEL HARD POINT SPRINGS

computer runs was to match the observed fuselage crushing from the test. The most noticeable changes involved the hard point locations. The revised load-deflection curves for these locations (figure 5-26) allow for more deformation and energy absorption prior to restiffening. The frame springs, except for a minor modification in the forward fuselage region, were unchanged. It can be deduced from figures 5-25 and 5-26, that the most significant influence on the results comes from representation of hard point behavior. In particular, the bulkhead springs at FS960, 820 and 620 appear to be the driving forces which influence the damage results.

### 5.3 REVISED CID STICK MODEL RESULTS

Using the revised springs (figures 5-25 and 5-26) the CID stick model shown in figure 4-2, was rerun in the following conditions and sequence:

	<u>Sink Speed</u> <u>Ft/Sec</u>	<u>Forward Velocity</u> <u>(Kts)</u>	<u>Lift</u>
1.	17	0	0
2.	17	0	wing upload, tail download
3.	17	155	wing upload, tail download

The results for conditions one through three are similar to the B707 stick model results, but overall slightly higher. The addition of aerodynamic loading which induces an initial high tail down load and significant wing lift changes the characteristics of the responses somewhat. The most significant change is that the aft fuselage bending increases, while the contribution of shear loads from wing loading is lessened around the wing center box region. A comparison of analysis results for fuselage load-interaction curve (LIC) ratios, acceleration, and fuselage underside crush are shown in table 5-2. LIC values above one indicate that a potential for combined shear moment failure exists. These values are substantially lower than the preliminary results presented in Section 4. The LIC envelopes used in this analysis have higher allowables than those used in Section 4. The LIC envelopes are shown in figures 5-27 through 5-29. The dashed lines indicate the envelopes used in the KRASH



TABLE 5-2. COMPARISON OF ANALYSIS RESULTS  $\Delta$ 

FS	B707*	CID CONDITIONS		
		1	2	3
Load Interaction Curve (LIC) Ratios $\Delta_2$				
350	0.81	0.79	0.69	0.84
620	0.81	0.85	0.83	1.10
960	0.54	0.51	0.68	0.79
990	0.55	0.55	0.80	0.97
1080	0.64	0.58	0.95	1.02
1160	0.72	0.67	0.94	1.05
1240	0.50	0.55	0.70	0.85
1320	0.56	0.53	0.68	0.74
1400	0.74	0.70	0.83	0.89
Peak Vertical Accelerations - g's $\Delta_3$				
300	15. (20.)	16. (19)	18.3 (18.6)	12.5 (17)
460	10.5 (12.7)	10.4 (13)	11.2 (12.8)	12.6 (12)
620	9.2 (9.8)	9.2 (9.8)	10.3 (9.6)	12.1 (9)
820	6.9 (8.0)	6.0 (8.0)	7.4 (8.2)	7.8 (8.5)
960	6.3 (7.6)	6.4 (7.5)	7.2 (8.4)	8. (8.6)
1040	6.5 (7.4)	5.6 (7.4)	6.6 (8.4)	8.6 (8.6)
1200	6.6 (7.8)	6.8 (7.2)	8. (8.2)	9.6 (10)
1400	10.2 (8.2)	9.4 (7.8)	9.5 (9.2)	14. (10)
Maximum Crushing - Inches				
300	5.7	5.2	4.	5.9
460	5.4	5.2	3.7	4.9
620	6.6	6.7	4.8	5.4
820	9.2	9.9	7.3	7.2
960	12.1	12.9	10.2	9.0
1040	14.5	13.5	11.	10.2
1200	7.1	5.7	3.4	2.3
<div>1. 17 ft/sec sink speed, no aero, no fwd. velocity</div> <div>2. 17 ft/sec sink speed, aero, no fwd. velocity</div> <div>3. 17 ft/sec sink speed, aero, fwd. velocity</div> <div>* 17 ft/sec, no aero, no fwd. velocity</div> <div><math>\Delta_1</math> Maximum analysis time = 0.160 seconds</div> <div><math>\Delta_2</math> Based on revised LIC curves (Figures 5-27 through 5-29)</div> <div><math>\Delta_3</math> 50 Hz filtered data</div> <div>( ) Triangular Pulse Peak <math>\sim \frac{\text{Impulse} \times 2}{\Delta t}</math></div>				

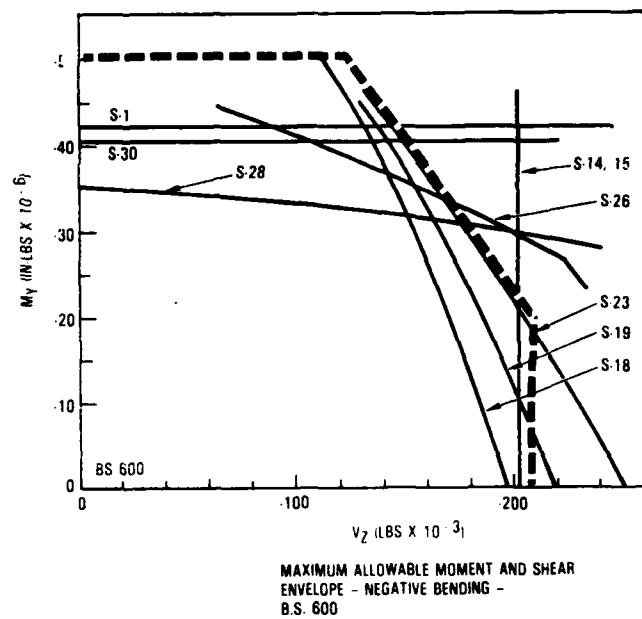
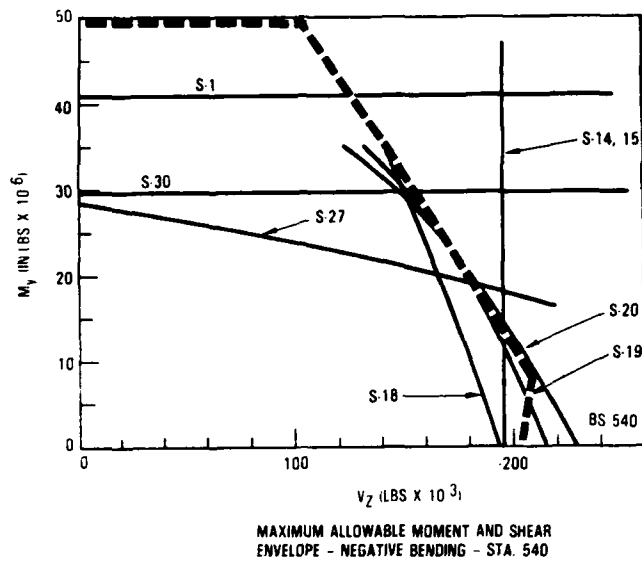
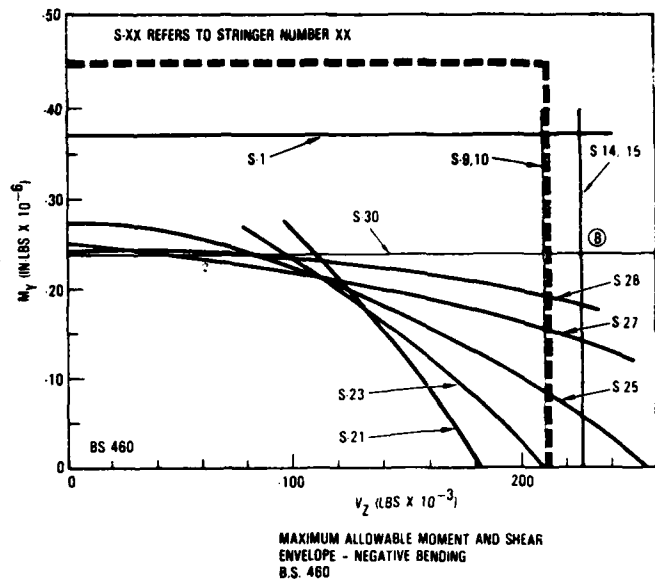
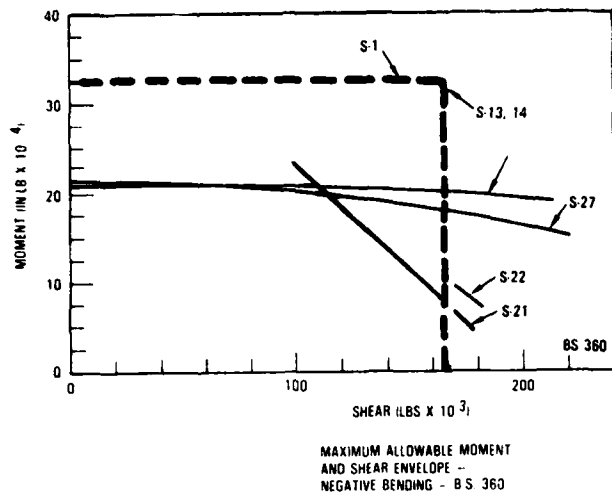
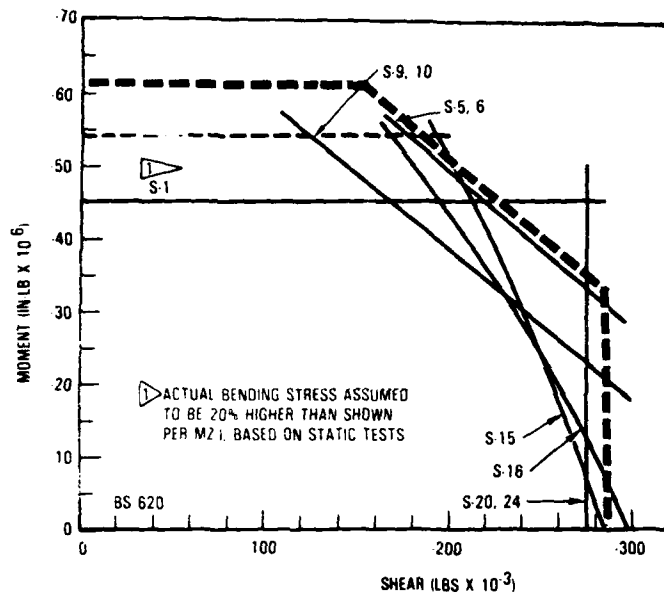
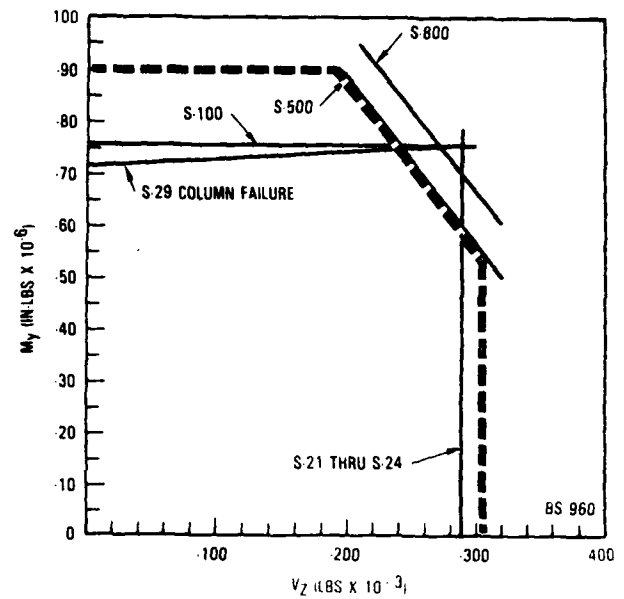


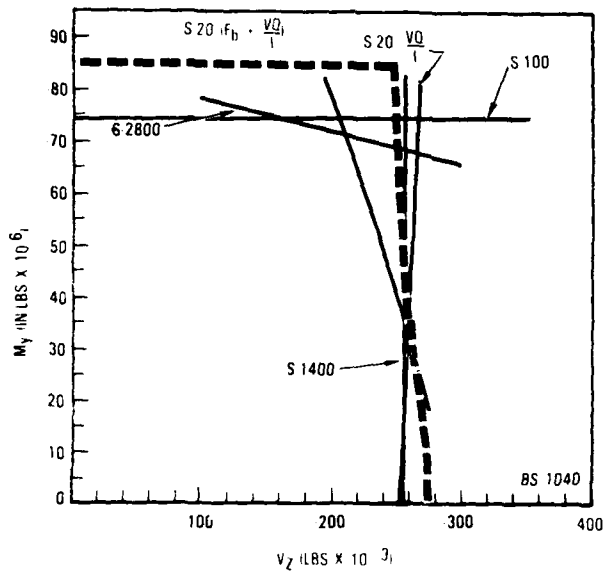
FIGURE 5-27. MAXIMUM ALLOWABLE MOMENT AND SHEAR ENVELOPE -  
NEGATIVE BENDING



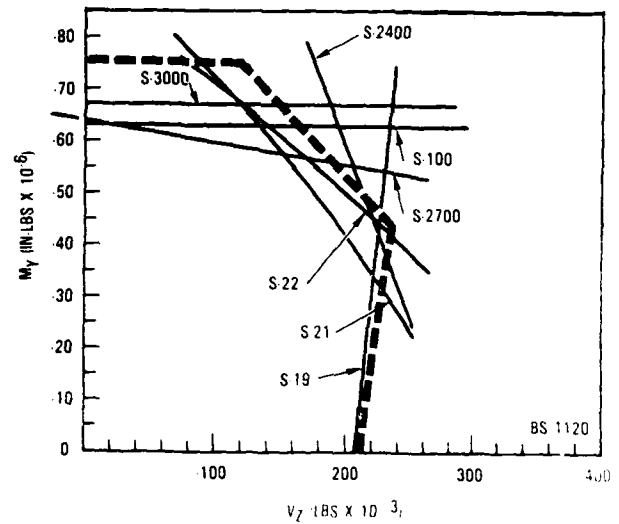
MAXIMUM ALLOWABLE MOMENT AND SHEAR  
ENVELOPE - NEGATIVE BENDING S.S. 620



MAXIMUM ALLOWABLE MOMENT AND SHEAR  
ENVELOPE - NEGATIVE BENDING -  
STATION 960



MAXIMUM ALLOWABLE MOMENT AND SHEAR  
ENVELOPE - NEGATIVE BENDING -  
STATION 1040



MAXIMUM ALLOWABLE MOMENT AND SHEAR  
ENVELOPE - NEGATIVE BENDING -  
STATION 1120

FIGURE 5-28. MAXIMUM ALLOWABLE MOMENT AND SHEAR ENVELOPE -  
NEGATIVE BENDING

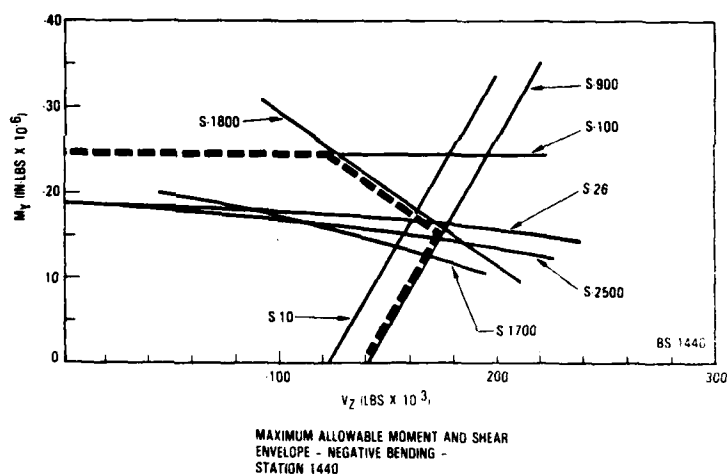
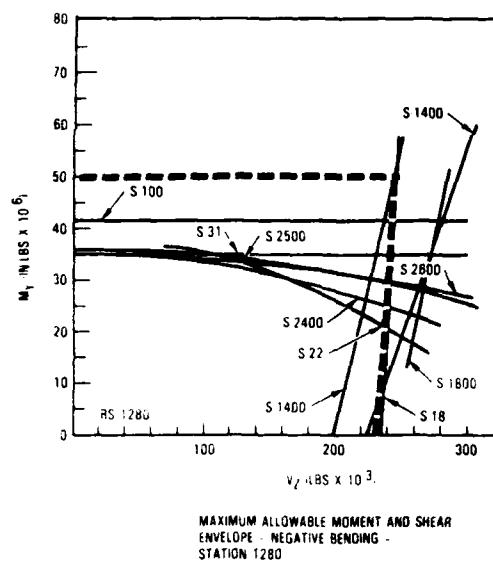
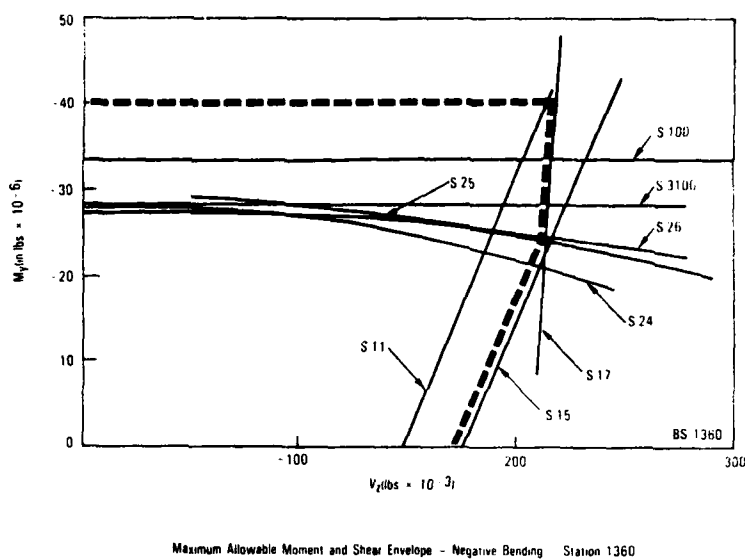
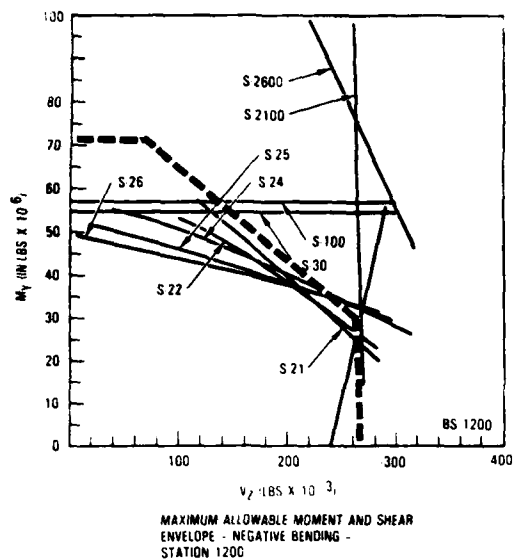


FIGURE 5-29. MAXIMUM ALLOWABLE MOMENT AND SHEAR ENVELOPE -  
NEGATIVE BENDING

analysis to obtain LIC ratios. The rationale behind the selection of the allowables was as follows:

- Critical failure would most likely occur due to tension at the fuselage upper crown (stringer 1) and due to shear at the side (S15-20), or due to some combination of moment and shear.
- Failure at the lower extremities of the fuselage (S30) is due to compression and thus not critical with regard to loss of fuselage structural integrity. Impact with the ground could easily account for crushing of several lower stringers without seriously jeopardizing the shell's protective capability.
- Where test results indicated a strength increase over analysis results, such data were used.

Figures 5-30 and 5-31 show comparisons of the KRASH stick model results between the use of the original load-deflection curves and LIC's (Section 4 Analysis) versus the revised load-deflection and LIC data described earlier in this section. The data envelope plotted includes the B707 Laurinburg drop test analysis as well as the three B720 conditions noted in Table 5-2. Figure 5-30 shows the peak vertical acceleration for the equivalent triangular pulse. As noted earlier the equivalent triangular pulse is obtained by integrating the acceleration data over the time period of interest. This yields an average acceleration, which when multiplied by two provides the equivalent peak for a triangular shaped pulse for the duration of the interval being considered. The presentation of the data in this form provides for a more consistent interpretation of the response. If only peaks are used then the question of whether the peak was plotted has to be resolved as well as how long the peak value is sustained. If filtered acceleration data is used then the filter characteristics (i.e., cut-off frequency and decay rate) can influence the results. From Figure 5-30 it can be observed that the revised load-deflection curve produce lower acceleration values. Since the revised curves tend to have lower peak forces, the aforementioned results appear to be consistent. The longitudinal pulse for condition no. 3 (Table 5-2) is also shown in Figure 5-30, since that is the only case run which included a forward velocity. The peak longitudinal acceleration is approximately 4g throughout the fuselage. Figure 5-31 compares the LIC ratios and crush distances. The results from the use of revised load-deflection data show lower LIC ratios and greater crush distances, both of which are consistent with the "Laurinburg" test results.

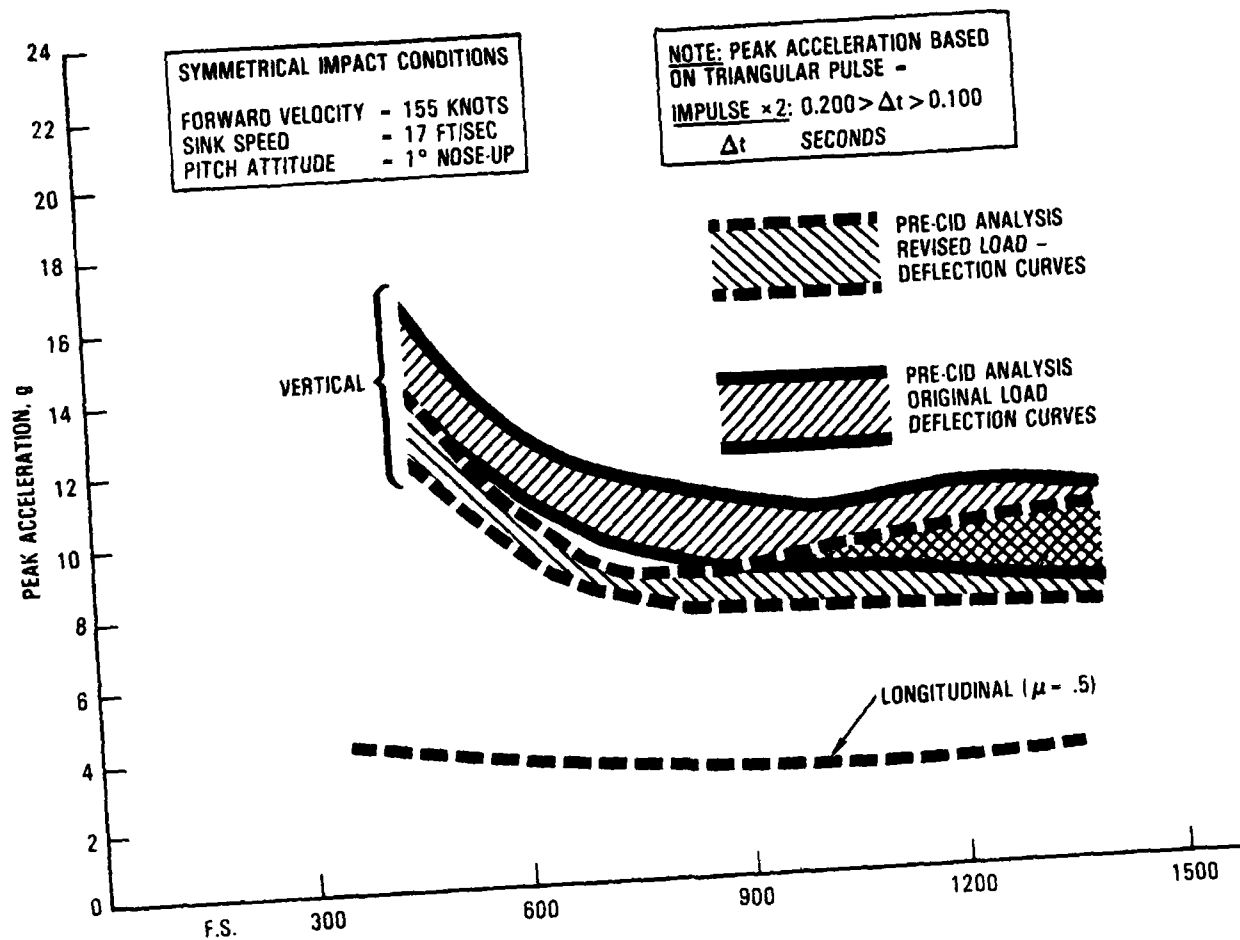


FIGURE 5-30. COMPARISON OF PRE-CID KRASH STICK MODEL ANALYSES ACCELERATION RESULTS - FOR PLANNED SYMMETRICAL IMPACT CONDITION, ORIGINAL VERSUS REVISED LOAD DEFLECTION CURVES

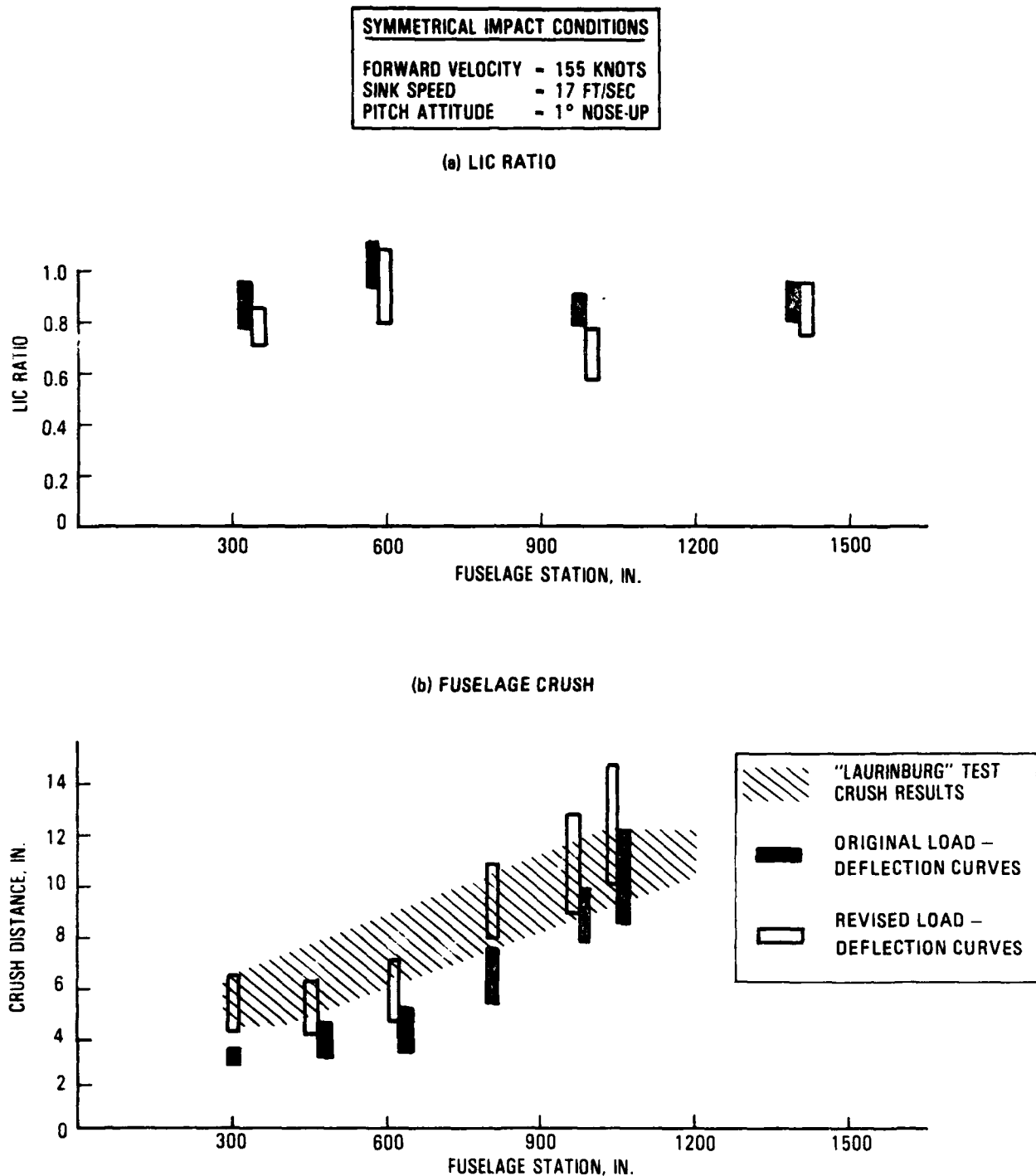


FIGURE 5-31. COMPARISON PRE-CID KRASH STICK MODEL LIC AND FUSELAGE CRUSH FOR THE PLANNED IMPACT CONDITION - ORIGINAL VERSUS REVISED LOAD-DEFLECTION CURVES

Figures 5-32 through 5-39 show representative KRASH analysis acceleration responses along the fuselage for condition no. 3, Table 5-2. From the data presented in these figures it can be observed that for the KRASH model results:

- differences exist in the peak acceleration values between unfiltered and filtered (50 Hz) data,
- at a particular location the pulse that is observed cannot always be described as a standard shape (i.e. triangular, trapezoidal),
- the plot interval selected may not provide the maximum value, and
- the impulse data provides a better indication of the overall pulse definition, and is independent of plot interval and/or filter characteristics.

Using the data at FS820 (figure 5-35), for example, the difference between plotted peak acceleration values is 7.753 g filtered vs 9.037 g unfiltered ( ~14 percent). The time history response indicates two or three acceleration peaks. However, from the mass impulse data an average acceleration of  $\approx 4$  g for a duration of .150 seconds can be surmised. An equivalent triangular pulse value of 8 g with a .150 second base duration is representative of the vertical pulse. Correspondingly, a 3.8 g triangular pulse of .150 second base duration is representative of longitudinal acceleration at this location. The response of the seat/occupant system is best evaluated in the manner described in Section 4.3, since the airframe pulse is not a definitive sinusoidal, trapezoidal or triangular shape.



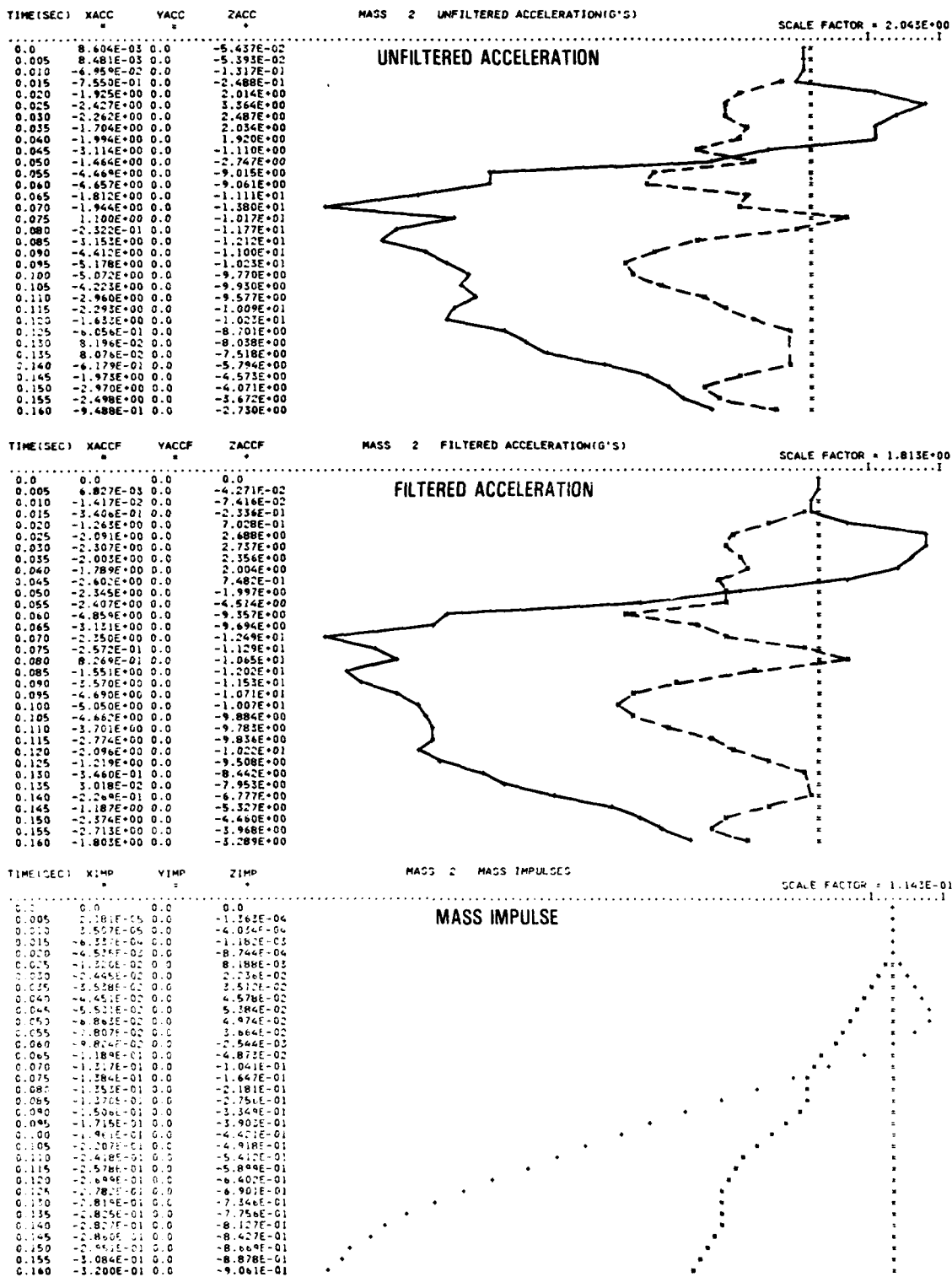


FIGURE 5-32. ACCELERATION RESPONSE AT FS300, CONDITION NO. 3

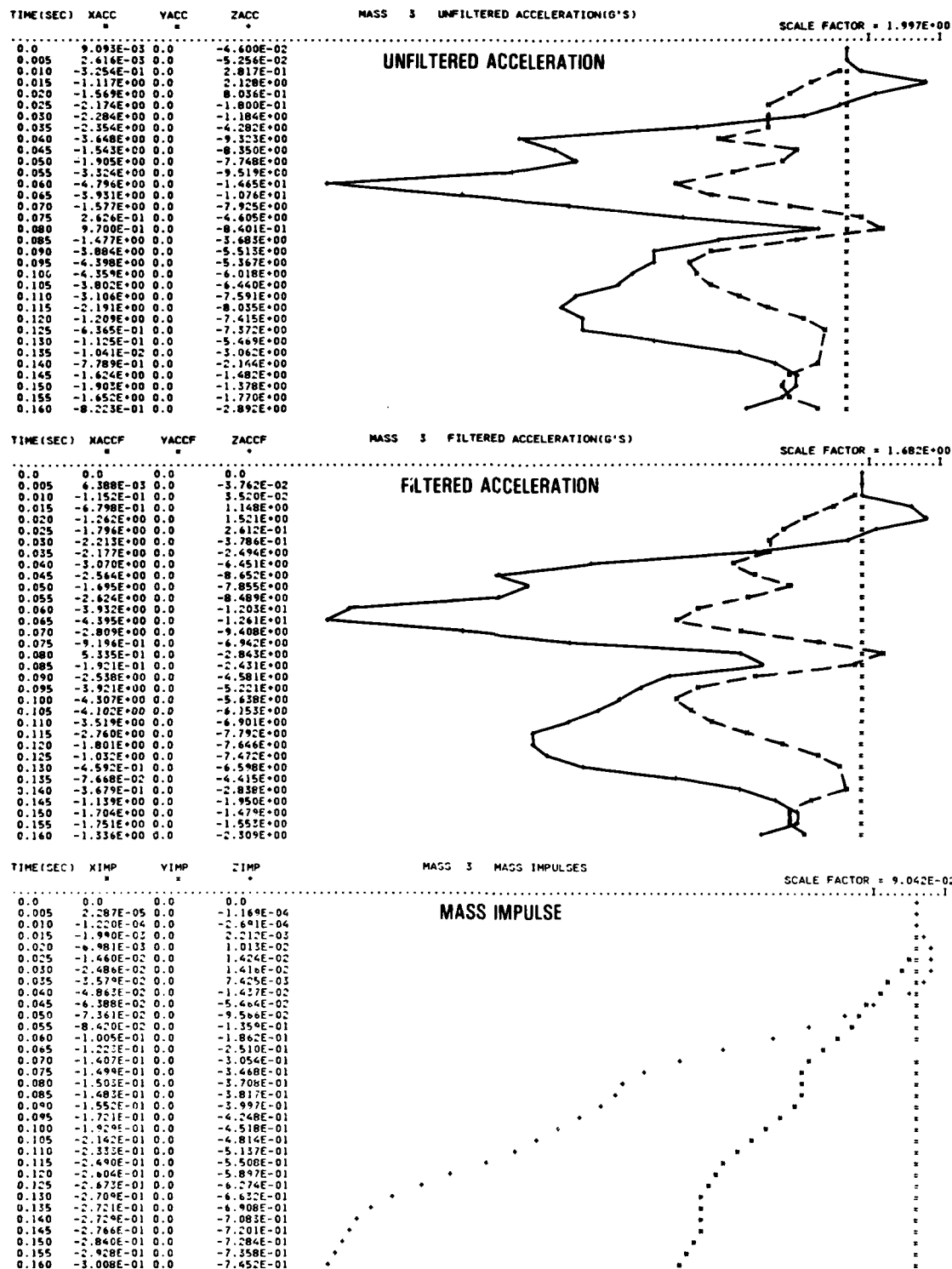


FIGURE 5-33. ACCELERATION RESPONSE AT FS460, CONDITION NO. 3

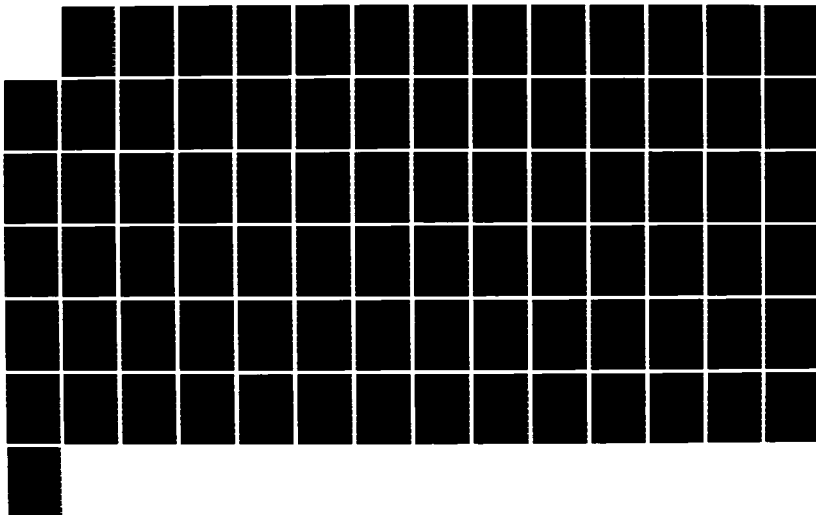
AD-A168 975

KRASH DYNAMICS ANALYSIS MODELING - TRANSPORT AIRPLANE  
CONTROLLED IMPACT D. (U) LOCKHEED AIRCRAFT CORP BURBANK  
CALIF 8 MITTLIN ET AL. MAR 86 LR-38776 DOT/FAA/CT-85/9  
DTFA83-84-C-80004 F/G 1/2

2/2

UNCLASSIFIED

NL





UNIT 1

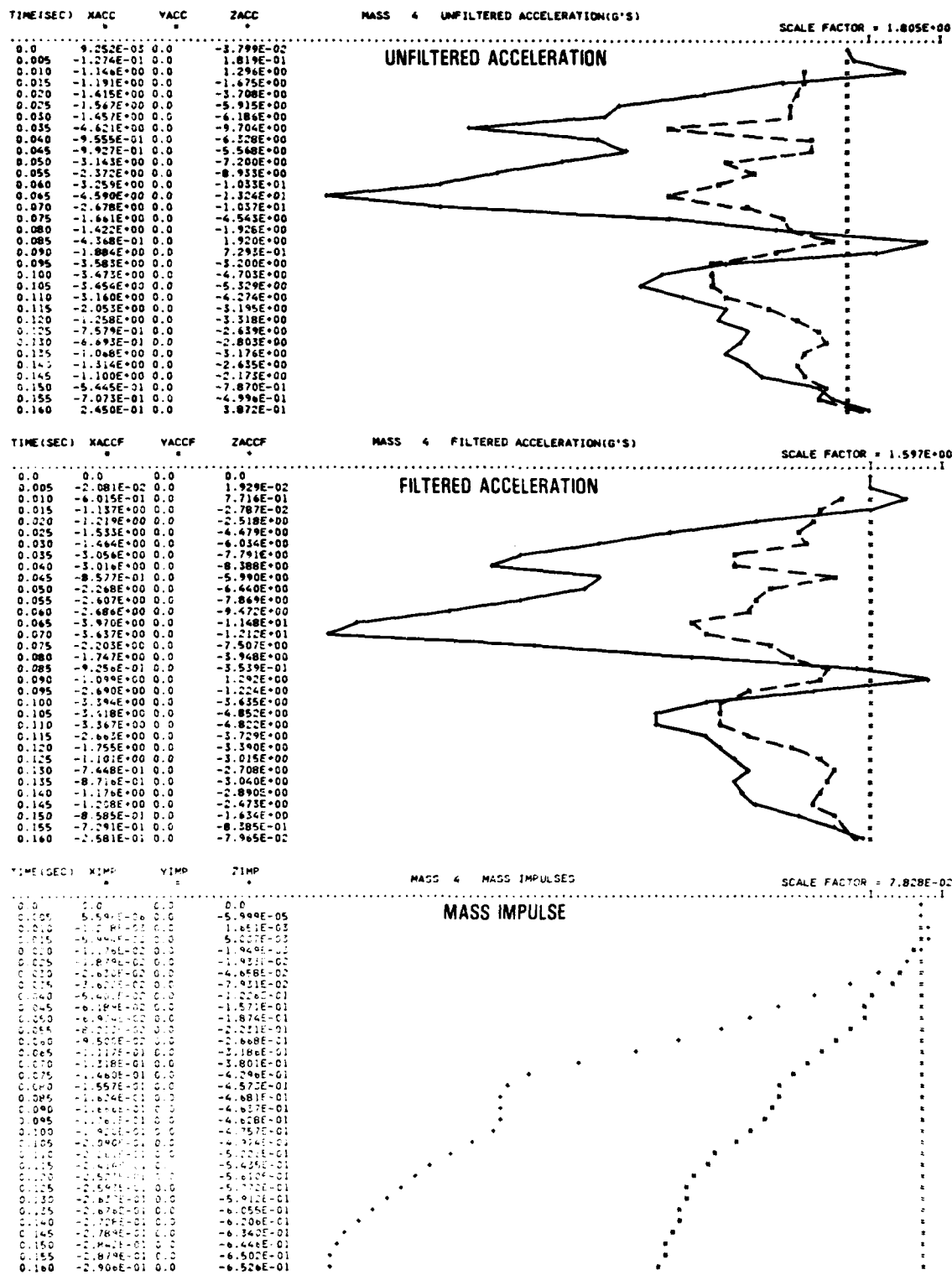


FIGURE 5-34. ACCELERATION RESPONSE AT FS620, CONDITION NO. 3

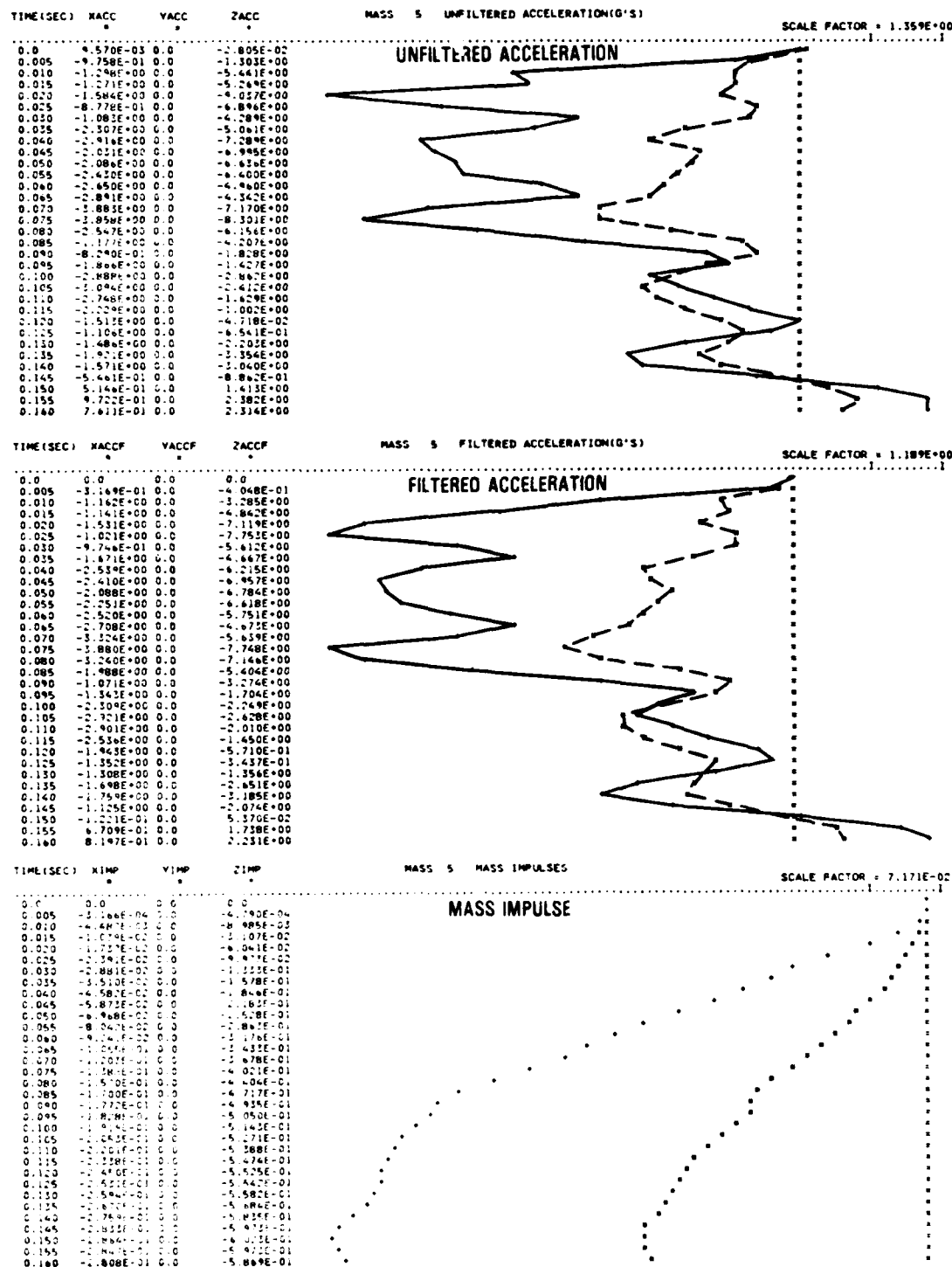


FIGURE 5-35. ACCELERATION RESPONSE AT FS820, CONDITION NO. 3

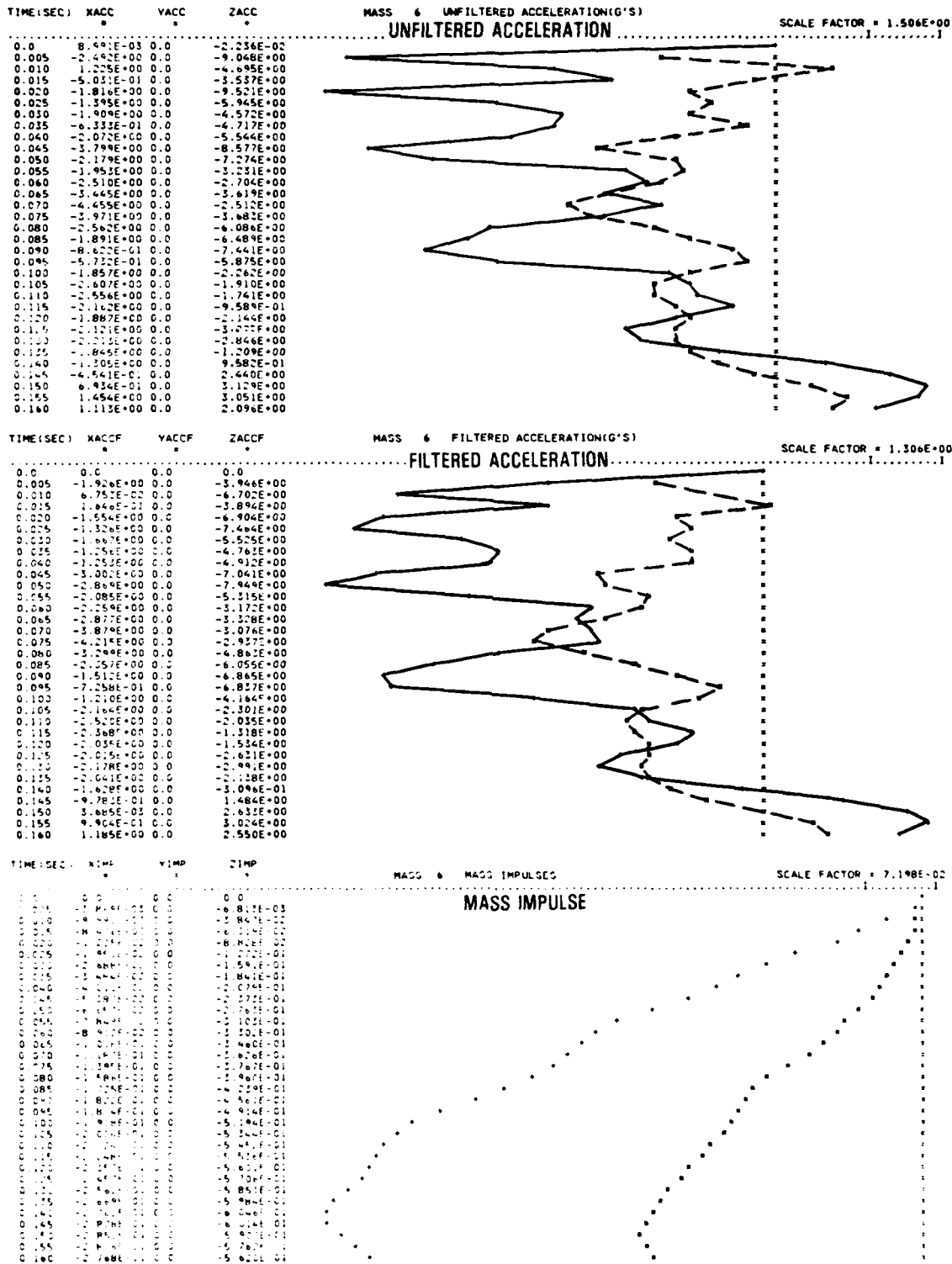


FIGURE 5-36. ACCELERATION RESPONSE AT FS960, CONDITION NO. 3

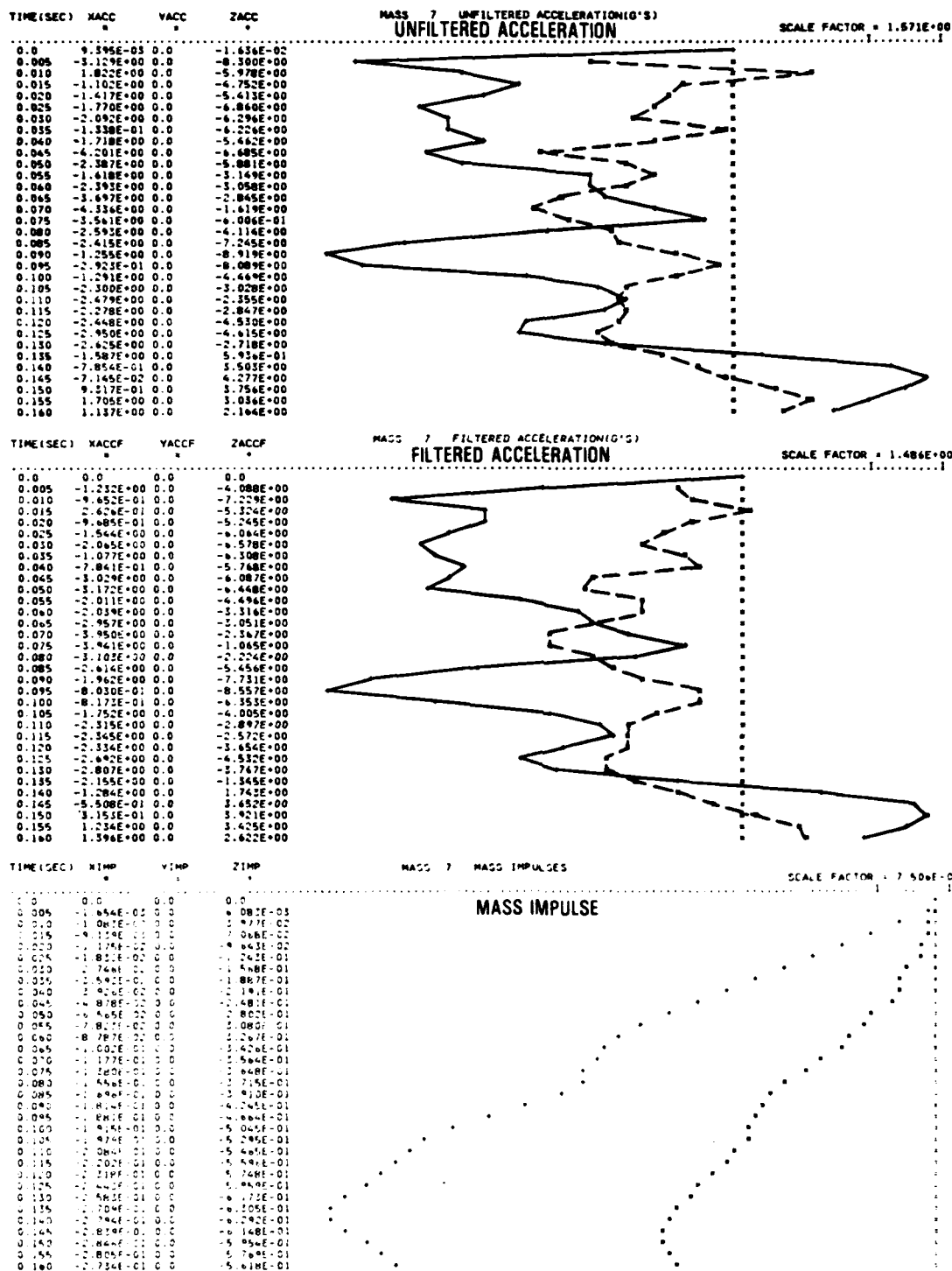


FIGURE 5-37. ACCELERATION RESPONSE AT FS1040, CONDITION NO. 3



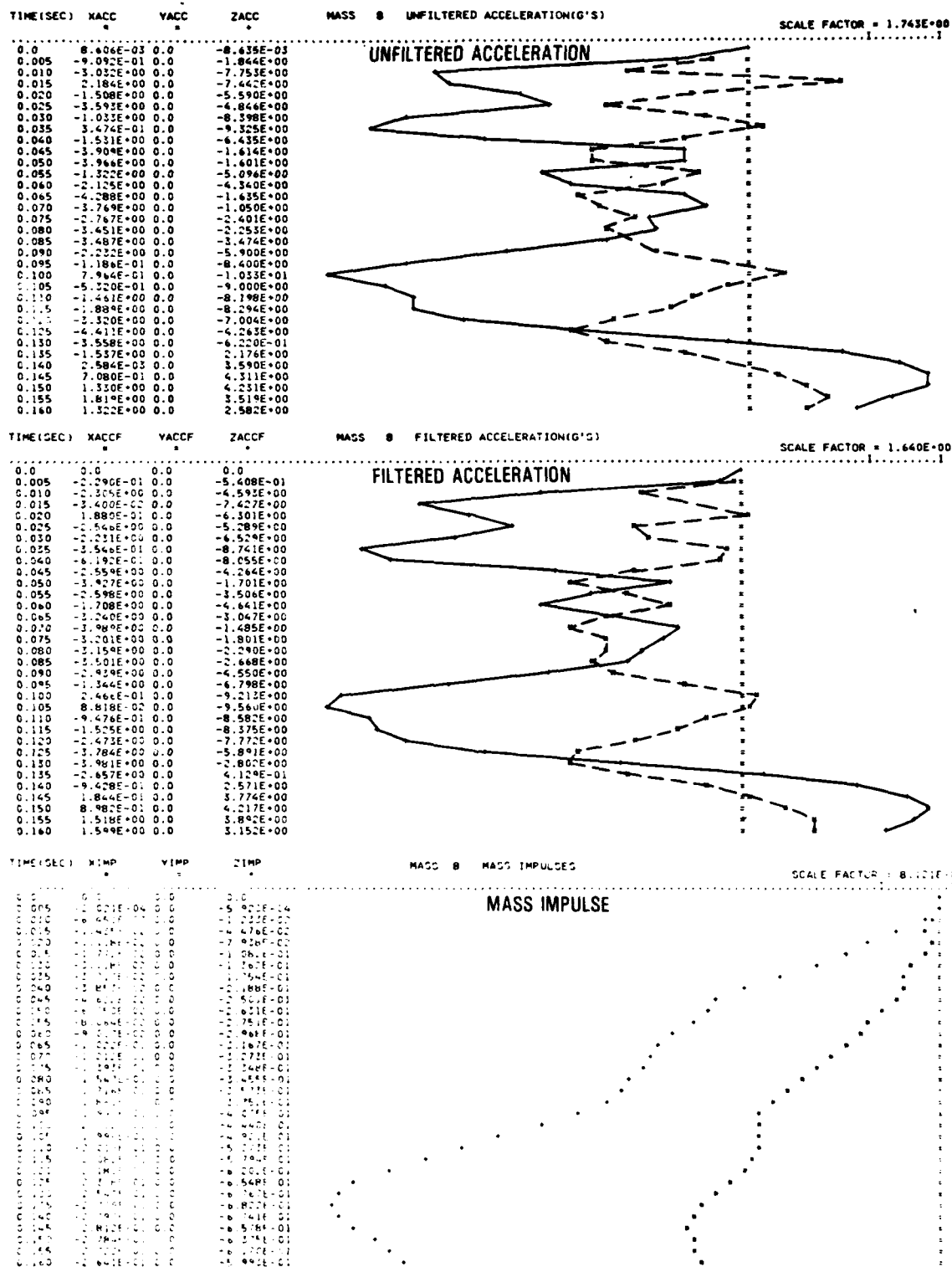


FIGURE 5-38. ACCELERATION RESPONSE AT FS1200, CONDITION NO. 3

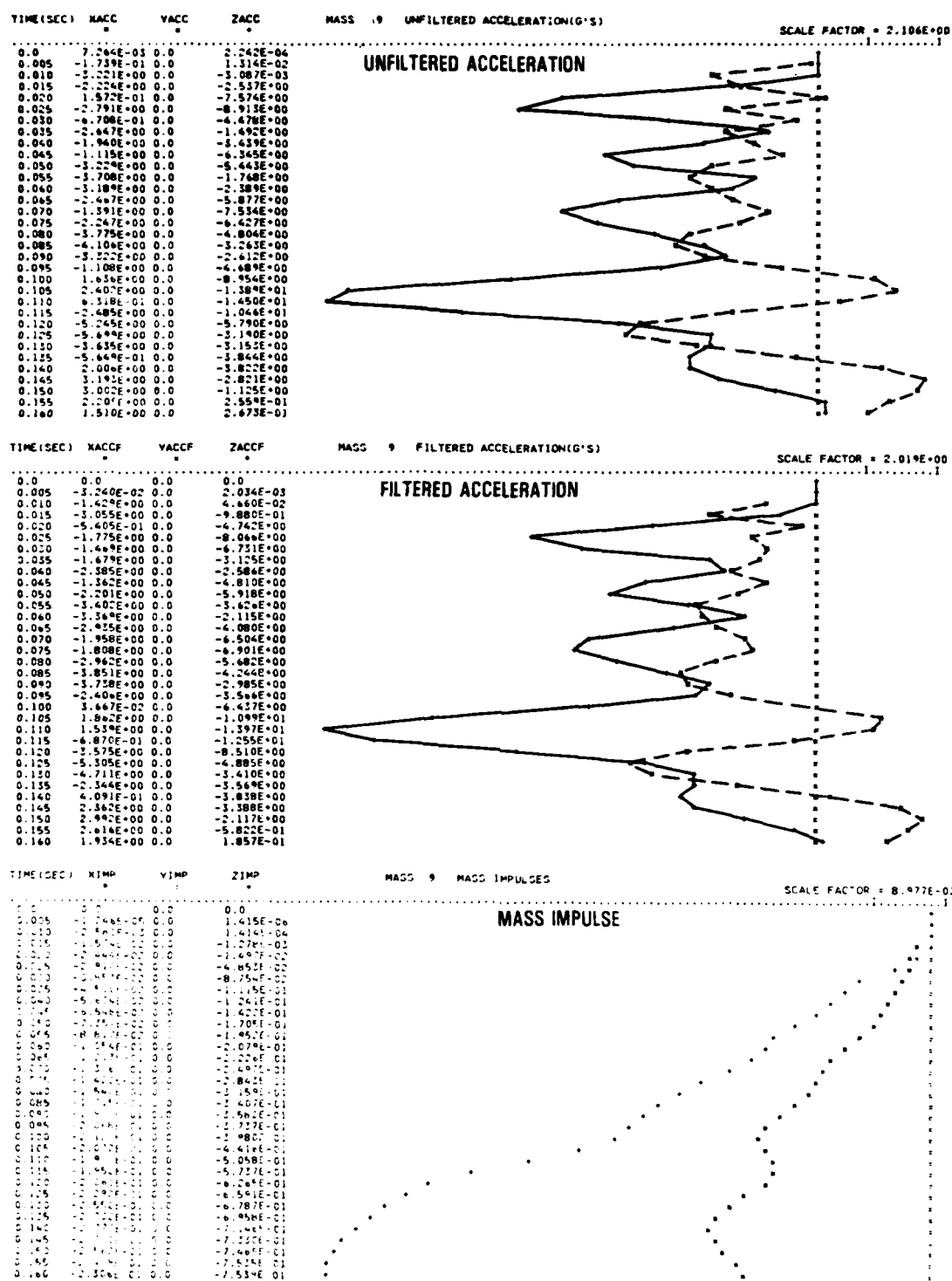


FIGURE 5-39. ACCELERATION RESPONSE AT FS1400, CONDITION NO. 3

## SECTION 6

### CID PRE-TEST ANALYSIS

#### 6.1 KRASH MODEL

The expanded KRASH model for the CID test, shown in figure 6-1, is a symmetrical half-airplane representation consisting of 48 masses and 137 beam elements. The overall weight, c.g., and stiffnesses are compared with similar characteristics for the 19 mass 18 beam stick model (figure 4-2). The initial static deflections were obtained using the IC coding (via NASTRAN) for both the stick and expanded models. A comparison of these results is shown in table 6-1. The expanded model shows approximately 2.4 inches more deflection at the extreme forward fuselage station as compared to the stick model which is attributed to differences in stiffness and/or initial loading between the two models. At the wing and aft fuselage locations the initial static deflections for both the stick and expanded models are in good agreement. Subsequent expanded model changes to improve the fuselage stiffness representation and wing representation shows better agreement with regard to static deflections (<1.0 inch difference), as noted in parentheses in Table 6-1. Since these changes were incorporated after the study was concluded, the analysis results described in this section are based on the more flexible model. A comparison of model parameters for the stick and expanded models is shown in figure 6-2. The models show good agreement with regard to weight, cg, mass inertia and overall vehicle forces. The overall vehicle forces and accelerations show the six net loads at the airplane c.g., and the resulting six rigid body accelerations. In KRASH those c.g. accelerations are used to calculate the rigid body accelerations at each mass point in the model. These mass point accelerations yield inertia relief loads at each mass point. When these inertia relief loads are calculated in KRASH and included in the total airplane force moment balance, the net c.g. loads and accelerations should ideally be zero. For both models they are

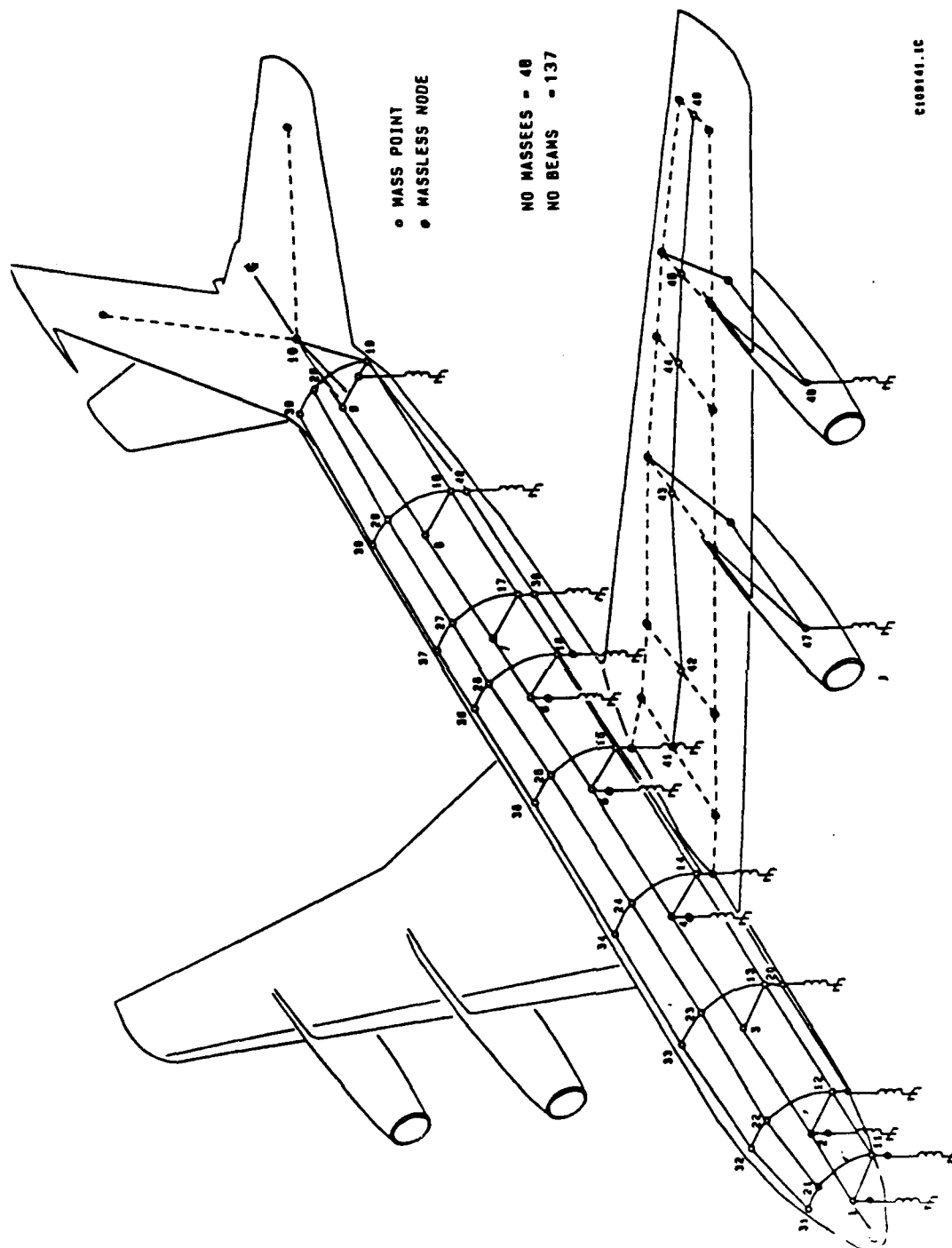


FIGURE 6-1. EXPANDED CID KRASH MODEL.

TABLE 6-1. STATIC DEFLECTIONS

LOCATION	DEFLECTION, in.		DIFFERENCE IN inches
	STICK MODEL FIG. 4-1	CID MODEL FIG. 6-1	
<b><u>FUSELAGE</u></b>			
FS 199	-1.07	-3.42 (-1.90)	2.35 (0.83)
FS 300	-0.83	-2.99 (-1.71)	2.09 (0.88)
FS 460	-0.45	-2.25 (-1.35)	1.80 (0.90)
FS 620	-0.16	-1.32 (-0.80)	1.16 (0.64)
FS 820	0	0 (0)	0 (0)
FS 960	-0.21	-0.03 (-0.09)	0.18 (0.12)
FS 1040	-0.49	-0.16 (-0.23)	0.33 (0.26)
FS 1200	-1.25	-0.94 (-0.99)	0.31 (0.26)
FS 1400	-2.65	-2.54 (-2.57)	0.11 (0.08)
FS 1570	-4.07	-4.03 (-4.10)	0.04 (0.03)
<b><u>WING</u></b>			
Root	+0.81	+0.61 (+0.65)	0.20 (0.18)
Tip	+40.5	+41.2 (+39.9)	0.70 (0.60)
+ upward displacement - downward displacement (XXX) REVISED MODEL RESULTS			

extremely small, which is satisfactory. The analysis results using the KRASH stick model have been presented in Section 5.0. The pre-CID analysis results using the expanded KRASH model are described in this section. The variations in allowing failure as opposed to yielding that were investigated using the expanded model are summarized in the following table:

Condition	Number of Masses	Number of Beams	Number of Nonlinear Beams	Aerodynamic Loading
1	48	137	44	Yes
2	48	137	19	Yes
3	48	137	19	No

(A) Stick

MODEL PARAMETERS

VEHICLE MT = 1.924740D 05

VEHICLE CG POSITION

X (FS) = 8.44728D 02

Y (BL) = 0.0

Z (WL) = 2.18312D 02

VEHICLE INERTIAS (IN-LB-SEC\*\*2)

I(XX) = 3.54622D 07

I(VY) = 3.92783D 07

I(ZZ) = 7.32031D 07

I(XY) = 0.0

I(YZ) = 0.0

I(XZ) = 2.31423D 06

VEHICLE CG INITIAL GROUND COORDINATES

XCG IS THE DISTANCE FROM SLOPE/GROUND INTERSECTION TO VEHICLE CG,+FORWARD

ZCG IS THE DISTANCE FROM GROUND PLANE TO VEHICLE CG,+DOWN

XCG = 0.0

ZCG = -8.55505D 01

OVERALL VEHICLE FORCES AND ACCELS(G-S), A/P AXES

FX= 1.66961D 03 AX= 8.67446D-03

FY= 0.0 AY= 0.0

FZ= -5.17204D 03 AZ= -2.68714D-02

MX= 0.0 PDT= 0.0

MY= 7.50458D 05 QDT= 1.91062D-02

MZ= 0.0 RDT= 0.0

OVERALL VEHICLE FORCES AND ACCELS(G-S), INCLUDING INERTIA RELIEF, A/P AXES

FX= 4.12115D-13 AX= 2.14115D-18

FY= 0.0 AY= 0.0

FZ= 1.09139D-11 AZ= 5.67034D-17

MX= 0.0 PDT= 0.0

MY= 4.94765D-10 QDT= 1.25964D-17

MZ= 0.0 RDT= 0.0

(B) Expanded

MODEL PARAMETERS

VEHICLE MT = 1.924746D+05

VEHICLE CG POSITION

X (FS) = 8.44131D+02

Y (BL) = 0.0

Z (WL) = 2.13005D+02

VEHICLE INERTIAS (IN-LB-SEC\*\*2)

I(XX) = 3.43332D+07

I(VY) = 3.82381D+07

I(ZZ) = 7.17985D+07

I(XY) = 0.0

I(YZ) = 0.0

I(XZ) = 1.67203D+06

VEHICLE CG INITIAL GROUND COORDINATES

XCG IS THE DISTANCE FROM SLOPE/GROUND INTERSECTION TO VEHICLE CG,+FORWARD

ZCG IS THE DISTANCE FROM GROUND PLANE TO VEHICLE CG,+DOWN

XCG = 0.0

ZCG = -7.94658D+01

OVERALL VEHICLE FORCES AND ACCELS(G-S), A/P AXES

FX= 2.51821D+03 AX= 1.30833D-02

FY= 0.0 AY= 0.0

FZ= -5.07993D+03 AZ= -2.63927D-02

MX= 0.0 PDT= 0.0

MY= 2.42083D+05 QDT= 6.33095D-03

MZ= 0.0 RDT= 0.0

OVERALL VEHICLE FORCES AND ACCELS(G-S), INCLUDING INERTIA RELIEF, A/P AXES

FX= 1.76215D-12 AX= 9.15521D-18

FY= 0.0 AY= 0.0

FZ= 1.36424D-11 AZ= 7.08791D-17

MX= 0.0 PDT= 0.0

MY= 1.33878D-09 QDT= 3.50116D-17

MZ= 0.0 RDT= 0.0

FIGURE 6-2. KRASH MODELS PARAMETERS

The echo of input data for the CID model is provided in Appendix Section A-4 for condition 1 which considers an initial aerodynamic lift distribution.

The load interaction curves described in Section 5.3 were used to compare static (time = 0) internal beam loading for both the stick and expanded model. These results are presented in table 6-2. With the exception of the ratios at the wing leading (FS 620) and trailing edge (FS 820) attachments to the fuselage, all the ratios are in excellent agreement. As in the comparison of static deflections the subsequent revised expanded, not used in the analysis, showed some improvement as noted by the numbers in parentheses in Table 6-2. The major contributor to the LIC ratio difference is the manner in which the wing attaches to the fuselage for each model. In the stick model, one beam connects the wing root to the fuselage centerline. In the expanded model, the wing root is represented as a box beam which connects at two locations to the fuselage at FS 620 and with two more beams at FS 820. The effect of these modeling differences will be pursued in the post-CID analyses.

The stick and expanded models also show comparable pertinent wing and fuselage fundamental frequencies and mode shapes, which are also in agreement with published airplane data (Reference 16). A summary of pertinent free-free modal frequencies is noted in the following table.

Mode	Frequency, Hz		
	Stick Model	Expanded Model	Reference (16) Data
Wing vertical bending	1.03	1.04	1.09
Fuselage vertical bending	3.37	3.29	3.19 - 3.40

Each Model contains the same mass and beam designations, but differ either in external force loading or treatment of post-failure loads. Each of the analyses was performed to a simulated .160 second impact, which encompasses the time for peak responses to occur. A description of the masses and beams for

TABLE 6-2. COMPARISON OF BEAM INITIAL LIC RATIOS

CURVE NO.	FUSELAGE STATION	LOAD INTERACTION CURVE RATIO	
		STICK MODEL	EXPANDED MODEL
1	300	0.011	0.009 (0.009)
2	350	0.061	0.062 (0.062)
3	450	0.058	0.052 (0.052)
4	480	0.122	0.120 (0.118)
5	540	0.122	0.120 (0.118)
6	600	0.124	0.121 (0.121)
7	620	0.151	0.258 (0.233)
8	820	0.209	0.360 (0.326)
9	820	0.426	0.431 (0.429)
10	960	0.203	0.205 (0.204)
11	960	0.203	0.205 (0.204)
12	1000	0.249	0.251 (0.250)
13	1080	0.245	0.248 (0.247)
14	1160	0.273	0.276 (0.275)
15	1240	0.190	0.192 (0.191)
16	1320	0.158	0.163 (0.162)
17	1400	0.199	0.203 (0.202)
18	1400	0.177	0.181 (0.181)
( ) REVISED MODEL RESULTS			

the CID models is shown in tables 6-3 and 6-4, respectively. The diagonal beams (beam numbers 90-137) are tension only members to account for shear loads between frames and m bulkheads.

TABLE 6-3. CID MODEL MASS DESCRIPTION

MASS NO.	REPRESENTATION
1 - 19, 20, 30, 40	Floor, occupant and lower fuselage
21 - 29, 31 - 39	Upper Fuselage shell and cabin
41 - 46	Wing
47, 48	Inboard, outboard engines



TABLE 6-4. CID MODEL BEAM DESCRIPTIONS

BEAM NO.	BEAM CONNECTIVITY	REPRESENTATION
1-9	1-11, 2-12, ..., 9-19	Floor transverse beams
10-27	11-21, ..., 19-29, 21-31, ..., 29-39	Upper shell frames
28, 29, 30	13-20, 17-30, 18-40	Lower shell vertical beams
31-38	21-22, ..., 28-29	Upper shell longitudinal beams
39-46	31-32, ..., 38-39	Upper shell longitudinal beams
47-54	1-2, ..., 8-9	Inboard floor longitudinal beams
55-62	11-12, ..., 18-19	Outboard floor longitudinal beams
63	9-10	Horizontal stabilizer - cabin
64-68	12-20, ..., 19-40	Lower fuselage longitudinal beams
69, 70	43 <sup>2</sup> -47 <sup>1</sup> , 45 <sup>2</sup> -48 <sup>1</sup>	Inboard, outboard engine rear attach points
71-74	15-41 <sup>1</sup> , 14-42 <sup>2</sup> , 41 <sup>3</sup> -0, 41 <sup>4</sup> -0	Wing root attachments to fuselage
75, 76	43 <sup>1</sup> -47, 45 <sup>1</sup> -48	Inboard, outboard engine forward attach points
77-81	41-42, ..., 45-46	Wing inboard to outboard members
82-89	1 <sup>2</sup> -2 <sup>3</sup> , 2 <sup>3</sup> -3 <sup>1</sup> , 3 <sup>1</sup> -4 <sup>1</sup> , ..., 8 <sup>1</sup> -9 <sup>1</sup>	Lower fuselage longitudinal members
90-93	2-12 <sup>1</sup> , 4-14 <sup>1</sup> , 5-15 <sup>1</sup> , 6-16 <sup>1</sup>	Bulkhead diagonals
94, 95	16 <sup>1</sup> -17, 16-30	FS 960-1040 lower diagonals
96, 97	17-40 <sup>1</sup> , 18-30	FS 1040-1200 lower diagonals
98, 99	12-20 <sup>1</sup> , 12 <sup>1</sup> -13	FS 300-460 lower diagonals
100, 101	14-20 <sup>1</sup> , 14 <sup>1</sup> -13	FS 460-620 lower diagonals
102-115	12-23, ..., 18-29, 13-22, ..., 19-28	FS 300-1400, upper diagonals, WL 205-270
116-129	22-33, ..., 28-39, 23-32, ..., 29-38	FS 300-1400, upper diagonals WL 270-293
130-137	5 <sup>1</sup> -15, ..., 2 <sup>3</sup> -12	FS 300, 620, 820 and 960 Bulkhead shear web diagonals

Prime designates Massless node.

## 6.2 KRASH ANALYSIS RESULTS

The analytical results based on the three cases noted in Section 6.1 are summarized in tables 6-5 through 6-10. Table 6-5 shows the amount of crush between FS300 to FS1200. For the most part the large deformation at FS300 is accompanied by an extremely low load level, as can be observed from the external spring description provided in figure 5-26. The amount of deflection noted in the forward fuselage may be exaggerated since the expanded model appears to be more flexible in that region (table 6-1). The impact sequence is shown in table 6-6. There are variations in impact sequence between the three cases as might be expected. Contact all along the fuselage occurs within the 60 milliseconds after impact. Peak deflections occur at all locations within 160 msec. after impact. Table 6-7 shows the yield and rupture sequence for the analytical cases that were run. The yield and rupture values used were those calculated in program KRASH for the respective beams, based on beam and material properties. The values are printed in the section of the output denoted "Model Parameter Data". For all the nonlinear beams a yield type 5 (load remains constant after a yield deflection is reached) was used. Each of the cases run contained 33 force rupture cutoff values. Case Number 1 contains 44 nonlinear beams. The "rupture allowable" cases (No's 2 and 3) contain 19 nonlinear beams, thus allowing for a rupture rather than a yield to occur for selected beams. Table 6-8 presents the beam deflections for the three cases analyzed. The three cases show a lateral deflection of up to 4.0 inches for the upper shell above the floor at FS960. This can be interpreted potentially as a bulge in that area. A floor maximum vertical deflection of 5.9 inches is noted in the FS620-820 region.

Table 6-9 shows the vertical acceleration values obtained from the analysis. Both the plotted peak and the equivalent triangular pulse peak values are noted in Table 6-9. The manner in which the equivalent triangular pulse is obtained and the reasons for showing it have been described in

TABLE 6-5. ANALYSIS RESULTS, FUSELAGE CRUSH

FUSELAGE STATION	MASS NUMBER	PEAK DEFLECTION, in.		
		1	2	3
300	2, 12	7.8, 7.6	9.4, 9.6	9.7, 9.8
460	20	5.0	6.9	7.5
620	4, 14	4.8, 5.1	5.7, 6.0	6.2, 7.1
820	5, 15	7.7, 8.2	7.3, 8.0	10.2, 11.0
960	6, 16	9.0, 9.8	6.0, 8.1	12.2, 12.6
1040	30	9.1	7.5	11.8
1200	40	3.4	4.1	4.9
* INCREASING AT FINAL TIME OF ANALYSIS				

Section 5. The higher peak values are associated with relatively short pulse durations as can be observed in the data presented in figure 6-3. The peak values tend to be higher than the values associated with an equivalent triangular pulse.

Program KRASH has provisions for printing and plotting mass axis component forces for selected beams. It also has provisions for internally summing up forces and moments at a particular station. Using this feature the mass axis component forces were determined for the condition 1 analysis. Table 6-10 summarizes the peak shear, moment and LIC ratios along the fuselage for condition 1. The input shear-moment envelope, representing the capability of the region of overall fuselage section, is not exceeded. At and aft of the MLG bulkhead the LIC ratios reach .820 (approximately 18% margin). The maximum shear and moment values obtained in the expanded model are 205,000 lb. and  $55.2 \times 10^6$  in-lb., respectively. The stick model showed both higher peak shear (225,000 lb) and higher peak moments ( $75 \times 10^6$  in-lb.) in the region between FS960-1000. Whether these differences are attributable to the manner in which structure is detailed or to differences in responses associated with more detail or some combination of both can only be determined when the test results are evaluated. The analysis results presented herein indicate that a CID test impacting at the conditions noted will most likely experience accelerations and structural damage similar to that sustained by the B707 airplane tested at Laurinburg, N.C. and described in Section 5. The results of the expanded model incorporating structural response information from the B707 airplane drop indicate that the results of the CID

TABLE 6-6. IMPACT SEQUENCE

CASE	INITIAL CONTACT TIME, MSEC <sup>(1)</sup>	PEAK DEFLECTION OCCURS TIME, MSEC <sup>(1)</sup>
<b>No. 1</b>		
Aft fuselage sta. 960	0	112.8 <sup>(2)</sup> , 105.1 <sup>(3)</sup>
MLG bulkhead, sta. 1040	4.3	108.1
Inboard engine	9.0	86.4
Wing center section T.E., sta. 820	10.6	100.9 <sup>(2)</sup> , 97.6 <sup>(3)</sup>
Wing center section L.E., sta. 620	27.7	90.5 <sup>(2)</sup> , 93.9 <sup>(3)</sup>
Forward fuselage sta. 460	36.5	114.1
NLG bulkhead sta. 300	40.7	105.3 <sup>(2)</sup> , 111.5 <sup>(3)</sup>
Aft fuselage, sta. 1200	50.	108.
<b>No. 2</b>		
Aft fuselage sta. 960	0	76.7
MLG bulkhead sta. 1040	4.3	51.4 <sup>(2)</sup> , 70.9 <sup>(3)</sup>
Inboard engine	9.0	85.8
Wing center section T.E., sta. 820	10.6	87.2 <sup>(2)</sup> , 87 <sup>(3)</sup>
Wing center section L.E. sta. 620	27.0	98.7 <sup>(2)</sup> , 102.3 <sup>(3)</sup>
Forward fuselage, sta. 460	36.5	127
NLG bulkhead, sta. 300	40.7	123.4 <sup>(2)</sup> , 124 <sup>(3)</sup>
Aft fuselage sta. 1200	50.0	160.
<b>No. 3</b>		
Inboard engine	0	77
Fuselage sta. 960	3.6	124.7 <sup>(2)</sup> , 117.4 <sup>(3)</sup>
MLG bulkhead sta. 1040	8.6	123.1
Wing center section T.E., sta. 820	13.9	108.5 <sup>(2)</sup> , 109.3 <sup>(3)</sup>
Wing center section L.E., sta. 620	35.8	107.7 <sup>(2)</sup> , 116.5 <sup>(3)</sup>
Forward fuselage sta. 460	47.9	136.5
NLG bulkhead sta. 300	54.5	155.1 <sup>(2)</sup> , 150.6 <sup>(3)</sup>
Outbd engine	114.8	—
NLG bulkhead sta. 199	114.9	147.9
Aft fuselage sta. 1200	55.3	141.
(1) Time after impact (2) Inboard location (3) Outboard location		

TABLE 6-7. ANALYSIS RESULTS, YIELD/RUPTURE SEQUENCE

TIME AFTER IMPACT SEC	CONDITION		
	1	2	3
0-0.015	16 <sup>1</sup> -30 Y	16 <sup>1</sup> -30 Y	43 <sup>1</sup> -47 R
0.015-0.030	43 <sup>1</sup> -47 R	43 <sup>1</sup> -47 R	
0.030-0.045	5 <sup>1</sup> -6 <sup>1</sup> Y	6 <sup>1</sup> -7 <sup>1</sup> R	
0.045-0.060	7 <sup>1</sup> -8 <sup>1</sup> Y	30-40 Y 16-17 R	
0.060-0.075 14	19-40 Y 14 <sup>1</sup> -20 Y 4 <sup>1</sup> -5 <sup>1</sup> Y	6-7 R 14 <sup>1</sup> -20 R	43 <sup>2</sup> -47 <sup>1</sup> R
0.075-0.090			14 <sup>1</sup> -20 Y
0.090-0.120	8 <sup>1</sup> -9 <sup>1</sup> Y 13-14 Y 3 <sup>1</sup> -4 <sup>1</sup> Y 3-4 Y		13-14 R 4 <sup>1</sup> -5 <sup>1</sup> R 5-15 R 14-41 <sup>1</sup> R 15-41 <sup>2</sup> R 14-15 R 4-5 R
0.120-0.150			45 <sup>1</sup> -48 R 45 <sup>2</sup> -48 <sup>1</sup> R
Y - YIELD R - RUPTURE SUPERScript DENOTES NODE POINT DESIGNATION			




TABLE 6-8. ANALYSIS RESULTS, BEAM DEFLECTIONS

LOCATION DIRECTION	BEAM NO.	MASS <sub>i</sub> -MASS <sub>j</sub>	DEFLECTIONS, in. CONDITIONS		
			1	2	3
Floor-Vertical	49	3-4	2.46	1.71	2.1
	50	4-5	2.36	1.81	5.9 R
	51	5-6	0.37	0.86	0.78
	52	6-7	0.32	3.1 R	0.33
	53	7-8	2.1	1.81	1.7
	57	13-14	0.69	1.44	0.83 R
	58	14-15	0.54	0.5	2.18 R
	59	15-16	0.95	0.98	0.91
	60	16-17	0.83	0.88 R	0.62
Upper Shell -	20	16-26	1.22	4.0	1.74
Lateral	21	26-36	1.17	1.7*	0.66
Floor transverse - Vertical	4	4-14	0.61	0.64	1.27
	5	5-15	1.05	0.84	1.6 R
	6	6-16	1.1	3.0	1.42
Cabin longerons - Vertical	33	23-24	0.67	0.93	1.06
	34	24-25	0.64	0.73	2.87
	35	25-26	0.56	0.78	0.58
	36	26-27	0.26	1.16	0.18
	37	27-28	1.34	2.7*	1.02
	41	33-34	0.52	0.34	0.69*
	42	34-35	0.81	0.76	1.9*
	43	35-36	0.40	1.04*	0.69*
	44	36-37	0.15	0.55	0.14
	45	37-38	0.62	1.69	0.36
* Increasing at end of analysis R Beam rupture occurred					

test will not be as damaging to the aircraft as noted in the pretest analysis presented in Section 4.

Subsequent to the analysis for the cases described in Section 6.1 a KRASH model was run in which all diagonal tension members representing fuselage shear webs were removed. This resulted in a 48 mass 101 beam representation. A comparison of peak accelerations and fuselage crushing and beam deflections are shown in tables 6-11, 6-12 and 6-13 respectively. The results are comparable because either 1) the beam properties selected didn't influence the response or 2) the shear loads do not significantly influence the overall airplane response. Unless

TABLE 6-9. ANALYSIS RESULTS, PEAK VERTICAL ACCELERATIONS

FUSELAGE STATION	MASS NO.	VERTICAL, g.   		
		1	2	3
300	2, 12	26.0 (16), 17.2 (15.2)	21.2 (12.6), 13.4 (12.4)	24 (11.4), 15.7 (11.4)
460	3, 13	16.4 (12), 18.1 (13)	15.8 (10.6), 17.5 (12.0)	14.5 (13.9), 16.1 (14.0)
620	4, 14	17.8 (12), 13.1 (11.8)	17.9 (12.6), 13.1 (11.8)	18.2 (14.4), 12.4 (11.6)
820	5, 15	12.0 (10.6), 8.2 (9.4)	12.1 (11.2), 10.0 (9.5)	12.2 (12.9), 19.4 (13.0)
960	6, 16	14.7 (8.8), 11.2 (9.2)	29.4 (11.6), 14.6 (11.6)	16.2 (10.6), 14.0 (8.5)
1040	7, 17	16.7 (9.2), 17.3 (9.4)	16.7 (11.6), 17.3 (10.4)	17.0 (13.0), 13.1 (8.5)
1200	8, 18	11.4 (10.2), 11.5 (8.8)	11.5 (8.6), 12.6 (9.7)	9.8 (9.3), 8.9 (8.2)




 50 Hz Filter  
 Upward Direction  
 A(B); A = plotted peak acceleration, (B) Equivalent Triangular Pulse =  $\frac{\text{IMPULSE} \times 2}{\Delta t}$

Table 6-10. SUMMARY OF FUSELAGE PEAK SHEAR AND MOMENT LOADS AND LIC RATIOS

CURVE NUMBER	FUSELAGE STATION	MAXIMUM SHEAR X E4	MAXIMUM MOMENT X E6	MAXIMUM LIC RATIO
1	300	3.5	3.7	0.248***
2	350	14.3	13.5	0.864***
3	450	14.4	18.0	0.760***
4	480	9.2	31.0	0.620*
5	540	9.3	34.1	0.684*
6	600	9.3	37.3	0.60*
7	620	9.5	39.2	0.63*
8/9	820	8.3	42.2	0.68*
10/11	960	20.5	55.2	0.65**
12	990	20.5	52.1	0.82**
13	1080	16.7	41.2	0.82**
14	1160	16.7	32.9	0.80*
15	1210	11.5	28.8	0.58*
16	1320	11.5	19.1	0.64**
17/18	1400	11.5	13.2	0.81**

\*Maximum Load Ratio Associated with Occurrence of Peak Moment  
 \*\*Maximum Load Ratio Associated with Occurrence of Peak Shear  
 \*\*\*Maximum Load Ratio Associated With Occurrence of Peak Shear and Peak Moment

TABLE 6-11. COMPARISON OF PEAK ACCELERATION WITH AND WITHOUT FUSELAGE SHELL SHEAR REPRESENTATION

MASS NO.	NO FUSELAGE SHELL SHEAR*	FUSELAGE SHELL SHEAR*
3,13	16.9 (12.0), 20.5 (13.2)	14.5 (13.9), 16.1 (14)
4,14	18.2 (14.0), 12.9 (12.2)	19.2 (14.4), 12.4 (11.6)
5,15	12.2 (11.5), 8.5 (11.0)	12.2 (12.9), 19.4 (13.0)
6,16	33.6 (11.0), 14.8 (11.5)	10.2 (10.6), 14.0 (8.5)
7,17	17.7 (10.0), 18.3 (11.0)	17.0 (13.0), 13.1 (8.5)
8,18	10.7 (8.2), 13.6 (9.6)	19.8 (9.3), 8.9 (8.2)
*Peak acceleration, g (pulse durations are short .03 to .06 seconds), based on 50 Hz filter ( ) Equivalent triangular pulse = $\frac{\text{Impulse} \times 2}{\Delta T}$		

TABLE 6-12. COMPARISON OF PEAK CRUSHING WITH AND WITHOUT FUSELAGE SHELL SHEAR REPRESENTATION

MASS NO. INBD/OUTBD	NO FUSELAGE SHELL SHEAR*	FUSELAGE SHELL SHEAR*
2/12	9.9/9.9	9.4/9.6
20	6.0	6.9
4/14	5.2/5.2	5.7/6.0
5/15	7.2/7.7	7.3/8.0
6/16	6.2/8.4	6.0/8.1
30	7.6	7.5
40	3.9	4.1
*Crushing distance, inches		

the test results prove otherwise, the model might be simplified by eliminating some beam members. The fuselage region below the passenger floor is most likely in compression in which case diagonal tension members in this region are not functional. Thus if diagonal tension members will be needed to better represent fuselage web shear the upper fuselage shell would be the preferred locations.



TABLE 6-13. COMPARISON OF BEAM DEFLECTIONS FOR MODELING WITH AND WITHOUT FUSELAGE SHELL SHEAR REPRESENTATION

LOCATION DIRECTION	BEAM NO.	MASS <sub>i</sub> -MASS <sub>j</sub>	DEFLECTIONS, in. CONDITIONS	
			(a)	(b)
Floor-Vertical	49	3-4	1.71	2.3
	50	4-5	1.81	2.2
	51	5-6	0.86	0.78
	52	6-7	3.1R	5.5 R
	53	7-8	1.81	2.9
	57	13-14	1.44	1.0 R
	58	14-15	0.50	0.73
	59	15-16	0.98	1.08
	60	16-17	0.88 R	1.2 R
Upper Shell -	20	16-26	4.0	3.6
Lateral	21	26-36	1.7*	1.4
Floor transverse -	4	4-14	0.64	0.59
Vertical	5	5-15	0.84	0.91
	6	6-16	3.0	3.0
Cabin longerons - Vertical	33	23-24	0.93	1.17
	34	24-25	0.73	0.75
	35	25-26	0.78	0.79
	36	26-27	1.16	1.04
	37	27-28	2.7*	2.3*
	41	33-34	0.34	0.66
	42	34-35	0.76	0.96
	43	35-36	1.04*	0.88
	44	36-37	0.55	0.55*
	45	37-38	1.69	1.98*
* Increasing at end of analysis			(a) Fuselage shell shear	
R Beam rupture occurred			(b) No fuselage shell shear	

### 6.3 SUMMARY OF CID PRE-TEST ANALYSIS RESULTS

The aft fuselage (FS960 and aft) could crush from 6 to 12 inches. The wing center section may experience 5 to 8 inches of crush. The midforward fuselage (FS460) shows 5 to 7 inches of crush. The fuselage underside adjacent to the nose gear aft bulkhead at FS300 shows nearly 10 inches of deflection. However, this value may be misleading because 1) the load-deflection curve allows deflection to occur with little accompanying load after about 2 inches, and 2) the flexibility of the model may contribute some additional deflection in the extreme forward region.

Table 6-14 shows a range of deflections for beams. Floor peak vertical deflection of up to 6 inches occurs along the centerline. Along the outboard region of the floor deflections range up to 2 inches. Transverse floor beam vertical displacements of up to 3.0 inches occur at stations between FS620 and FS960. These peak deflections occur for a condition in which rupture occurs. Lateral displacement of the upper cabin fuselage structure at around station 960 is between 1.4 and 3.6 inches.

The CID pre-test analysis was performed using the two models described: a stick model consisting of 17 masses and 16 beam elements (figure 4-2), and an expanded model consisting of 48 masses and 137 beam elements (figure 6-1). The stick model due to its coarseness tends to provide lower frequency acceleration responses than the finer expanded model. It is not uncommon to see substantially higher peak acceleration responses obtained from the expanded model than from the stick model. However, the higher peaks are generally associated with shorter duration pulses than the lower peaks. The triangular pulse shape equivalent responses obtained from the analysis are plotted in figure 6-3. Also shown in figure 6-3 is a curve depicting a constant  $\Delta V$

TABLE 6-14. SUMMARY OF BEAM PEAK DEFLECTION RANGE

DESCRIPTION	LOCATION	DEFLECTION, inches
Upper Shell Lateral	station 960 WL 205-271	1.22 to 4.0
Upper Shell Lateral	station 960 WL 271-290	0.66 to 1.7
Transverse Floor Beams-Vertical	station 620 station 820 station 960	0.61 to 1.27 0.84 to 1.6 1.1 to 3.0
Upper Cabin Longeron Vertical	station 460-620 WL 205-271/WL 271-290	0.67 to 1.06/0.34 to 0.69
	station 620-820 WL 205-271/WL 271-290	0.64 to 2.87/0.76 to 1.09
	station 820-960 WL 205-271/WL 271-290	0.56 to 0.78/0.40 to 1.04
	station 960-1040 WL 205-271/WL 271-290	0.26 to 1.16/0.15 to 0.55
	station 1040-1200 WL 205-271/WL 271-290	1.02 to 2.7/0.36 to 1.69
Floor Vertical Inboard	station 460-620 station 620-820 station 820-960 station 960-1040 station 1040-1200	1.71 to 2.46 1.81 to 5.9 0.37 to 0.86 0.33 to 3.1 1.7 to 2.1
Outboard	station 460-620 station 620-820 station 820-960 station 960-1040	0.69 to 1.44 0.50 to 2.18 0.91 to 0.98 0.62 to 0.88

of 17 ft/sec. The ensemble of data presented shows the inverse relationship between pulse amplitude and duration. The data cluster about the constant  $\Delta V$  curve. The stick model results tend to be of a lower amplitude and broader in duration than the refined model for 50 Hz filtered data. As the data are filtered lower to 25 Hz, the points shift to the right and lower. Lower filtering to 10 Hz (not shown) shifts the responses more to the right and lower and tends to show better agreement between the two models. The aforementioned observations are based on earlier models with the original load-deflection curves. While the results vary somewhat with the refined curves, the same relationship will hold, as can be observed from the response data in Tables 5-2 and 6-9.

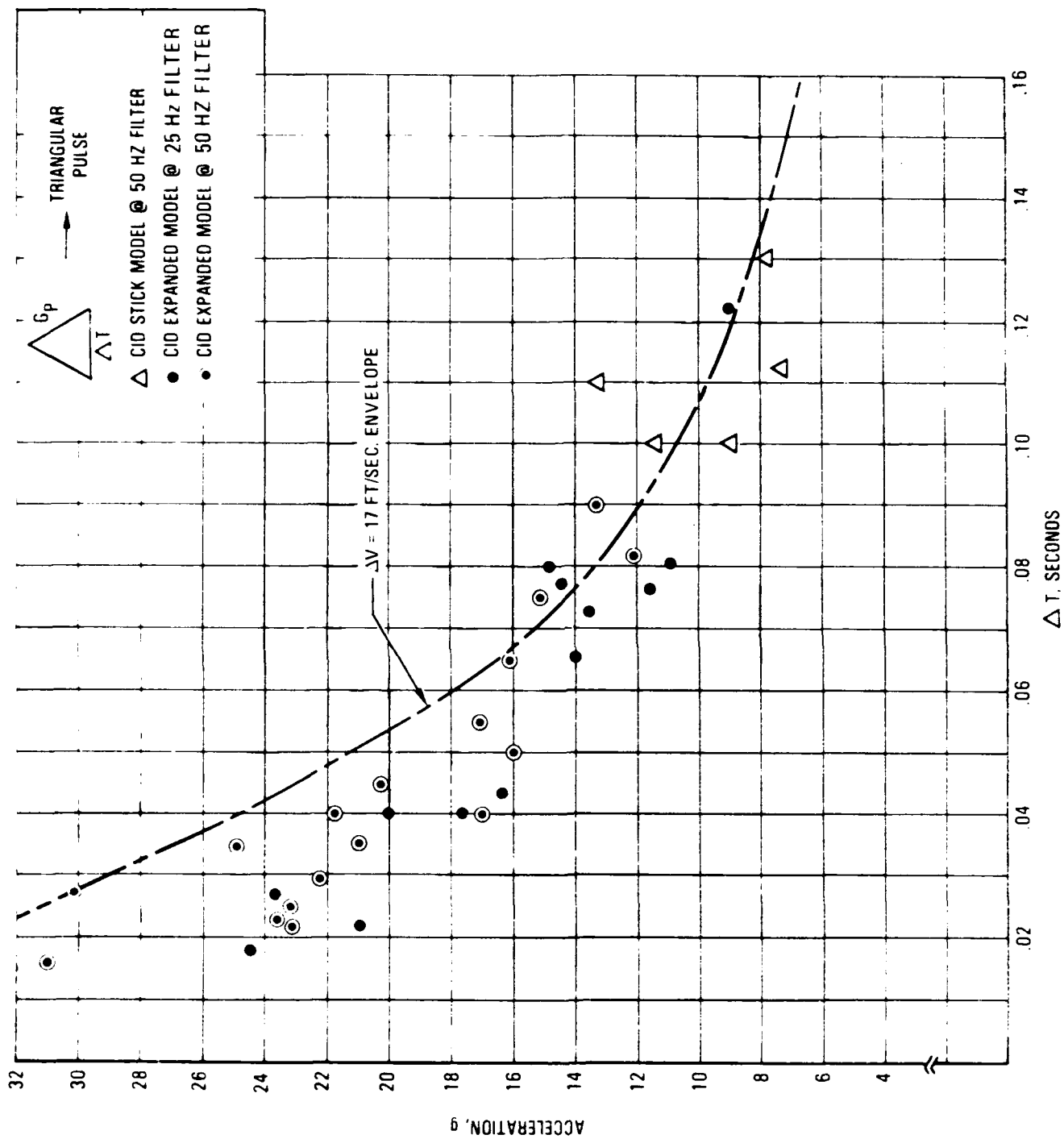


FIGURE 6-3. CID PRE-TEST ANALYSIS - VERTICAL ACCELERATION PULSES, 17 FT/SEC, +1 $\sigma$  NOISE-UP

A representative KRASH analysis result for the expanded model (condition 1) is shown in Figure 6-4. Unfiltered and filtered (50 Hz) accelerations, as well as impulse (g-sec) response data for FS820 (wing-center section) floor centerline is presented. The unfiltered peak acceleration values are 13.3 g and 2.8 g for the vertical and longitudinal directions, respectively. The corresponding filtered data shows 12.04 g and 2.5 g respectively. Two vertical pulses are detectable in the filtered data. A 12.05 g, .060 sec duration and a 8.78 g, .060 sec. duration. However from the impulse data a broader 120 second pulse can be deduced with an average acceleration value of 5.3 g, which translates to a 10.6 g peak for a triangular pulse of equal duration. The corresponding longitudinal triangular would be approximately 2.7 g for a .140 second duration. The floor responses at fuselage stations 300 to 1400, along both the centerline and at the floor/frame intersection for the expanded model, condition 1, are provided in Appendix B.

A comparison of the stick and expanded models for the ranges of conditions described in Section 5 and 6, based on impulse data is shown in Figure 6-5. The corresponding acceleration data for the two cases (stick model, condition 3 and expanded model, condition 1) which most resemble each other is shown in Figure 6-6. The predicted responses based on these two conditions are shown in Figure 6-7 for L10 ratios, accelerations and crush for the planned impact.

Based on the structural damage noted in the B707 airplane drop test at Laurinburg, N.C. (Section 5 discussion), the peak vertical acceleration would be expected to occur closer to FS820. If the test results substantiate this then the modeling of the center wing box region and its attachment to the wing should be further evaluated.

Based on the analysis results shown in Table 6-10 the highest potential for failures is from fuselage station 990 to 1080. However, from the model results it is doubtful that fuselage shell strength would be exceeded, unless the maropoint springs at FS620, 820 and 960 bottom out (restiffen) at a lower crush deflection than used in the analysis.

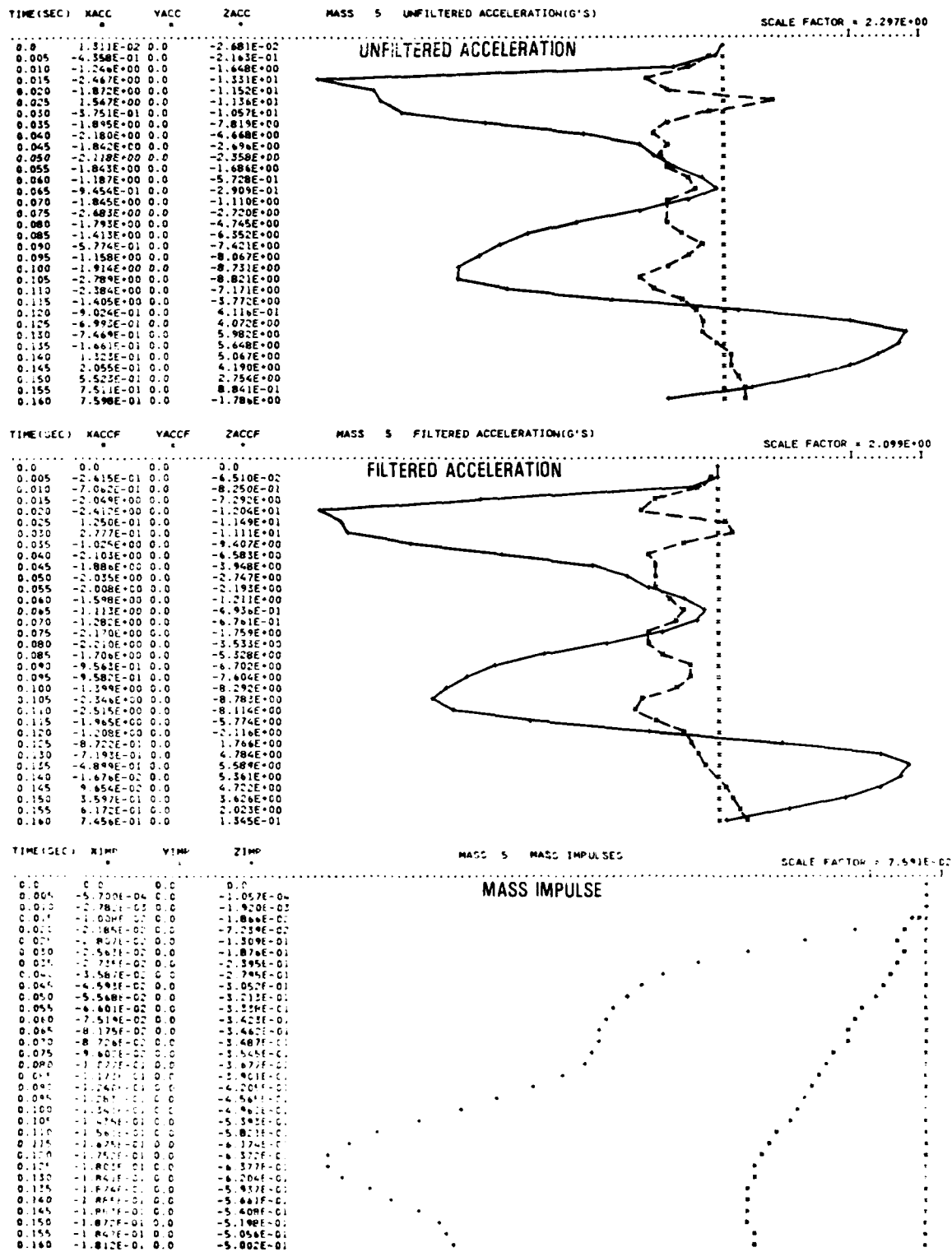


FIGURE 6-4. ACCELERATION RESPONSE AT FS820 CENTERLINE, EXPANDED MODEL CONDITION 1

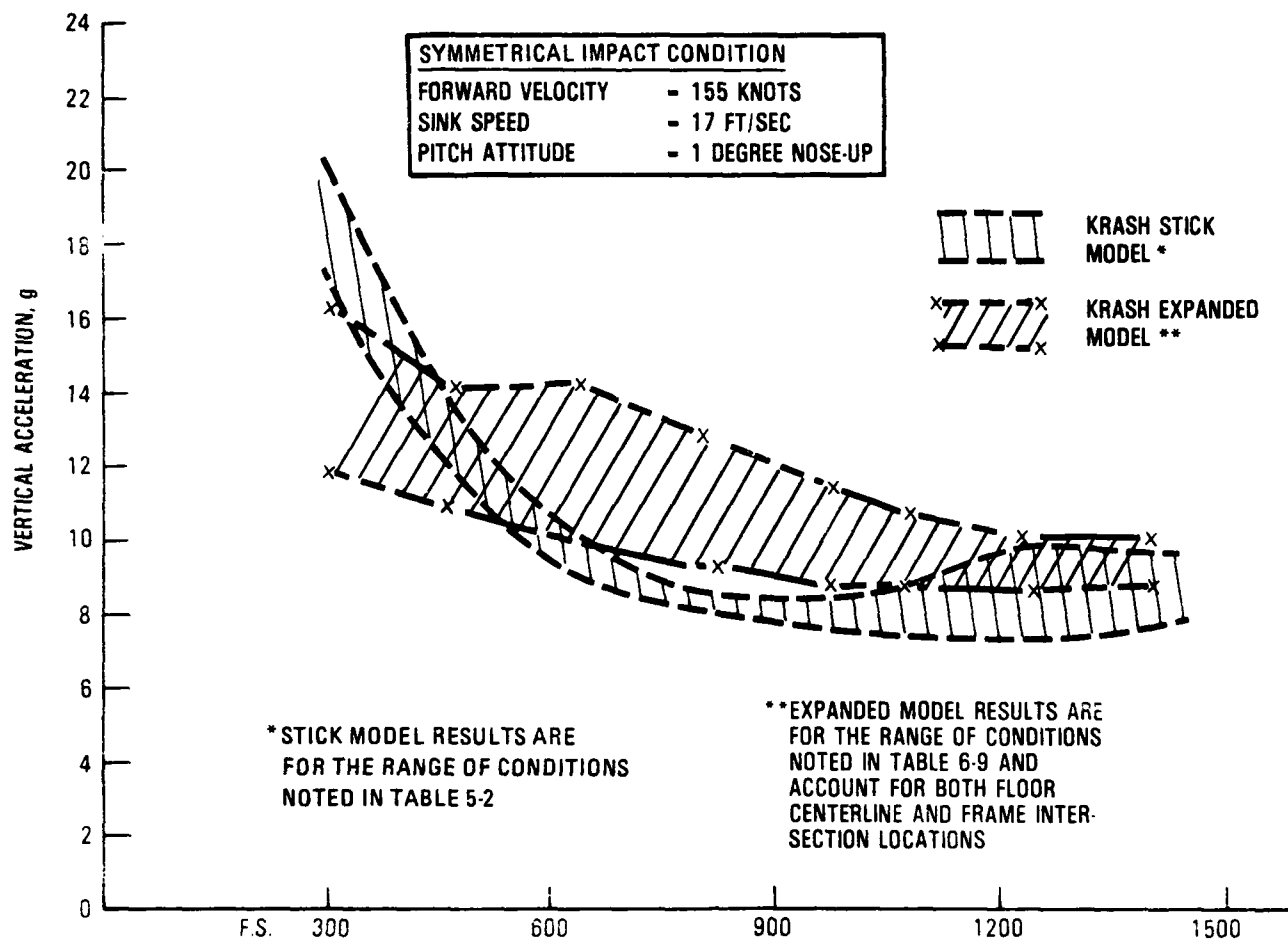


FIGURE 6-5. COMPARISON OF PRE-CID KRASH STICK MODEL ANALYSES VERSUS EXPANDED MODEL RESULTS FOR PLANNED SYMMETRICAL IMPACT CONDITION

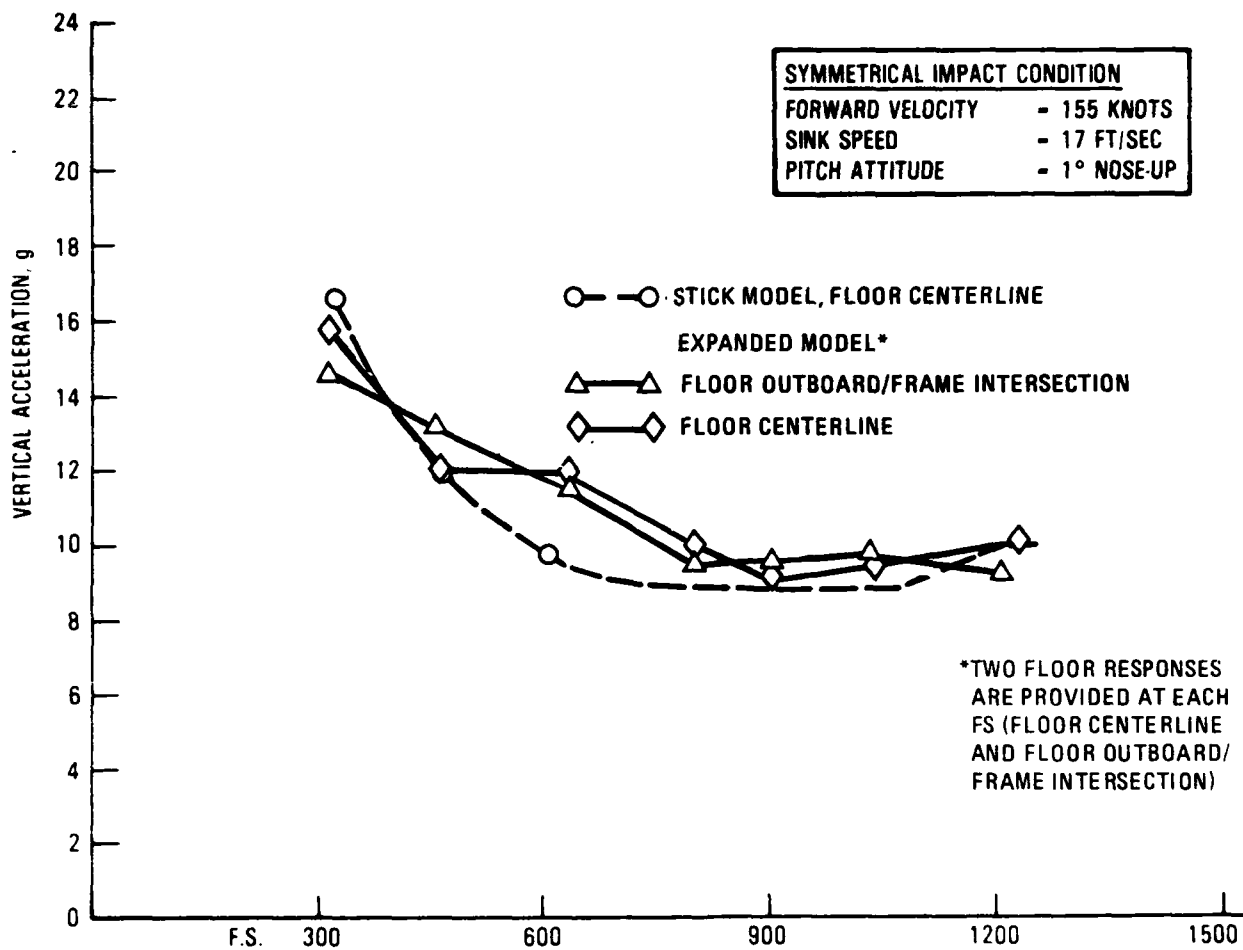


FIGURE 6-6. COMPARISON OF PRE-CID KRASH STICK AND EXPANDED MODELS ANALYSES RESULTS FOR PLANNED SYMMETRICAL IMPACT CONDITION



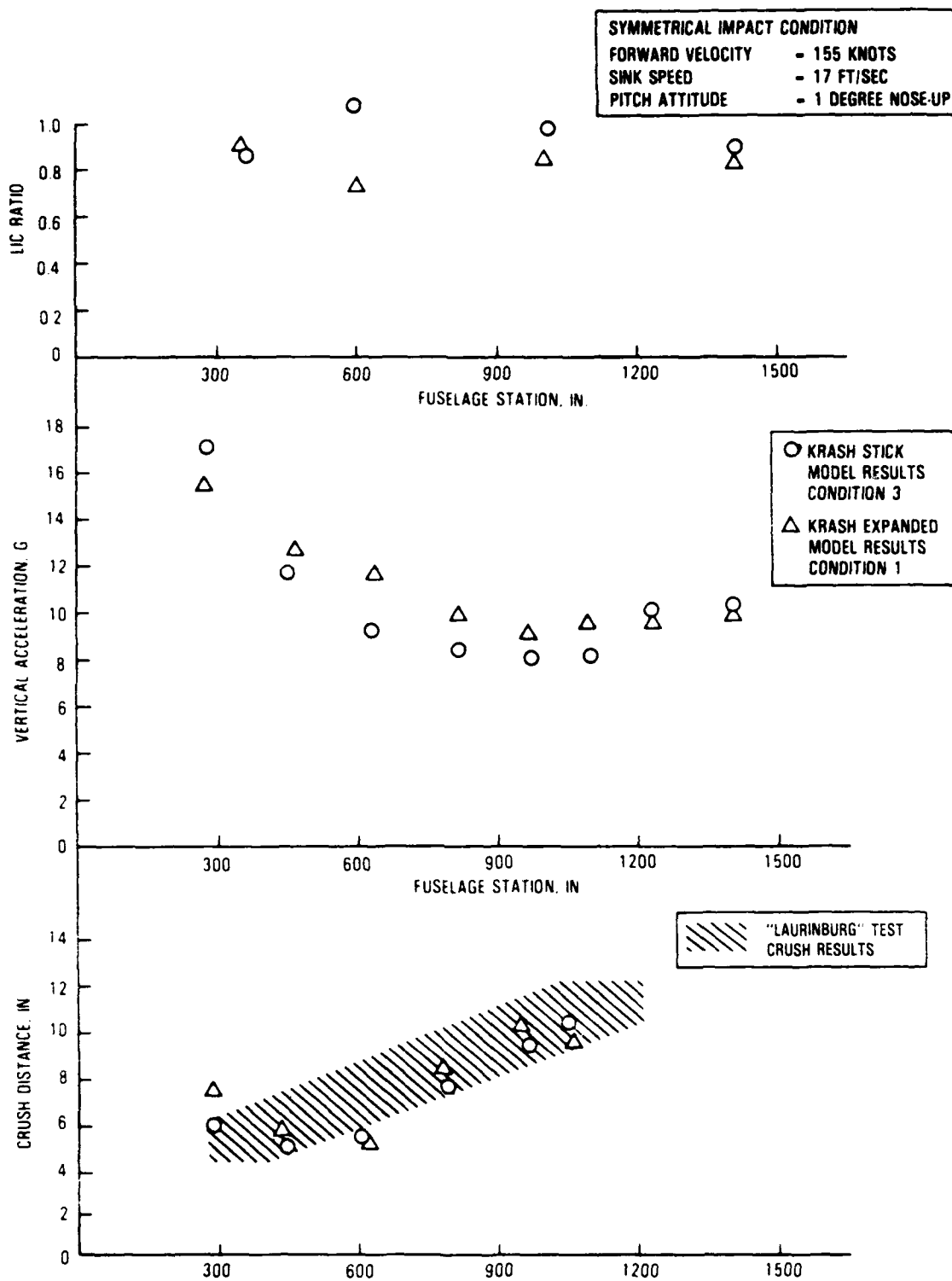


FIGURE 6-7. PRE-CID TESTS KRASH ANALYSIS RESULTS FOR PLANNED SYMMETRICAL IMPACT CONDITION

The analysis results are particularly sensitive to:

- The representation of the hard point load-deflection characteristics. Bottoming out loads could easily result in localized failures and subsequent disruption of structural integrity.
- Extent to which structure yields or fails. This is difficult to model because a large segment of structure, consisting of several frames and stringers, is defined by only a few beam elements.
- The expanded model results in higher frequency responses than the stick model. This is evidenced in the peak responses. The lower acceleration peaks with longer time durations obtained from the stick model results (Section 5) are probably more realistic than the expanded model results.

## SECTION 7

### CONCLUSIONS

#### CONCLUSIONS

1. The CID pre-test analysis indicates responses and structural damage similar to that experienced for the B707 airplane drop test conducted in Laurinburg N.C., for a symmetrical 17 ft/sec impact and the airplane at a 1 degree nose-up attitude.
2. Analysis of frame sections subjected to vertical impact loading can be performed to obtain overall section load-deflection behavior for use in larger airframe mathematical models.
3. The hard point load-deflection behavior is the most significant parameter which influences the potential for loss of structural integrity and cause of severe injury to occupants in a crash.
4. Analytical modeling results are influenced by the representation of yield and/or rupture allowables. Representation of large regions of structure by simpler elements will be enhanced with additional methodology development.

## REFERENCES

1. Wittlin, G., Gamon, M. A., and Shycoff, D. L., "Transport Aircraft Crash Dynamics," Lockheed-California Company, NASA CR 165851, FAA Report, DOT/FAA/CT-82/69, March 1982.
2. Widmayer, E. and Brende, O. B., "Commercial Jet Transport Crashworthiness," Boeing Airplane Company, NASA CR 65849, FAA Report DOT/FAA/CT-82/68 March 1982.
3. Cominsky, A., "Transport Aircraft Accident Dynamics," McDonnell Douglas Corp., NASA CR 165850, FAA Report DOT/FAA/CT-82/70 March 1982.
4. Thomson, R. G. and Caiafa, C., "Structural Response of Transport Airplanes in Crash Situations," NASA TM 85654, June 1983.
5. Federal Aviation Regulations, "FAR 25-Airworthiness Standards: Transport Category Airplanes," June 1974 (Amendments through April 1982).
6. Wittlin, G. and Lackey, D., "Analytical Modeling of Transport Aircraft Crash Scenarios to Obtain Floor Pulses," Lockheed-California Company, NASA-CR 166089, FAA Report DOT/FAA/CT - 83/23, April 1983.
7. Wittlin, G. and Gamon, M. A., "Experimental Program for the Development of Improved Helicopter Structural Crashworthiness Analytical and Design Techniques," Lockheed-California Company, USAAMRDL-TR-72-72, May 1973.
8. Wittlin, G. and Gamon, M. A., "Development, Verification, and Application of Program KRASH to General Aviation Airplane Crash Dynamics," Lockheed-California Company, FAA Report FAA-RD-77-188, February 1978.
9. Gamon, M.A., Wittlin G., LaBarge, W.L., "KRASH85 User's Manual" Lockheed-California Company, DOT/FAA/CT-85-10, Sept. 1984
10. Hayduk, R., Williams, S., "Vertical Drop Test of Transport Fuselage Section Located Forward of the Wing," NASA Tech Memo 85679, August 1983.
11. Park, K. C. and Wittlin, G., "Development and Experimental Verification of Procedures to Determine Nonlinear Load-Deflection Characteristics of Helicopter Substructures Subjected to Crash Forces," Lockheed-California Company, USAAMRDL-TR-74-12, May 1974.
12. B707 Fuselage Drop Test Report, Calspan Report No. 7252-1, March 1984.

13. DC-10 Fuselage Drop Test Report, Calspan Report No. 7251-1, September 1984.
14. Williams, S. A., Hayduk, R. J., "Vertical Drop Test of a Transport Fuselage Center Section Including the Wheel Wells," NASA TM 85706, October 1983.
15. Reed, W. H., et al, "Full-Scale Dynamic Crash Test of a Lockheed Constellation Model 1649 Aircraft," Aviation Safety Engineering and Research, FAA Technical Report ADS-38, Washington, D.C., October 1965.
16. Fuller, J.R., et al, "Contributions to the Development of a Power Spectral Gust Design Procedure For Civil Aircraft," The Boeing Company, FAA-ADS-54, January, 1966.

APPENDIX A

# A.1 NARROW-BODY AIRPLANE KRASH FRAME MODEL

## ECHO OF THE INPUT DATA IN CARD IMAGE FORMAT

CARD NO.	1	2	3	4	5	6	7	8
1	NBSTRUCT.MASS11.DATA 02-05-84 FULL FRAME REV.MT.4/4 CASE114 PL(1/7)=.60 00000010							
2	B707 SECT.PL=1.0 20FPS 10%DAMP SOFT TOP K(FR)=1 K(FL)=1 5E-5DT 50HZ 00000020							
3	1234567890123456789012345678901234567890123456789012345678901200000030							
4	NM	NSP	NB	NLB	NVP	NPIN	NUB	NDRINOLEO NACC MVP NVCH NMTL ND 00000040
5	11	4	12	2	3	7	0	0 0 0 0 0 0 0 3 00000050
6	NVBM	NFBM	NVBM	NFBM	NKM	NHI	NPH	TOL1 TOL2 TOL3 NSC NICNAERONBOMB 00000060
7	0	0	1	1	0	0	0	1000 1000 1000 0 1 0 1 00000070
8	NSCV NLICNHRGR NBAL ICDICITR 00000071							
9	00000072							
10	GRAPHIC AND DATA TRANSFER CARDS 00000080							
11	00000090							
12	00000100							
13	ONE START AND ONE RESTART CARD 00000110							
14	00000120							
15	00000130							
16	IPRINT DELTAT TMAX PLOWT FCUT RUNMOD 00000140							
17	100 0.00005 .000 40. 1.0 00000150							
18	BLANK CARD FOLLOWS 00000160							
19	00000170							
20	NSF	NTF	NDE	NSPD	NED	NS	NRP	NIMP: PRINT DAT 00000180
21	0	0	0	0	0	0	0	0 00000190
22	NMEP	NNEP	NBFP	NBDP	NSTP	NSEP	NENP	NDRP NPLTNPFCT:PLOT DATA 00000200
23	5	0	7	7	0	4	0	0 1 0 00000210
24	INITIAL CONDITION DATA:3 CARDS 00000220							
25	0.0	0.0	240.	00000230				
26	0.0	0.0	0.	00000240				
27	0.	0.	0.	0.	0.	0.	0.	00000250
28	MASS DATA:NM CARDS 00000260							
29	18.0	0.0	-20.	4.	4.	4.	4.	00000270
30	18.0	0.0	-37.	12.	4.	4.	4.	00000280
31	18.0	0.0	-52.	25.	4.	4.	4.	00000290
32	51.	0.0	-70.	69.	16.	16.	16.	00000300
33	51.	0.0	-45.4	69.	16.	16.	16.	00000310
34	51.	0.	-24.8	69.	16.	16.	16.	00000320
35	18.	0.	0.	1.	4.	4.	4.	00000330
36	450.	0.	-35.1	89.	125.	125.	125.	00000340
37	27.	0.	-72.	110.	8.	8.	8.	00000350
38	32.	0.	-60.	140.	8.	8.	8.	00000360
39	40.	0.	0.	176.	10.	10.	10.	00000370
40	NODE PT.DATA: NNP CARDS 00000380							
41	1	1	0.	0.	1.	00000390		
42	1	8	0.	-45.4	89.	00000400		
43	2	8	0.	-24.8	89.	00000410		
44	EXTERNAL SPRING DATA:2XNSP CARDS 00000420							
45	1	3	1.0	0.	10000.	0.	0.	00000430
46	7	3	1.	0.	10000.	0.	0.	00000440
47	2	3	1.0	0.	10000.	0.	0.	00000450
48	3	3	1.	0.	10000.	00000460		
49	0.6	0.65	.66	0.9	4000.	4000.	.00001	00000470
50	0.6	0.65	.66	0.9	4000.	4000.	0.00001	00000480

© 1999 by the American Psychological Association, 0893-3200/99/\$12.00 DOI: 10.1037/0893-3200.13.4.593

A-2



# ECHO OF THE INPUT DATA IN CARD IMAGE FORMAT

CARD NO.	1	2	3	4	5	6	7	8
102	3.5	1.0						00001030
103	BEAM NEG.DEFL.CUTOFF :NVBMN CARDS							00001040
104	1	7	1.E+10	1.E+10	100.	1.E+10	1.E+10	00001050
105	BEAM NEG.FORCE CUTOFF:NFBMN CARDS							00001060
106	1	7	1.E+10	1.E+10	1.E+10	1.E+10	1.E+10	00001070
107	POSITION PLOT DATA:2XNPLT CARDS							00001080
108	3	11	3	10.0	30.0			00001090
109	1	2	3	4	5	6	7	00001100
110	MASS PLOT DATA: NMEP CARDS							00001110
111	4	1	0	1			1	00001140
112	5	1	0	1			1	00001150
113	6	1	0	1			1	00001160
114	8	1	0	1			1	00001180
115	11	1	1				1	00001210
116	BEAM FORCE PLOT DATA:NBFP CARDS							00001220
117	1	1	1	1				00001235
118	4	1	1	1				00001240
119	5	1	1	1				00001250
120	6	1	1	1				00001260
121	7	1	1	1				00001270
122	11	1	1	1				00001310
123	12	1	1	1				00001320
124	BEAM DEFLECTION PLOT DATA:NBDF CARDS							00001330
125	1	1	1	1				00001335
126	4	1	1	1				00001350
127	5	1	1	1				00001360
128	6	1	1	1				00001370
129	7	1	1	1				00001380
130	11	1	1	1				00001420
131	12	1	1	1				00001430
132	EXTERNAL SPRING DATA:NSEP CARDS							00001440
133	1	1	1					00001450
134	2	1	1					00001460
135	3	1	1					00001470
136	7	1	1					00001480
137	END							00001490

# A.2 WIDE-BODY AIRPLANE KRASH FRAME MODEL

## ECHO OF THE INPUT DATA IN CARD IMAGE FORMAT

	1	2	3	4	5	6	7	8
CARD NO.	1234567890123456789012345678901234567890123456789012345678901234567890							
1	FRAME.MOD7.DATA 8-21-84							00000010
2	WIDE-BODY SECTION 14MASS 20FPS							00000020
3	123456789012345678901234567890123456789012345678901234567890123456789012							00000030
4	NM NSP NB NLB NNP NPIN NUB NDRINOLEO NACC MVP NVCH NMTL ND							00000040
5	14 3 16 0 2 4 0 0 0 0 0 0 0 0 0							00000050
6	NVBM NFBNNVBMNNFBNN NKM NHI NPH TOL1 TOL2 TOL3 NSC NICNAERONBOMB							00000060
7	0 1 0 0 0 0 0 1000 1000 1000 0 1 0 1							00000070
8	NSCV NLICNNRGR NBAL ICD							00000080
9	0 0 0 0 0 0							00000090
10	GRAPHIC AND DATA TRANSFER CARDS							00000100
11								00000110
12								00000120
13	ONE START AND ONE RESTART CARD							00000130
14								00000140
15								00000150
16	IPRINT DELTAT TMAX PLOWT FCUT RUNMOD							00000160
17	250 0.00001 .100 50. 1.0							00000170
18	BLANK CARD FOLLOWS							00000180
19								00000190
20	NSF NTF NDE NSPD NED NS NRP NIMP: PRINT DAT							00000200
21	1 1 1 1 1 0 1 0							00000210
22	NMEP NMEP NMEP NMEP NMEP NMEP NMEP NMEP NMEP NMEP NMEP NMEP NMEP NMEP NMEP							00000220
23	14 2 16 16 0 3 0 0 1 4							00000230
24	INITIAL CONDITION DATA:3 CARDS							00000240
25	0.0 0.0 240.							00000250
26	0.0 0.0 0.							00000260
27	0. 0.0 0. 0. 0. 0.							00000270
28	MASS DATA:NM CARDS							00000280
29	20. 0. 0. 2.0 2.0 2.0 2.0							00000290
30	25.00 0.00 17.0 3.24 4.00 4.00 4.00							00000300
31	35.00 0.00 55.00 15.00 6.00 6.00 6.00							00000310
32	30.00 0.00 83.00 36.00 6.00 6.00 6.00							00000320
33	30. 0. 100. 65. 6. 6. 6.							00000330
34	75.00 0.00 110.00 93.00 24.00 24.00 24.00							00000340
35	75.00 0.00 83.00 93.00 24.00 24.00 24.00							00000350
36	75.00 0.00 0.00 93.00 24.00 24.00 24.00							00000360
37	40.00 0.00 92.00 162.00 12.00 12.00 12.00							00000370
38	45.00 0.00 55.00 203.00 12.00 12.00 12.00							00000380
39	60.00 0.00 0.00 220.00 15.00 15.00 15.00							00000390
40	165. 0. 0. 113. 47.25 47.25 47.25							00000400
41	82.5 0. 83. 113. 23.63 23.63 23.63							00000410
42	20. 0. 17.0 15. 4. 4. 4.							00000420
43	MASSLESS NODE POINT DATA: NNP CARDS							00000430
44	1 2 0.3 17.0 3.24							00000440
45	1 14 0.3 17.0 15.0							00000450
46	EXTERNAL SPRING DATA:2XNSP CARDS							00000460
47	1 3 2.00 0.00 20000.00 0.00 0.00							00000470
48	2 3 2.00 0.00 20000.00 0.00 0.00							00000480
49	3 3 2.00 0.00 20000.00 0.00 0.00							00000490
50	0.40 0.75 0.85 1.00 4000.00 5000.00 0.00001 00000500							

# ECHO OF THE INPUT DATA IN CARD IMAGE FORMAT

CARD NO.	1	2	3	4	5	6	7	8
51	0.40	0.75	0.85	1.00	4000.00	5000.00	0.00001	00000510
52	0.40	0.75	0.85	1.00	4000.00	5000.00	0.00001	00000520
53	INTERNAL BEAM DATA:NB CARDS							00000530
54	3	14	0.47	0.5	1.3	1.3	1.0	1.0 400000540
55	2	3	2.32	3.0	3.34	3.34	3.0	1.5 400000550
56	4	71	0.39		0.77	0.77	1.50	1.5 400000560
57	3	4	2.28		3.30	3.30	1.50	1.0 400000570
58	4	5	2.38		4.5	4.5	2.25	1. 400000580
59	5	6	2.48		5.0	5.0	2.5	1. 400000590
60	6	7	0.75		15.20	15.20	5.00	1.0 400000600
61	7	8	0.75		15.20	15.20	5.00	1.0 400000610
62	6	9	2.27		4.20	4.20	2.00	1.0 400000620
63	9	10	2.11		3.90	3.90	2.00	1.0 400000630
64	10	11	1.90		3.60	3.60	1.80	1.0 400000640
65	8	121	0.80		0.04	0.04	0.50	0.5 100000650
66	7	131	0.80		0.04	0.04	0.50	0.5 100000660
67	1	2	141	0.328	0.0195	0.537	.57	1.7 400000670
68	1	2	2.28	3.0	3.95	3.95	3.0	1.5 400000680
69	14	0	0.47		1.3	1.3	1.0	1.0 400000690
70	BEAM END FIXITY DATA: NPIN CARDS							00000700
71	1	2	1	1	0	0 0.75	0.75	0.0 00000710
72	2	3	1	1	0	0 0.75	0.75	0.0 00000720
73	3	4	1	1	0	0 1.0	1.0	0.0 00000730
74	7	8	0	0	1	1 0.0	0.0	1.0 00000740
75	DAMPC CARD							00000770
76	0.01000							00000780
77	NON STANDARD MAX BEAM ELEMENT POS LOAD: NFBM CARD							00000790
78	1	2	1	14	1.0E10	1.0E10	1.0E10	1.0E10 1500.0 1.0E10 00000800
79	POSITION PLOT DATA:2XNPLT CARDS							00000810
80	3	14	3		20.0	40.0		00000820
81	1	2	3	4	5	6	7	8 9 10 11 12 13 14 00000830
82	MASS PLOT DATA: NMEP CARDS							00000840
83	1	1	1	1				1 00000850
84	2	1	1	1				1 00000860
85	3	1	1	1				1 00000870
86	4	1	1	1				1 00000880
87	5	1	1	1				1 00000890
88	6	1	1	1				1 00000900
89	7	1	1	1				1 00000910
90	8	1	1	1				1 00000920
91	9	1	1	1				1 00000930
92	10	1	1	1				1 00000940
93	11	1	1	1				1 00000950
94	12	1	1	1				1 00000960
95	13	1	1	1				1 00000970
96	14	1	1	1				1 00000980
97	MASSLESS NODE POINT DATA: NNEP CARDS							00000990
98	1	2	1					00001000
99	1	14	1					00001010
100	BEAM FORCE PLOT DATA:NBFP CARDS							00001020
101	1	1	1	1				00001030

# ECHO OF THE INPUT DATA IN CARD IMAGE FORMAT

CARD NO.	1	2	3	4	5	6	7	8
102	2	1	1	1				00001040
103	3	1	1	1				00001050
104	4	1	1	1				00001060
105	5	1	1	1				00001070
106	6	1	1	1				00001080
107	7	1	1	1				00001090
108	8	1	1	1				00001100
109	9	1	1	1				00001110
110	10	1	1	1				00001120
111	11	1	1	1				00001130
112	12	1	1	1				00001140
113	13	1	1	1				00001150
114	14	1	1	1				00001160
115	15	1	1	1				00001170
116	16	1	1	1				00001180
117	BEAM DEFLECTION PLOT DATA:NBDP CARDS							00001190
118	1	1	1	1				00001200
119	2	1	1	1				00001210
120	3	1	1	1				00001220
121	4	1	1	1				00001230
122	5	1	1	1				00001240
123	6	1	1	1				00001250
124	7	1	1	1				00001260
125	8	1	1	1				00001270
126	9	1	1	1				00001280
127	10	1	1	1				00001290
128	11	1	1	1				00001300
129	12	1	1	1				00001310
130	13	1	1	1				00001320
131	14	1	1	1				00001330
132	15	1	1	1				00001340
133	16	1	1	1				00001350
134	EXTERNAL SPRING DATA:NSEP CARDS							00001360
135	1	1	1	1				00001370
136	2	1	1	1				00001380
137	3	1	1	1				00001390
138	END							00001400

# A.3 KRASH CID STICK MODEL

## ECHO OF THE INPUT DATA IN CARD IMAGE FORMAT

	1	2	3	4	5	6	7	8
CARD NO.	12345678901	23456789012	34567890123	45678901234	56789012345	67890123456	78901234567	8901234567890
1	B720.NASTI.LICK.DATA 8-07-84 1E-4DT ELKD 100%A.I.MOM.80%STR. 193K							00000010
2	155 KTS. 01 PTCH GYM.17 ROD-RIG.GRD MU=.35RAT.AERO DAMPC=.100 TMAX=.16							00000020
3	12345678901234567890123456789012345678901234567890123456789012000000030							000000030
4	NM	NSP	NB	NLB	NNP	NPIN	NUB	NDRINOLEO NACC MVP NVCH NMTL ND
5	17	12	16	0	11	6	0	0 0 0 17 0 0 0 0
6	NVBM	NFBMNVBMNNFBMN	NKM	NHI	NPH	TOL1	TOL2	TOL3 NSC NICNAERONBOMB
7	0	0	0	2	0	0	0	1000 1000 1000 0 0 0 1
8	NSCV	MLICNWRGR	NBAL	ICDICITR				
9	1	16	0	5	1	1		
10	GRAPHICS							00000100
11								00000110
12								00000120
13	ONE RESTART AND ONE SAVE CARD FOLLOWS							00000130
14								00000140
15								00000150
16	IPRINT	DELTAT	TMAX	PLOWT	FCUT	RUNMOD		00000160
17	50	.000100	0.160	0.000	50.	1.		00000170
18	BLANK CARD FOLLOWS							00000180
19								00000190
20	NSF	NTF	NDE	NSPD	NED	NS	NRP	NIMP : PRINT DATA
21	0	0	0	0	0	0	0	0
22	NMEP	NNEP	NBFP	NBDP	NSTP	NSEP	NENP	NDRP NPLTNPFCT : PLOT DATA
23	11	0	16	16	0	9	0	0 0 0 0
24	INITIAL CONDITION DATA : 3 CARDS							00000240
25	3140.00	000.00	204.00					00000250
26	000.00	000.00	000.00					00000260
27	000.00	0.01745	000.00	000.00	000000.	0.001.1463E-07		00000270
28	MASS DATA : NM CARDS							00000280
29	1585.0	199.0	0.0	219.0.11514E+05.4	E+05.15	E+05		00000290
30	10064.5	300.0	0.0	217.9.89080E+05.3	E+06.99	E+05		00000300
31	15318.1	460.0	0.0	208.3.16278E+06.96935E+05.10309E+06				00000310
32	13096.0	620.0	0.0	205.8.19627E+06.66715E+05.79389E+05				00000320
33	21752.6	820.0	0.0	200.0.49106E+06.12567E+06.14651E+06				00000330
34	7901.5	960.0	0.0	211.9.81383E+05.12	E+06.2	E+06		00000340
35	9190.7	1043.5	0.0	206.6.87536E+05.14	E+06.2	E+06		00000350
36	9938.4	1201.1	0.0	222.4.88098E+05.18	E+06.3	E+06		00000360
37	5702.0	1400.0	0.0	255.8.96249E+05.41788E+05.26039E+05				00000370
38	6175.2	1570.0	0.0	297.0.21530E+06.10798E+06.15863E+06				00000380
39	9670.6	801.3	118.3	189.0.15213E+05.13858E+06.36	E+06			00000390
40	15065.6	852.3	271.8	208.3.19510E+05.12263E+06.3	E+06			00000400
41	5286.5	943.5	430.7	234.3.72715E+04.52619E+05.11	E+06			00000410
42	3759.0	1045.8	583.5	272.0.44083E+04.25823E+05.60	E+05			00000420
43	1542.3	1112.6	740.6	300.4.16708E+04.90137E+04.18	E+05			00000430
44	5400.0	719.0	321.6	169.3 3651.56	25746.	29374.6		00000440
45	5151.0	902.8	551.6	212.6 3712.	24588.2	28178.		00000450
46	NODE POINT DATA : NNP CARDS							00000460
47	1	5	820.0	48.0	181.0			00000470
48	1	11	773.9	118.3	187.0			00000480
49	2	11	887.0	131.6	180.4			00000490
50	1	12	811.8	321.6	204.8			00000500

## ECHO OF THE INPUT DATA IN CARD IMAGE FORMAT

CARD NO.	1	2	3	4	5	6	7	8
1234567890123456789012345678901234567890123456789012345678901234567890								
51	1	14	994.5	551.6	249.0			00000510
52	1	15	1148.0	740.6	306.6			00000520
53	1	16	735.7	321.6	203.1			00000530
54	1	17	918.4	551.6	249.0			00000540
55	1	2	279.0	0.0	146.5			00000550
56	2	2	380.	0.	217.9			00000560
57	1	3	530.	0.	207.			00000570
58	EXTERNAL SPRING DATA : 2 X NSP CARDS							
59	1	3	74.2	0.50	100000.0			00000580
60	2	3	82.1	0.50	100000.0			00000590
61	3	3	72.2	0.50	100000.0			00000600
62	4	3	70.0	0.50	300000.0			00000610
63	5	3	64.2	0.50	300000.0			00000620
64	6	3	76.1	0.50	300000.0			00000630
65	7	3	69.3	0.50	100000.0			00000640
66	8	3	72.6	0.50	100000.0			00000650
67	9	3	62.0	0.50	300000.0			00000660
68	10	3	82.0	0.40	300000.0			00000670
69	16	3	38.3	0.50	272000.			00000680
70	17	3	28.0	0.50	272000.			00000690
71	1.1	1.5	4.0	10.	100000.	5000.	0.00	00000700
72	1.1	3.3	4.4	18.	200000.	5000.	0.00	00000710
73	4.0	5.0	6.0	24.0	128000.	128000.	0.00	00000720
74	1.1	3.3	9.9	10.	200000.	200000.	0.00	00000730
75	1.1	3.3	9.9	10.	250000.	200000.	0.00	00000740
76	1.1	3.3	9.9	18.	250000.	200000.	0.00	00000750
77	4.0	5.0	5.5	24.0	55000.	55000.	0.00	00000760
78	4.0	5.0	5.5	24.	75000.	75000.	0.00	00000770
79	1.0	1.1	2.0	3.0	300000.	30000.	0.00	00000780
80	1.0	1.1	2.0	3.0	300000.	30000.	0.00	00000790
81	1.	8.0	9.	16.	50000.	100000.	0.00	00000800
82	1.	8.0	9.	16.0	50000.	100000.	0.00	00000810
83	INTERNAL BEAM DATA : NB CARDS							
84	1	2	32.00	0.00	6.20E+04	3.70E+04	0.00	96. 96. 500000840
85	2	3	36.00	0.00	7.70E+04	4.30E+04	0.00	99. 99. 500000850
86	3	4	36.00	0.00	8.64E+04	4.30E+04	0.00	56. 56. 500000860
87	4	5	59.00	0.00	13.60E+04	4.65E+04	0.00	56. 56. 500000870
88	5	6	59.00	0.00	11.60E+04	4.65E+04	0.00	66. 66. 500000880
89	6	7	57.00	0.00	13.60E+04	5.70E+04	0.00	88. 88. 500000890
90	7	8	48.00	0.00	11.60E+04	6.20E+04	0.00	91. 91. 500000900
91	8	9	37.00	0.00	5.60E+04	3.35E+04	0.00	51. 51. 500000910
92	9	10	25.00	0.00	9.00E+04	9.50E+03	0.00	50. 50. 500000920
93	5	11	54.00	4.800E+04	1.59E+04	1.14E+05	0.00	1.0 1.0 500000930
94	1	11	63.20	2.600E+04	1.14E+04	1.02E+05	0.00	1.0 1.0 500000940
95	12	13	56.3	1.000E+04	4.70E+03	5.80E+04	0.00	1.0 1.0 500000950
96	13	14	40.7	4.800E+03	2.00E+03	2.10E+04	0.00	1.0 1.0 500000960
97	14	15	20.	2.700E+03	1.20E+03	8.00E+03	0.00	1.0 1.0 500000970
98	1	12	8.0	2.208E+02	7.32E+02	1.00E+02	0.00	1.0 1.0 400000980
99	1	14	8.0	2.208E+02	7.32E+02	1.00E+02	0.00	1.0 1.0 400000990
100	BEAM END FIXITY CARDS: NPIN CARDS							
101	1	2	0	0	1	1	0.	00001000
						1.55	1.55	00001010

ECHO OF THE INPUT DATA IN CARD IMAGE FORMAT

CARD NO.	1	2	3	4	5	6	7	8
102	2	3	0	0	1	1	0.	00001020
103	3	4	0	0	1	1	0.	00001030
104	6	7	1	1	0	0	1.6	00001040
105	7	8	1	1	0	0	1.5	00001050
106	8	9	1	1	0	0	1.35	00001060
107	DAMPC CARD							00001070
108	.100							00001080
109	NEG BEAM CUTOFF:NFBMN X 2 CARDS							00001090
110	1	12	1	16	30000.	1.E10	1.E10	00001100
111	1	14	1	17	30000.	1.E10	1.E10	00001110
112	LOAD INTERACTION SIGN CONVENTIONS(NSCV CARDS):							00001120
113	1	2	-3	4	5	6		00001130
114	LOAD INTERACTION DATA(NLIC+ CARDS):							00001140
115	1	3	5	1	0	300.	1000.	00001150
116						166000.	32.5E+06 -166000.	00001160
117	1	1	215000.	42.5	E+06			00001170
118	2	3	5	1	0	350.	1000.	00001180
119						188000.	39.0E+06 -188000.	00001190
120	1	1	260000.	70.0	E+06			00001200
121	2	3	5	1	0	450.	1000.	00001210
122						210000.	45.0E+06 -210000.	00001220
123	1	1	300000.	100.	E+06			00001230
124	3	3	5	1	0	480.	1000.	00001240
125						210000.	50.0E+06 -210000.	00001250
126	1	1	400000.	80.	E+06			00001260
127	3	3	5	1	0	540.	1000.	00001270
128						210000.	50.0E+06 -210000.	00001280
129	1	1	400000.	100.	E+06			00001290
130	3	3	5	2	0	600.	1000.	00001300
131						280000.	62.5E+06 -280000.	00001310
132	1	1	318000.	206.6	E+06			00001320
133	1	1	422400.	88.7	E+06			00001330
134	4	3	5	2	0	620.	1000.	00001340
135						280000.	62.5E+06 -280000.	00001350
136	1	1	318000.	206.6	E+06			00001360
137	1	1	422400.	88.7	E+06			00001370
138	5	3	5	2	1	960.	1000.	00001380
139						315000.	96.0E+06 -315000.	00001390
140	1	0	-5.7617E06	96.5E+06				00001400
141	1	1	521500.	200.8E+06				00001410
142	6	3	5	2	1	960.	1000.	00001420
143						315000.	96.0E+06 -315000.	00001430
144	1	0	-5.7617E06	96.5E+06				00001440
145	1	1	521500.	200.8E+06				00001450
146	6	3	5	2	1	990.	1000.	00001460
147						270000.	84.0E+06 -270000.	00001470
148	1	1	301000.	228.7E+06				00001480
149	1	11.3581E 06	84.2E+06					00001490
150	7	3	5	3	1	1090.	1000.	00001500
151						270000.	75.0E+06 -270000.	00001510
152	0	1	210000.	-555.88E06				00001520

# ECHO OF THE INPUT DATA IN CARD IMAGE FORMAT

CARD NO.	1	2	3	4	5	6	7	8
153	1	1	327700.	107.75E06				00001530
154	1	1	1.5738E06	64.0 E06				00001540
155	7	3	5	3	1	1160.	1000.	00001550
156						270000.	66.0E+06 -270000.	00001560
157	0	1	239000.	-265.64E06			-66.0E+06	00001570
158	1	1	372214.	85.0E 06				00001580
159	1	1	804840.	50.0E 06				00001590
160	8	3	5	1	1	1210.	1000.	00001600
161						235000.	50.0 E 06 -235000.	00001610
162	0	1	200000.	-217.32E06			-50.0E06	00001620
163	8	3	5	1	1	1320.	1000.	00001630
164						180000.	40.0 E 06 -180000.	00001640
165	0	1	148000.	-91.818E06			-40.0E06	00001650
166	8	3	5	2	1	1400.	1000.	00001660
167						160000.	30.0 E+06 -160000.	00001670
168	0	1	125000.	-54.998E06			-30.0E+06	00001680
169	1	1	260000.	45.0E 06				00001690
170	9	3	5	2	1	1400.	1000.	00001700
171						160000.	30.0 E+06 -160000.	00001710
172	0	1	125000.	-54.998E06			-30.0E+06	00001720
173	1	1	260000.	45.0E 06				00001730
174	FORCE	TIME	HISTORY	DATA:	NACC	+	CARDS	00001740
175	1	3	2	1				00001750
176	2	3	2	1				00001760
177	3	3	2	1				00001770
178	4	3	2	1				00001780
179	5	3	2	1				00001790
180	6	3	2	1				00001800
181	7	3	2	1				00001810
182	8	3	2	1				00001820
183	9	3	2	1				00001830
184	10	3	2	1				00001840
185	11	3	2	1				00001850
186	12	3	2	1				00001860
187	13	3	2	1				00001870
188	14	3	2	1				00001880
189	15	3	2	1				00001890
190	16	3	2	1				00001900
191	17	3	2	1				00001910
192	0.		-95.					00001920
193	1.		-95.					00001930
194	0.		-624.5					00001940
195	1.		-624.5					00001950
196	0.		-1861.					00001960
197	1.		-1861.					00001970
198	0.		-4715.					00001980
199	1.		-4715.					00001990
200	0.		-7901.					00002000
201	1.		-7901.					00002010
202	0.		-1991.					00002020
203	1.		-1991.					00002030



# ECHO OF THE INPUT DATA IN CARD IMAGE FORMAT

CARD NO.	1	2	3	4	5	6	7	8
204	0.	-2316.						00002040
205	1.	-2316.						00002050
206	0.	-785.4						00002060
207	1.	-785.4						00002070
208	0.	-450.						00002080
209	1.	-450.0						00002090
210	0.	17445.6						00002100
211	1.	17445.6						00002110
212	0.	-23129.2						00002120
213	1.	-23129.2						00002130
214	0.	-28188.2						00002140
215	1.	-28188.2						00002150
216	0.	-21394.1						00002160
217	1.	-21394.1						00002170
218	0.	-17818.8						00002180
219	1.	-17818.8						00002190
220	0.	-6240.9						00002200
221	1.	-6240.9						00002210
222	0.	-270.8						00002220
223	1.	-270.8						00002230
224	0.	-258.3						00002240
225	1.	-258.3						00002250
226	MASS PLOT PARAMETERS: NMEP							00002260
227	1	1	0	0	0	0	1	0
228	2	1	0	0	0	0	1	1
229	3	1	0	0	0	0	1	0
230	4	1	0	0	0	0	1	0
231	5	1	1	1	1	1	1	1
232	6	1	0	0	0	0	1	1
233	7	1	0	0	0	0	1	1
234	8	1	0	0	0	0	1	1
235	9	1	0	0	0	0	1	1
236	16	1	0	0	0	0	1	1
237	17	1	0	0	0	0	1	1
238	BEAM ELEMENT LOAD PLOT PARAMETERS:NBFP PLOTS							00002370
239	1	1	1	1	1	1	1	1
240	2	1	1	1	1	1	1	1
241	3	1	1	1	1	1	1	1
242	4	1	1	1	1	1	1	1
243	5	1	1	1	1	1	1	1
244	6	1	1	1	1	1	1	1
245	7	1	1	1	1	1	1	1
246	8	1	1	1	1	1	1	1
247	9	1	1	1	1	1	1	1
248	10	1	1	1	1	1	1	1
249	11	1	1	1	1	1	1	1
250	12	1	1	1	1	1	1	1
251	13	1	1	1	1	1	1	1
252	14	1	1	1	1	1	1	1
253	15	1	1	1	1	1	1	1
254	16	1	1	1	1	1	1	1

ECHO OF THE INPUT DATA IN CARD IMAGE FORMAT

	1	2	3	4	5	6	7	8
CARD NO.	1234567890123456789012345678901234567890123456789012345678901234567890							
255	BEAM ELEMENT DEFLECTION PLOT PARAMETERS: NBDP							00002550
256	1	1	1	1				00002560
257	2	1	1	1				00002570
258	3	1	1	1				00002580
259	4	1	1	1				00002590
260	5	1	1	1				00002600
261	6	1	1	1				00002610
262	7	1	1	1				00002620
263	8	1	1	1				00002630
264	9	1	0	1				00002640
265	10	1	1	1				00002650
266	11	1	1	1				00002660
267	12	1	1	1				00002670
268	13	1	1	1				00002680
269	14	1	1	1				00002690
270	15	1	0	1				00002700
271	16	1	0	1				00002710
272	EXTERNAL SPRING LOAD-DEFLECTION PLOT PARAMETERS: NSEP							00002720
273	2	0	1	1				00002730
274	3	0	1	1				00002740
275	4	0	1	1				00002750
276	5	0	1	1				00002760
277	6	0	1	1				00002770
278	7	0	1	1				00002780
279	8		1	1				00002790
280	16	0	1	1				00002800
281	17		1	1				00002810
282	END							00002820

#### A.4 KRASH CID AIRPLANE EXPANDED MODEL ECHO

### ECHO OF THE INPUT DATA IN CARD IMAGE FORMAT

CARD NO. 1 2 3 4 5 6 7 8  
1234567890123456789012345678901234567890123456789012345678901234567890

1	GILS.PRECID.OLDENG44.DATA 6-25-85 193K WT FWD FUS8WING8ENG T=1.16										00000010				
2	155 KTS.+1. PITCH 00 YAW 00 ROLL 17 ROD-RIG.GRD MU=.50 .DIAGS. NLB=44										00000020				
3	12345678901234567890123456789012345678901234567890123456789012										00000030				
4	NM	NSP	NB	NLB	NMP	NPIN	NUB	NDRINOLEO	NACC	MVP	NVCH	NMTL	ND	00000040	
5	48	18	137	44	34	66	48	0	0	48	0	0	0	00000050	
6	NVBM	NFBM	NVBM	NFBM	NKM	NMI	NPH	TOL1	TOL2	TOL3	NSC	NICNAERON	BOMB	00000060	
7	0	12	0	31	0	0	0	1000	1000	1000	0	1	0	1	00000070
8	NSCV		NLICNWRGR		NBAL		ICDICITR							00000080	
9	1	18	0	5	1	1								00000090	
10	GRAPHICS													00000100	
11														00000110	
12														00000120	
13	ONE RESTART AND ONE SAVE CARD FOLLOWS													00000130	
14														00000140	
15														00000150	
16	IPRINT		DELTAT		TMAX		PLOWT		FCUT		RUNMOD		00000160		
17	50		.000100		0.160		0.000		50.		1.		00000170		
18	BLANK CARD FOLLOWS													00000180	
19														00000190	
20	NSF	NTF	NDE	NSPD	NED	NS	NRP	NIMP	NBC : PRINT DATA					00000200	
21	0	0	0	0	0	0	0	0	0					00000210	
22	NMEP	NNEP	NBFP	NBDP	NSTP	NSEP	NENP	NDRP	NPLTNPFCT : PLOT DATA					00000220	
23	20	0	0	0	0	0	0	0	0					00000230	
24	INITIAL CONDITION DATA : 3 CARDS													00000240	
25	3140.00		000.00		204.00									00000250	
26	000.00		000.00		000.00									00000260	
27	000.00		+.01730		000.00		000.00		000.00		0.001.1463E-07		00000270		
28	MASS DATA : NM CARDS													00000280	
29	525.6		199.0		0.0		205.0.37996E+04		.13200E+04		.49500E+03		00000290		
30	4476.0		300.0		0.0		205.0.29396E+04		.99000E+04		.32670E+04		00000300		
31	6418.0		460.0		0.0		205.0.53717E+04		.31989E+04		.34020E+04		00000310		
32	5745.0		620.0		0.0		205.0.64769E+04		.22016E+04		.26198E+04		00000320		
33	9438.0		820.0		0.0		205.0.16205E+05		.41471E+04		.48348E+04		00000330		
34	3585.0		960.0		0.0		205.0.26856E+04		.39600E+04		.66000E+04		00000340		
35	3759.0		1040.0		0.0		205.0.28887E+04		.46200E+04		.66000E+04		00000350		
36	4083.0		1200.0		0.0		205.0.29072E+04		.59400E+04		.99000E+04		00000360		
37	2505.0		1400.0		0.0		205.0.31762E+04		.13790E+04		.85929E+03		00000370		
38	6175.0		1570.0		0.0		297.0.21530E+06		.10798E+06		.15863E+06		00000380		
39	277.5		199.0		46.0		205.0.51468E+03		.17880E+04		.67050E+03		00000390		
40	2238.0		300.0		66.0		205.0.39819E+04		.13410E+05		.44253E+04		00000400		
41	3352.0		460.0		70.0		205.0.72763E+04		.43330E+04		.46081E+04		00000410		
42	2994.0		620.0		70.0		205.0.87733E+04		.29822E+04		.35487E+04		00000420		
43	4920.0		820.0		70.0		205.0.21950E+05		.56174E+04		.65490E+04		00000430		
44	1864.0		960.0		70.0		205.0.36378E+04		.53640E+04		.89400E+04		00000440		
45	1968.0		1040.0		70.0		205.0.39129E+04								

## ECHO OF THE INPUT DATA IN CARD IMAGE FORMAT

CARD NO.	1	2	3	4	5	6	7	8
51	594.0	460.0	65.0	270.0.66740E+04.	39743E+04.	42267E+04	00000510	
52	505.0	620.0	65.0	270.0.80471E+04.	27353E+04.	32549E+04	00000520	
53	837.0	820.0	65.0	270.0.20133E+05.	51525E+04.	60069E+04	00000530	
54	305.0	960.0	65.0	270.0.33367E+04.	49200E+04.	82000E+04	00000540	
55	356.0	1040.0	65.0	270.0.35890E+04.	57400E+04.	82000E+04	00000550	
56	383.0	1200.0	65.0	270.0.36120E+04.	73800E+04.	12300E+05	00000560	
57	221.0	1400.0	40.0	240.0.39462E+04.	17133E+04.	10676E+04	00000570	
58	260.0	1040.0	70.0	181.0.36516E+04.	25746E+05.	29375E+05	00000580	
59	48.0	199.0	0.0	270.0.34887E+03.	12120E+04.	45450E+03	00000590	
60	304.0	300.0	0.0	280.0.26991E+04.	90900E+04.	29997E+04	00000600	
61	440.0	460.0	0.0	293.0.49322E+04.	29371E+04.	31236E+04	00000610	
62	374.0	620.0	0.0	293.0.59470E+04.	20215E+04.	24055E+04	00000620	
63	620.0	820.0	0.0	293.0.14879E+05.	38078E+04.	44392E+04	00000630	
64	226.0	960.0	0.0	293.0.24659E+04.	36360E+04.	60600E+04	00000640	
65	264.0	1040.0	0.0	293.0.26523E+04.	42420E+04.	60600E+04	00000650	
66	284.0	1200.0	0.0	293.0.26694E+04.	54540E+04.	90900E+04	00000660	
67	164.0	1400.0	0.0	280.0.29163E+04.	12662E+04.	78898E+03	00000670	
68	277.0	1200.0	70.0	181.0.36520E+04.	25788E+05.	29478E+05	00000680	
69	9786.0	801.3	118.3	188.3.07642E+05.	69387E+05.	18000E+06	00000690	
70	4835.0	825.3	176.8	195.7.07642E+05.	69387E+05.	18000E+06	00000700	
71	10065.0	852.3	271.8	203.1.19542E+06.	12387E+06.	30000E+06	00000710	
72	5286.0	943.5	430.7	219.9.72715E+04.	52619E+05.	11000E+06	00000720	
73	3759.0	1045.8	583.5	243.5.44083E+04.	25823E+05.	60000E+05	00000730	
74	1542.0	1112.6	740.6	255.0.16708E+04.	90137E+04.	18000E+05	00000740	
75	5400.0	719.0	321.6	169.3.36516E+04.	25746E+05.	29375E+05	00000750	
76	5151.0	902.8	551.6	188.1.37120E+04.	24588E+05.	28178E+05	00000760	
77	NODE POINT DATA : NNP CARDS							
78	1	14	620.	70.	181.		00000770	
79	1	16	960.	70.	181.		00000790	
80	1	12	300.	66.	181.		00000800	
81	1	15	820.	70.	181.		00000810	
82	1	41	650.0	118.3	205.		00000820	
83	2	41	833.0	118.3	205.		00000830	
84	3	41	650.	118.3	171.6		00000840	
85	4	41	833.	118.3	171.6		00000850	
86	1	42	770.0	176.8	195.7		00000860	
87	2	42	900.0	176.8	195.7		00000870	
88	1	43	790.0	271.8	203.1		00000880	
89	2	43	919.0	271.8	203.1		00000890	
90	1	44	893.0	430.7	219.9		00000900	
91	2	44	993.0	430.7	219.9		00000910	
92	1	45	1010.0	583.5	243.5		00000920	
93	2	45	1080.0	583.5	243.5		00000930	
94	1	46	1087.0	740.0	255.0		00000940	
95	2	46	1137.0	740.0	255.0		00000950	
96	1	47	735.7	321.6	199.6		00000960	
97	1	48	918.4	551.6	220.5		00000970	
98	1	2	300.0	0.0	205.0		00000980	
99	2	2	279.0	0.0	147.5		00000990	
100	1	1	199.0	0.0	205.0		00001000	
101	1	11	199.	46.0	205.		00001010	

# ECHO OF THE INPUT DATA IN CARD IMAGE FORMAT

CARD NO.	1	2	3	4	5	6	7	8
102	2	1	199.	0.0	150.			00001020
103	3	2	300.	0.0	150.			00001030
104	1	3	460.	0.0	150.			00001040
105	1	4	620.	0.0	140.			00001050
106	1	5	820.	0.0	140.			00001060
107	1	6	960.	0.0	140.			00001070
108	1	7	1040.0	0.0	150.			00001080
109	1	8	1200.	0.0	150.			00001090
110	1	9	1400.	0.0	150.			00001100
111	2	9	1400.	0.0	253.1			00001110
112	EXTERNAL	SPRING DATA : 2 X NSP	CARDS					00001120
113	1	3	60.2	0.35	100000.0			00001130
114	2	3	69.2	0.35	100000.0			00001140
115	20	3	44.2	0.35	100000.0			00001150
116	4	3	68.2	0.35	300000.0			00001160
117	5	3	69.4	0.35	300000.0			00001170
118	6	3	69.1	0.35	300000.0			00001180
119	30	3	42.7	0.35	100000.0			00001190
120	40	3	32.2	0.35	100000.0			00001200
121	9	3	13.0	0.35	300000.0			00001210
122	10	3	82.0	0.35	300000.0			00001220
123	12	3	69.2	0.35	100000.0			00001230
124	14	3	68.2	0.35	100000.0			00001240
125	15	3	69.4	0.35	100000.0			00001250
126	16	3	69.1	0.35	100000.0			00001260
127	42	3	14.0	0.35	100000.0			00001270
128	41	3	28.0	0.35	100000.0			00001280
129	47	3	38.3	0.35	272000.0			00001290
130	48	3	28.0	0.35	272000.0			00001300
131	1.1	1.5	4.0	10.	50000.	2500.	0.00	00001310
132	1.1	3.3	4.4	18.0	100000.	2500.	0.00	00001320
133	4.0	5.0	6.0	24.0	64000.	64000.	0.00	00001330
134	1.1	3.3	6.6	10.	100000.	100000.	0.00	00001340
135	1.1	3.3	6.6	10.	125000.	100000.	0.00	00001350
136	1.1	3.3	6.6	18.	125000.	100000.	0.00	00001360
137	4.0	5.0	6.0	18.0	27500.	27500.	0.00	00001370
138	4.0	5.0	6.0	18.0	37500.	37500.	0.00	00001380
139	1.0	1.1	2.0	3.0	150000.	15000.	0.00	00001390
140	1.0	1.1	2.0	3.0	150000.	15000.	0.00	00001400
141	1.1	3.3	4.4	18.	50000.	1250.		00001410
142	1.1	3.3	6.6	10.	50000.	50000.		00001420
143	1.1	3.3	6.6	10.	62500.	50000.		00001430
144	1.1	3.3	6.6	18.	62500.	50000.		00001440
145	1.	1.5	2.	7.	330000.	330000.		00001450
146	1.	1.5	2.	7.	330000.	330000.	0.00	00001460
147	1.	8.	9.	16.	50000.	100000.		00001470
148	1.	8.	9.	16.	50000.	100000.		00001480
149	INTERNAL BEAM DATA : NB CARDS							00001490
150	1	11	4.35	840.0	53.00	1000.0	3	1 500001500
151	2	12	6.30	1200.0	74.00	2400.0	3	1 500001510
152	3	13	7.20	1380.0	84.00	4000.0	3	1 500001520

ECHO OF THE INPUT DATA IN CARD IMAGE FORMAT

CARD NO.	1	2	3	4	5	6	7	8
153	4	14	8.10	1560.0	95.00	6000.0	3	1
154	5	15	8.10	1560.0	95.00	6000.0	3	1
155	6	16	5.40	1018.0	64.00	1500.0	3	1
156	7	17	5.40	1018.0	64.00	1500.0	3	1
157	8	18	8.10	1560.0	95.00	6000.0	3	1
158	9	19	4.50	840.0	53.00	1000.0	3	1
159	11	21	6.60	250.0	400.0	9.0	1.8	1.8
160	21	31	6.60	250.0	9.00	400.0	1.8	1.8
161	12	22	8.75	334.0	1000.0	12.6	1.8	1.8
162	22	32	8.75	334.0	12.60	1000.0	1.8	1.8
163	13	23	10.0	383.0	1600.	14.4	1.8	1.8
164	23	33	10.0	383.0	14.40	1600.0	1.8	1.8
165	14	24	11.3	432.0	2400.	16.2	1.8	1.8
166	24	34	11.3	432.0	16.20	2400.0	1.8	1.8
167	15	25	11.3	432.0	2400.	16.2	1.8	1.8
168	25	35	11.3	432.0	16.20	2400.0	1.8	1.8
169	16	26	7.50	285.0	600.	10.8	1.8	1.8
170	26	36	7.50	285.0	10.80	600.0	1.8	1.8
171	17	27	7.50	285.0	600.0	10.8	1.8	1.8
172	27	37	7.50	285.0	10.80	600.0	1.8	1.8
173	18	28	11.2	432.0	2000.	16.2	1.8	1.8
174	28	38	11.2	432.0	16.20	2000.0	1.8	1.8
175	19	29	6.30	250.0	400.	9.0	1.8	1.8
176	29	39	6.30	250.0	9.00	400.0	1.8	1.8
177	13	20	10.0	383.0	1600.0	14.4	1.8	1.8
178	17	30	7.50	285.0	600.0	10.8	1.8	1.8
179	18	40	11.2	432.0	2000.0	16.2	1	1
180	21	22	3.10	0.0	982.00	20.00	1	1
181	22	23	3.86	0.0	1228.00	24.70	1	1
182	23	24	5.53	0.0	1763.00	35.50	1	1
183	24	25	5.53	0.0	1763.00	35.50	1	1
184	25	26	5.55	0.0	1763.00	35.50	1	1
185	26	27	5.18	0.0	1650.00	33.20	1	1
186	27	28	4.23	0.0	592.00	11.90	1	1
187	28	29	3.10	0.0	434.00	8.70	1	1
188	31	32	8.02	0.0	874.00	11092.0	1	1
189	32	33	10.1	0.0	1012.00	13865.0	1	1
190	33	34	12.86	0.0	1307.00	17616.0	1	1
191	34	35	12.86	0.0	1307.00	17616.0	1	1
192	35	36	14.02	0.0	1511.00	19616.0	1	1
193	36	37	12.75	0.0	1375.00	17462.0	1	1
194	37	38	12.00	0.0	1296.00	16453.0	1	1
195	38	39	10.32	0.0	1116.00	14172.0	1	1
196	1	2	2.32	500.	8.25	1000.00	4	1
197	2	3	2.54	750.	8.25	4000.00	4	1
198	3	4	2.54	800.	8.25	4000.00	4	1
199	4	5	4.35	800.	16.50	8000.00	4	1
200	5	6	4.35	800.	16.50	8000.00	4	1
201	6	7	4.00	800.	16.50	8000.00	4	1
202	7	8	3.40	700.	12.75	6000.00	4	1
203	8	9	2.54	500.	8.25	4000.00	4	1

## ECHO OF THE INPUT DATA IN CARD IMAGE FORMAT

CARD NO.	1	2	3	4	5	6	7	8
204	11	12	2.20	100.	11.80	500.00	4	1
205	12	13	1.40	100.	8.20	347.00	4	1
206	13	14	1.28	100.	5.90	243.00	4	1
207	14	15	1.28	200.	5.90	243.00	4	1
208	15	16	2.84	200.	12.70	535.00	4	1
209	16	17	3.00	200.	16.30	687.00	4	1
210	17	18	1.45	100.	8.30	351.00	4	1
211	18	19	1.36	100.	5.90	250.00	4	1
212	2	9	10	25.00	0.0	1.4E05	1.4E04	1
213	1	12	20	0.76	0.0	6.50	6.60	1
214	1	14	20	0.63	0.0	5.40	6.30	1
215	1	16	30	.49	0.0	4.20	6.00	1
216	30	40	.67	0.0	5.70	6.40	1	1
217	19	40	.33	0.0	2.85	3.20	1	1
218	2	43	1	2.00	55.5	183.00	25.00	1
219	2	45	1	2.00	55.4	183.00	25.00	1
220	15	2	41	13.50	1.2E04	3200.00	.29E04	1
221	14	1	41	13.50	1.2E04	3200.00	.29E04	1
222	3	41	0	13.5	1.2E04	3200.00	.29E04	1
223	4	41	0	13.5	1.2E04	3200.00	.29E04	1
224	1	43	47	2.00	55.4	183.00	25.00	1
225	1	45	48	2.00	55.4	183.00	25.00	1
226	41	42	63.20	26000.0	11400.00	102000.00	1	1
227	42	43	60.00	18000.0	8100.00	80000.00	1	1
228	43	44	56.00	10000.0	4700.00	58000.00	1	1
229	44	45	40.70	4800.0	2000.00	21000.00	1	1
230	45	46	20.00	2700.0	1200.00	8000.00	1	1
231	2	1	3	2	4.5	100.	592.	6985.
232	3	2	1	3	5.54	100.	700.	82
233	1	3	1	4	3.84	100.	500.	15.6
234	1	4	1	5	3.84	100.	500.	15.6
235	1	5	1	6	6.0	100.	800.	26.
236	1	6	1	7	9.3	100.	1120.00	13200.
237	1	7	1	8	6.6	100.	840.	9920.
238	1	8	1	9	5.4	100.	629.	7425.
239	2	1	12	4.5	100.	592.	6985.	1
240	4	1	14	5.6	100.	700.	82	1
241	5	1	15	7.2	100.	800.	26.	1
242	6	1	16	4.4	100.	1120.00	13200.	1
243	1	16	17	5.0	100.	840.	9920.	1
244	16	30	5.0	100.	629.	7425.	1	1
245	17	40	5.	100.	629.	7425.	1	1
246	18	30	5.	100.	629.	7425.	1	1
247	12	20	5.	100.	629.	7425.	1	1
248	1	12	13	5.	100.	629.	7425.	1
249	14	20	5.	100.	629.	7425.	1	1
250	13	1	14	5.	100.	629.	7425.	1
251	12	23	5.	100.	629.	7425.	1	1
252	13	22	5.	100.	629.	7425.	1	1
253	13	24	5.	100.	629.	7425.	1	1
254	14	23	5.	100.	629.	7425.	1	1

## ECHO OF THE INPUT DATA IN CARD IMAGE FORMAT

CARD NO.	1	2	3	4	5	6	7	8
12345678901234567890123456789012345678901234567890123456789012345678901234567890								
255	14	25	5.					400002550
256	15	24	5.					400002560
257	15	26	5.					400002570
258	16	25	5.					400002580
259	16	27	5.0					400002590
260	17	26	5.0					400002600
261	17	28	5.					400002610
262	18	27	5.					400002620
263	18	29	5.					400002630
264	19	28	5.					400002640
265	22	33	5.					400002650
266	23	32	5.					400002660
267	23	34	5.					400002670
268	24	33	5.					400002680
269	24	35	5.					400002690
270	25	34	5.					400002700
271	25	36	5.					400002710
272	26	35	5.					400002720
273	26	37	5.0					400002730
274	27	36	5.0					400002740
275	27	38	5.					400002750
276	28	37	5.					400002760
277	28	39	5.					400002770
278	29	38	5.					400002780
279	1 5	15	7.2					400002790
280	1 4	14	5.6					400002800
281	1 6	16	4.4					400002810
282	1 4	5	4.					400002820
283	4 1	5	4.					400002830
284	1 5	6	4.					400002840
285	5 1	6	4.					400002850
286	3 2	12	4.					400002860
287	BEAM END FIXITY CARDS: NPIN CARDS							00002870
288	21	31	0	0	1	0	0.	00002880
289	22	32	0	0	1	0	0.	00002890
290	23	33	0	0	1	0	0.	00002900
291	24	34	0	0	1	0	0.	00002910
292	25	35	0	0	1	0	0.	00002920
293	26	36	0	0	1	0	0.	00002930
294	27	37	0	0	1	0	0.	00002940
295	28	38	0	0	1	0	0.	00002950
296	29	39	0	0	1	0	0.	00002960
297	11	21	0	1	0	1	0.	00002970
298	12	22	0	1	0	1	0.	00002980
299	13	23	0	1	0	1	0.	00002990
300	14	24	0	1	0	1	0.	00003000
301	15	25	0	1	0	1	0.	00003010
302	16	26	0	1	0	1	0.	00003020
303	17	27	0	1	0	1	0.	00003030
304	18	28	0	1	0	1	0.	00003040
305	19	29	0	1	0	1	0.	00003050



# ECHO OF THE INPUT DATA IN CARD IMAGE FORMAT

CARD NO.	1	2	3	4	5	6	7	8
306	2 1 12	1	1	1	1			00003060
307	4 1 14	1	1	1	1			00003070
308	5 1 15	1	1	1	1			00003080
309	6 1 16	1	1	1	1			00003090
310	1 4 5	1	1	1	1			00003100
311	4 1 5	1	1	1	1			00003110
312	1 5 6	1	1	1	1			00003120
313	5 1 6	1	1	1	1			00003130
314	3 2 12	1	1	1	1			00003140
315	1 6 16	1	1	1	1			00003150
316	1 5 15	1	1	1	1			00003160
317	1 4 14	1	1	1	1			00003170
318	1 16 17	1	1	1	1			00003180
319	16 30	1	1	1	1			00003190
320	17 40	1	1	1	1			00003200
321	18 30	1	1	1	1			00003210
322	12 20	1	1	1	1			00003220
323	1 12 13	1	1	1	1			00003230
324	14 20	1	1	1	1			00003240
325	13 1 14	1	1	1	1			00003250
326	12 23	1	1	1	1			00003260
327	13 22	1	1	1	1			00003270
328	13 24	1	1	1	1			00003280
329	14 23	1	1	1	1			00003290
330	14 25	1	1	1	1			00003300
331	15 24	1	1	1	1			00003310
332	15 26	1	1	1	1			00003320
333	16 25	1	1	1	1			00003330
334	16 27	1	1	1	1			00003340
335	17 26	1	1	1	1			00003350
336	17 28	1	1	1	1			00003360
337	18 27	1	1	1	1			00003370
338	18 29	1	1	1	1			00003380
339	19 28	1	1	1	1			00003390
340	22 33	1	1	1	1			00003400
341	23 32	1	1	1	1			00003410
342	23 34	1	1	1	1			00003420
343	24 33	1	1	1	1			00003430
344	24 35	1	1	1	1			00003440
345	25 34	1	1	1	1			00003450
346	25 36	1	1	1	1			00003460
347	26 35	1	1	1	1			00003470
348	26 37	1	1	1	1			00003480
349	27 36	1	1	1	1			00003490
350	27 38	1	1	1	1			00003500
351	28 37	1	1	1	1			00003510
352	28 39	1	1	1	1			00003520
353	29 38	1	1	1	1			00003530
354	UNSYM.BEAM ELEMENTS:NUB CARDS							00003540
355	2 1 12	1						00003550
356	4 1 14	1						00003560

ECHO OF THE INPUT DATA IN CARD IMAGE FORMAT

CARD NO.	1	2	3	4	5	6	7	8
357	5	1	15	1				00003570
358	6	1	16	1				00003580
359	1	16	17	1				00003590
360	16	30	1					00003600
361	17	40	1					00003610
362	18	30	1					00003620
363	12	20	1					00003630
364	1	12	13	1				00003640
365	14	20	1					00003650
366	13	1	14	1				00003660
367	12	23	1					00003670
368	13	22	1					00003680
369	13	24	1					00003690
370	14	23	1					00003700
371	14	25	1					00003710
372	15	24	1					00003720
373	15	26	1					00003730
374	16	25	1					00003740
375	16	27	1					00003750
376	17	26	1					00003760
377	17	28	1					00003770
378	18	27	1					00003780
379	1	5	15	1				00003790
380	1	4	14	1				00003800
381	1	6	16	1				00003810
382	1	4	5	1				00003820
383	4	1	5	1				00003830
384	1	5	6	1				00003840
385	5	1	6	1				00003850
386	3	2	12	1				00003860
387	18	29	1					00003870
388	19	28	1					00003880
389	22	33	1					00003890
390	23	32	1					00003900
391	23	34	1					00003910
392	24	33	1					00003920
393	24	35	1					00003930
394	25	34	1					00003940
395	25	36	1					00003950
396	26	35	1					00003960
397	26	37	1					00003970
398	27	36	1					00003980
399	27	38	1					00003990
400	28	37	1					00004000
401	28	39	1					00004010
402	29	38	1					00004020
403	DAMPC CARD							00004030
404	.10							00004040
405	NONLINEAR BEAMS:NLB CARDS							00004050
406	21	22	1	5	.32			00004060
407	22	23	1	5	.48			00004070

ECHO OF THE INPUT DATA IN CARD IMAGE FORMAT

CARD NO.	1	2	3	4	5	6	7	8	
408	23	24	1	5	.48			00004080	
409	24	25	1	5	.6			00004090	
410	25	26	1	5	.4			00004100	
411	26	27	1	5	.24			00004110	
412	27	28	1	5	.48			00004120	
413	31	32	1	8	.39			00004130	
414	32	33	1	8	.59			00004140	
415	33	34	1	8	.59			00004150	
416	34	35	1	8	.75			00004160	
417	35	36	1	8	.52			00004170	
418	36	37	1	8	.3			00004180	
419	37	38	1	8	.59			00004190	
420	1	2	1	5	.32			00004200	
421	2	3	1	5	.48			00004210	
422	3	4	1	5	.48			00004220	
423	4	5	1	5	.60			00004230	
424	5	6	1	5	.40			00004240	
425	6	7	1	5	.24			00004250	
426	7	8	1	5	.48			00004260	
427	11	12	1	5	.32			00004270	
428	12	13	1	5	.48			00004280	
429	13	14	1	5	.48			00004290	
430	14	15	1	5	.60			00004300	
431	15	16	1	5	.40			00004310	
432	16	17	1	5	.24			00004320	
433	17	18	1	5	.48			00004330	
434	1	12	20	1	5	.48		00004340	
435	1	14	20	1	5	.48		00004350	
436	1	16	30	1	5	.24		00004360	
437		30	40	1	5	.48		00004370	
438		19	40	1	5	.6		00004380	
439	2	1	3	2	1	5	.32	00004390	
440	3	2	1	3	1	5	.48	00004400	
441	1	3	1	4	1	5	.48	00004410	
442	1	4	1	5	1	5	.60	00004420	
443	1	5	1	6	1	5	.4	00004430	
444	1	6	1	7	1	5	.24	00004440	
445	1	7	1	8	1	5	.48	00004450	
446	1	8	1	9	1	5	.48	00004460	
447		6	16	1	5	.2		00004470	
448		7	17	1	5	.2		00004480	
449		8	18	1	5	.2		00004490	
450	POS	BEAM	CUTOFF:	NFBM	X	2	CARDS	00004500	
451	2	12	2.10E5	7.2E04	7.2E04	1.E10	1.E10	00004510	
452	3	13	2.44E5	8.2E04	8.2E04	1.E10	1.E10	00004520	
453	4	14	2.75E5	9.2E04	9.2E04	1.E10	1.E10	00004530	
454	5	15	2.75E5	9.2E04	9.2E04	1.E10	1.E10	00004540	
455	6	16	1.80E5	6.2E04	6.2E04	1.E10	1.E10	00004550	
456	7	17	1.83E5	6.2E04	6.2E04	1.E10	1.E10	00004560	
457	2	9	8.50E5	1.0E10	1.5E05	1.E10	2.E07	00004570	
458	1	3	1	4	134000	1.0E10	4.3E04	1.E10	00004580

## ECHO OF THE INPUT DATA IN CARD IMAGE FORMAT

CARD NO.	1	2	3	4	5	6	7	8
1234567890	1234567890	1234567890	1234567890	1234567890	1234567890	1234567890	1234567890	1234567890
459	15 2 41	4.60E5	1.5E05	1.5E05	1.E10	1.E10	1.E10	00004590
460	14 1 41	4.60E5	1.5E05	1.5E05	1.E10	1.E10	1.E10	00004600
461	3 41 0	4.60E5	1.5E05	1.5E05	1.E10	1.E10	1.E10	00004610
462	4 41 0	4.60E5	1.5E05	1.5E05	1.E10	1.E10	1.E10	00004620
463	NEG BEAM CUTOFF:NFBMN X 2 CARDS							
464	2 43 1 47	30000.	1.E10	1.25E5	1.E10	1.E10	1.E10	00004640
465	1 43 47	30000.	1.E10	1.25E5	1.E10	1.E10	1.E10	00004650
466	2 45 1 48	30000.	1.E10	1.25E5	1.E10	1.E10	1.E10	00004660
467	1 45 48	30000.	1.E10	1.25E5	1.E10	1.E10	1.E10	00004670
468	1 3 1 4	134000.	1.E10	4.3E4	1.E10	1.E10	1.E10	00004680
469	1 4 1 5	134000.	1.E10	4.3E4	1.E10	1.E10	1.E10	00004690
470	1 5 1 6	210000.	1.E10	6.8E4	1.E10	1.E10	1.E10	00004700
471	1 6 1 7	265000.	1.E10	1.1E5	1.E10	1.E10	1.E10	00004710
472	1 7 1 8	231000.	1.E10	7.1E4	1.E10	1.E10	1.E10	00004720
473	1 8 1 9	183000.	6.2E4	6.2E4	1.E10	1.E10	1.E10	00004730
474	2 9 10	8.5E5	1.E10	1.5E5	1.E10	2.E07	1.E10	00004740
475	3 4	1.2E5	1.E10	2.9E4	1.E10	1.E10	1.E10	00004750
476	4 5	1.5E5	1.E10	4.9E4	1.E10	1.E10	1.E10	00004760
477	5 6	1.5E5	1.E10	4.9E4	1.E10	1.E10	1.E10	00004770
478	6 7	1.4E5	1.E10	4.5E4	1.E10	1.E10	1.E10	00004780
479	7 8	1.2E5	1.E10	3.9E4	1.E10	1.E10	1.E10	00004790
480	13 14	4.0E4	1.E10	1.5E4	1.E10	1.E10	1.E10	00004800
481	14 15	4.4E4	1.E10	1.5E4	1.E10	1.E10	1.E10	00004810
482	15 16	9.6E4	1.E10	3.2E4	1.E10	1.E10	1.E10	00004820
483	16 17	1.0E5	1.E10	3.4E4	1.E10	1.E10	1.E10	00004830
484	17 18	1.E10	1.E10	1.E10	1.E10	1.E10	1.E10	00004840
485	2 12	2.1E5	7.2E4	7.2E4	1.E10	1.E10	1.E10	00004850
486	3 13	2.4E5	8.2E4	8.2E4	1.E10	1.E10	1.E10	00004860
487	4 14	2.7E5	9.2E4	9.2E4	1.E10	1.E10	1.E10	00004870
488	5 15	2.7E5	9.2E4	9.2E4	1.E10	1.E10	1.E10	00004880
489	6 16	1.8E5	6.2E4	6.2E4	1.E10	1.E10	1.E10	00004890
490	7 17	1.8E5	6.2E4	6.2E4	1.E10	1.E10	1.E10	00004900
491	15 2 41	4.6E5	1.5E5	1.5E5	1.E10	1.E10	1.E10	00004910
492	14 1 41	4.6E5	1.5E5	1.5E5	1.E10	1.E10	1.E10	00004920
493	3 41 0	4.6E5	1.5E5	1.5E5	1.E10	1.E10	1.E10	00004930
494	4 41 0	4.6E5	1.5E5	1.5E5	1.E10	1.E10	1.E10	00004940
495	LOAD INTERACTION SIGN CONVENTIONS(NSCV CARDS):							
496	1 2 -3 4 5 6							00004960
497	LOAD INTERACTION DATA(NLIC+ CARDS):							
498	47 3 5 1 0 5	300.				1000.		00004980
499		166000.	32.5E+06	-166000.	-32.5E+06			00004990
500	1 1 215000.	42.5 E+06						00005000
501	216.6 215.7							00005010
502	31 39 47 55 82							00005020
503	48 3 5 1 0 10	350.				1000.		00005030
504		166000.	39.0E+06	-166000.	-39.0E+06			00005040
505	1 1 260000.	70.0 E+06						00005050
506	215.7 206.4							00005060
507	32 40 48 56 64 83	102 103	116 117					00005070
508	48 3 5 1 0 10	450.				1000.		00005080
509		210000.	45.0E+06	-210000.	-45.0E+06			00005090

# ECHO OF THE INPUT DATA IN CARD IMAGE FORMAT

CARD NO.	1	2	3	4	5	6	7	8
510	1	1	300000.	100. E+06				00005100
511	215.7	206.4						00005110
512	32	40	48	56	64	83	102 103 116 117	00005120
513	49	3	5	1	0	10	480. 1000.	00005130
514							210000. 50.0E+06 -210000. -50.0E+06	00005140
515	1	1	400000.	80.0 E+06				00005150
516	206.4	204.7						00005160
517	33	41	49	57	65	84	104 105 118 119	00005170
518	49	3	5	1	0	10	540. 1000.	00005180
519							210000. 50.0E+06 -210000. -50.0E+06	00005190
520	1	1	400000.	100.0 E+06				00005200
521	206.4	204.7						00005210
522	33	41	49	57	65	84	104 105 118 119	00005220
523	49	3	5	2	0	10	600. 1000.	00005230
524							280000. 62.5E+06 -280000. -62.5E+06	00005240
525	1	1	318000.	206.6 E+06				00005250
526	1	1	422400	88.7 E+06				00005260
527	206.4	204.7						00005270
528	33	41	49	57	65	84	104 105 118 119	00005280
529	50	3	5	2	0	11	620. 1000.	00005290
530							280000. 62.5E+06 -280000. -62.5E+06	00005300
531	1	1	318000.	206.6 E+06				00005310
532	1	1	422400	88.7 E+06				00005320
533	204.7	202.0						00005330
534	34	42	50	58	85	106	107 120 121 133 134	00005340
535	50	3	5	2	1	11	820. 1000.	00005350
536							288000. 62.5E+06 -288000. -62.5E+06	00005360
537	1	0-5.2317E06	71.5E+06					00005370
538	1	1	474500.	152.8E+06				00005380
539	204.7	202.0						00005390
540	34	42	50	58	85	106	107 120 121 133 134	00005400
541	51	3	5	2	1	11	820. 1000.	00005410
542							288000. 62.5E+06 -288000. -62.5E+06	00005420
543	1	0-5.2317E06	71.5E+06					00005430
544	1	1	474500.	152.8E+06				00005440
545	202.0	212.4						00005450
546	35	43	51	59	86	108	109 122 123 135 136	00005460
547	51	3	5	2	1	11	960. 1000.	00005470
548							315000. 96.0E+06 -315000. -96.0E+06	00005480
549	1	0-5.7617E06	96.5E+06					00005490
550	1	1	521500.	200.8E+06				00005500
551	202.0	212.4						00005510
552	35	43	51	59	86	108	109 122 123 135 136	00005520
553	52	3	5	2	1	10	960. 1000.	00005530
554							315000. 96.0E+06 -315000. -96.0E+06	00005540
555	1	0-5.7617E06	96.5E+06					00005550
556	1	1	521500.	200.8E+06				00005560
557	202.0	207.7						00005570
558	36	44	52	60	66	87	124 125 110 111	00005580
559	52	3	5	2	1	10	990. 1000.	00005590
560							270000. 84.0E+06 -270000. -84.0E+06	00005600

ECHO OF THE INPUT DATA IN CARD IMAGE FORMAT

CARD NO.	1	2	3	4	5	6	7	8
561	1	1	301000.	228.7E+06				00005610
562	1	11.3581E 06	84.2E+06					00005620
563	202.0	207.7						00005630
564	36	44	52	60	66	87	124 125 110 111	00005640
565	53	3	5	3	1	10	1090.	00005650
566							270000. 75.0E+06 -270000. -75.0E+06	00005660
567	0	1	210000.	-555.88E06				00005670
568	1	1	327700.	107.75E06				00005680
569	1	1	1.5738E06	64.0 E06				00005690
570	207.7	224.2						00005700
571	37	45	53	61	67	88	112 113 126 127	00005710
572	53	3	5	3	1	10	1160.	00005720
573							270000. 66.0E+06 -270000. -66.0E+06	00005730
574	0	1	239000.	-265.64E06				00005740
575	1	1	372214.	85.0E 06				00005750
576	1	1	804840.	50.0E 06				00005760
577	207.7	224.2						00005770
578	37	45	53	61	67	88	112 113 126 127	00005780
579	54	3	5	1	1	10	1210.	00005790
580							235000. 50.0 E 06 -235000. -50.0E06	00005800
581	0	1	200000.	-217.32E06				00005810
582	224.2	257.5						00005820
583	38	46	54	62	68	89	114 115 128 129	00005830
584	54	3	5	1	1	10	1320.	00005840
585							180000. 40.0 E 06 -180000. -40.0E06	00005850
586	0	1	148000.	-91.818E06				00005860
587	224.2	257.5						00005870
588	38	46	54	62	68	89	114 115 128 129	00005880
589	54	3	5	2	1	10	1400.	00005890
590							160000. 30.0 E 06 -160000. -30.0E06	00005900
591	0	1	123500.	-54.998E06				00005910
592	1	1	350720.	24.2E 06				00005920
593	224.2	257.5						00005930
594	38	46	54	62	68	89	114 115 128 129	00005940
595	63	3	5	2	1	1	1400.	00005950
596							160000. 30.0 E 06 -160000. -30.0E06	00005960
597	0	1	123500.	-54.998E06				00005970
598	1	1	350720.	24.2E 06				00005980
599	257.2	298.						00005990
600	63							00006000
601	FORCE	TIME	HISTORY	DATA:	NACC	+ CARDS		00006010
602	1	3	2	1				00006020
603	11	3	2	1				00006030
604	21	3	2	1				00006040
605	31	3	2	1				00006050
606	2	3	2	1				00006060
607	12	3	2	1				00006070
608	22	3	2	1				00006080
609	32	3	2	1				00006090
610	3	3	2	1				00006100
611	13	3	2	1				00006110

# ECHO OF THE INPUT DATA IN CARD IMAGE FORMAT

CARD NO.	1	2	3	4	5	6	7	8
612	23	3	2	1				00006120
613	33	3	2	1				00006130
614	4	3	2	1				00006140
615	14	3	2	1				00006150
616	24	3	2	1				00006160
617	34	3	2	1				00006170
618	5	3	2	1				00006180
619	15	3	2	1				00006190
620	25	3	2	1				00006200
621	35	3	2	1				00006210
622	6	3	2	1				00006220
623	16	3	2	1				00006230
624	26	3	2	1				00006240
625	36	3	2	1				00006250
626	7	3	2	1				00006260
627	17	3	2	1				00006270
628	27	3	2	1				00006280
629	37	3	2	1				00006290
630	8	3	2	1				00006300
631	18	3	2	1				00006310
632	28	3	2	1				00006320
633	38	3	2	1				00006330
634	9	3	2	1				00006340
635	19	3	2	1				00006350
636	29	3	2	1				00006360
637	39	3	2	1				00006370
638	10	3	2	1				00006380
639	20	3	2	1				00006390
640	30	3	2	1				00006400
641	40	3	2	1				00006410
642	41	3	2	1				00006420
643	42	3	2	1				00006430
644	43	3	2	1				00006440
645	44	3	2	1				00006450
646	45	3	2	1				00006460
647	46	3	2	1				00006470
648	47	3	2	1				00006480
649	48	3	2	1				00006490
650	0.		-31.50					00006500
651	1.		-31.50					00006510
652	0.		-16.75					00006520
653	1.		-16.75					00006530
654	0.		-3.9					00006540
655	1.		-3.9					00006550
656	0.		-3.9					00006560
657	1.		-3.9					00006570
658	0.		-282.0					00006580
659	1.		-282.0					00006590
660	0.		-131.0					00006600
661	1.		-131.0					00006610
662	0.		-25.44					00006620

## ECHO OF THE INPUT DATA IN CARD IMAGE FORMAT

CARD NO.	1	2	3	4	5	6	7	8
663	1.	-25.44						00006630
664	0.	-18.86						00006640
665	1.	-18.86						00006650
666	0.	-780.						00006660
667	1.	-780.						00006670
668	0.	-408.						00006680
669	1.	-408.						00006690
670	0.	-72.16						00006700
671	1.	-72.16						00006710
672	0.	-53.46						00006720
673	1.	-53.46						00006730
674	0.	-2066.						00006740
675	1.	-2066.						00006750
676	0.	-1068.						00006760
677	1.	-1068.						00006770
678	0.	-181.8						00006780
679	1.	-181.8						00006790
680	0.	-134.7						00006800
681	1.	-134.7						00006810
682	0.	-3428.6						00006820
683	1.	-3428.6						00006830
684	0.	-1786.8						00006840
685	1.	-1786.8						00006850
686	0.	-304.0						00006860
687	1.	-304.0						00006870
688	0.	-228.2						00006880
689	1.	-228.2						00006890
690	0.	-1012.0						00006900
691	1.	-1012.4						00006910
692	0.	-438.6						00006920
693	1.	-438.6						00006930
694	0.	-76.8						00006940
695	1.	-76.8						00006950
696	0.	-57.0						00006960
697	1.	-57.0						00006970
698	0.	-948.2						00006980
699	1.	-948.2						00006990
700	0.	-496.5						00007000
701	1.	-496.5						00007010
702	0.	-89.7						00007020
703	1.	-89.7						00007030
704	0.	-66.5						00007040
705	1.	-66.5						00007050
706	0.	-322.5						00007060
707	1.	-322.5						00007070
708	0.	-168.5						00007080
709	1.	-168.5						00007090
710	0.	-30.2						00007100
711	1.	-30.2						00007110
712	0.	-13.9						00007120
713	1.	-13.9						00007130



# ECHO OF THE INPUT DATA IN CARD IMAGE FORMAT

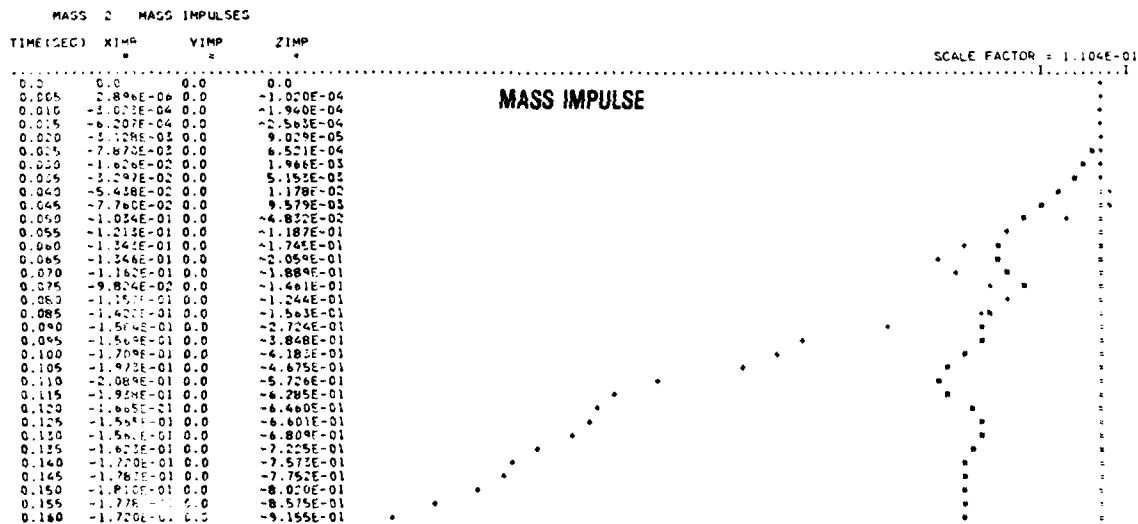
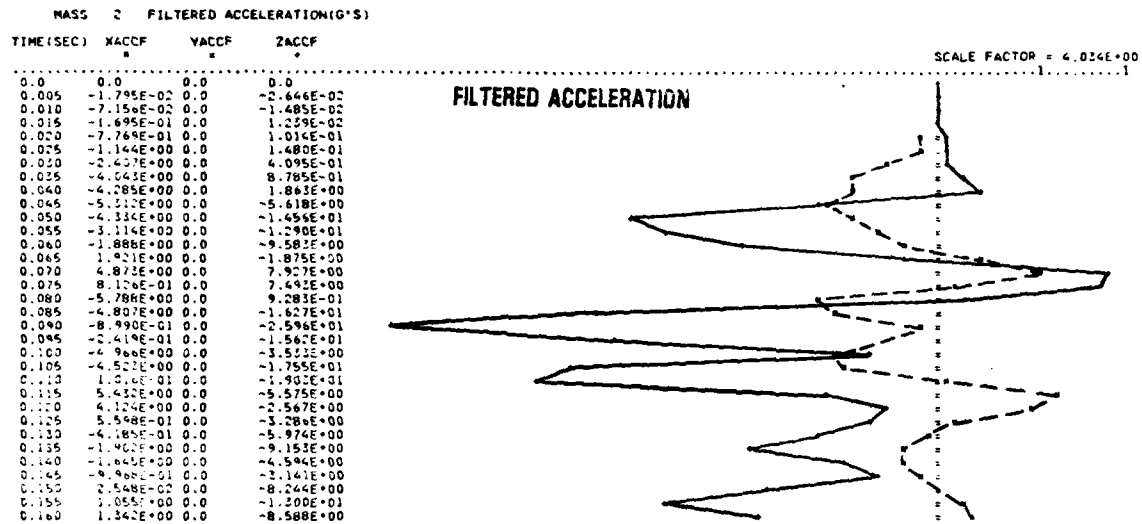
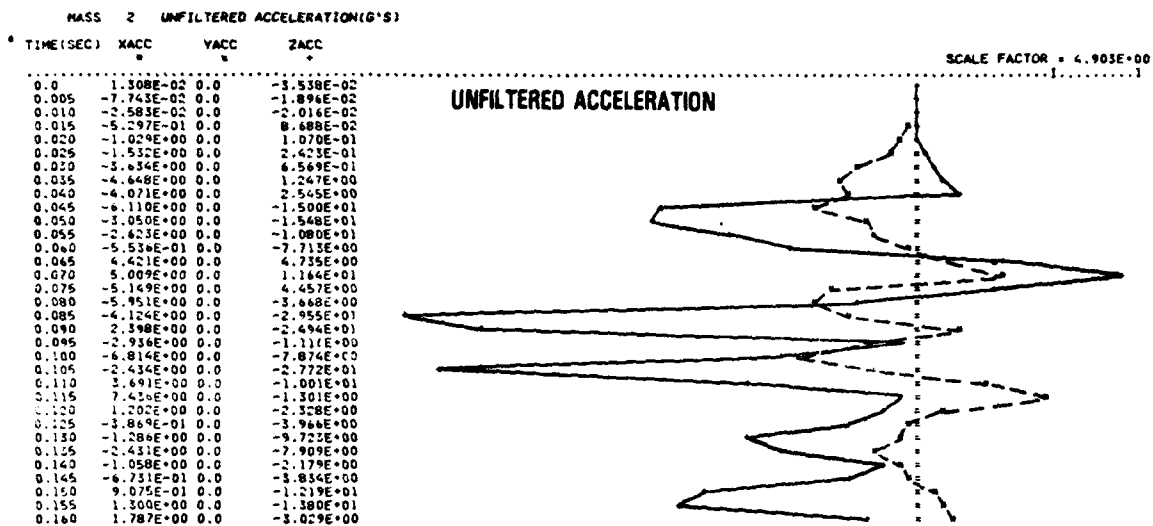
CARD NO.	1	2	3	4	5	6	7	8
714	0.	-202.						00007140
715	1.	-202.						00007150
716	0.	-103.						00007160
717	1.	-103.						00007170
718	0.	-17.4						00007180
719	1.	-17.4						00007190
720	0.	-12.9						00007200
721	1.	-12.9						00007210
722	0.	17545.6						00007220
723	1.	17545.6						00007230
724	0.	-52.8						00007240
725	1.	-52.8						00007250
726	0.	-65.5						00007260
727	1.	-65.5						00007270
728	0.	-21.9						00007280
729	1.	-21.9						00007290
730	0.	-15420.						00007300
731	1.	-15420.						00007310
732	0.	-7710.						00007320
733	1.	-7710.						00007330
734	0.	-28190.						00007340
735	1.	-28190.						00007350
736	0.	-21390.						00007360
737	1.	-21390.						00007370
738	0.	-17820.						00007380
739	1.	-17820.						00007390
740	0.	-6240.						00007400
741	1.	-6240.						00007410
742	0.	-270.8						00007420
743	1.	-270.8						00007430
744	0.	-258.						00007440
745	1.	-258.						00007450
746	MASS PLOTS:NMEP CARDS							00007460
747	1			1	1	1	1	00007470
748	2			1	1	1	1	00007480
749	3			1	1	1	1	00007490
750	4			1	1	1	1	00007500
751	5			1	1	1	1	00007510
752	6			1	1	1	1	00007520
753	7			1	1	1	1	00007530
754	8			1	1	1	1	00007540
755	9			1	1	1	1	00007550
756	11			1	1	1	1	00007560
757	12			1	1	1	1	00007570
758	13			1	1	1	1	00007580
759	14			1	1	1	1	00007590
760	15			1	1	1	1	00007600
761	16			1	1	1	1	00007610
762	17			1	1	1	1	00007620
763	18			1	1	1	1	00007630
764	19			1	1	1	1	00007640

# ECHO OF THE INPUT DATA IN CARD IMAGE FORMAT

CARD NO.	1	2	3	4	5	6	7	8
1234567890123456789012345678901234567890123456789012345678901234567890								
765	47							
766	48							
767	END							
			1	1	1			00007650
			1	1	1			00007660
								00008400

APPENDIX B

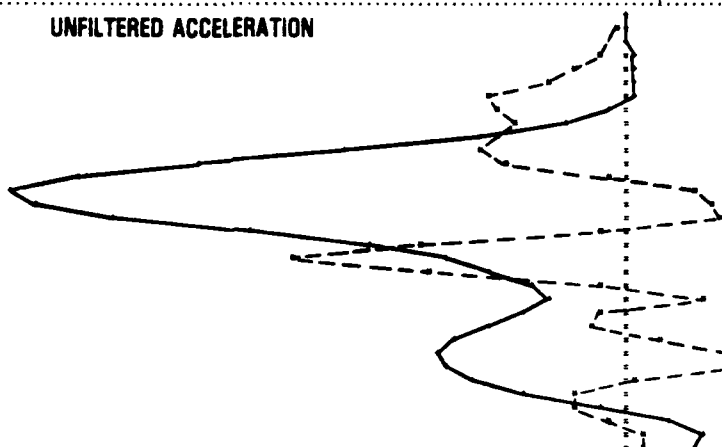
# APPENDIX B: KRASH TIME HISTORY RESPONSES - EXPANDED MODEL



# MASS 3 UNFILTERED ACCELERATION(G'S)

TIME(SEC)	XACC	YACC	ZACC
0.0	0.0	0.0	0.0
0.005	-3.15E-02	0.0	-3.280E-02
0.010	-9.755E-02	0.0	-1.543E-01
0.015	-6.40E-02	0.0	2.404E-01
0.020	-6.720E-01	0.0	1.909E-01
0.025	-1.201E+00	0.0	2.388E-01
0.030	-2.157E+00	0.0	2.445E-01
0.035	-3.713E+00	0.0	2.641E-01
0.040	-3.273E+00	0.0	3.412E-01
0.045	-2.954E+00	0.0	1.540E+00
0.050	-3.50E+00	0.0	-3.950E+00
0.055	-3.975E+00	0.0	-7.780E+00
0.060	-3.305E+00	0.0	-1.167E+01
0.065	-4.702E+01	0.0	-1.499E+01
0.070	1.83E+00	0.0	-1.680E+01
0.075	2.349E+00	0.0	-1.418E+01
0.080	2.602E+00	0.0	-1.389E+01
0.085	-6.462E-01	0.0	-1.056E+01
0.090	-5.462E+00	0.0	-6.990E+00
0.095	-8.992E+00	0.0	-4.818E+00
0.100	-5.420E+00	0.0	-3.719E+00
0.105	-8.077E-01	0.0	-2.645E+00
0.110	-2.095E+00	0.0	-2.178E+00
0.115	-6.919E-01	0.0	-2.797E+00
0.120	-8.700E-01	0.0	-3.653E+00
0.125	8.878E-01	0.0	-4.624E+00
0.130	2.828E+00	0.0	-5.091E+00
0.135	2.751E+00	0.0	-4.935E+00
0.140	2.285E-01	0.0	-4.747E+00
0.145	-1.478E+00	0.0	-2.722E+00
0.150	-1.315E+00	0.0	-6.925E-01
0.155	-3.400E-01	0.0	1.75E+00
0.160	4.000E-01	0.0	2.00E+00
0.165	5.65E-01	0.0	1.93E+00

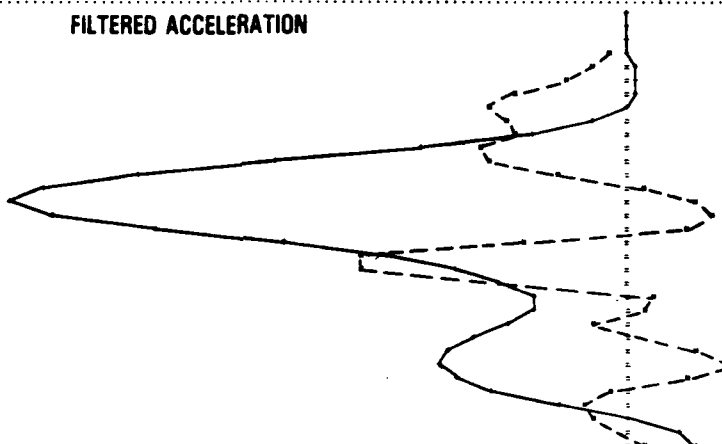
## UNFILTERED ACCELERATION



# MASS 3 FILTERED ACCELERATION(G'S)

TIME(SEC)	XACF	YACF	ZACF
0.0	0.0	0.0	0.0
0.005	-2.724E-02	0.0	-1.897E-02
0.010	-7.447E-02	0.0	-3.806E-01
0.015	-3.449E-01	0.0	7.611E-02
0.020	-8.785E-01	0.0	2.054E-01
0.025	-1.577E+00	0.0	2.396E-01
0.030	-2.892E+00	0.0	2.459E-01
0.035	-3.529E+00	0.0	2.852E-02
0.040	-2.102E+00	0.0	-8.427E-01
0.045	-3.000E+00	0.0	-2.457E+00
0.050	-3.876E+00	0.0	-5.512E+00
0.055	-3.771E+00	0.0	-9.266E+00
0.060	-1.920E+00	0.0	-1.287E+01
0.065	4.17E-01	0.0	-1.599E+01
0.070	1.89E-03	0.0	-1.659E+01
0.075	1.20E+00	0.0	-1.518E+01
0.080	1.644E+00	0.0	-1.245E+01
0.085	-2.642E+00	0.0	-9.069E+00
0.090	-7.074E+00	0.0	-6.268E+00
0.095	-7.070E+00	0.0	-4.555E+00
0.100	-2.429E+00	0.0	-2.360E+00
0.105	6.52E-01	0.0	-2.482E+00
0.110	4.350E-01	0.0	-2.514E+00
0.115	-8.149E-01	0.0	-3.149E+00
0.120	3.726E-02	0.0	-4.026E+00
0.125	1.764E+00	0.0	-4.782E+00
0.130	2.764E+00	0.0	-4.976E+00
0.135	1.595E+00	0.0	-4.648E+00
0.140	-5.099E-01	0.0	-3.929E+00
0.145	-1.024E+00	0.0	-1.919E+00
0.150	-8.921E-01	0.0	-1.891E-02
0.155	6.960E-05	0.0	1.401E+00
0.160	3.926E-01	0.0	1.932E+00

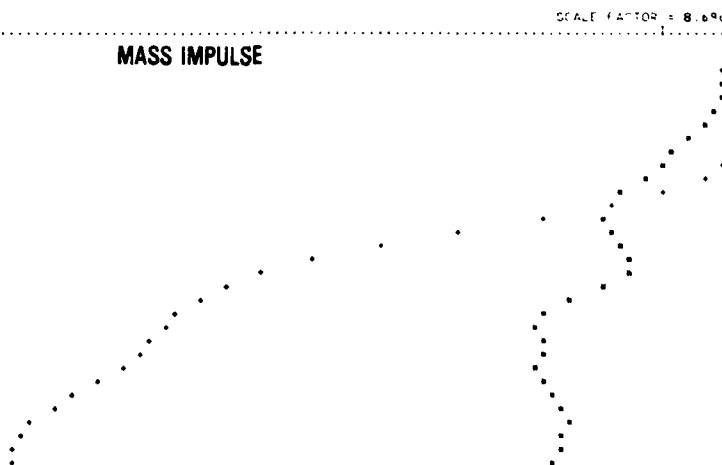
## FILTERED ACCELERATION



# MASS 3 MASS IMPULSES

TIME(SEC)	XIMP	YIMP	ZIMP
0.0	0.0	0.0	0.0
0.005	-5.311E-05	0.0	-9.084E-05
0.010	-5.711E-04	0.0	-1.124E-04
0.015	-1.144E-03	0.0	-4.427E-06
0.020	-4.184E-02	0.0	7.710E-04
0.025	-1.025E-02	0.0	1.401E-03
0.030	-2.102E-02	0.0	3.084E-03
0.035	-3.788E-02	0.0	4.031E-03
0.040	-5.422E-02	0.0	2.117E-03
0.045	-6.924E-02	0.0	-5.705E-03
0.050	-8.705E-02	0.0	-2.522E-02
0.055	-1.062E-01	0.0	-6.243E-02
0.060	-1.209E-01	0.0	-1.182E-01
0.065	-1.246E-01	0.0	-1.401E-01
0.070	-1.182E-01	0.0	-2.711E-01
0.075	-1.079E-01	0.0	-3.506E-01
0.080	-9.61E-02	0.0	-4.200E-01
0.085	-9.868E-02	0.0	-4.725E-01
0.090	-1.226E-01	0.0	-5.112E-01
0.095	-1.614E-01	0.0	-5.277E-01
0.100	-1.86E-01	0.0	-5.575E-01
0.105	-1.929E-01	0.0	-5.716E-01
0.110	-1.894E-01	0.0	-5.827E-01
0.115	-1.921E-01	0.0	-5.978E-01
0.120	-1.927E-01	0.0	-6.157E-01
0.125	-1.892E-01	0.0	-6.380E-01
0.130	-1.775E-01	0.0	-6.627E-01
0.135	-1.657E-01	0.0	-6.869E-01
0.140	-1.635E-01	0.0	-7.079E-01
0.145	-1.684E-01	0.0	-7.218E-01
0.150	-1.742E-01	0.0	-7.264E-01
0.155	-1.762E-01	0.0	-7.222E-01
0.160	-1.750E-01	0.0	-7.135E-01

## MASS IMPULSE

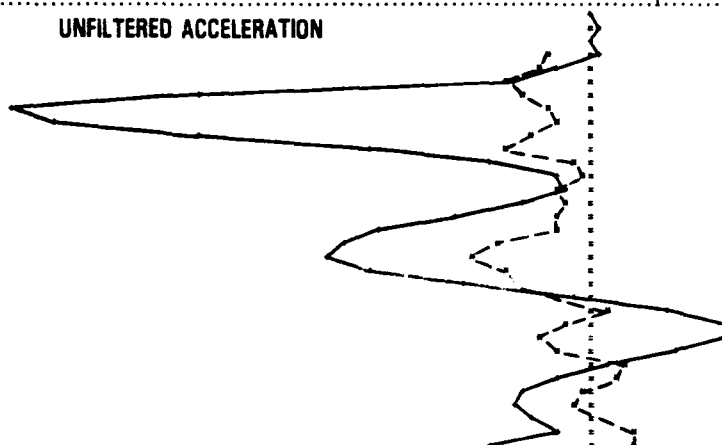


# MASS 4 UNFILTERED ACCELERATION(G'S)

TIME(SEC)	XACC	YACC	ZACC
0.0	1.316E-02	0.0	-3.009E-02
0.005	-2.156E-01	0.0	6.345E-02
0.010	-1.114E-01	0.0	1.833E-02
0.015	-1.453E+00	0.0	8.585E-02
0.020	-1.848E+00	0.0	-1.085E+00
0.025	-2.804E+00	0.0	-2.708E+00
0.030	-2.338E+00	0.0	-1.283E+01
0.035	-1.416E+00	0.0	-1.897E+01
0.040	-1.286E+00	0.0	-1.752E+01
0.045	-2.290E+00	0.0	-1.292E+01
0.050	-2.92E+00	0.0	-7.415E+00
0.055	-5.279E-01	0.0	-3.363E+00
0.060	-3.830E-01	0.0	-1.242E+00
0.065	-1.095E+00	0.0	-8.733E-01
0.070	-8.522E-01	0.0	-2.202E+00
0.075	-1.121E+00	0.0	-4.620E+00
0.080	-1.140E+00	0.0	-7.005E+00
0.085	-3.283E+00	0.0	-8.284E+00
0.090	-3.981E+00	0.0	-8.670E+00
0.095	-2.847E+00	0.0	-7.234E+00
0.100	-2.468E+00	0.0	-4.378E+00
0.105	-2.023E-01	0.0	-7.189E-01
0.110	-4.812E-01	0.0	2.427E+00
0.115	-9.179E-01	0.0	4.309E+00
0.120	-1.732E+00	0.0	4.337E+00
0.125	-1.084E+00	0.0	2.712E+00
0.130	1.057E+00	0.0	5.410E-01
0.135	8.445E-01	0.0	-1.277E+00
0.140	-2.691E-01	0.0	-2.232E+00
0.145	-6.445E-01	0.0	-2.574E+00
0.150	-3.726E-02	0.0	-2.096E+00
0.155	1.182E+00	0.0	-1.128E+00
0.160	1.405E+00	0.0	-3.296E+00

SCALE FACTOR = 2.775E+00

## UNFILTERED ACCELERATION

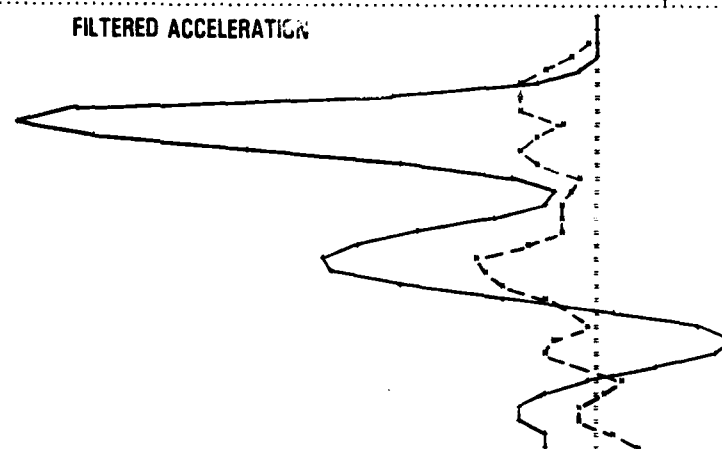


# MASS 4 FILTERED ACCELERATION(G'S)

TIME(SEC)	XACCF	YACCF	ZACCF
0.0	0.0	0.0	0.0
0.005	-1.089E-01	0.0	5.584E-03
0.010	-1.268E-01	0.0	5.156E-02
0.015	-8.226E-01	0.0	7.158E-02
0.020	-1.523E+00	0.0	-4.046E-01
0.025	-2.341E+00	0.0	-1.774E+00
0.030	-2.348E+00	0.0	-6.243E+00
0.035	-2.348E+00	0.0	-1.583E+01
0.040	-2.152E+00	0.0	-1.777E+01
0.045	-1.895E+00	0.0	-1.545E+01
0.050	-2.357E+00	0.0	-1.068E+01
0.055	-1.741E+00	0.0	-5.906E+00
0.060	-5.534E-01	0.0	-2.754E+00
0.065	7.326E-01	0.0	-1.263E+00
0.070	-1.109E+00	0.0	-1.511E+00
0.075	-1.066E+00	0.0	-3.216E+00
0.080	-9.275E-01	0.0	-5.562E+00
0.085	-2.120E+00	0.0	-7.400E+00
0.090	-3.590E+00	0.0	-8.375E+00
0.095	-3.271E+00	0.0	-8.028E+00
0.100	-2.839E+00	0.0	-8.045E+00
0.105	-1.458E+00	0.0	-2.926E+00
0.110	-4.412E-02	0.0	4.594E-01
0.115	-2.506E-01	0.0	3.047E+00
0.120	-1.272E+00	0.0	4.193E+00
0.125	-1.520E+00	0.0	3.582E+00
0.130	-8.179E-02	0.0	1.825E+00
0.135	8.677E-01	0.0	-1.870E-01
0.140	2.588E-01	0.0	-1.556E+00
0.145	-3.944E-01	0.0	-2.210E+00
0.150	-3.815E-01	0.0	-2.322E+00
0.155	5.516E-01	0.0	-1.671E+00
0.160	1.245E+00	0.0	-1.494E+00

SCALE FACTOR = 2.614E+00

## FILTERED ACCELERATION

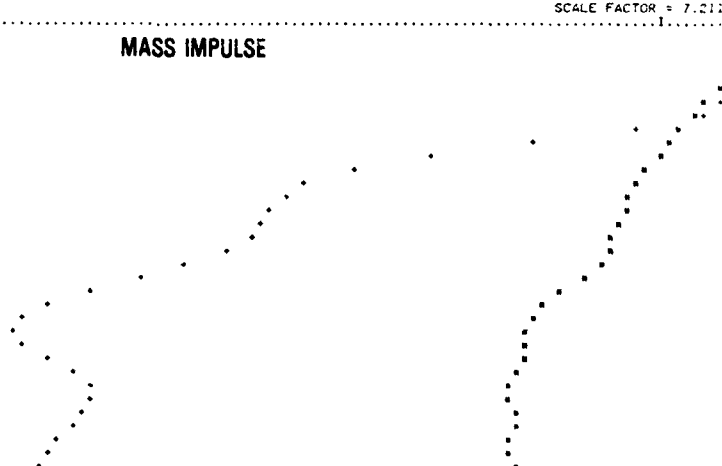


# MASS 4 MASS IMPULSES

TIME(SEC)	XIMP	YIMP	ZIMP
0.0	0.0	0.0	0.0
0.005	-1.785E-04	0.0	-6.751E-05
0.010	-8.829E-04	0.0	1.467E-04
0.015	-2.759E-03	0.0	3.760E-04
0.020	-8.971E-03	0.0	-1.857E-06
0.025	-1.852E-02	0.0	-5.377E-03
0.030	-3.253E-02	0.0	-2.167E-02
0.035	-6.280E-02	0.0	-8.026E-02
0.040	-5.361E-02	0.0	-1.666E-01
0.045	-5.826E-02	0.0	-2.511E-01
0.050	-6.852E-02	0.0	-3.165E-01
0.055	-8.304E-02	0.0	-3.572E-01
0.060	-8.491E-02	0.0	-2.779E-01
0.065	-8.782E-02	0.0	-3.871E-01
0.070	-8.243E-02	0.0	-3.433E-01
0.075	-9.800E-02	0.0	-4.048E-01
0.080	-1.079E-01	0.0	-4.269E-01
0.085	-1.049E-01	0.0	-4.597E-01
0.090	-1.248E-01	0.0	-4.996E-01
0.095	-1.426E-01	0.0	-5.412E-01
0.100	-1.578E-01	0.0	-5.770E-01
0.105	-1.691E-01	0.0	-5.996E-01
0.110	-1.719E-01	0.0	-6.053E-01
0.115	-1.717E-01	0.0	-5.959E-01
0.120	-1.757E-01	0.0	-5.770E-01
0.125	-1.832E-01	0.0	-5.670E-01
0.130	-1.876E-01	0.0	-5.434E-01
0.135	-1.843E-01	0.0	-5.346E-01
0.140	-1.817E-01	0.0	-5.442E-01
0.145	-1.822E-01	0.0	-5.543E-01
0.150	-1.846E-01	0.0	-5.662E-01
0.155	-1.812E-01	0.0	-5.764E-01
0.160	-1.795E-01	0.0	-5.830E-01

SCALE FACTOR = 7.212E-02

## MASS IMPULSE



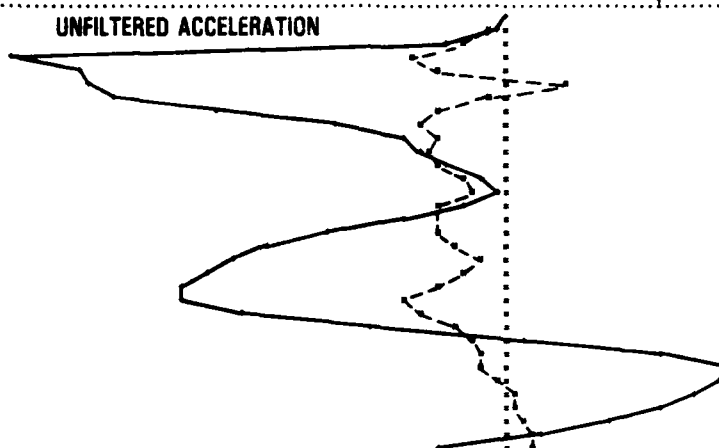
# MASS 5 UNFILTERED ACCELERATION(G'S)

TIME(SEC) XACC YACC ZACC

SCALE FACTOR = 2.297E+00

0.0	1.311E-02	0.0	-2.481E-02
0.005	-4.358E-01	0.0	-2.163E-01
0.010	-1.244E+00	0.0	-1.648E+00
0.015	-2.467E+00	0.0	-1.331E+01
0.020	-1.175E+00	0.0	-1.152E+01
0.025	1.547E+00	0.0	-1.154E+01
0.030	-3.751E-01	0.0	-1.057E+01
0.035	-1.895E+00	0.0	-7.819E+00
0.040	-2.180E+00	0.0	-4.668E+00
0.045	-1.842E+00	0.0	-2.696E+00
0.050	-2.118E+00	0.0	-2.358E+00
0.055	-1.843E+00	0.0	-1.684E+00
0.060	-1.187E+00	0.0	-5.728E-01
0.065	-9.454E-01	0.0	-2.909E-01
0.070	-1.845E+00	0.0	-1.110E+00
0.075	-2.683E+00	0.0	-2.720E+00
0.080	-1.793E+00	0.0	-4.745E+00
0.085	-1.413E+00	0.0	-6.352E+00
0.090	-5.774E-01	0.0	-7.421E+00
0.095	-1.158E+00	0.0	-8.067E+00
0.100	-1.914E+00	0.0	-8.731E+00
0.105	-2.789E+00	0.0	-8.821E+00
0.110	-2.384E+00	0.0	-7.171E+00
0.115	-1.405E+00	0.0	-3.772E+00
0.120	-9.024E-01	0.0	-4.114E-01
0.125	-6.992E-01	0.0	4.072E+00
0.130	-7.469E-01	0.0	5.982E+00
0.135	-1.661E-01	0.0	5.648E+00
0.140	1.323E-01	0.0	5.067E+00
0.145	2.055E-01	0.0	4.190E+00
0.150	5.523E-01	0.0	2.754E+00
0.155	7.511E-01	0.0	8.841E-01
0.160	7.598E-01	0.0	-1.786E+00

## UNFILTERED ACCELERATION



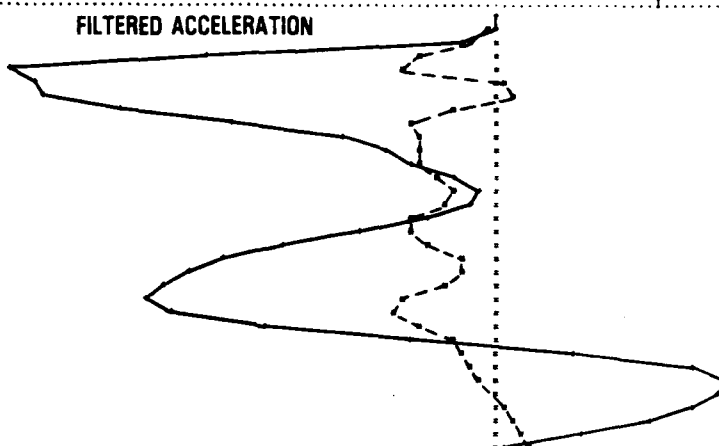
# MASS 5 FILTERED ACCELERATION(G'S)

TIME(SEC) XACCF YACCF ZACCF

SCALE FACTOR = 2.099E+00

0.0	0.0	0.0	0.0
0.005	-2.615E-01	0.0	-6.510E-02
0.010	-7.062E-01	0.0	-8.250E-01
0.015	-2.049E+00	0.0	-7.292E+00
0.020	-2.412E+00	0.0	-1.204E+01
0.025	1.250E-01	0.0	-1.149E+01
0.030	2.777E-01	0.0	-1.111E+01
0.035	-1.025E+00	0.0	-9.407E+00
0.040	-2.103E+00	0.0	-6.583E+00
0.045	-1.884E+00	0.0	-3.968E+00
0.050	-2.035E+00	0.0	-2.767E+00
0.055	-2.008E+00	0.0	-2.193E+00
0.060	-1.598E+00	0.0	-1.211E+00
0.065	-1.113E+00	0.0	-4.936E-01
0.070	-1.288E+00	0.0	-6.761E-01
0.075	-2.170E+00	0.0	-1.759E+00
0.080	-2.210E+00	0.0	-3.533E+00
0.085	-1.704E+00	0.0	-5.328E+00
0.090	-9.562E-01	0.0	-6.702E+00
0.095	-9.582E-01	0.0	-7.604E+00
0.100	-1.394E+00	0.0	-8.292E+00
0.105	-2.344E+00	0.0	-8.782E+00
0.110	-2.515E+00	0.0	-8.114E+00
0.115	-1.965E+00	0.0	-5.774E+00
0.120	-1.208E+00	0.0	-2.116E+00
0.125	-8.722E-01	0.0	1.766E+00
0.130	-7.193E-01	0.0	4.784E+00
0.135	-4.899E-01	0.0	5.589E+00
0.140	-1.674E-02	0.0	5.361E+00
0.145	9.654E-02	0.0	4.722E+00
0.150	3.597E-01	0.0	3.624E+00
0.155	6.172E-01	0.0	2.023E+00
0.160	7.456E-01	0.0	1.345E-01

## FILTERED ACCELERATION



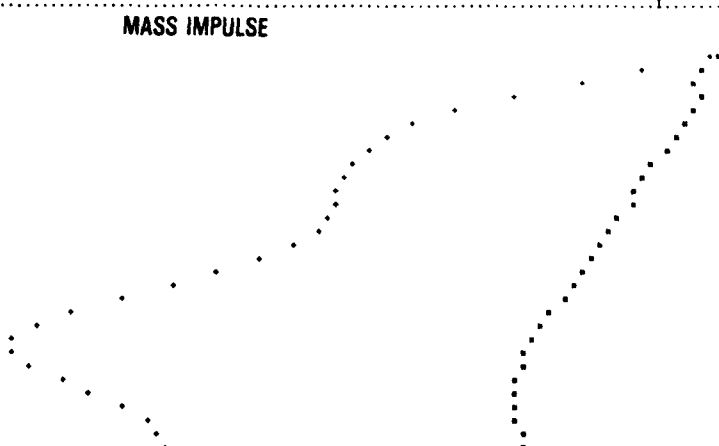
# MASS 5 MASS IMPULSES

TIME(SEC) XIMP YIMP ZIMP

SCALE FACTOR = 7.591E-02

0.0	0.0	0.0	0.0
0.005	-5.700E-04	0.0	-1.057E-04
0.010	-2.782E-03	0.0	-1.920E-03
0.015	-1.009E-02	0.0	-1.866E-02
0.020	-2.165E-02	0.0	-7.239E-02
0.025	-2.807E-02	0.0	-1.309E-01
0.030	-2.562E-02	0.0	-1.876E-01
0.035	-2.725E-02	0.0	-2.395E-01
0.040	-3.587E-02	0.0	-2.795E-01
0.045	-4.592E-02	0.0	-3.052E-01
0.050	-5.568E-02	0.0	-3.213E-01
0.055	-6.401E-02	0.0	-3.338E-01
0.060	-7.519E-02	0.0	-3.423E-01
0.065	-8.175E-02	0.0	-3.462E-01
0.070	-8.726E-02	0.0	-3.487E-01
0.075	-9.602E-02	0.0	-3.565E-01
0.080	-1.077E-01	0.0	-3.677E-01
0.085	-1.173E-01	0.0	-3.901E-01
0.090	-1.240E-01	0.0	-4.205E-01
0.095	-1.283E-01	0.0	-4.565E-01
0.100	-1.341E-01	0.0	-4.963E-01
0.105	-1.435E-01	0.0	-5.393E-01
0.110	-1.561E-01	0.0	-5.821E-01
0.115	-1.675E-01	0.0	-6.174E-01
0.120	-1.752E-01	0.0	-6.372E-01
0.125	-1.802E-01	0.0	-6.377E-01
0.130	-1.841E-01	0.0	-6.204E-01
0.135	-1.874E-01	0.0	-5.937E-01
0.140	-1.885E-01	0.0	-5.661E-01
0.145	-1.882E-01	0.0	-5.408E-01
0.150	-1.872E-01	0.0	-5.198E-01
0.155	-1.847E-01	0.0	-5.056E-01
0.160	-1.812E-01	0.0	-5.002E-01

## MASS IMPULSE

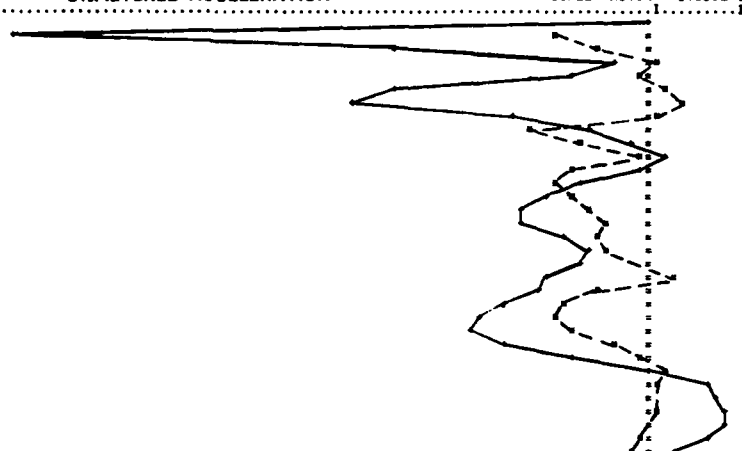


MASS 6 UNFILTERED ACCELERATION(G'S)

TIME(SEC)	XACC	YACC	ZACC
0.0	1.317E-02	0.0	-2.453E-02
0.005	-3.382E+00	0.0	-2.290E+01
0.010	-1.899E+00	0.0	-9.225E+00
0.015	3.846E-01	0.0	-1.274E+00
0.020	-2.889E-01	0.0	-2.580E+00
0.025	4.944E-01	0.0	-9.100E+00
0.030	1.363E+00	0.0	-1.058E+01
0.035	3.491E-01	0.0	-4.975E+00
0.040	-4.172E+00	0.0	-1.982E+00
0.045	-2.444E+00	0.0	-7.142E-01
0.050	-2.972E-01	0.0	5.131E-01
0.055	-2.822E+00	0.0	-1.475E-01
0.060	3.415E+00	0.0	-2.335E+00
0.065	-2.772E+00	0.0	-3.504E+00
0.070	-2.185E+00	0.0	-4.459E+00
0.075	-1.445E+00	0.0	-4.525E+00
0.080	-1.657E+00	0.0	-3.035E+00
0.085	-1.585E+00	0.0	-2.100E+00
0.090	6.893E-03	0.0	-2.537E+00
0.095	8.533E-01	0.0	-3.561E+00
0.100	-1.887E+00	0.0	-4.006E+00
0.105	-3.154E+00	0.0	-5.119E+00
0.110	-3.186E+00	0.0	-5.982E+00
0.115	-2.727E+00	0.0	-4.504E+00
0.120	-1.094E+00	0.0	-5.285E+00
0.125	-2.249E-01	0.0	-2.598E+00
0.130	5.229E-01	0.0	1.100E-01
0.135	2.869E-01	0.0	2.033E+00
0.140	4.707E-02	0.0	2.621E+00
0.145	2.728E-01	0.0	2.657E+00
0.150	3.513E-02	0.0	2.775E+00
0.155	-2.040E-01	0.0	2.295E+00
0.160	-4.985E-01	0.0	1.085E+00

UNFILTERED ACCELERATION

SCALE FACTOR = 3.056E+00

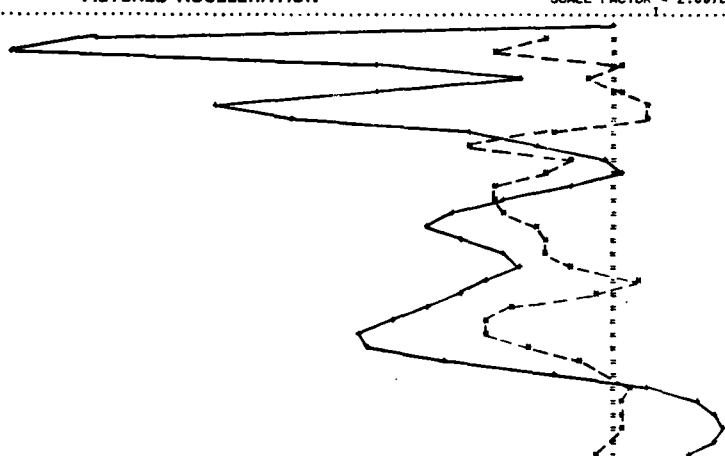


MASS 6 FILTERED ACCELERATION(G'S)

TIME(SEC)	XACCF	YACCF	ZACCF
0.0	0.0	0.0	0.0
0.005	-1.578E+00	0.0	-1.267E+01
0.010	-2.859E+00	0.0	-1.466E+02
0.015	1.841E-01	0.0	-5.812E+00
0.020	-5.739E-01	0.0	-2.281E+00
0.025	1.467E-01	0.0	-5.848E+00
0.030	9.428E-01	0.0	-4.650E+00
0.035	9.092E-01	0.0	-7.915E+00
0.040	-1.407E+00	0.0	-3.570E+00
0.045	-3.426E+00	0.0	-1.845E+00
0.050	-1.099E+00	0.0	-1.920E-01
0.055	-1.692E+00	0.0	1.315E-01
0.060	-2.980E+00	0.0	-1.110E+00
0.065	-2.975E+00	0.0	-2.714E+00
0.070	-2.591E+00	0.0	-3.826E+00
0.075	-1.854E+00	0.0	-4.501E+00
0.080	-1.631E+00	0.0	-3.803E+00
0.085	-1.628E+00	0.0	-2.651E+00
0.090	-9.453E-01	0.0	-2.325E+00
0.095	5.226E-01	0.0	-3.071E+00
0.100	-4.947E-01	0.0	-3.634E+00
0.105	-2.414E+00	0.0	-4.475E+00
0.110	-2.984E+00	0.0	-5.432E+00
0.115	-3.047E+00	0.0	-6.192E+00
0.120	-1.953E+00	0.0	-5.960E+00
0.125	-8.210E-01	0.0	-4.138E+00
0.130	6.878E-02	0.0	-1.535E+00
0.135	3.542E-01	0.0	7.838E-01
0.140	1.292E-01	0.0	2.145E+00
0.145	2.152E-01	0.0	2.534E+00
0.150	1.234E-01	0.0	2.701E+00
0.155	-2.463E-02	0.0	2.579E+00
0.160	-4.108E-01	0.0	1.781E+00

FILTERED ACCELERATION

SCALE FACTOR = 2.067E+00

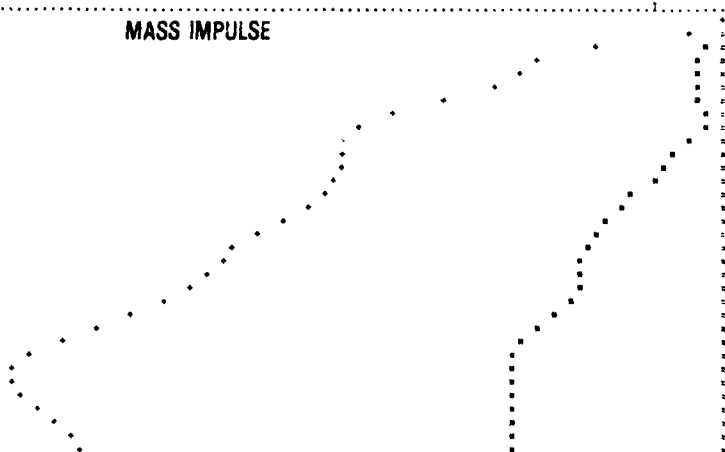


MASS 6 MASS IMPULSES

TIME(SEC)	XIMP	YIMP	ZIMP
0.0	0.0	0.0	0.0
0.005	-3.202E-03	0.0	-2.638E-02
0.010	-1.815E-02	0.0	-1.070E-01
0.015	-2.200E-02	0.0	-1.570E-01
0.020	-2.347E-02	0.0	-1.738E-01
0.025	-2.440E-02	0.0	-1.925E-01
0.030	-2.172E-02	0.0	-2.330E-01
0.035	-1.647E-02	0.0	-2.794E-01
0.040	-1.589E-02	0.0	-3.067E-01
0.045	-3.076E-02	0.0	-3.199E-01
0.050	-4.187E-02	0.0	-3.245E-01
0.055	-4.737E-02	0.0	-3.240E-01
0.060	-5.471E-02	0.0	-3.259E-01
0.065	-7.506E-02	0.0	-3.359E-01
0.070	-8.914E-02	0.0	-3.524E-01
0.075	-1.030E-01	0.0	-3.737E-01
0.080	-1.064E-01	0.0	-3.946E-01
0.085	-1.178E-01	0.0	-4.108E-01
0.090	-1.258E-01	0.0	-4.227E-01
0.095	-1.240E-01	0.0	-4.361E-01
0.100	-1.221E-01	0.0	-4.530E-01
0.105	-1.221E-01	0.0	-4.731E-01
0.110	-1.244E-01	0.0	-4.980E-01
0.115	-1.272E-01	0.0	-5.273E-01
0.120	-1.301E-01	0.0	-5.583E-01
0.125	-1.296E-01	0.0	-5.840E-01
0.130	-1.316E-01	0.0	-5.980E-01
0.135	-1.301E-01	0.0	-5.995E-01
0.140	-1.278E-01	0.0	-5.916E-01
0.145	-1.270E-01	0.0	-5.790E-01
0.150	-1.270E-01	0.0	-5.665E-01
0.155	-1.270E-01	0.0	-5.521E-01
0.160	-1.278E-01	0.0	-5.420E-01

MASS IMPULSE

SCALE FACTOR = 7.137E-02



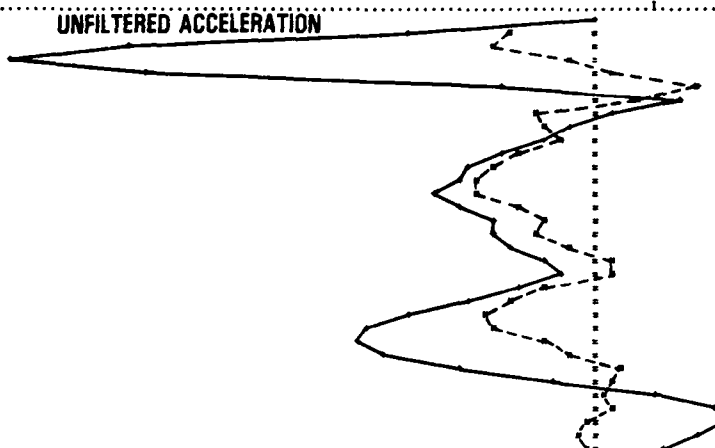


# MASS 7 UNFILTERED ACCELERATION(G'S)

TIME(SEC)	XACC	YACC	ZACC
0.0	1.334E-02	0.0	-2.314E-02
0.005	-2.783E+00	0.0	-6.028E+00
0.010	-3.181E+00	0.0	-1.479E+01
0.015	-6.711E-01	0.0	-1.863E+01
0.020	6.854E-01	0.0	-1.417E+01
0.025	5.421E+00	0.0	-2.970E+00
0.030	1.310E+00	0.0	2.668E+00
0.035	-1.958E+00	0.0	6.915E-01
0.040	-1.554E+00	0.0	-6.347E-01
0.045	-1.0.3E+00	0.0	-1.472E+00
0.050	-2.265E+00	0.0	-2.958E+00
0.055	-5.299E+00	0.0	-4.061E+00
0.060	-3.765E+00	0.0	-4.308E+00
0.065	-3.618E+00	0.0	-5.057E+00
0.070	-2.403E+00	0.0	-4.294E+00
0.075	-1.556E+00	0.0	-3.183E+00
0.080	-1.837E+00	0.0	-3.129E+00
0.085	-6.631E-01	0.0	-2.761E+00
0.090	6.043E-01	0.0	-1.620E+00
0.095	6.547E-01	0.0	-9.400E-01
0.100	-1.521E+00	0.0	-2.424E+00
0.105	-2.597E+00	0.0	-4.136E+00
0.110	-3.560E+00	0.0	-6.005E+00
0.115	-5.063E+00	0.0	-7.376E+00
0.120	-1.678E+00	0.0	-7.650E+00
0.125	-7.491E-01	0.0	-6.720E+00
0.130	7.913E-01	0.0	-4.393E+00
0.135	7.190E-01	0.0	-1.342E+00
0.140	3.180E-01	0.0	1.866E+00
0.145	5.757E-01	0.0	3.935E+00
0.150	-2.737E-01	0.0	6.124E+00
0.155	-5.231E-01	0.0	3.215E+00
0.160	-1.460E-01	0.0	2.178E+00

SCALE FACTOR = 2.709E+06

## UNFILTERED ACCELERATION

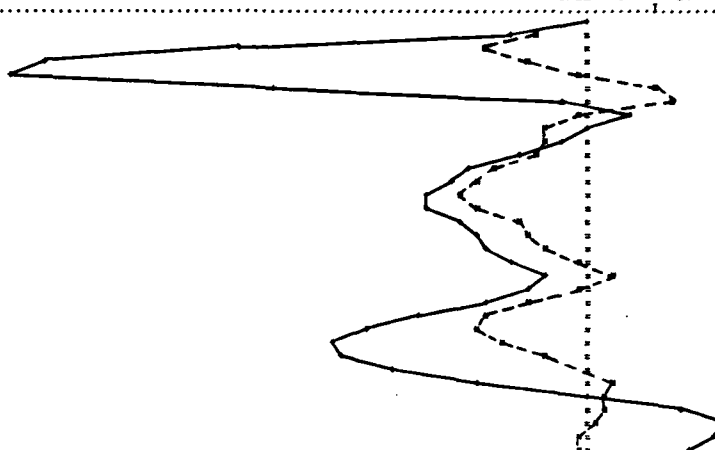


# MASS 7 FILTERED ACCELERATION(G'S)

TIME(SEC)	XACCF	YACCF	ZACCF
0.0	0.0	0.0	0.0
0.005	-1.483E+00	0.0	-2.326E+00
0.010	-2.935E+00	0.0	-1.003E+01
0.015	-1.834E+00	0.0	-1.582E+01
0.020	-1.875E-01	0.0	-1.671E+01
0.025	1.897E+00	0.0	-8.039E+00
0.030	2.358E+00	0.0	-8.857E-01
0.035	-1.941E-01	0.0	1.235E+00
0.040	-1.320E+00	0.0	-8.622E-02
0.045	-1.197E+00	0.0	-8.500E-01
0.050	-1.570E+00	0.0	-2.079E+00
0.055	-2.738E+00	0.0	-3.372E+00
0.060	-3.334E+00	0.0	-4.059E+00
0.065	-3.656E+00	0.0	-4.667E+00
0.070	-3.183E+00	0.0	-4.705E+00
0.075	-2.011E+00	0.0	-3.750E+00
0.080	-1.887E+00	0.0	-3.251E+00
0.085	-1.242E+00	0.0	-3.019E+00
0.090	-2.292E-01	0.0	-2.306E+00
0.095	6.766E-01	0.0	-1.272E+00
0.100	-4.189E-01	0.0	-1.697E+00
0.105	-1.851E+00	0.0	-3.110E+00
0.110	-2.971E+00	0.0	-4.854E+00
0.115	-3.307E+00	0.0	-6.502E+00
0.120	-2.404E+00	0.0	-7.403E+00
0.125	-1.378E+00	0.0	-7.222E+00
0.130	-1.060E-01	0.0	-5.754E+00
0.135	6.672E-01	0.0	-3.186E+00
0.140	4.441E-01	0.0	-1.091E-01
0.145	6.820E-01	0.0	2.595E+00
0.150	2.044E-01	0.0	3.859E+00
0.155	-4.096E-01	0.0	3.647E+00
0.160	-2.580E-01	0.0	2.781E+00

SCALE FACTOR = 2.649E+00

## FILTERED ACCELERATION

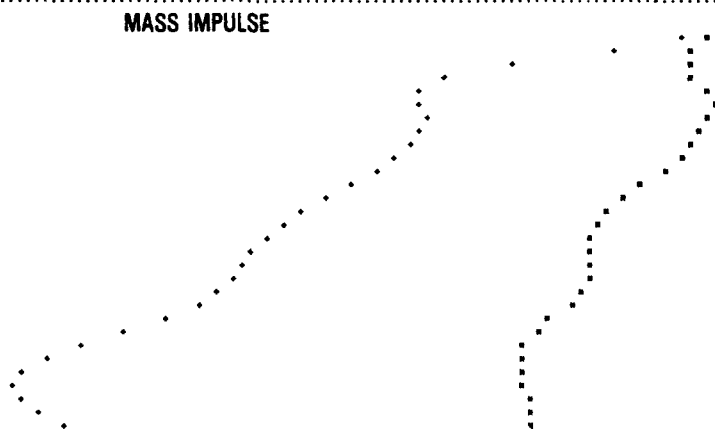


# MASS 7 MASS IMPULSES

TIME(SEC)	XIMP	YIMP	ZIMP
0.0	0.0	0.0	0.0
0.005	-5.009E-03	0.0	-3.402E-03
0.010	-1.501E-02	0.0	-3.421E-02
0.015	-2.765E-02	0.0	-1.004E-01
0.020	-3.228E-02	0.0	-1.855E-01
0.025	-2.848E-02	0.0	-2.516E-01
0.030	-1.804E-02	0.0	-2.742E-01
0.035	-1.035E-02	0.0	-2.705E-01
0.040	-1.539E-02	0.0	-2.679E-01
0.045	-2.194E-02	0.0	-2.702E-01
0.050	-2.829E-02	0.0	-2.774E-01
0.055	-3.924E-02	0.0	-2.912E-01
0.060	-5.448E-02	0.0	-3.102E-01
0.065	-7.228E-02	0.0	-3.319E-01
0.070	-8.980E-02	0.0	-3.559E-01
0.075	-1.025E-01	0.0	-3.770E-01
0.080	-1.119E-01	0.0	-3.942E-01
0.085	-1.200E-01	0.0	-4.100E-01
0.090	-1.259E-01	0.0	-4.235E-01
0.095	-1.221E-01	0.0	-4.322E-01
0.100	-1.207E-01	0.0	-4.389E-01
0.105	-1.248E-01	0.0	-4.508E-01
0.110	-1.340E-01	0.0	-4.708E-01
0.115	-1.552E-01	0.0	-4.995E-01
0.120	-1.698E-01	0.0	-5.347E-01
0.125	-1.791E-01	0.0	-5.717E-01
0.130	-1.829E-01	0.0	-6.047E-01
0.135	-1.809E-01	0.0	-6.271E-01
0.140	-1.780E-01	0.0	-6.353E-01
0.145	-1.759E-01	0.0	-6.285E-01
0.150	-1.758E-01	0.0	-6.115E-01
0.155	-1.744E-01	0.0	-5.923E-01
0.160	-1.744E-01	0.0	-5.762E-01

SCALE FACTOR = 7.563E-02

## MASS IMPULSE

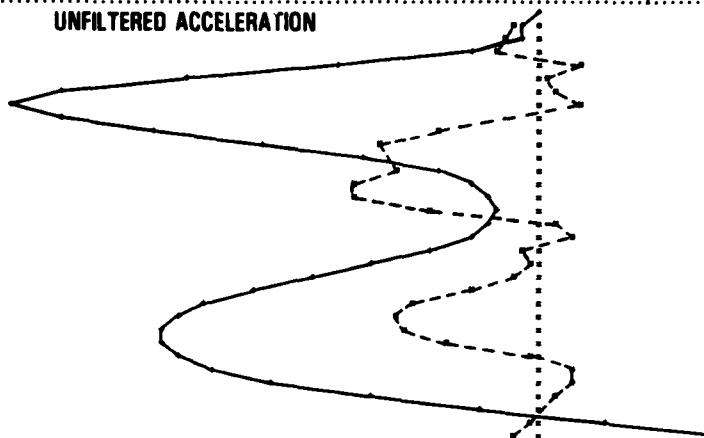


MASS 8 UNFILTERED ACCELERATION(G'S)

TIME(SEC)	XACC	YACC	ZACC
0.0	1.320E-02 0.0	-2.052E-02	-3.282E-01
0.005	-5.487E-01 0.0	-4.240E-01	-1.587E+00
0.010	-1.045E+00 0.0	-4.535E+00	-8.037E+00
0.015	9.613E-01 0.0	-1.091E+01	-1.199E+01
0.020	9.848E-02 0.0	-1.092E+01	-8.795E+00
0.025	3.448E-01 0.0	-6.287E+00	-3.923E+00
0.030	0.869E-01 0.0	-2.372E+00	-1.617E+00
0.035	-1.017E-02 0.0	-1.234E+00	-1.055E+00
0.040	-2.306E+00 0.0	-1.084E+00	-1.499E+00
0.045	-3.679E+00 0.0	-2.396E+00	-3.747E+00
0.050	-4.099E+00 0.0	-5.158E+00	-6.434E+00
0.055	-3.330E+00 0.0	-7.547E+00	-8.245E+00
0.060	-4.247E+00 0.0	-8.623E+00	-8.652E+00
0.065	-4.252E+00 0.0	-8.652E+00	-8.265E+00
0.070	-2.435E+00 0.0	-7.446E+00	-6.066E+00
0.075	4.324E-01 0.0	-5.889E+00	-1.278E+00
0.080	7.521E-01 0.0	-1.488E+00	1.488E+00
0.085	-3.135E-01 0.0	3.975E+00	
0.090	-2.536E-01 0.0		
0.095	-5.854E-01 0.0		
0.100	-1.495E+00 0.0		
0.105	-2.794E+00 0.0		
0.110	-3.258E+00 0.0		
0.115	-3.037E+00 0.0		
0.120	-2.115E+00 0.0		
0.125	-1.925E 01 0.0		
0.130	7.199E-01 0.0		
0.135	8.195E-01 0.0		
0.140	3.054E-01 0.0		
0.145	-4.308E-03 0.0		
0.150	-1.496E-01 0.0		
0.155	-5.241E-01 0.0		
0.160			

SCALE FACTOR = 1.900E+00

UNFILTERED ACCELERATION

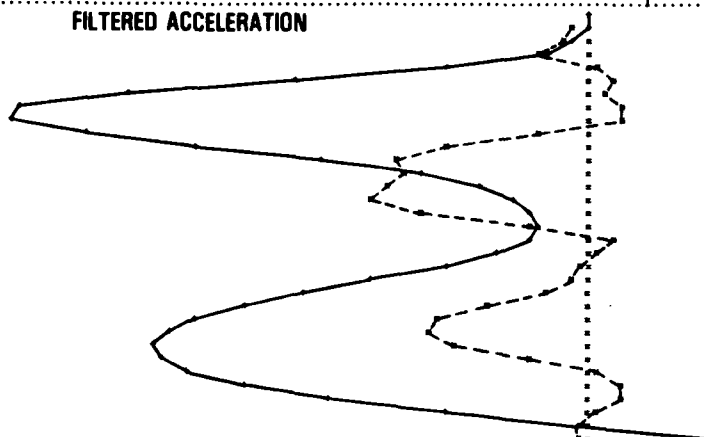


MASS 8 FILTERED ACCELERATION(G'S)

TIME(SEC)	XACCF	YACCF	ZACCF
0.0	0.0	0.0	0.0
0.005	-3.582E-01 0.0	-1.571E-01	-3.565E-01
0.010	-5.274E-01 0.0	-8.327E-01	-2.846E+00
0.015	-1.018E+00 0.0	-5.900E+00	-9.106E+00
0.020	1.572E-02 0.0	-1.120E+01	-1.142E+01
0.025	3.937E-01 0.0	-9.999E+00	-7.818E+00
0.030	1.748E-01 0.0	-5.395E+00	-3.396E+00
0.035	5.218E-01 0.0	-2.179E+00	-1.527E+00
0.040	6.127E-01 0.0	-1.190E+00	-1.083E+00
0.045	-1.124E+00 0.0	-1.256E+00	-1.865E+00
0.050	-2.817E+00 0.0	-2.929E+00	-4.290E+00
0.055	-3.790E+00 0.0	-5.613E+00	-6.835E+00
0.060	-3.634E+00 0.0	-7.781E+00	-8.341E+00
0.065	-3.950E+00 0.0	-8.607E+00	-8.478E+00
0.070	-4.362E+00 0.0	-7.935E+00	-6.879E+00
0.075	-3.374E+00 0.0	-5.177E+00	-2.885E+00
0.080	-1.238E+00 0.0	-2.350E-01	2.389E+00
0.085	4.191E-01 0.0		
0.090	1.949E-02 0.0		
0.095	-1.757E-01 0.0		
0.100	-3.974E-01 0.0		
0.105	-9.046E-01 0.0		
0.110	-2.005E+00 0.0		
0.115	-2.964E+00 0.0		
0.120	-3.127E+00 0.0		
0.125	-2.674E+00 0.0		
0.130	-1.264E+00 0.0		
0.135	9.540E-02 0.0		
0.140	6.613E-01 0.0		
0.145	5.810E-01 0.0		
0.150	1.256E-01 0.0		
0.155	-4.642E-02 0.0		
0.160	-2.876E-01 0.0		

SCALE FACTOR = 1.644E+00

FILTERED ACCELERATION

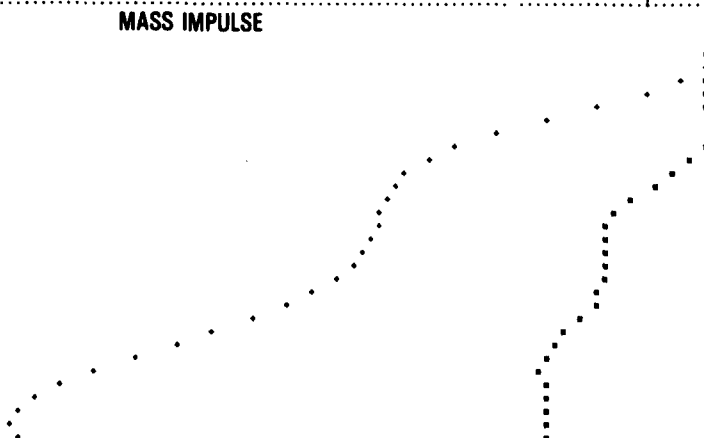


MASS 8 MASS IMPULSES

TIME(SEC)	XIMP	YIMP	ZIMP
0.0	0.0	0.0	0.0
0.005	-6.444E-04 0.0	-3.011E-04	-1.691E-03
0.010	-2.791E-03 0.0	-4.243E-03	-1.295E-02
0.015	-4.934E-03 0.0	-1.242E-01	-1.612E-01
0.020	-1.012E-02 0.0	-2.356E-01	-2.802E-01
0.025	-8.173E-03 0.0	-3.130E-01	-3.346E-01
0.030	-7.154E-03 0.0	-3.481E-01	-3.572E-01
0.035	-5.535E-03 0.0	-3.638E-01	-3.694E-01
0.040	-2.189E-03 0.0	-3.751E-01	-3.828E-01
0.045	-3.237E-03 0.0	-3.946E-01	-4.127E-01
0.050	-1.342E-02 0.0	-4.689E-01	-5.056E-01
0.055	-3.034E-02 0.0	-5.462E-01	-5.886E-01
0.060	-4.961E-02 0.0	-6.316E-01	-6.728E-01
0.065	-6.806E-02 0.0	-7.100E-01	-7.402E-01
0.070	-8.903E-02 0.0	-7.605E-01	-7.682E-01
0.075	-1.088E-01 0.0	-7.626E-01	
0.080	-1.207E-01 0.0		
0.085	-1.216E-01 0.0		
0.090	-1.200E-01 0.0		
0.095	-1.206E-01 0.0		
0.100	-1.270E-01 0.0		
0.105	-1.250E-01 0.0		
0.110	-1.323E-01 0.0		
0.115	-1.451E-01 0.0		
0.120	-1.606E-01 0.0		
0.125	-1.753E-01 0.0		
0.130	-1.855E-01 0.0		
0.135	-1.890E-01 0.0		
0.140	-1.897E-01 0.0		
0.145	-1.823E-01 0.0		
0.150	-1.807E-01 0.0		
0.155	-1.805E-01 0.0		
0.160	-1.813E-01 0.0		

SCALE FACTOR = 9.146E-02

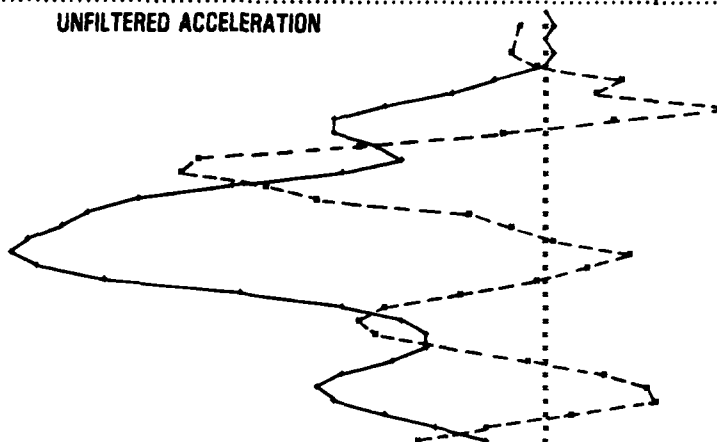
MASS IMPULSE



# MASS 9 UNFILTERED ACCELERATION(G'S)

TIME(SEC)	XACC	YACC	ZACC
0.0	1.418E-02	0.0	-1.727E-02
0.005	-5.585E-01	0.0	1.521E-01
0.010	2.544E-02	0.0	1.010E-01
0.015	-7.404E-01	0.0	2.875E-01
0.020	-9.840E-02	0.0	3.151E-02
0.025	1.715E+00	0.0	-9.553E-01
0.030	1.070E+00	0.0	-1.927E+00
0.035	5.778E+00	0.0	-3.337E+00
0.040	1.529E+00	0.0	-5.349E+00
0.045	-8.339E-01	0.0	-4.466E+00
0.050	-3.976E+00	0.0	-3.538E+00
0.055	-7.303E+00	0.0	-3.057E+00
0.060	-7.597E+00	0.0	-4.277E+00
0.065	-5.865E+00	0.0	-6.659E+00
0.070	-4.782E+00	0.0	-5.388E+00
0.075	-1.544E+00	0.0	-9.492E+00
0.080	-6.228E-01	0.0	-1.017E+01
0.085	2.724E-01	0.0	-1.078E+01
0.090	1.802E+00	0.0	-1.122E+01
0.095	9.535E-01	0.0	-1.074E+01
0.100	-1.934E-01	0.0	-9.215E+00
0.105	-1.715E+00	0.0	-4.395E+00
0.110	-3.422E+00	0.0	-4.208E+00
0.115	-3.947E+00	0.0	-2.921E+00
0.120	-3.487E+00	0.0	-2.473E+00
0.125	-2.555E+00	0.0	-2.530E+00
0.130	-3.922E-01	0.0	-3.237E+00
0.135	1.241E+00	0.0	-4.226E+00
0.140	2.147E+00	0.0	-4.716E+00
0.145	2.349E+00	0.0	-4.418E+00
0.150	5.074E-01	0.0	-3.397E+00
0.155	-1.142E+00	0.0	-2.246E+00
0.160	-2.597E+00	0.0	-1.178E+00

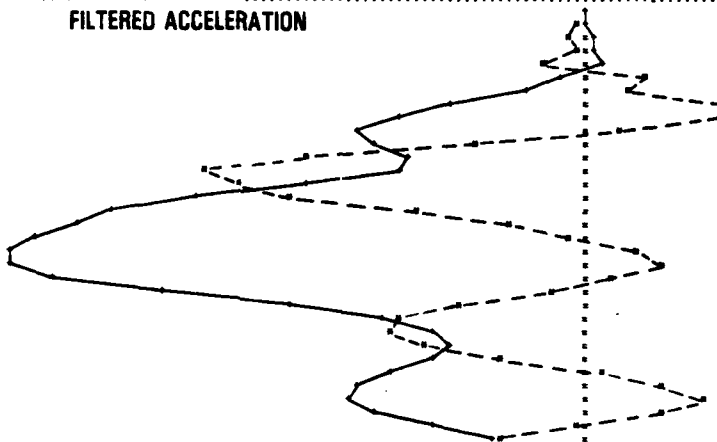
## UNFILTERED ACCELERATION



# MASS 9 FILTERED ACCELERATION(G'S)

TIME(SEC)	XACCF	YACCF	ZACCF
0.0	0.0	0.0	0.0
0.005	-1.805E-01	0.0	2.707E-03
0.010	-3.412E-01	0.0	1.524E-01
0.015	-1.392E-01	0.0	1.383E-01
0.020	-8.610E-01	0.0	2.659E-01
0.025	1.161E+00	0.0	-4.981E-01
0.030	8.588E-01	0.0	-1.217E+00
0.035	2.542E+00	0.0	-2.576E+00
0.040	2.493E+00	0.0	-3.634E+00
0.045	5.684E-01	0.0	-4.423E+00
0.050	-2.046E+00	0.0	-3.963E+00
0.055	-5.264E+00	0.0	-3.344E+00
0.060	-7.336E+00	0.0	-3.576E+00
0.065	-4.574E+00	0.0	-5.388E+00
0.070	-5.481E+00	0.0	-7.375E+00
0.075	-3.219E+00	0.0	-8.962E+00
0.080	-1.425E+00	0.0	-9.752E+00
0.085	-3.323E-01	0.0	-1.045E+01
0.090	1.004E+00	0.0	-1.094E+01
0.095	1.407E+00	0.0	-1.096E+01
0.100	4.948E-01	0.0	-1.014E+01
0.105	-6.826E-01	0.0	-8.019E+00
0.110	-2.355E+00	0.0	-5.576E+00
0.115	-3.555E+00	0.0	-3.800E+00
0.120	-3.671E+00	0.0	-2.842E+00
0.125	-3.124E+00	0.0	-2.544E+00
0.130	-1.649E+00	0.0	-2.843E+00
0.135	2.332E-01	0.0	-3.656E+00
0.140	1.443E+00	0.0	-4.402E+00
0.145	2.236E+00	0.0	-4.552E+00
0.150	1.439E+00	0.0	-3.972E+00
0.155	-1.914E-01	0.0	-2.949E+00
0.160	-1.682E+00	0.0	-1.841E+00

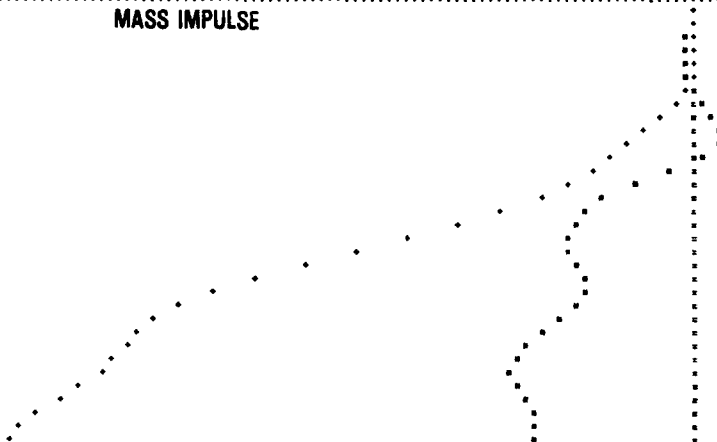
## FILTERED ACCELERATION



# MASS 9 MASS IMPULSES

TIME(SEC)	XIMP	YIMP	ZIMP
0.0	0.0	0.0	0.0
0.005	-1.932E-04	0.0	-2.022E-04
0.010	-2.054E-03	0.0	3.476E-04
0.015	-2.544E-03	0.0	9.165E-04
0.020	-6.090E-03	0.0	2.194E-03
0.025	-5.029E-03	0.0	1.703E-03
0.030	1.685E-04	0.0	-2.460E-03
0.035	8.054E-03	0.0	-1.202E-02
0.040	2.224E-02	0.0	-2.763E-02
0.045	3.002E-02	0.0	-4.829E-02
0.050	2.647E-02	0.0	-6.952E-02
0.055	8.063E-03	0.0	-8.767E-02
0.060	-2.475E-02	0.0	-1.043E-01
0.065	-6.012E-02	0.0	-1.243E-01
0.070	-9.078E-02	0.0	-1.583E-01
0.075	-1.134E-01	0.0	-1.996E-01
0.080	-1.242E-01	0.0	-2.461E-01
0.085	-1.284E-01	0.0	-2.972E-01
0.090	-1.270E-01	0.0	-3.505E-01
0.095	-1.200E-01	0.0	-4.057E-01
0.100	-1.152E-01	0.0	-4.588E-01
0.105	-1.155E-01	0.0	-5.044E-01
0.110	-1.237E-01	0.0	-5.382E-01
0.115	-1.385E-01	0.0	-5.612E-01
0.120	-1.570E-01	0.0	-5.774E-01
0.125	-1.741E-01	0.0	-5.906E-01
0.130	-1.884E-01	0.0	-6.019E-01
0.135	-1.897E-01	0.0	-6.200E-01
0.140	-1.852E-01	0.0	-6.404E-01
0.145	-1.755E-01	0.0	-6.631E-01
0.150	-1.657E-01	0.0	-6.847E-01
0.155	-1.626E-01	0.0	-7.020E-01
0.160	-1.674E-01	0.0	-7.159E-01

## MASS IMPULSE



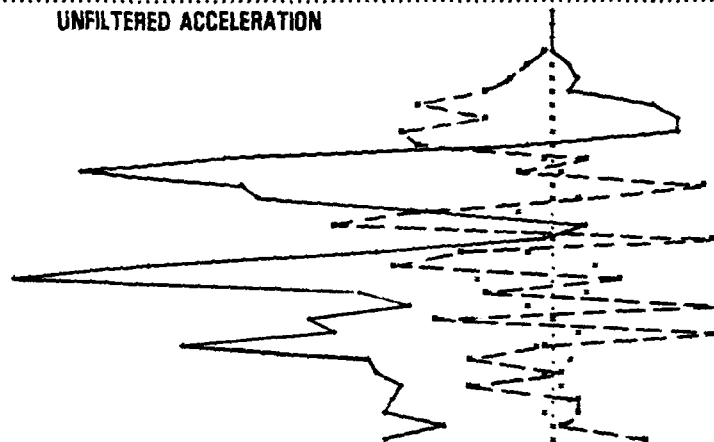
# MASS 11 UNFILTERED ACCELERATION(G'S)

TIME(SEC) XACC YACC ZACC

0.0	1.294E-02	-5.773E-05	-3.655E-02
0.005	-1.719E-02	4.171E-03	-3.374E-02
0.010	-9.650E-02	8.805E-03	2.222E-01
0.015	-5.750E-01	4.434E-03	9.875E-02
0.020	-1.029E+00	-1.399E-02	6.873E-01
0.025	-1.955E+00	1.124E-02	1.320E+00
0.030	-2.800E+00	-1.049E-01	8.859E-01
0.035	-5.898E+00	9.558E-02	4.345E+00
0.040	-2.948E+00	1.437E-01	5.787E+00
0.045	-4.707E+00	1.802E-01	5.628E+00
0.050	-5.905E+00	-5.978E-02	-1.242E+00
0.055	1.373E+00	-2.237E-01	-1.434E+01
0.060	-1.572E+00	5.068E-01	-2.070E+01
0.065	6.591E+00	2.040E-01	-1.352E+01
0.070	8.132E+00	2.258E-01	-1.294E+01
0.075	-6.197E+00	-1.491E+00	-5.502E+00
0.080	-9.736E+00	1.715E+00	1.380E+00
0.085	7.251E+00	1.091E+00	-3.305E-01
0.090	-4.132E+00	-1.205E+00	-7.630E+00
0.095	-4.977E+00	8.084E+00	-1.747E+01
0.100	2.858E+00	-3.295E+00	-2.371E+01
0.105	-2.905E+00	1.520E+00	-8.587E+00
0.110	7.336E+00	-9.852E-01	-6.338E+00
0.115	-5.157E+00	-1.654E-02	-1.083E+01
0.120	7.483E+00	1.195E+00	-9.552E+00
0.125	-1.516E+01	-6.438E-01	-1.191E+01
0.130	-3.826E+00	7.551E-01	-7.946E+00
0.135	4.476E-01	-1.311E-01	-7.541E+00
0.140	-5.502E+00	2.402E-01	-6.702E+00
0.145	1.228E+00	7.343E-01	-7.106E+00
0.150	1.156E+00	-1.933E-01	-7.305E+00
0.155	3.844E-01	1.016E-01	-6.883E+00
0.160	3.994E+00	-1.823E-02	-7.413E+00

SCALE FACTOR = 5.715E+00

## UNFILTERED ACCELERATION



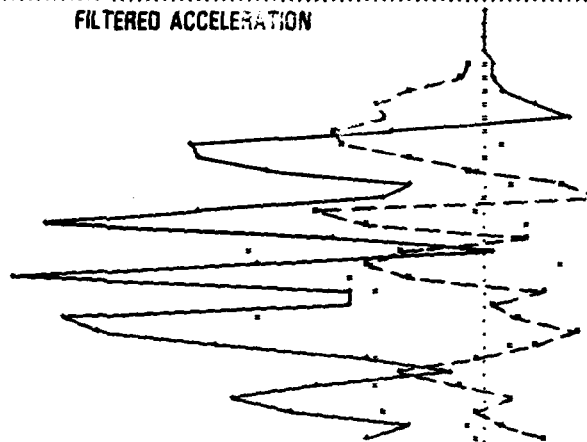
# MASS 12 FILTERED ACCELERATION(G'S)

TIME(SEC) XACCF YACCF ZACCF

0.0	0.0	0.0	0.0
0.005	6.878E-03	0.711E-04	-2.554E-02
0.010	-1.001E-02	-3.430E-03	-1.648E-02
0.015	-1.390E-01	-3.348E-04	-1.859E-03
0.020	-6.939E-01	-4.128E-03	4.948E-02
0.025	-1.142E+00	1.608E-02	2.001E-01
0.030	-2.755E+00	-2.699E-02	4.442E-01
0.035	-6.185E+00	2.024E-03	1.624E+00
0.040	-3.756E+00	-8.078E-02	2.935E+00
0.045	-5.584E+00	-1.691E-02	-3.602E+00
0.050	-5.336E+00	5.530E-01	-1.088E+01
0.055	-2.905E+00	-1.858E-01	-1.055E+01
0.060	-8.468E-01	-3.817E-01	-8.113E+00
0.065	2.434E+00	6.490E-01	-2.949E+00
0.070	4.274E+00	-1.804E-01	-3.662E+00
0.075	-6.172E+00	-3.846E-01	-1.044E+01
0.080	-4.407E+00	1.282E+00	-1.588E+01
0.085	1.495E+00	8.083E+00	-5.542E+00
0.090	-3.152E+00	-8.683E+00	2.484E-01
0.095	-4.510E+00	2.642E+00	-8.463E+00
0.100	-2.990E+00	-4.882E+00	-1.717E+01
0.105	2.104E+00	-4.104E+00	-4.959E+00
0.110	9.324E-02	7.719E+00	-6.941E+00
0.115	9.581E-01	-8.207E+00	-1.532E+01
0.120	3.361E+00	8.404E+00	-1.409E+01
0.125	1.814E+00	9.097E-01	-9.716E+00
0.130	-4.078E-01	-3.988E+00	-4.344E+00
0.135	-3.197E+00	3.713E+00	-1.376E+00
0.140	-1.099E+00	-3.936E+00	-6.285E+00
0.145	8.542E-01	5.746E+00	-9.361E+00
0.150	-4.781E-01	-3.697E+00	-7.143E+00
0.155	4.074E-01	-7.545E-01	-2.916E+00
0.160	1.943E+00	-2.728E-01	-4.467E+00

SCALE FACTOR = 5.046E+00

## FILTERED ACCELERATION



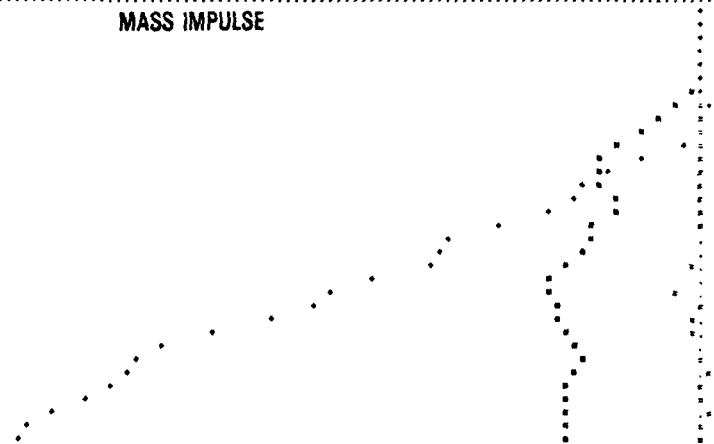
# MASS 12 MASS IMPULSES

TIME(SEC) XIMP YIMP ZIMP

0.0	0.0	0.0	0.0
0.005	2.932E-05	1.417E-06	-7.760E-05
0.010	1.834E-05	-2.577E-06	-1.982E-04
0.015	-2.043E-04	-2.170E-05	-2.292E-04
0.020	-2.388E-03	-1.782E-05	-1.774E-04
0.025	-6.594E-03	-1.143E-05	4.697E-04
0.030	-1.431E-02	7.448E-06	1.985E-03
0.035	-2.397E-02	1.149E-06	6.744E-03
0.040	-5.434E-02	-3.090E-06	1.871E-02
0.045	-7.414E-02	-3.642E-06	2.281E-02
0.050	-1.058E-01	1.480E-06	-1.912E-02
0.055	-1.262E-01	1.392E-05	-7.407E-02
0.060	-1.261E-01	-1.089E-05	-1.218E-01
0.065	-3.18E-01	1.700E-06	-1.490E-01
0.070	-1.119E-01	1.907E-05	-1.621E-01
0.075	-1.101E-01	-4.031E-06	-1.948E-01
0.080	-1.459E-01	1.836E-05	-2.645E-01
0.085	-1.469E-01	2.403E-05	-3.244E-01
0.090	-1.502E-01	3.016E-06	-3.301E-01
0.095	-1.715E-01	-1.651E-05	-3.435E-01
0.100	-1.918E-01	2.949E-06	-4.199E-01
0.105	-1.920E-01	-3.713E-06	-4.777E-01
0.110	-1.853E-01	2.781E-05	-4.911E-01
0.115	-1.858E-01	-1.695E-05	-5.488E-01
0.120	-1.730E-01	1.509E-06	-6.247E-01
0.125	-1.596E-01	1.965E-06	-6.844E-01
0.130	-1.558E-01	-2.077E-06	-7.204E-01
0.135	-1.458E-01	5.055E-06	-7.307E-01
0.140	-1.786E-01	2.942E-06	-7.494E-01
0.145	-1.771E-01	9.931E-06	-7.844E-01
0.150	-1.743E-01	-1.155E-06	-8.324E-01
0.155	-1.772E-01	-5.555E-06	-8.548E-01
0.160	-1.713E-01	-2.415E-06	-8.720E-01

SCALE FACTOR = 1.074E-01

## MASS IMPULSE

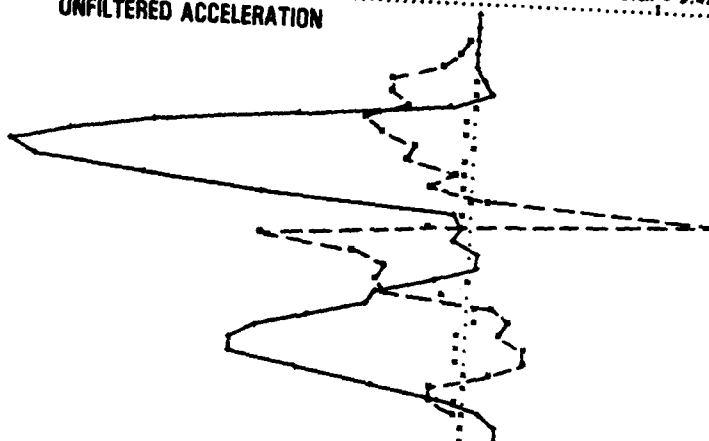


# MASS 13 UNFILTERED ACCELERATION(G'S)

TIME(SEC)	XACC	YACC	ZACC
0.0	1.240E-02	1.465E-04	3.160E-02
0.005	-3.602E-03	2.923E-04	1.913E-02
0.010	-7.372E-03	3.932E-03	1.100E-02
0.015	-5.071E-01	2.407E-03	2.853E-02
0.020	-1.047E-00	1.905E-02	2.409E-01
0.025	-3.149E-00	9.608E-04	5.708E-01
0.030	-3.400E-00	6.190E-02	1.000E+00
0.035	-2.539E-00	9.469E-02	7.037E-00
0.040	-4.239E-00	5.965E-02	7.037E-00
0.045	-3.680E-00	1.007E-01	1.270E+01
0.050	-3.370E-00	8.109E-02	1.627E+01
0.055	-2.467E-00	5.657E-02	1.862E+01
0.060	-6.436E-01	1.950E-01	1.777E+01
0.065	-7.535E-00	1.237E-01	1.326E+01
0.070	6.690E-01	1.069E-03	8.396E+00
0.075	1.002E-01	6.916E-02	3.870E-01
0.080	-1.597E-00	5.546E-01	2.501E-01
0.085	-0.323E-00	5.163E-01	5.591E-01
0.090	-4.663E+00	3.647E-01	4.113E-01
0.095	-3.115E+00	3.769E-01	5.275E-01
0.100	-3.452E+00	1.391E-02	1.345E+00
0.105	-5.562E-00	7.738E-01	3.698E+00
0.110	-1.114E-00	3.873E-01	3.852E+00
0.115	1.902E-00	4.148E-01	6.386E+00
0.120	1.438E-00	1.966E-01	6.337E+00
0.125	2.364E-00	3.327E-01	9.546E+00
0.130	2.385E-00	3.422E-01	9.258E+00
0.135	1.099E-00	1.922E-01	6.571E+00
0.140	-1.248E-00	6.881E-02	3.754E+00
0.145	-1.250E-00	1.495E-01	1.023E+00
0.150	-6.445E-02	9.201E-02	7.021E-01
0.155	6.387E-02	2.029E-01	1.372E+00
0.160	9.868E-02	1.692E-01	1.586E+00

## UNFILTERED ACCELERATION

SCALE FACTOR = 3.418E+00

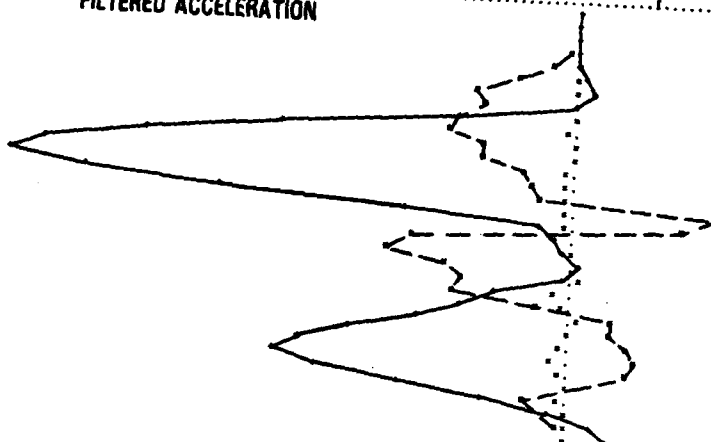


# MASS 13 FILTERED ACCELERATION(G'S)

TIME(SEC)	XACCF	YACCF	ZACCF
0.0	0.0	0.0	0.0
0.005	-5.185E-03	1.385E-04	2.036E-02
0.010	-2.370E-02	1.422E-03	1.233E-02
0.015	-7.583E-01	4.929E-03	2.912E-02
0.020	-1.862E-00	1.291E-01	3.446E-01
0.025	-3.158E-00	3.074E-02	7.261E-01
0.030	-2.961E-00	7.723E-02	8.159E-02
0.035	-3.595E-00	8.591E-02	3.662E+00
0.040	-2.787E-00	6.463E-02	9.323E+00
0.045	-2.885E-00	1.755E-02	1.378E+01
0.050	-1.582E-00	1.294E-01	1.813E+01
0.055	-1.188E-00	1.479E-01	1.580E+01
0.060	-9.689E-01	5.801E-02	1.124E+01
0.065	4.700E-00	7.790E-02	5.316E+00
0.070	3.689E-00	1.298E-01	9.473E-01
0.075	-5.040E-00	5.406E-01	5.369E-01
0.080	-6.003E-00	4.594E-02	7.826E-02
0.085	-5.918E-00	3.000E-01	2.217E-01
0.090	-3.449E-00	2.755E-01	1.634E-01
0.095	-3.734E-00	6.695E-01	2.402E+00
0.100	-1.125E-00	1.498E-01	3.583E+00
0.105	1.397E-00	3.924E-01	6.892E+00
0.110	1.494E-00	7.046E-02	7.070E+00
0.115	1.891E-00	2.122E-01	8.749E+00
0.120	2.332E-00	1.437E-01	9.446E+00
0.125	1.943E-00	8.505E-02	7.992E+00
0.130	3.636E-02	1.511E-01	5.192E+00
0.135	-1.171E-00	8.207E-02	2.767E+00
0.140	-5.824E-01	5.405E-03	4.421E-01
0.145	-1.012E-01	1.293E-01	8.575E-01
0.150	1.640E-02	1.861E-01	1.407E+00

## FILTERED ACCELERATION

SCALE FACTOR = 2.718E+00

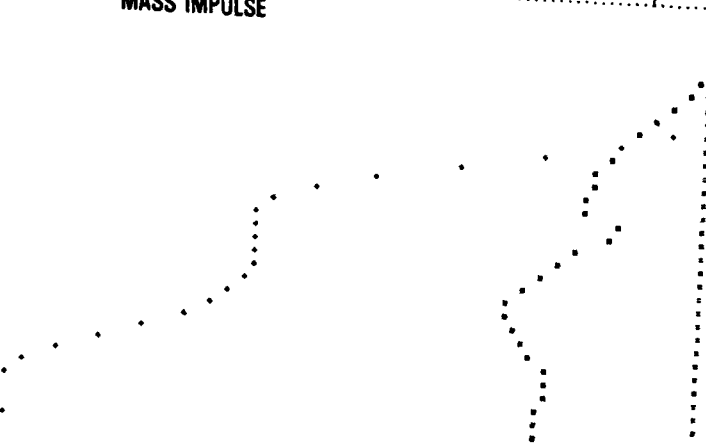


# MASS 13 MASS IMPULSES

TIME(SEC)	XIMP	YIMP	ZIMP
0.0	0.0	0.0	0.0
0.005	2.702E-05	1.186E-07	4.731E-05
0.010	4.135E-06	1.657E-06	1.438E-04
0.015	-5.099E-04	1.680E-05	2.477E-04
0.020	-3.078E-03	2.405E-05	2.209E-04
0.025	-9.000E-03	9.352E-05	8.529E-04
0.030	-2.235E-02	6.026E-05	3.581E-03
0.035	-3.833E-02	2.110E-04	4.461E-03
0.040	-5.381E-02	5.477E-04	6.374E-04
0.045	-7.298E-02	3.504E-04	3.567E-02
0.050	-8.987E-02	7.321E-05	9.224E-02
0.055	-1.062E-01	2.077E-04	1.705E-01
0.060	-1.156E-01	4.922E-05	2.400E-01
0.065	-1.215E-01	8.243E-04	3.461E-01
0.070	-1.286E-01	1.372E-03	4.136E-01
0.075	-1.228E-01	1.662E-03	4.544E-01
0.080	-9.484E-02	2.024E-03	4.687E-01
0.085	-1.008E-01	3.906E-03	4.722E-01
0.090	-1.318E-01	5.581E-03	4.742E-01
0.095	-1.561E-01	4.675E-03	4.739E-01
0.100	-1.740E-01	3.012E-03	4.727E-01
0.105	-1.925E-01	3.526E-03	4.792E-01
0.110	-2.055E-01	5.642E-03	4.950E-01
0.115	-2.035E-01	4.635E-03	5.154E-01
0.120	-1.879E-01	3.780E-03	5.457E-01
0.125	-1.769E-01	5.252E-03	6.318E-01
0.130	-1.657E-01	4.507E-03	6.761E-01
0.135	-1.405E-01	6.158E-03	7.095E-01
0.140	-1.642E-01	6.029E-03	7.298E-01
0.145	-1.690E-01	6.369E-03	7.372E-01
0.150	-1.705E-01	6.014E-03	7.357E-01
0.155	-1.704E-01	5.159E-03	7.298E-01

## MASS IMPULSE

SCALE FACTOR = 8.854E-02



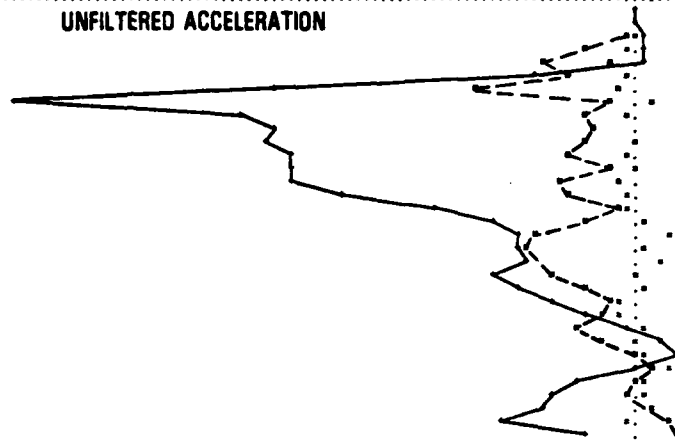
# MASS 14 UNFILTERED ACCELERATION(G'S)

TIME(SEC) XACC YACC ZACC

0.0 1.277E-02 2.443E-04 3.096E-02  
0.005 -9.452E-02 7.684E-04 1.738E-02  
0.010 -3.058E-01 9.787E-03 9.884E-02  
0.015 -1.249E-00 3.372E-01 1.708E-01  
0.020 -2.338E-00 4.733E-01 2.181E-01  
0.025 -1.649E-00 2.690E-01 2.633E-00  
0.030 -4.135E-00 4.504E-01 9.369E-00  
0.035 -5.953E-01 4.044E-01 1.592E-01  
0.040 -1.351E-00 2.049E-01 1.017E-01  
0.045 -1.108E-00 1.282E-00 9.536E-00  
0.050 -1.343E-00 3.081E-02 9.515E-00  
0.055 -1.645E-00 2.835E-01 8.769E-00  
0.060 -6.177E-01 6.225E-02 8.767E-00  
0.065 -1.942E-00 5.480E-01 8.864E-00  
0.070 -1.736E-00 1.585E-01 7.680E-00  
0.075 -4.289E-01 1.798E-01 5.274E-00  
0.080 -1.310E-00 2.338E-01 5.580E-00  
0.085 -2.631E-00 9.100E-01 3.107E-00  
0.090 -2.867E-00 2.725E-01 2.970E-00  
0.095 -2.905E-00 6.762E-01 2.878E-00  
0.100 -2.077E-00 4.490E-02 3.618E-00  
0.105 -1.241E-00 2.447E-01 2.894E-00  
0.110 -5.946E-01 4.047E-01 2.216E-00  
0.115 -8.001E-01 3.539E-01 1.291E-00  
0.120 -1.523E-00 1.546E-01 3.109E-01  
0.125 -9.183E-01 1.290E-01 5.215E-01  
0.130 -2.946E-02 1.237E-01 1.873E-00  
0.135 3.320E-01 8.747E-01 5.687E-02  
0.140 -7.840E-02 1.443E-01 1.501E-00  
0.145 -2.261E-01 1.454E-01 2.113E-00  
0.150 4.740E-01 3.224E-01 2.418E-00  
0.155 9.218E-01 2.884E-01 3.563E-00  
0.160 1.029E-00 2.125E-00 1.222E-00

SCALE FACTOR = 2.149E+00

## UNFILTERED ACCELERATION



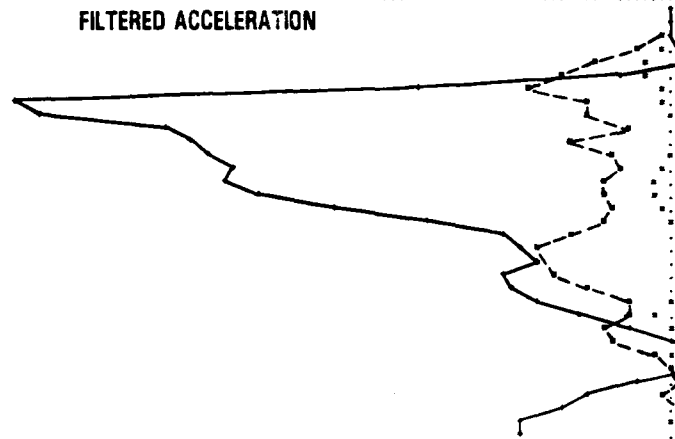
# MASS 14 FILTERED ACCELERATION(G'S)

TIME(SEC) XACCF YACCF ZACCF

0.0 0.0 0.0 0.0  
0.005 -3.047E-02 4.332E-03 6.450E-03  
0.010 -1.841E-01 1.029E-02 5.958E-02  
0.015 -7.120E-01 1.346E-01 9.402E-02  
0.020 -1.528E-00 5.411E-01 3.380E-01  
0.025 -2.178E-00 5.279E-01 1.016E-00  
0.030 -2.943E-00 2.152E-01 5.039E-00  
0.035 -1.695E-00 2.515E-01 1.310E-01  
0.040 -1.422E-00 2.725E-02 1.255E-01  
0.045 -8.241E-01 5.754E-01 1.003E-01  
0.050 -2.046E-00 5.710E-01 9.534E-00  
0.055 -1.159E-00 9.615E-02 9.193E-00  
0.060 -1.008E-00 1.014E-01 8.767E-00  
0.065 -1.198E-00 3.815E-01 8.843E-00  
0.070 -1.352E-00 3.019E-01 8.287E-00  
0.075 -1.203E-00 2.384E-01 6.650E-00  
0.080 -1.347E-00 7.705E-03 4.796E-00  
0.085 -2.057E-00 6.639E-01 3.417E-00  
0.090 -2.713E-00 4.420E-01 2.960E-00  
0.095 -2.780E-00 5.147E-01 2.747E-00  
0.100 -2.392E-00 3.185E-01 3.376E-00  
0.105 -1.708E-00 1.928E-01 3.212E-00  
0.110 -8.997E-01 4.211E-02 2.690E-00  
0.115 -7.897E-01 4.109E-01 1.854E-00  
0.120 -1.339E-00 6.524E-02 8.601E-01  
0.125 -1.115E-00 3.654E-02 1.650E-03  
0.130 3.450E-01 1.636E-02 7.126E-01  
0.135 5.544E-02 3.652E-01 5.516E-01  
0.140 8.799E-02 4.787E-01 7.234E-01  
0.145 -1.330E-01 1.341E-01 1.447E-00  
0.150 9.919E-02 3.063E-01 2.213E-00  
0.155 5.504E-01 1.394E-02 2.954E-00  
0.160 9.922E-01 4.038E-01 2.991E-00

SCALE FACTOR = 1.677E+00

## FILTERED ACCELERATION



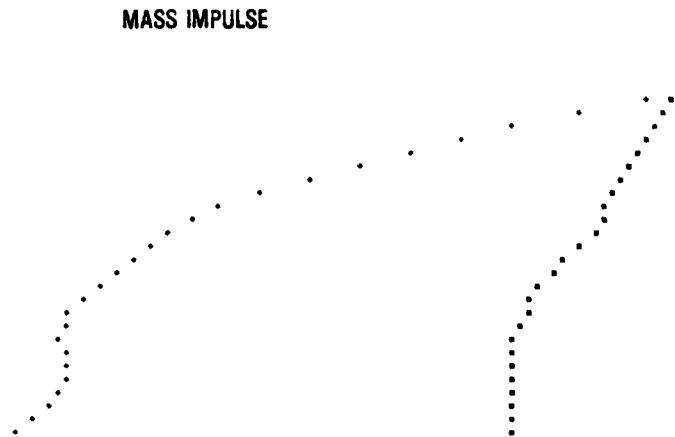
# MASS 14 MASS IMPULSES

TIME(SEC) XIMP YIMP ZIMP

0.0 0.0 0.0 0.0  
0.005 -1.824E-05 1.947E-05 2.942E-05  
0.010 -5.272E-04 4.419E-05 8.832E-05  
0.015 -2.445E-03 9.568E-05 4.738E-04  
0.020 -7.882E-03 1.853E-03 1.682E-03  
0.025 -1.813E-02 4.742E-03 8.831E-04  
0.030 -2.927E-02 6.234E-03 1.244E-02  
0.035 -4.725E-02 8.049E-03 5.868E-02  
0.040 -4.494E-02 7.998E-02 1.265E-01  
0.045 -5.597E-02 7.281E-03 1.815E-01  
0.050 -6.386E-02 3.437E-03 2.298E-01  
0.055 -7.047E-02 2.619E-02 2.769E-01  
0.060 -7.885E-02 3.302E-03 3.214E-01  
0.065 -8.198E-02 4.354E-03 3.655E-01  
0.070 -8.404E-02 6.255E-03 4.090E-01  
0.075 -9.446E-02 7.518E-03 4.466E-01  
0.080 -1.024E-01 8.211E-03 4.748E-01  
0.085 -1.106E-01 8.589E-03 4.945E-01  
0.090 -1.226E-01 3.570E-03 5.101E-01  
0.095 -1.360E-01 1.444E-03 5.243E-01  
0.100 -1.491E-01 9.424E-04 5.378E-01  
0.105 -1.593E-01 1.988E-03 5.545E-01  
0.110 -1.657E-01 2.653E-03 5.714E-01  
0.115 -1.697E-01 1.187E-03 5.827E-01  
0.120 -1.748E-01 9.808E-04 5.894E-01  
0.125 -1.811E-01 1.315E-04 5.915E-01  
0.130 -1.852E-01 4.418E-04 5.895E-01  
0.135 -1.891E-01 1.634E-04 5.856E-01  
0.140 -1.854E-01 2.890E-03 5.800E-01  
0.145 -1.858E-01 4.161E-03 5.922E-01  
0.150 -1.840E-01 5.272E-03 6.021E-01  
0.155 -1.843E-01 8.202E-03 6.149E-01  
0.160 -1.802E-01 5.909E-03 6.313E-01

SCALE FACTOR = 7.589E-02

## MASS IMPULSE



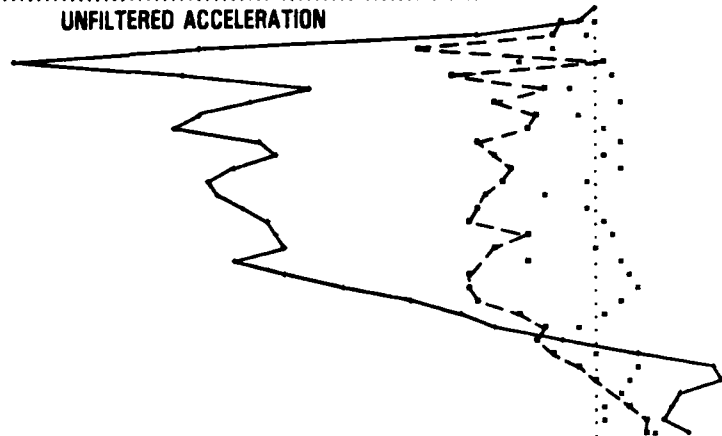
MASS 15 UNFILTERED ACCELERATION(G'S)

TIME(SEC) KACC YACC ZACC

SCALE FACTOR = 1.385E+00

0.0 1.294E-02 1.525E-04 2.777E-02  
0.005 -6.111E-01 4.255E-03 2.587E-01  
0.010 -7.440E-01 1.553E-01 1.914E+00  
0.015 -2.974E+00 7.131E-01 6.541E+00  
0.020 1.776E-01 1.296E+00 9.586E+00  
0.025 -2.548E+00 2.605E-01 6.828E+00  
0.030 -8.738E-01 4.587E-01 6.721E+00  
0.035 -1.625E+00 4.274E-01 5.709E+00  
0.040 -9.445E-01 2.951E-01 6.571E+00  
0.045 -1.158E+00 5.777E-02 6.887E+00  
0.050 -1.966E+00 4.120E-01 5.613E+00  
0.055 -1.758E+00 1.144E-01 5.354E+00  
0.060 -1.425E+00 4.304E-01 5.955E+00  
0.065 -1.540E+00 2.010E-01 6.370E+00  
0.070 -1.841E+00 7.918E-01 6.218E+00  
0.075 -1.987E+00 1.843E-01 5.810E+00  
0.080 -2.066E+00 8.942E-02 5.371E+00  
0.085 -1.097E+00 2.345E-01 5.245E+00  
0.090 -1.734E+00 2.080E-02 5.164E+00  
0.095 -1.113E+00 4.217E-01 5.949E+00  
0.100 -2.172E+00 4.860E-01 5.144E+00  
0.105 -2.145E+00 6.031E-01 6.225E+00  
0.110 -2.016E+00 3.298E-01 5.145E+00  
0.115 -1.297E+00 4.943E-02 5.241E+00  
0.120 -8.738E-01 2.813E-01 1.624E+00  
0.125 -1.014E+00 6.045E-01 5.601E-01  
0.130 -7.091E-01 9.744E-02 6.885E-01  
0.135 -3.283E-01 6.072E-01 1.944E+00  
0.140 3.140E-03 5.304E-01 2.048E+00  
0.145 3.986E-01 3.352E-01 1.327E+00  
0.150 5.411E-01 6.254E-02 1.232E+00  
0.155 7.654E-01 1.551E-01 1.032E+00  
0.160 8.270E-01 9.348E-01 1.458E+00

UNFILTERED ACCELERATION



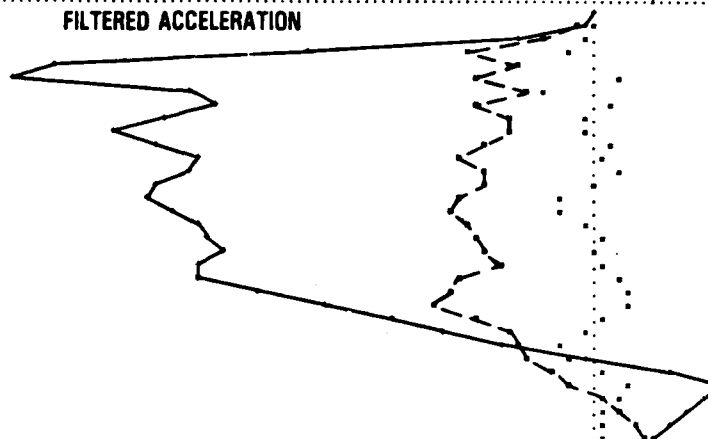
MASS 15 FILTERED ACCELERATION(G'S)

TIME(SEC) KACCF YACCF ZACCF

SCALE FACTOR = 1.194E+00

0.0 0.0 0.0 0.0  
0.005 -7.284E-01 3.401E-04 6.700E-02  
0.010 -7.144E-01 4.743E-02 1.032E+00  
0.015 -1.795E+00 3.245E-01 3.971E+00  
0.020 -1.012E+00 1.172E+00 7.584E+00  
0.025 -1.601E+00 3.519E-01 8.204E+00  
0.030 -8.584E-01 6.682E-01 5.638E+00  
0.035 -1.601E+00 2.940E-01 5.542E+00  
0.040 -1.159E+00 8.278E-02 6.051E+00  
0.045 -1.149E+00 1.028E-01 6.767E+00  
0.050 -1.502E+00 2.927E-01 6.212E+00  
0.055 -1.895E+00 1.341E-01 5.537E+00  
0.060 -1.467E+00 3.724E-01 5.625E+00  
0.065 -1.490E+00 9.518E-02 6.124E+00  
0.070 -1.893E+00 4.541E-01 6.531E+00  
0.075 -2.037E+00 4.619E-01 5.984E+00  
0.080 -1.782E+00 1.209E-01 5.630E+00  
0.085 -1.571E+00 1.895E-01 5.430E+00  
0.090 -1.535E+00 7.572E-02 5.164E+00  
0.095 -1.271E+00 2.235E-01 5.622E+00  
0.100 -1.839E+00 4.495E-01 5.825E+00  
0.105 -2.042E+00 5.071E-01 4.741E+00  
0.110 -2.185E+00 5.057E-01 3.779E+00  
0.115 -1.581E+00 1.075E-01 2.804E+00  
0.120 -1.196E+00 4.424E-02 2.087E+00  
0.125 -8.879E-01 4.513E-01 1.221E+00  
0.130 -9.335E-01 3.495E-01 6.740E-02  
0.135 -5.379E-01 2.199E-01 1.151E+00  
0.140 -2.924E-01 5.485E-01 1.843E+00  
0.145 2.030E-01 4.198E-01 1.624E+00  
0.150 4.140E-01 2.207E-01 1.328E+00  
0.155 6.443E-01 1.108E-01 1.171E+00  
0.160 7.803E-01 2.129E-01 9.234E-01

FILTERED ACCELERATION



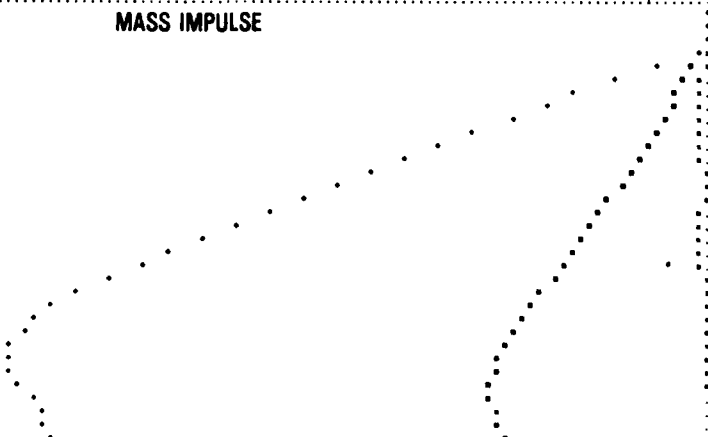
MASS 15 MASS IMPULSES

TIME(SEC) XIMP YIMP ZIMP

SCALE FACTOR = 7.355E-02

0.0 0.0 0.0 0.0  
0.005 -2.574E-04 4.108E-06 1.201E-04  
0.010 -2.902E-03 1.040E-04 2.431E-03  
0.015 -7.499E-02 9.271E-04 1.332E-02  
0.020 -1.692E-02 4.862E-03 4.310E-02  
0.025 -2.207E-02 6.473E-03 8.497E-02  
0.030 -2.882E-02 7.874E-03 1.190E-01  
0.035 -3.524E-02 8.621E-03 1.454E-01  
0.040 -4.227E-02 7.932E-03 1.740E-01  
0.045 -4.798E-02 8.621E-03 2.063E-01  
0.050 -5.428E-02 8.114E-03 2.392E-01  
0.055 -6.320E-02 6.952E-03 2.682E-01  
0.060 -7.147E-02 5.728E-03 2.958E-01  
0.065 -7.887E-02 4.351E-03 3.253E-01  
0.070 -8.734E-02 5.241E-03 3.567E-01  
0.075 -9.704E-02 7.992E-03 3.875E-01  
0.080 -1.042E-01 9.353E-03 4.166E-01  
0.085 -1.152E-01 9.054E-03 4.442E-01  
0.090 -1.225E-01 8.333E-03 4.705E-01  
0.095 -1.299E-01 7.754E-03 4.972E-01  
0.100 -1.374E-01 5.943E-03 5.257E-01  
0.105 -1.472E-01 3.404E-03 5.515E-01  
0.110 -1.580E-01 8.719E-04 5.728E-01  
0.115 -1.674E-01 7.992E-04 5.892E-01  
0.120 -1.744E-01 1.213E-03 6.013E-01  
0.125 -1.794E-01 1.079E-03 6.096E-01  
0.130 -1.845E-01 2.378E-03 6.128E-01  
0.135 -1.881E-01 2.767E-03 6.101E-01  
0.140 -1.905E-01 5.384E-04 6.025E-01  
0.145 -1.904E-01 1.899E-03 5.932E-01  
0.150 -1.888E-01 3.494E-03 5.860E-01  
0.155 -1.861E-01 4.230E-03 5.797E-01  
0.160 -1.825E-01 5.010E-03 5.746E-01

MASS IMPULSE



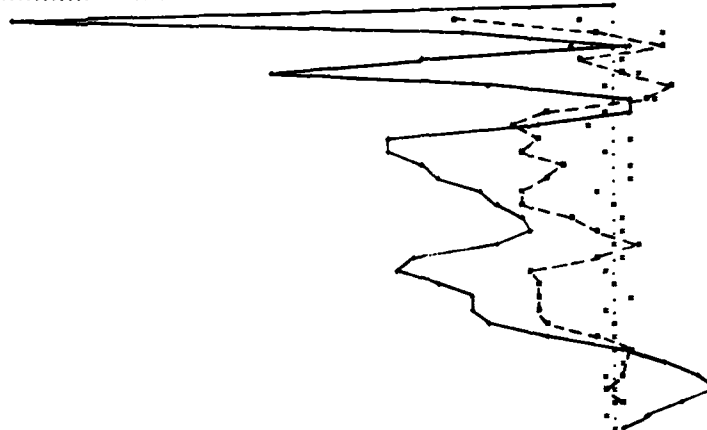
MASS 16 UNFILTERED ACCELERATION(G'S)

TIME(SEC) XACC YACC ZACC

UNFILTERED ACCELERATION

SCALE FACTOR = 2.656E+00

0.0 1.510E-02-4.482E-05-2.451E-02  
0.005 -5.141E+00-1.151E+00-1.913E-01  
0.010 -5.855E-01 1.497E+00-4.852E+00  
0.015 1.631E+00-1.227E+00 5.724E-01  
0.020 -9.790E-01 1.584E-01-6.019E+00  
0.025 1.510E-01 6.799E-01-1.093E-01  
0.030 1.904E+00-3.658E-01-3.917E+00  
0.035 1.050E+00 1.196E+00 6.019E-01  
0.040 -2.243E+00-3.394E-01 6.401E-01  
0.045 -3.257E+00-7.521E-01-2.501E+00  
0.050 -2.266E+00 5.448E-01-7.088E+00  
0.055 -2.821E+00-2.540E-01-7.077E+00  
0.060 -1.670E+00 4.794E-01-6.065E+00  
0.065 -2.131E+00 4.821E-01-5.625E+00  
0.070 -2.942E+00-5.834E-01-4.344E+00  
0.075 -2.961E+00 2.937E-02-3.624E+00  
0.080 -1.240E+00 3.182E-01-2.970E+00  
0.085 -5.792E-01 1.892E-01-2.720E+00  
0.090 8.744E-01 1.292E-01-3.430E+00  
0.095 -4.845E-01 1.684E-01-4.334E+00  
0.100 -2.527E+00-2.580E-01-6.850E+00  
0.105 -2.474E+00 7.019E-02-5.480E+00  
0.110 -2.502E+00 6.149E-01-4.520E+00  
0.115 -2.395E+00-1.389E-01-4.411E+00  
0.120 -2.194E+00-4.281E-02-3.883E+00  
0.125 -5.424E-01 1.234E-02-2.179E+00  
0.130 4.829E-01-4.224E-02 3.557E-01  
0.135 1.823E-01 1.651E-01 1.640E+00  
0.140 1.436E-01-1.874E-01 2.719E+00  
0.145 -2.797E-01 4.596E-02 3.184E+00  
0.150 1.419E-01 1.232E-01 2.080E+00  
0.155 -2.924E-01-1.649E-01 9.499E-01  
0.160 2.051E-02 3.444E-02 3.235E-01



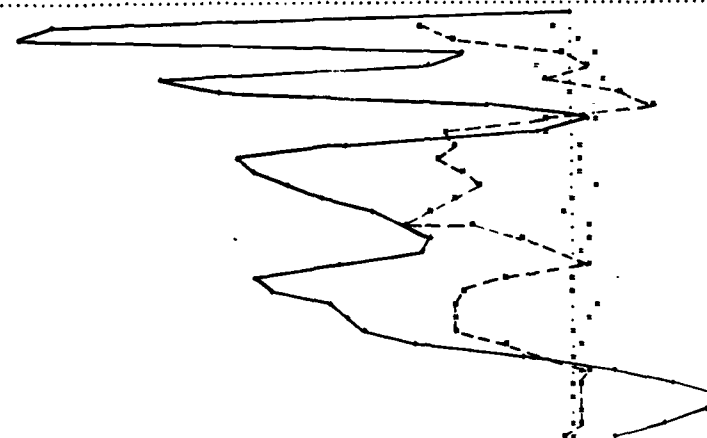
MASS 16 FILTERED ACCELERATION(G'S)

TIME(SEC) XACCF YACCF ZACCF

FILTERED ACCELERATION

SCALE FACTOR = 1.688E+00

0.0 0.0 0.0 0.0  
0.005 -3.097E+00-4.495E-01-1.057E-01  
0.010 -2.404E+00 5.824E-02-1.122E-01  
0.015 -1.655E-01 3.877E-01-2.299E+00  
0.020 3.139E-01-8.128E-01-2.942E+00  
0.025 -1.149E-01 4.008E-01-8.169E+00  
0.030 8.697E-01-9.093E-02-7.218E+00  
0.035 1.655E+00 5.132E-01-1.818E+00  
0.040 -5.540E-01 4.853E-01 2.034E-01  
0.045 -2.662E+00-6.462E-01-7.432E-01  
0.050 -2.489E+00 4.554E-02-6.424E+00  
0.055 -2.712E+00 4.255E-02-6.857E+00  
0.060 -2.222E+00 5.361E-02-6.470E+00  
0.065 -1.914E+00 5.167E-01-5.861E+00  
0.070 -2.499E+00-9.596E-02-5.122E+00  
0.075 -2.963E+00-2.573E-01-4.112E+00  
0.080 -2.078E+00 2.033E-01-3.627E+00  
0.085 -1.101E+00 2.051E-01-2.884E+00  
0.090 4.981E-02 1.736E-01-3.106E+00  
0.095 2.477E-01 1.519E-01-4.817E+00  
0.100 -1.494E+00-1.419E-02-6.564E+00  
0.105 -2.351E+00-1.403E-01-6.168E+00  
0.110 -2.454E+00 1.881E-01-5.031E+00  
0.115 -2.411E+00 2.047E-01-4.661E+00  
0.120 -2.364E+00-8.872E-02-4.318E+00  
0.125 -1.449E+00 3.103E-02-3.207E+00  
0.130 -1.292E-01-7.178E-02-1.107E+00  
0.135 2.489E-01 8.454E-02 7.972E-01  
0.140 1.398E-01-2.916E-02 1.951E+00  
0.145 -4.981E-02-7.578E-02 2.946E+00  
0.150 1.522E-02 1.204E-01 2.585E+00  
0.155 4.640E-02-6.211E-02 1.704E+00  
0.160 -2.473E-01-4.458E-02 7.445E-01



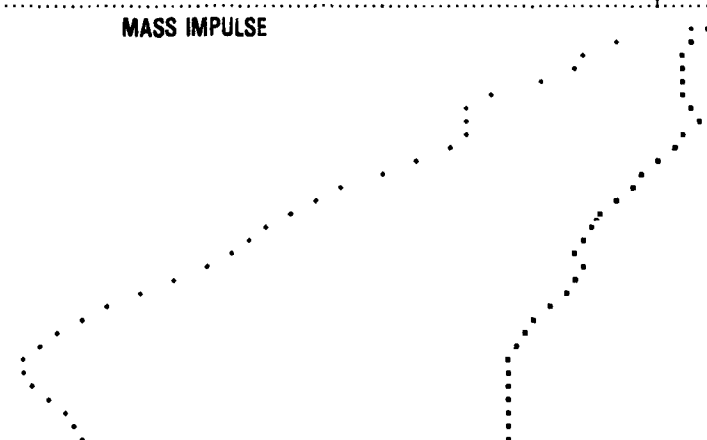
MASS 16 MASS IMPULSES

TIME(SEC) XIMP YIMP ZIMP

MASS IMPULSE

SCALE FACTOR = 7.417E-02

0.0 0.0 0.0 0.0  
0.005 -4.515E-03-4.881E-04-2.110E-02  
0.010 -2.227E-02-3.297E-03-8.684E-02  
0.015 -2.946E-02 2.544E-04-1.174E-01  
0.020 -2.682E-02-2.923E-03-1.246E-01  
0.025 -2.923E-02-2.456E-03-1.553E-01  
0.030 -2.851E-02-1.207E-03-1.981E-01  
0.035 -2.099E-02-8.018E-04-2.197E-01  
0.040 -1.775E-02 2.774E-03-2.224E-01  
0.045 -2.665E-02 1.778E-03-2.224E-01  
0.050 -4.007E-02-9.452E-03-2.355E-01  
0.055 -5.283E-02 7.627E-04-2.659E-01  
0.060 -4.561E-02 5.385E-04-2.995E-01  
0.065 -7.538E-02 2.285E-03-3.301E-01  
0.070 -8.433E-02 3.628E-03-3.581E-01  
0.075 -1.002E-01 2.199E-03-3.809E-01  
0.080 -1.134E-01 2.228E-03-3.997E-01  
0.085 -1.211E-01 3.325E-03-4.153E-01  
0.090 -1.238E-01 4.244E-03-4.298E-01  
0.095 -1.220E-01 5.050E-03-4.490E-01  
0.100 -1.150E-01 5.586E-03-4.785E-01  
0.105 -1.353E-01 4.867E-03-5.109E-01  
0.110 -1.474E-01 5.503E-03-5.387E-01  
0.115 -1.549E-01 7.377E-03-5.626E-01  
0.120 -1.716E-01 7.363E-03-5.853E-01  
0.125 -1.816E-01 7.285E-03-6.044E-01  
0.130 -1.852E-01 7.154E-03-6.154E-01  
0.135 -1.844E-01 7.153E-03-6.154E-01  
0.140 -1.835E-01 7.462E-03-6.086E-01  
0.145 -1.830E-01 7.001E-03-5.958E-01  
0.150 -1.834E-01 7.210E-03-5.815E-01  
0.155 -1.830E-01 7.424E-03-5.708E-01  
0.160 -1.841E-01 7.040E-03-5.650E-01



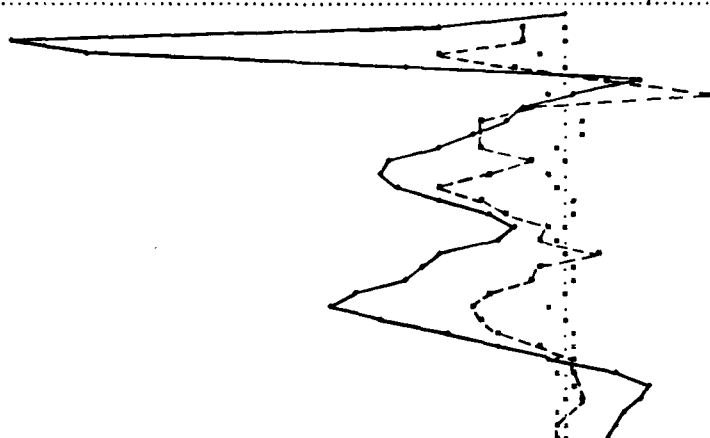


# MASS 17 UNFILTERED ACCELERATION(G'S)

TIME(SEC)	XACC	YACC	ZACC
0.0	1.290E-02	2.097E-05	2.310E-02
0.005	-1.342E-02	1.500E-01	4.225E-00
0.010	-1.216E-00	6.140E-02	1.913E-01
0.015	-4.212E-00	8.374E-01	1.646E-01
0.020	-1.017E-00	8.233E-02	5.407E-00
0.025	2.745E-00	1.611E-00	2.618E-00
0.030	5.271E-00	5.440E-01	3.182E-01
0.035	-1.144E-00	1.214E-00	1.430E-00
0.040	-2.970E-00	7.201E-01	1.071E-00
0.045	-3.279E-00	7.375E-01	3.275E-00
0.050	-2.722E-00	1.243E-01	4.299E-00
0.055	-1.074E-00	6.007E-02	6.101E-00
0.060	-2.495E-00	4.724E-01	6.483E-00
0.065	-4.227E-00	1.015E-01	5.750E-00
0.070	-2.822E-00	4.041E-01	4.344E-00
0.075	-2.001E-00	3.042E-01	2.581E-00
0.080	-4.704E-01	9.785E-02	1.756E-00
0.085	-8.706E-01	3.872E-01	2.301E-00
0.090	1.095E-00	1.749E-02	4.443E-00
0.095	-7.744E-01	2.485E-01	4.999E-00
0.100	-1.225E-00	3.640E-01	5.423E-00
0.105	-2.599E-00	8.640E-02	7.343E-00
0.110	-3.292E-00	4.432E-01	7.972E-00
0.115	-2.918E-00	1.022E-01	6.275E-00
0.120	-2.553E-00	2.803E-01	4.027E-00
0.125	-7.872E-01	2.454E-01	2.181E-00
0.130	4.115E-01	1.141E-01	4.540E-01
0.135	1.892E-01	1.994E-01	1.750E-00
0.140	4.040E-01	2.842E-01	3.043E-00
0.145	7.237E-01	3.078E-02	2.573E-00
0.150	-1.557E-01	1.442E-01	2.041E-00
0.155	-2.795E-01	5.902E-03	1.741E-00
0.160	-3.724E-01	1.840E-02	1.592E-00

## UNFILTERED ACCELERATION

SCALE FACTOR = 2.905E+00

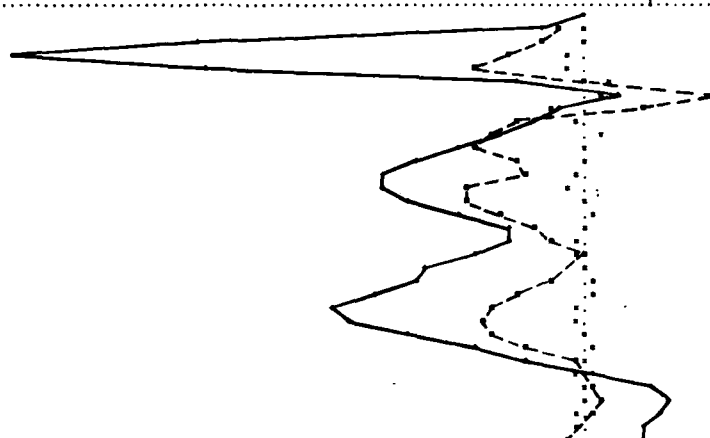


# MASS 17 FILTERED ACCELERATION(G'S)

TIME(SEC)	XACCF	YACCF	ZACCF
0.0	0.0	0.0	0.0
0.005	-5.786E-01	3.700E-02	1.115E-00
0.010	-1.293E-00	1.745E-01	1.178E-01
0.015	-2.259E-00	3.400E-01	1.728E-01
0.020	-3.281E-00	4.659E-01	1.132E-01
0.025	1.257E-01	9.119E-01	1.988E-00
0.030	1.181E-00	5.285E-01	1.038E-00
0.035	1.893E-00	9.871E-01	4.702E-01
0.040	-1.897E-00	2.313E-01	1.424E-00
0.045	-2.829E-00	7.248E-01	2.549E-00
0.050	-2.139E-00	2.158E-01	3.624E-00
0.055	-1.859E-00	6.708E-02	5.098E-00
0.060	-1.750E-00	2.059E-01	4.158E-00
0.065	-3.277E-00	3.480E-01	4.052E-00
0.070	-3.514E-00	1.158E-01	5.151E-00
0.075	-2.424E-00	3.318E-01	3.718E-00
0.080	-1.386E-00	2.127E-01	2.240E-00
0.085	-9.687E-01	1.189E-01	2.105E-00
0.090	1.177E-01	1.954E-01	2.245E-00
0.095	1.020E-01	1.444E-01	4.447E-00
0.100	-9.316E-01	2.573E-01	5.002E-00
0.105	-1.832E-00	2.867E-01	6.342E-00
0.110	-2.814E-00	2.073E-01	7.577E-00
0.115	-3.075E-00	1.500E-01	7.126E-00
0.120	-2.459E-00	1.831E-01	5.344E-00
0.125	-1.751E-00	2.534E-01	3.335E-00
0.130	-2.200E-01	1.083E-01	1.645E-00
0.135	1.646E-01	1.889E-01	3.201E-01
0.140	2.839E-01	1.232E-01	2.209E-00
0.145	6.440E-01	2.090E-01	2.452E-00
0.150	2.755E-01	8.409E-02	2.299E-00
0.155	-2.070E-01	4.473E-02	1.983E-00
0.160	-2.494E-01	4.637E-02	1.932E-00

## FILTERED ACCELERATION

SCALE FACTOR = 2.554E+00

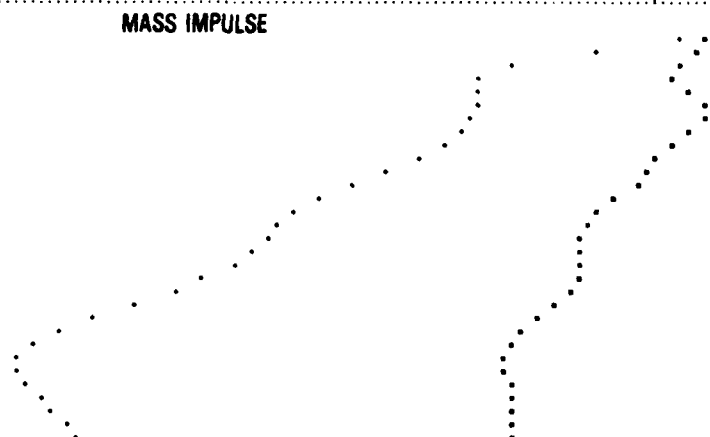


# MASS 17 MASS IMPULSES

TIME(SEC)	XIMP	YIMP	ZIMP
0.0	0.0	0.0	0.0
0.005	-8.541E-04	2.892E-05	1.124E-03
0.010	-8.189E-03	7.124E-04	5.118E-02
0.015	-1.381E-02	5.720E-04	1.098E-01
0.020	-3.054E-02	2.442E-03	1.842E-01
0.025	-3.859E-02	1.561E-03	2.160E-01
0.030	-2.458E-02	5.452E-03	2.146E-01
0.035	-8.742E-03	1.889E-02	2.141E-01
0.040	-1.044E-02	1.882E-02	2.196E-01
0.045	-2.272E-02	2.094E-04	2.295E-01
0.050	-2.871E-02	2.325E-02	2.451E-01
0.055	-5.088E-02	2.784E-03	2.667E-01
0.060	-5.884E-02	2.615E-03	2.954E-01
0.065	-7.170E-02	9.184E-04	3.242E-01
0.070	-9.004E-02	2.797E-04	3.540E-01
0.075	-1.049E-01	1.631E-03	3.769E-01
0.080	-1.143E-01	3.020E-03	3.914E-01
0.085	-1.197E-01	3.565E-03	4.019E-01
0.090	-1.224E-01	2.230E-03	4.147E-01
0.095	-1.208E-01	2.222E-03	4.252E-01
0.100	-1.232E-01	3.213E-03	4.392E-01
0.105	-1.298E-01	4.785E-03	4.872E-01
0.110	-1.417E-01	4.972E-03	5.224E-01
0.115	-1.549E-01	5.742E-03	5.600E-01
0.120	-1.712E-01	5.961E-03	5.912E-01
0.125	-1.857E-01	5.111E-03	6.128E-01
0.130	-1.877E-01	6.174E-03	6.252E-01
0.135	-1.870E-01	5.810E-03	6.288E-01
0.140	-1.859E-01	5.475E-03	6.219E-01
0.145	-1.827E-01	6.615E-03	6.091E-01
0.150	-1.812E-01	6.870E-03	5.964E-01
0.155	-1.812E-01	6.419E-03	5.859E-01
0.160	-1.828E-01	6.201E-03	5.760E-01

## MASS IMPULSE

SCALE FACTOR = 7.567E-02

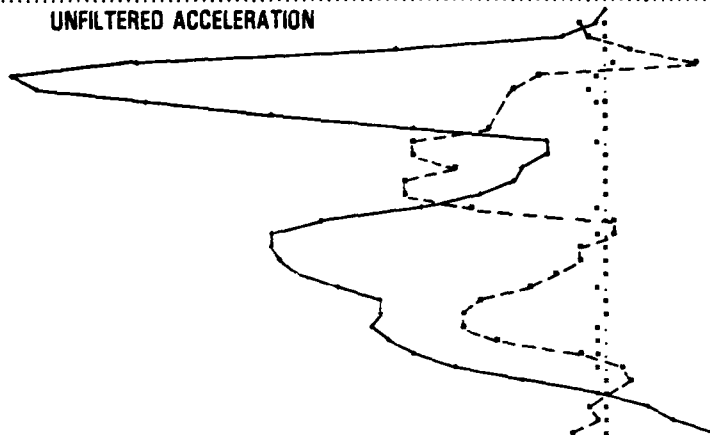


MASS 18 UNFILTERED ACCELERATION(G'S)

TIME(SEC)	KACC	YACC	ZACC
0.0	1.345E-02	2.237E-05	2.245E-02
0.005	-4.641E-01	5.476E-03	8.807E-02
0.010	-3.030E-01	1.147E-02	8.156E-01
0.015	5.557E-01	4.745E-02	-6.077E+00
0.020	1.847E+00	1.493E-01	-9.252E+00
0.025	-1.266E+00	-1.151E-01	-1.184E+01
0.030	-1.831E+00	-2.540E-01	-1.141E+01
0.035	2.932E-03	-1.587E-01	-9.161E+00
0.040	1.124E-01	5.735E-02	-6.641E+00
0.045	-2.509E+00	2.782E-02	-5.748E+00
0.050	-3.810E+03	-6.290E-02	-1.116E+00
0.055	-3.825E+00	7.846E-02	-1.180E+00
0.060	-3.040E+00	6.179E-02	-1.706E+00
0.065	-5.455E+00	1.028E-02	-1.836E+00
0.070	-3.498E+00	4.141E-02	-2.424E+00
0.075	-2.578E+00	3.565E-02	-2.715E+00
0.080	1.347E-01	-1.507E-02	-5.600E+00
0.085	2.601E-01	-5.272E-02	-6.648E+00
0.090	-4.870E-01	-8.375E-03	-6.593E+00
0.095	-4.515E-01	1.248E-02	-6.441E+00
0.100	-8.704E-01	1.747E-02	-6.135E+00
0.105	1.347E-01	-5.507E-02	-5.257E+00
0.110	-2.495E+00	-3.666E-03	-4.482E+00
0.115	-2.870E+00	-2.614E-02	-4.554E+00
0.120	-2.821E+00	-1.011E-01	-4.658E+00
0.125	-2.091E+00	-4.477E-02	-4.343E+00
0.130	-3.736E-01	-9.525E-03	-3.871E+00
0.135	3.424E-01	-1.019E-01	-2.970E+00
0.140	5.397E-01	-1.574E-02	-1.650E+00
0.145	-6.910E-02	4.897E-03	-1.504E-01
0.150	-2.444E-01	7.888E-02	8.071E-01
0.155	-8.689E-02	1.755E-01	1.406E+00
0.160	-5.524E-01	6.442E-02	2.230E+00

SCALE FACTOR = 1.675E+00

### UNFILTERED ACCELERATION

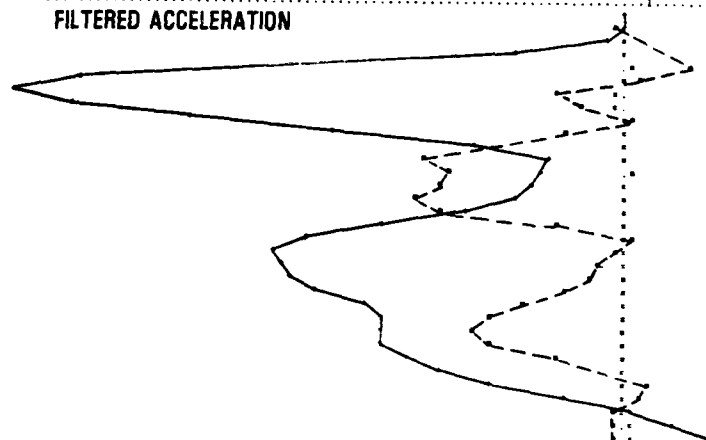


MASS 18 FILTERED ACCELERATION(G'S)

TIME(SEC)	KACCF	YACCF	ZACCF
0.0	0.0	0.0	0.0
0.005	-1.569E-01	1.451E-03	-2.242E-02
0.010	-5.732E-01	9.494E-02	-2.620E-01
0.015	6.026E-02	1.025E-02	-2.104E+00
0.020	1.256E+00	1.014E-01	-6.293E+00
0.025	-1.141E-01	-2.862E-02	-1.015E+01
0.030	-1.344E+00	-1.782E-01	-1.145E+01
0.035	-8.318E-01	-1.474E-01	-1.024E+01
0.040	6.214E-02	5.979E-02	-8.181E+00
0.045	-1.070E+00	4.615E-02	-5.572E+00
0.050	-2.821E+00	3.577E-02	-2.774E+00
0.055	-3.801E+00	1.205E-02	-1.454E+00
0.060	-3.587E+00	6.992E-02	-1.548E+00
0.065	-3.405E+00	2.851E-02	-1.746E+00
0.070	-3.979E+00	3.512E-02	-2.062E+00
0.075	-3.442E+00	2.449E-02	-2.425E+00
0.080	-1.322E+00	2.112E-02	-4.508E+00
0.085	8.017E-02	1.876E-02	-6.004E+00
0.090	-1.881E-01	-1.855E-02	-6.522E+00
0.095	-4.429E-01	1.214E-02	-6.512E+00
0.100	-7.149E-01	1.421E-02	-6.320E+00
0.105	-1.092E+00	-1.025E-02	-5.755E+00
0.110	-1.881E+00	-2.222E-02	-4.908E+00
0.115	-2.579E+00	-4.457E-02	-4.558E+00
0.120	-2.777E+00	-6.702E-02	-4.417E+00
0.125	-2.565E+00	-7.819E-02	-4.464E+00
0.130	-1.119E+00	-7.607E-02	-4.156E+00
0.135	-8.409E-02	1.042E-01	-2.517E+00
0.140	4.528E-01	5.735E-02	-2.455E+00
0.145	2.584E-01	1.204E-01	-1.071E+00
0.150	-1.101E-01	2.479E-02	1.547E-01
0.155	-1.081E-01	1.025E-01	4.672E-01
0.160	-2.446E-01	9.326E-02	1.692E+00

SCALE FACTOR = 1.565E+00

### FILTERED ACCELERATION

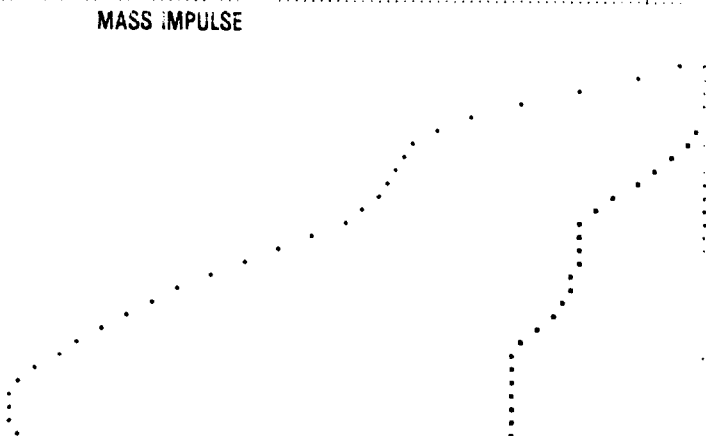


MASS 18 MASS IMPULSES

TIME(SEC)	KIMP	YIMP	ZIMP
0.0	0.0	0.0	0.0
0.005	0.0	0.0	0.0
0.010	-1.792E-02	3.194E-05	-7.691E-04
0.015	-2.490E-02	5.414E-05	-6.044E-02
0.020	1.463E-04	2.201E-04	-2.666E-02
0.025	5.607E-02	6.771E-04	-6.889E-02
0.030	-2.120E-02	2.564E-04	-1.241E-01
0.035	-4.211E-02	7.751E-04	-1.194E-01
0.040	-5.514E-02	1.464E-02	-2.259E-01
0.045	-7.155E-02	1.549E-02	-2.601E-01
0.050	-1.718E-02	1.564E-02	-2.804E-01
0.055	-3.447E-02	1.490E-02	-2.904E-01
0.060	-5.571E-02	1.224E-02	-2.944E-01
0.065	-8.618E-02	9.829E-03	-3.082E-01
0.070	-8.741E-02	8.247E-03	-3.154E-01
0.075	-1.066E-01	6.991E-03	-3.276E-01
0.080	-1.191E-01	7.810E-03	-3.461E-01
0.085	-1.212E-01	8.676E-03	-3.726E-01
0.090	-1.212E-01	9.732E-03	-4.045E-01
0.095	-1.212E-01	1.022E-02	-4.422E-01
0.100	-1.259E-01	9.801E-03	-4.860E-01
0.105	-1.207E-01	9.577E-03	-5.372E-01
0.110	-1.175E-01	1.074E-02	-5.967E-01
0.115	-1.489E-01	1.128E-02	-6.649E-01
0.120	-1.625E-01	1.217E-02	-7.425E-01
0.125	-1.767E-01	1.709E-02	-8.364E-01
0.130	-1.861E-01	2.069E-02	-9.471E-01
0.135	-1.892E-01	2.526E-02	-1.076E-01
0.140	-1.902E-01	2.962E-02	-1.215E-01
0.145	-1.851E-01	3.115E-02	-1.360E-01
0.150	-1.840E-01	3.073E-02	-1.512E-01
0.155	-1.867E-01	3.073E-02	-1.671E-01
0.160	-1.874E-01	3.066E-02	-1.837E-01

SCALE FACTOR = 1.565E+00

### MASS IMPULSE



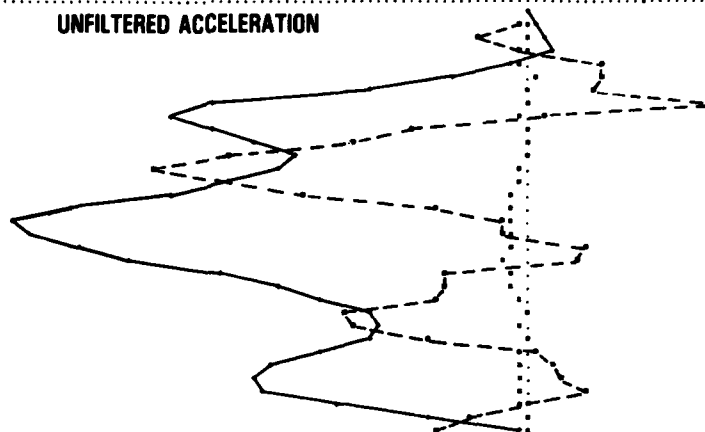
# MASS 19 UNFILTERED ACCELERATION(G'S)

TIME(SEC) XACC YACC ZACC

0.0 1.32E-02 2.86E-04 1.76E-02  
0.005 -2.08E-01 1.86E-02 6.10E-02  
0.010 -9.65E-01 2.67E-02 2.47E-01  
0.015 -1.16E-01 1.01E-02 4.41E-01  
0.020 1.37E+00 1.09E-01 5.70E-01  
0.025 1.34E+00 1.86E-01 1.49E+00  
0.030 1.19E+00 1.46E-02 3.08E+00  
0.035 5.51E+00 8.66E-01 6.21E+00  
0.040 2.16E-01 1.22E-01 6.09E+00  
0.045 -2.32E+00 2.44E-02 6.07E+00  
0.050 -3.39E+00 1.97E-02 5.30E+00  
0.055 -5.76E+00 7.52E-02 4.58E+00  
0.060 -7.21E+00 1.21E-01 4.79E+00  
0.065 -5.04E+00 1.95E-01 5.01E+00  
0.070 -4.46E+00 2.76E-01 6.07E+00  
0.075 -1.75E+00 2.80E-01 6.91E+00  
0.080 -5.09E-01 5.09E-01 1.00E+01  
0.085 -5.01E-01 5.75E-01 9.66E+00  
0.090 1.07E+00 3.95E-01 8.64E+00  
0.095 9.62E-01 4.97E-01 7.69E+00  
0.100 -1.71E+00 5.66E-01 6.02E+00  
0.105 -1.68E+00 5.22E-01 4.80E+00  
0.110 -1.75E+00 4.75E-01 4.11E+00  
0.115 -3.62E+00 1.02E-01 5.06E+00  
0.120 -5.36E+00 1.27E-01 2.80E+00  
0.125 -1.09E+00 7.19E-02 5.15E+00  
0.130 6.56E-02 1.97E-01 4.07E+00  
0.135 4.92E-01 2.26E-01 5.08E+00  
0.140 6.52E-01 1.10E-01 5.29E+00  
0.145 1.15E+00 2.76E-01 5.16E+00  
0.150 -7.72E-02 1.20E-01 5.70E+00  
0.155 -1.23E+00 9.29E-02 1.09E+01  
0.160 -1.79E+00 5.52E-02 2.57E-01

SCALE FACTOR = 1.609E+00

## UNFILTERED ACCELERATION



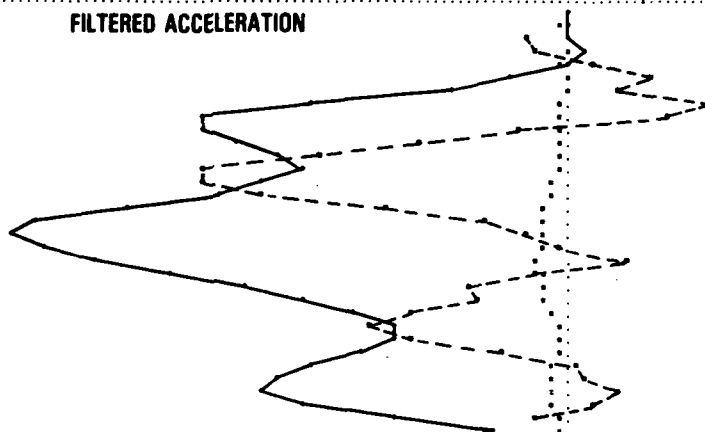
# MASS 19 FILTERED ACCELERATION(G'S)

TIME(SEC) XACF YACF ZACF

0.0 0.0 0.0 0.0  
0.005 -2.45E-02 5.45E-03 5.59E-02  
0.010 -6.41E-01 4.62E-05 1.29E-01  
0.015 -4.76E-01 2.24E-02 3.45E-01  
0.020 6.46E-01 7.99E-02 1.14E-01  
0.025 1.50E+00 5.22E-02 8.64E-01  
0.030 9.77E-01 4.48E-02 2.01E+00  
0.035 2.57E+00 8.11E-02 4.45E+00  
0.040 1.89E+00 8.65E-02 6.58E+00  
0.045 -8.51E-01 9.15E-02 6.58E+00  
0.050 -2.59E+00 1.57E-02 7.99E+00  
0.055 -4.29E+00 5.90E-02 5.06E+00  
0.060 -6.15E+00 8.59E-02 4.99E+00  
0.065 -6.27E+00 1.59E-01 5.29E+00  
0.070 -5.61E+00 2.10E-01 6.15E+00  
0.075 -5.22E+00 1.40E-01 7.74E+00  
0.080 -1.69E+00 2.54E-01 9.29E+00  
0.085 -7.20E-01 5.17E-01 9.77E+00  
0.090 -4.22E-02 5.54E-01 9.14E+00  
0.095 1.04E+00 4.44E-01 8.31E+00  
0.100 -4.44E-01 4.27E-01 7.06E+00  
0.105 -1.85E+00 2.44E-01 5.59E+00  
0.110 -1.51E+00 5.06E-01 4.67E+00  
0.115 -2.70E+00 1.74E-01 5.67E+00  
0.120 -2.45E+00 1.21E-01 5.04E+00  
0.125 -2.70E+00 9.82E-02 5.02E+00  
0.130 -1.04E+00 1.30E-01 5.52E+00  
0.135 1.72E-01 1.28E-01 4.59E+00  
0.140 4.24E-01 2.06E-01 5.14E+00  
0.145 9.67E-01 2.50E-01 5.32E+00  
0.150 5.61E-01 1.72E-01 4.59E+00  
0.155 -5.67E-01 1.15E-01 5.01E+00  
0.160 -1.33E+00 7.29E-02 1.31E+00

SCALE FACTOR = 1.470E+00

## FILTERED ACCELERATION



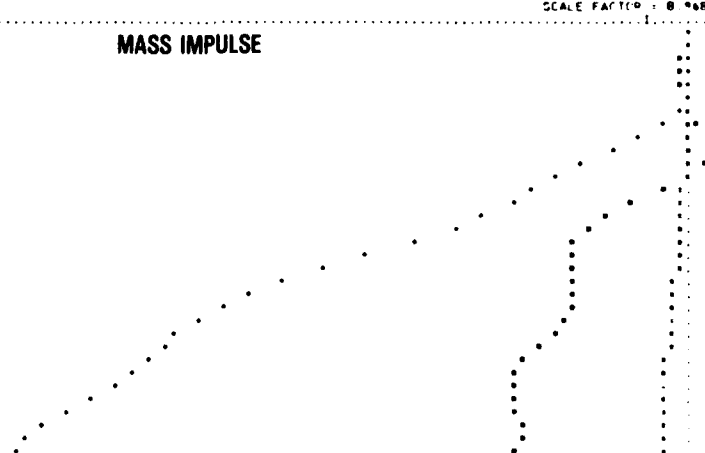
# MASS 19 MASS IMPULSES

TIME(SEC) XIMP YIMP ZIMP

0.0 0.0 0.0 0.0  
0.005 3.09E-05 4.86E-06 1.91E-04  
0.010 -1.57E-05 3.22E-05 5.46E-04  
0.015 -4.81E-05 6.67E-05 1.75E-03  
0.020 -5.71E-05 8.01E-05 2.29E-03  
0.025 4.82E-04 2.86E-04 1.27E-02  
0.030 6.29E-03 1.75E-04 5.62E-03  
0.035 1.46E-02 5.67E-05 2.14E-02  
0.040 2.76E-02 4.57E-04 6.95E-02  
0.045 2.98E-02 9.71E-04 8.20E-02  
0.050 2.02E-02 1.18E-03 1.14E-01  
0.055 5.92E-02 1.27E-03 1.29E-01  
0.060 -2.35E-02 1.72E-03 1.63E-01  
0.065 -5.50E-02 2.23E-03 1.86E-01  
0.070 -9.54E-02 2.24E-03 2.17E-01  
0.075 -1.07E-01 4.67E-03 2.41E-01  
0.080 -1.18E-01 6.58E-03 2.96E-01  
0.085 -1.23E-01 7.96E-03 3.42E-01  
0.090 -1.26E-01 9.65E-03 3.90E-01  
0.095 -1.29E-01 1.16E-02 4.33E-01  
0.100 -1.29E-01 1.39E-02 4.74E-01  
0.105 -1.26E-01 1.58E-02 5.02E-01  
0.110 -1.24E-01 1.76E-02 5.29E-01  
0.115 -1.44E-01 1.86E-02 5.50E-01  
0.120 -1.60E-01 1.92E-02 5.66E-01  
0.125 -1.76E-01 1.99E-02 5.81E-01  
0.130 -1.89E-01 2.06E-02 5.97E-01  
0.135 -1.89E-01 2.17E-02 6.17E-01  
0.140 -1.89E-01 2.24E-02 6.42E-01  
0.145 -1.85E-01 2.35E-02 6.69E-01  
0.150 -1.78E-01 2.45E-02 6.92E-01  
0.155 -1.78E-01 2.57E-02 7.12E-01  
0.160 -1.83E-01 2.57E-02 7.25E-01

SCALE FACTOR = 8.96E-02

## MASS IMPULSE



# APPENDIX C

## STANDARD DISTRIBUTION LIST

### Region Libraries

Alaska	AAL-64
Central	ACE-66
Eastern	AEA-62
Great Lakes	AGL-60
New England	ANE-40
Northwest-Mountain	ANM-60
Western-Pacific	AWP-60
Southern	ASO-63d
Southwest	ASW-40

### Center Libraries

Technical Center	ACT-64
Aeronautical Center	AAC-44.4

Civil Aviation Authority  
Aviation House  
129 Kingsway  
London WC2B 6NN England

Embassy of Australia  
Civil Air Attache  
1601 Mass Ave. NW  
Washington, D. C. 20036

Scientific & Tech. Info FAC  
Attn: NASA Rep.  
P.O. Box 8757 BWI Aprt  
Baltimore, Md. 21240

DOT-FAA AEU-500  
American Embassy  
APO New York, N. Y. 09667

### Headquarters (Wash. DC)

ADL-1  
ADL-32 (North)  
APM-1  
APM-13 (Nigro)  
ALG-300  
APA-300  
API-19  
AAT-1  
AWS-1  
AES-3

### OST Headquarters Library

M-493.2 (Bldg. 10A)

University of California  
Sers Dpt Inst of Trsp Std Lib  
412 McLaughlin Hall  
Berkeley, CA 94720

British Embassy  
Civil Air Attache ATS  
3100 Mass Ave. NW  
Washington, DC 20008

Dir. DuCentre Exp DE LA  
Navigation Aerineene  
941 Orly, France

Northwestern University  
Trisnet Repository  
Transportation Center Lib  
Evanston, Ill. 60201

Government ActivitiesNo. of Copies

FAA, Washington, DC 20591 (2)  
(Attn: Harold W. Becker, ASF-300; Thomas McSweeney, AWS-100)

FAA, 4344 Donald Douglas Drive, Long Beach, CA 90808 (1)  
(Attn: Stephen Soltis, ANW-102N)

FAA, Mike Monroney Aeronautical Center, P.O. Box 25082, Oklahoma City, OK 73125 (1)  
(Attn: Richard Chandler, AAM-119)

NASA, Langley Research Center, Hampton, VA 23365 (2)  
(Attn: Emilio Alfaro-Bou, MA-495; Huey Cardin, MS-495)

U.S. Army Aviation Applied Technology Directorate, USAARTA, (AVSCOM), (2)  
Fort Eustis, VA 23604  
(Attn: Roy Burrows, Code SAVRT-TY-ASV)

U.S. Navy Naval Air Development Center, Warminster, PA 18974 (1)  
(Attn: Leon Domzalski, Code 60322)

NTSB, 800 Independence Ave. S.E., Washington, DC 20594 (1)  
(Attn: John C. Clark, TE 60)

Non-Government Activities

Beech Aircraft Corp., P.O. Box 85, Wichita, KS 67201 (3)  
(Attn: Dayton L. Hartley; James E. Terry; William Schultz)

Bell Helicopter Co., P.O. Box 482, Fort Worth, TX 76101 (2)  
(Attn: James Cronkite, MS 11; Roy G. Fox)

Boeing Airplane Co., P.O. Box 3707, Seattle, WA 98124 (1)  
(Attn: Edward Widmayer, MC-9W-22)

Boeing Co., Vertol Division, P.O. Box 16858, Philadelphia, PA 91942 (1)  
(Attn: Denise Vassilakos, MS P30-27)

Cessna Aircraft Co., P.O. Box 7704, Wichita, KS 67277 (3)  
(Attn: John Berwick; Robert Held; Richard Soloski)

Fairchild Aircraft Corp., P.O. Box 3246, San Antonio, TX 78284 (1)  
(Attn: Walt Dwyer)

General Dynamics/Convair, P.O. Box 80847, San Diego, CA 92138 (1)  
(Attn: L. Mastny, MA 80-6030)

Grumman Aerospace Corp., So. Oyster Bay Road,, Bethpage, (2)  
L.I., NY 11714  
(Attn: Robert Winter, A08-35; Allan B. Difko, A08-35)

Gulfstream Aerospace Corp., P.O. Box 2206, Savannah, GA 31402 (Attn: George Westphal)	(1)
Gulfstream Aerospace Corp., P.O. Box 22500, Oklahoma City, OK 73123 (Attn: Richard Southard)	(1)
Lockheed-California Co., Burbank, CA 91503 (Attn: Gil Wittlin, D 76-12, B 63G, PLT A-1)	(1)
McDonnell Douglas Corp., 3855 Lakewood Drive, Long Beach, CA 90846 (Attn: J. Webster; John L. Galligher)	(2)
McDonnell Douglas Helicopter, 4645 S. Ash Ave., Tempe, AZ 85182 (Attn: Lyndon Landborne; J.K. Sen)	(2)
Piper Aircraft Corp., 2925 Piper Drive, Vero Beach, FL 32960 (Attn: Marion Dees)	(1)
Sikorsky Aircraft, North Maint Street, Stratford, CT 06601 (Attn: Brain Cornell, MS 5207A; Pramoni Mukunda, MS 5207A)	(2)

END

DTIC

8-86